OBSERVATIONS AND MODELING OF EROSION FROM SPATIALLY AND TEMPORALLY DISTRIBUTED SOURCES IN THE (SEMI) HUMID ETHIOPIAN HIGHLANDS

A Dissertation

Presented to the Faculty of the Graduate School

of Cornell University

in Partial Fulfillment of the Requirements for the Degree of

Doctor of Philosophy

by

Seifu Admassu Tilahun

August 2012

OBSERVATIONS AND MODELING OF EROSION FROM SPATIALLY AND TEMPORALLY DISTRIBUTED SOURCES IN THE (SEMI) HUMID ETHIOPIAN HIGHLANDS

Seifu Admassu Tilahun, Ph.D.

Cornell University 2012

Despite long term efforts to reduce erosion in the Blue Nile Basin, river sediment concentrations have not declined. Lack of progress on sediment reduction indicates that runoff and erosion processes are not fully understood. The objective of this dissertation was, therefore, to understand runoff and erosion processes by investigating where runoff and erosion takes place in the landscape and to use this information to model erosion. Runoff processes were investigated in Debre Mawi, a 95-ha watershed south of Lake Tana. During the rainy period of the 2010 and 2011 monsoons, storm runoff and sediment concentrations were measured from four sub-watersheds and at the main watershed outlet. In addition, perched groundwater tables, infiltration rates, rill erosion from agricultural fields and gully expansion were measured. The results show that saturation excess runoff was the main runoff mechanism because median infiltration rate was only exceeded 3% of the time. Early during rainy period, runoff produced from shallow soils upslope infiltrated before it reached the outlet, and sediment concentrations were very high as rill networks developed on the ploughed land. At the end of July, the bottom lands became saturated, the runoff coefficient at the outlet became greater than upslope areas and rill networks were fully developed reducing the velocities and thereby the sediment concentrations.

A semi-distributed hillslope erosion model relating sediment concentration with overland flow using only four calibrated sediment parameters was developed based on input data from various

watersheds in Blue Nile Basin. The erosion model assumed that sediment concentration is transport limiting at the beginning of the rainy phase when lands are plowed and source limited at the end. Overland flow was simulated with the semi-distributed water balance hydrology model. The model predicted daily sediment concentrations well in three small watersheds including the Debre Mawi as well as in the Blue Nile Basin at the Sudanese border. The implication of this research is that shallow degraded soils and bottom lands with gullies are the greatest sediment sources and should be targeted for erosion control.

BIOGRAPHICAL SKETCH

Seifu Admassu Tilahun was born in 1978 and grew up in Addis Ababa, Ethiopia. After he completed high school at Kolfe Comprehensive Secondary School, he joined Bahir Dar University in 1996 to study for a Bachelor of Science in Civil Engineering. During his five year stay at the university, he became interested in fulfilling his career goals in Hydrology. After finishing his B. Sc., he received a faculty position in the same university and worked for one year. He then joined Addis Ababa University in 2002 to obtain a Masters of Science in Civil Engineering with a specialization in Hydraulic Engineering. His M. Sc. research involved an evaluation of the performance of remotely-sensed rainfall measurements and rainfall trend in Ethiopia which led him to work even more on hydrology. After finishing his M. Sc. in 2004, he returned back to Bahir Dar University and became Chair of the Department of Water Resources Engineering for two years. In addition, he taught courses in the area of hydrology and numerical methods. He then became Chair for the Department of Civil Engineering in August, 2008. In January 2009, Seifu joined Cornell University to start his Ph.D. program at the Department of Biological and Environmental Engineering.

Dedicated to my parents Admassu Tilahun and Elfenesh Ejigu, who guided my education since my childhood, and my wife Eleni Shimeles who has always taken care of our family and given love.

ACKNOWLEDGEMENTS

It would have not been possible to complete this work without a large number of people whom I owe immense gratitude and appreciation. First, I am very much grateful to Tammo Steenhuis who provided invaluable support, supervision, encouragement and constructive critiques as an advisor and chair of my special committee. He was also a friend and academic father that shared his research and life experience since 2009. Second, I would like to express my gratitude to my special committee members Lawrence M. Cathles, J. Yves Parlange and Wilfried Brutsaert for their invaluable conversation, support and guidance throughout my academic program and PhD research. Their conversations and course lectures were unforgettable and helped me in formulating ideas for my research work, and beyond that, to understand the physical process of water and land. I am at last deeply indebted to my friend, Amy S. Collick, to motivate me to do better and for her tireless effort to escalate the quality of my field work and dissertation writing. She had always time to sit and deal with any of my issues.

Funding for the research work was provided by the International Foundation for Science (IFS), Higher Education for Development (HED) and USDA International Science and Education (ISE) program. The field work in Ethiopia would not have been possible without this funding and help of Bahir Dar University (BDU) in providing resources such as vehicle, lab space and equipments.

I would like to acknowledge Christian Guzman, Steve Pacenka and Larry D. Geohring from the Soil and Water Lab for helping me in the field and getting me instruments that I needed from the Soil and Water Lab. I am also grateful for Ali Yassin and Abebaw Azagi, undergraduate BDU students, and local people from Debre Mawi, such as Tewachew Alebachew, Yaregal

Tewachew, Adugna Takele, Tsegawe Alenhe, Wubetu Worekete and all the farmers with whom I discussed, for their continuous help in collecting primary data during day and night and their presence in the field all the time when I needed them.

All runoff and sediment data that I used as secondary data were made available by Amhara Regional Agricultural Research Institute (ARARI). I am very much grateful to Dr Birru Yitaferu from ARARI and Assefa Derebe from Adet Research Center for allowing me to work in Debre Mawi watershed and getting the secondary data. I would like to thank also Hans Hurni and his research groups for providing information when we requested and foresight in establishing the SCRP watersheds (Anjeni and Andit Tid) for runoff and sediment data collection. Finally, I sincerely appreciate New York City Department of Environmental Protection for providing data for Esoups Creek watershed in Catskill region.

I would like to express my sincere appreciation to Addisu Tesfaye from City of Ithaca, friends and colleagues in the School of Civil and Water Resources Engineering of BDU, and all the other people at BDU and in other organizations from where I received help and discussed my research work. I express finally my extended appreciation to my parents, my three sisters (Mekdes Admassu, Fasika Admassu and Mahlet Admassu), my wife, my 5-years old daughter (Abigail Seifu) and my sister in law (Haimanot Azezew) for giving me care and love during my research work.

TABLE OF CONTENTS

LIST OF FIGURES

LIST OF TABLES

CHAPTER 1: INTRODUCTION

Soil erosion is a hazard traditionally associated with agriculture in tropical and semi-arid areas and is a threat to long-term soil productivity and sustainable agriculture (Morgan, 2005) by 1) reducing soil depth and thereby plant available water (Tessema et al., 2010), 2) loss in fertility which can be, for newly developed lands, considerable in magnitude (Mitiku et al, 2006) and cause a decline in land productivity (Bewkete & Sterk, 2003), and finally, 3) silting of small ponds for irrigation, water supply large reservior systems for hydropower in the Ethiopian highlands (Tamene et al, 2006). One of the many examples is the loss of storage capacity of Alemaya Lake that has served as the water supply for the Ethiopian city of Harer, with a population of 100,000 people, and became unusable because the lake filled up with sediment (Muleta et al., 2006).

This problem of reservior sedimentation is particularly significant in the Blue Nile Basin and the downstream countries of Sudan and Egypt (Shahin, 1993). The basin contibutes 60 to 70% of water and suspended sediment load at the Aswan dam in the Nile (Shukri, 1949 and Garzanti et al., 2006). The average annual rate of soil loss has increased from 0.053–0.080 mm/yr from 29 Ma (million years) ago to 0.080–0.12 mm/yr 10 Ma ago to the current rate of 0.5 mm/year when avaraged uniformly over the whole basin (Gani et al., 2007; Garzanti et al, 2006).

Many authors (Hurni, 1983; Hurni, 1988; Bewkete and Sterk, 2003; Nyssen et al., 2004) associated this current severe soil loss with human induced changes, such as land use changes in order to meet high food demands, while others argued that the high soil loss rate after approximately 10Ma is in line with major volcanic episodes that occurred between 10.6 and 8.4 Ma and 4 Ma (Abebe et al., 2005), indicating a dramatic plateau rise that caused a nonequilibrium Ethiopian Plateau landscape (Gani et al., 2007). With continued population growth, it is true that there is demand for more crop production and further need to develop irrigation and hydropower; therefore, human activity is likely to accelerate the geological erosion rate today and in the future (Mitiku et al, 2006).

The most common degradation processes throught the highlands of Ethiopia including the Blue Nile Basin are sheet, rill, and gully erosion (Nyssen et al, 2004). Rill erosion is a result of surface runoff and associated sheet wash, which is a process that selectively removes fine material and organic matter that are very important determinants of land productivity (Bewket and Sterk, 2003). Zegeye et al. (2010) and Beweket and Sterk (2003) reported that the total soil loss by rill and inter-rill erosion in the watersheds of the Blue Nile Basin is in the range of 18 to 80 t/ha, well exceeding permissible values of 1–6 t/ha (Hurni,1983).

Furthermore, gully erosion has become more common since the land reform ("Land to the Tiller") of the Derg regime 30 years ago (Tebebu et al., 2010; Tarekegn, 2012). Gully erosion threatens soil resources leading to lower crop yields in inter-gully areas due to enhanced drainage and desiccation, aggravated flooding and reservoir siltation (Nyssen et al., 2006), which in turn promotes ecosystem instability (Daba, et al, 2003), the most serious threat to reservoirs and crop production (Tamene et al., 2006). Gully erosion can transport large quantities of sediment. For example in the Debre Mawi watershed, gully erosion removed soil with an equivalent depth of 4 cm per year over the watershed (Tebebu et al., 2010).

Past efforts to reduce erosion have been less successful mainly because many of the implemented soil and water conservation (SWC) structures originated from the "dust bowl" era of the 1930's in the United States. These practices which effectively controlled erosion in the US were designed for undulating landscapes with rainfall in the order of 600 mm/year. In contrast to the American mid-west, Ethiopian highland is characterized by steep slopes and rainfall patterns that can yield 300 mm of rain in a single month. In most cases, the hydrology of runoff generation has not been considered (Steenhuis et al, 2009). For example, upslope areas are targeted for practices while in reality most runoff and erosion is produced on the lower slopes near the rivers and saturated valley bottoms (Tebubu et al, 2010 and Zegeye et al, 2010). It is thus not surprising that Beweket and Sterk (2002) and Herweg and Ludi (1999) found that in many cases soil and water conservation (SWC) structures were not effective. Research has shown that in humid monsoon climates conventional soil and water conservation (SWC) structures promote saturation-induced erosion due to the over-retention of soil moisture (Herweg and Ludi, 1999; Mitiku et al., 2006).

As shown in the chapters of this dissertation, erosion modeling in Ethiopia where saturation excess conditions dominate is in its infancy. Based on experimentally observed data in the Debre Mawi watershed and discussed in Chapter 2 and 3, a realistic hillslope erosion model is developed for saturation excess condition and validated for a number of headwater watersheds and the Blue Nile River at the Sudan border. The hillslope erosion model described in Chapter 4 and Chapter 5 is based on the semi-distributed conceptual water balance model (Steenhuis et al., 2009) that is a semi-spatially distributed, topographically-derived water balance model in which the shallow degraded soil depth area and valley bottom are runoff producing areas and on the non-degraded hillslopes, rainfall infiltrates and eventually becomes interflow and baseflow. Both the hydrology and erosion model is then further tested in the Debre Mawi watershed (Chapter 6) where measurements of rainfall, runoff, infiltration, perched water table, sediment concentration, rill erosion and gully erosion during 2010 and 2011 rainy periods were conducted to understand where runoff and erosion takes place on the landscape scale. The dissertation therefore started with Chapter 2 and 3 to explain the spatially distributed runoff and sediment producing areas with additional discussion of runoff mechanism and sediment dynamics on the landscape of the Debre Mawi watershed and then modeling.

References

Abebe, T., Maetti, P., Bonini, M., Corti, G., Innocenti, F., Mazzarini, F., and Pecksay, Z.: Geological map of the northern Main Ethiopian Rift and its implications for the volcano-tectonic evolution of the rift: Geological Society of America Map and Chart Series MCH094, scale 1:200,000, 20 p, 2005.

Bewket, W. and Sterk, G.: Farmers' participation in soil and water conservation activities in the Chemoga watershed, Blue Nile Basin, Ethiopia. Land Degradation and Development 13, 189-200, 2002.

Bewket, W. & Sterk G.: Assessment of soil erosion in cultivated fields using a survey methodology for rills in Chemoga watershed, Ethiopia. Agriculture, Ecosystem and Environment 97,81-93, 2003.

Daba S., Rieger W; Strauss P.: Assessment of gully erosion in eastern Ethiopia using photogrammetric techniques, Catena, 50: 273-291, 2003.

Gani, N. D. Gani, M. R. and Abdelsalam, M. G.: Blue Nile incision on the Ethiopian Plateau: Pulsed plateau growth, Pliocene uplift, and hominin evolution, GSA Today, v. 17, p. 4-11, 2007.

Garzanti, E., Ando, S., Vezzoli, G., Ali Abdel Megid, A., and El Kammar, A.: Petrology of Nile River sands (Ethiopia and Sudan): sediment budgets and erosion patterns, Earth Planet. Sc. Lett., 252(3–4), 327–341, 2006.

Herweg, K. and Ludi, E.: The performance of selected soil and water conservation measures-case studies from Ethiopia and Eritrea. Catena, 36, 99-114, 1999.

Hurni, H.: Soil Erosion and Soil Formation in Agricultural Ecosystems: Ethiopia and Northern Thailand. Mountain Research and Development, 3(2): 131-142, 1983.

Hurni, H.: Degradation and Conservation of the Resources in the Ethiopian highlands. Mountain Research and Development 8(2/3): 123-130, 1988.

Mitiku , H., Herweg, K., Stillhardt, B.: Sustaiable land management –A new approach to soil and water conservation in Ethiopia. Mekelle, Ethiopia: Land Resource Management and Environmental Protection Department, Mekelle University; Bern, Switzerland: Center for

Development and Environment (CDE), University of Bern and Swiss National Center of Competence in Research (NCCR) North-South, 269pp, 2006.

Morgan, R. P. C.: Soil erosion and conservation, 3rd edition, Blackwell publishing, p316, 2005.

Muleta S. Yohannes F and Rashid S.M.: Soil erosion assessment of Lake Alemaya catchment, Ethiopia. Land Degrad. Develop. 17: 333–341, 2006

Nyssen J, Poesen J, Moeyersons J, Mitiku Haile, Deckers J, and Lang A.: Human impacts on the environment in the Ethiopian and Eritrean highlands-a states of the art. Earth Science Reviews 64: 270-320, 2004.

Nyssen, J., Poesen, J., Veyret-Picot, M., Moeyersons, J., Haile , M., Deckers J., Dewit, J., Naudts, J., Teka, K., Govers, G.: Assessment of gully erosion rates through interviews and measurements: a case study from northern Ethiopia. Earth Surface Processes and Landforms 31, 167-185, 2006.

Shahin, M. M. A.: An overview of reservoir sedimentation in some African river basins, in: Sediment Problems: Strategies for Monitoring, Prediction and Control (Proceedings of the Yokohama Symposium, July 1993), IAHS Publ. no. 217, 1993.

Shukri, N.M.: The mineralogy of some Nile sediments, Quarterly Journal of Geological Society of London, v. 105, p. 511-534, 1949.

Steenhuis, T.S., A.S. Collick, Z. M. Easton, E.S. Leggesse, H. K. Bayabil, E. D. White, S.B. Awulachew, E. Adgo5, A.A. Ahmed.: Predicting Discharge and Erosion for the Abay (Blue Nile) with a Simple Model. Hydrological Processes 23: 3728–3737, 2009.

Tamene L, Park S. J, Dikau R, P.L.G. Vlek.: Analysis of factors determining sediment yield variability in the highlands of northern Ethiopia. Gemprphology 76: 76-91, 2006.

Tarekegn, B. C.: A Case Study of Gully Erosion in the Ethiopian Highlands: The Warke Watershed, A Thesis Presented to the Faculty of the Graduate School of Cornell University In Partial Fulfillment of the Requirements for the Degree of Master of Professional Studies, Ithaca, NY, 2012.

Tesemma, Z. K., Mohamed, Y. A., and Steenhuis, T. S.: Trends in rainfall and runoff in the Blue Nile Basin: 1964–2003, Hydrol. Process., 24(25), 3747–3758, doi:10.1002/hyp.7893, 2010.

Zegeye, A.D., T.S. Steenhuis, R.W. Blake, S. Kidnau, A.S. Collick and F. Dadgari.: Assessment of Upland Erosion Processes and Farmer Perception of Land Conservation in Debre-Mewi Watershed, near Lake Tana, Ethiopia. Ecohydrologica 10: 297-306, 2010.

CHAPTER 2: STORM RUNOFF PROCESSES IN THE UPPER BLUE NILE BASIN OF ETHIOPIA: THE DEBRE MAWI WATERSHED

Abstract

Despite long term efforts to reduce erosion in the Blue Nile basin, river sediment concentrations have not declined. Lack of progress on sediment reduction indicates that runoff and erosion processes are not fully understood. For that reason, runoff processes were investigated in the 95 ha Debre Mawi watershed in the headwaters of the Blue Nile basin where the rain starts in the middle of June and last to the end of September. During the 2010 and 2011 monsoon, precipitation and runoff were measured in four sub-watersheds and at the main outlet. Perched water table heights and infiltration rates were recorded in 2010. The results show that during the period of observation the median infiltration rate was only exceeded 3% of the time by the rainfall intensity indicating that saturation excess runoff was the main runoff mechanism. This was confirmed by a better fit between 7-day cumulative runoff with 7-day cumulative effective rainfall amount than with rainfall intensity. In a monsoon climate where the watershed is dry when the rainfall starts, the saturated areas and the runoff coefficients increase with time. During June and July the bottom part of the watershed was not saturated, and the runoff coefficients from the upslope watersheds were greater than for the whole watershed, indicating that water infiltrated in the lower parts. In August and the beginning of September when the water table in the lower part of the watershed reached the ground surface, the runoff coefficients were greater for the whole watershed than the upslope sub-watershed. At the end of the rainy period at least 40 percent of the rainfall in the watershed became runoff. Ten percent of the

runoff originates from saturated areas and the remaining 30% is from shallow degraded areas on the hillside that saturate during the storm. .

2.1 Introduction

Understanding the storm runoff producing mechanisms and knowing the locations where runoff is produced on the landscape in a watershed are useful as they are fundamental in simulating the transport mechanisms of sediment, nutrients and pollutants. Previous efforts to predict the runoff and erosion processes on the Ethiopian highlands (Haregeweyn and Yohannes, 2003; Mohammed et al., 2004; Setegn et al., 2008; 2011; Zeleke, 2000) were based on infiltration excess runoff mechanisms without first investigating the possibility of other governing hydrologic processes (Steenhuis et al., 2009). Over the past decades, the soil and water conservation practices on these highlands were not effective (Beweket and Sterk, 2002) and Herweg and Ludi, 1999) as the permissible values of soil loss are still exceeded in the Blue Nile basin (Easton et al., 2010) and sediment concentration has not decreased.

Recent research using hydrological data from three of the Soil Conservation Research Program experimental watersheds (Anjeni, Andit Tid and Maybar) by Liu et al. (2008), Collick et al. (2009), Steenhuis et al. (2009), Bayabil et al. (2010), Engda et al. (2011), Tilahun et al. (2011) and Tilahun et al. (2012) showed that storm runoff is mainly generated by saturation excess runoff. Both Bayabil et al (2010) and Engda et al (2011) found that infiltration rates in Maybar and Andit Tid watersheds are rarely exceeded by rainfall intensities and most rain falling on the hillsides flowed down hill as lateral shallow subsurface flow over the hardpan.

Modeling of hydrology based on saturation excess runoff mechanisms on the Ethiopian highland (Tilahun et al., 2011, Tilahun et al., 2012, Steenhuis et al., 2009, Easton et al., 2010; White et al.,

2010) performs better at a shorter time scale than the infiltration excess based models. The semi-distributed water balance model (Steenhuis et al., 2009) that divide the watershed in to three areas (i.e., saturated, degraded and infiltration zone) representing the common landscape on the Ethiopian highland were able to capture the hydrologic processes on the area (Tessema et al. 2010, Tilahun et al., 2011, Tilahun et al., 2012). Since actual locations of the conceptualized runoff producing areas in the model are not available, this study is interested in validating both the spatial variation of runoff and dominant runoff mechanisms in an additional outside of the three SCRP watersheds of the model.

The research is carried out in the Debre Mawi watershed where previously Tebebu et al. (2010) and Zegeye et al. (2010) investigated gully and upland erosion processes. They showed that erosion from the wet down slope areas were greater than from the dryer upland fields.

2.2 Material and Methods

The present study investigates the differences in runoff processes from the upland and lowland areas through field measurements of runoff from four nested locations and at the outlet of the watershed, the perched water tables along six transects, rainfall amounts and intensities in the center and infiltration rates throughout the watershed. These data are then used to identify the dominant runoff mechanism that is either based on infiltration or saturation excess mechanisms.

2.2.1 Site Description

The Debre Mawi watershed research site, named after the Kebele Debre Mawi in Yilmana-Densa Woreda (district), covers a total area of 523 ha. It is situated 30 km south of Bahir Dar adjacent to the Bahir Dar-Adet road at 37°22’ East and 11°18’ North (Figure 2-1) in the western plateau of the Ethiopian highlands at the northern source region of the Blue Nile River. A sub-watershed of approximately 95 ha was selected for this study and is located in the upstream portion of the whole watershed. Its slope ranges from 1 to 30% and topography ranges from 2,212 m above sea level (m.a.s.l.) near the outlet to 2,306 m.a.s.l. in the southeast.

The watershed is underlain by shallow, highly weathered and fractured basalt overlain by dark brown compacted clay, then by light brown wet and sticky clay soil and then finally by black clay and organic rich soil sequences (Abiy, 2009). The fractures are highly interconnected with limited clay infillings. Intrusive lava dykes are seen across the stream nearly perpendicular to the flow direction of the watershed (Figure 2-1) interrupting the connection in fissures and giving rise to several springs. The dominant soil types in the watershed are Nitisols, Vertisols and Vertic Nitisols: Nitisols (locally, *Dewel*) are found in the upper part of the watershed. This is a very deep, volcanic derived well-drained permeable red clay loam soil and is very productive. The Vertisols (locally called *Walka*) are black and cover the lower slope positions. This soil forms deep wide cracks during dry phase of the monsoon and, it swells and develops stickiness during rainy period. Vertic Nitisols (locally known as *Silehana*) are located mid-slope between the Vertisols and Nitisols. It is reddish-brown well drained permeable soil with a high moisture retention and forms cracks when dry. It is well suitable for tef production.

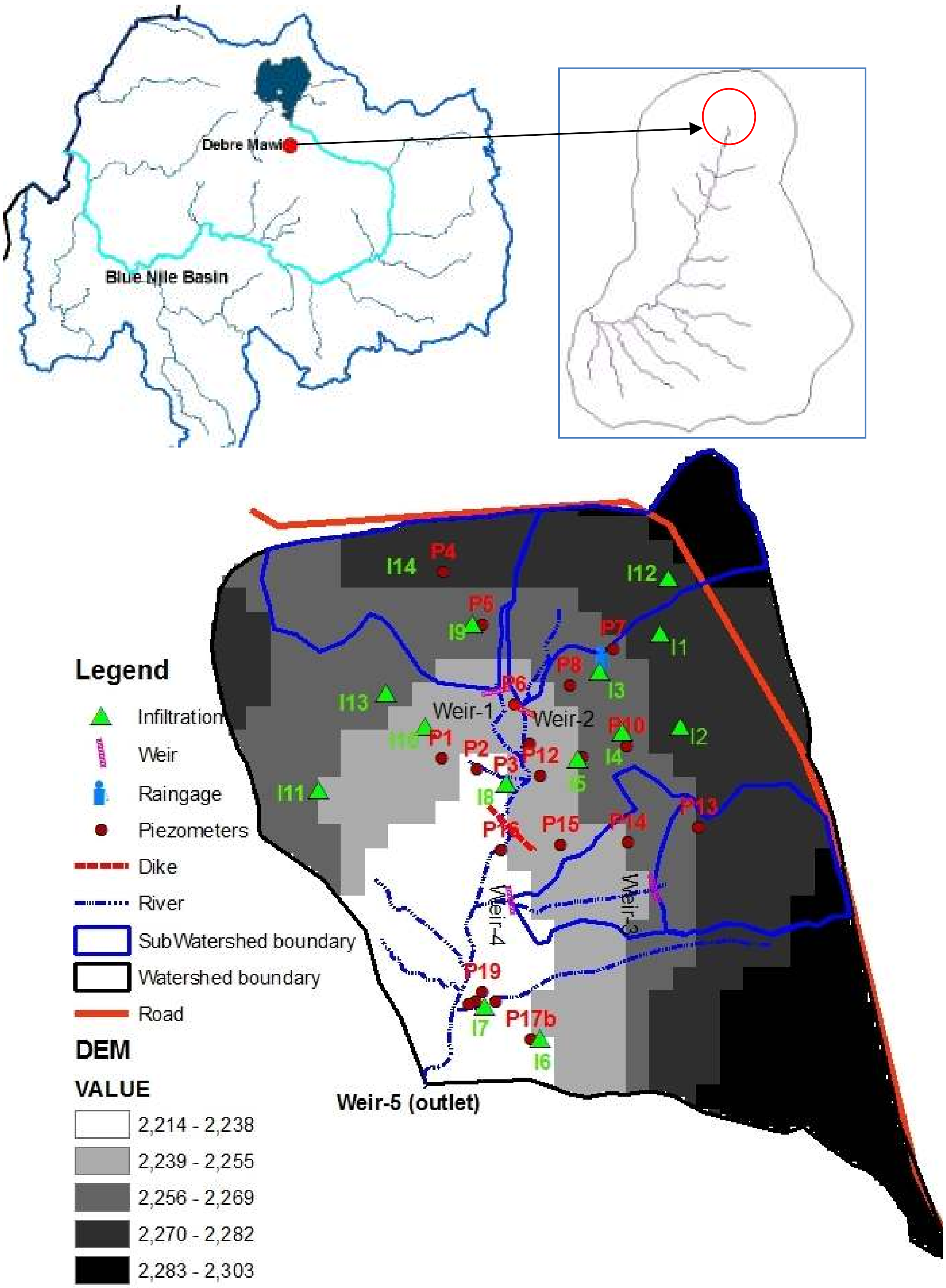

Figure 2-1: Location, boundary and drainage map of Debre Mawi storm runoff monitoring sites (weirs), perched water table sampling and infiltration test sites within the watershed (piezometer is abbreviated as P, and I stands for infiltration)

Most of the upper (slope of 0 to 6%) and middle area (slope of 6 to 27%) of the watershed (Figure 2-2a) is used for cultivation. The lower watershed with slopes of 0 to 6% (Figure 2-2b) is usually saturated during the rainy season and covered with grass. These lower grassy areas of the watershed serve as grazing land. Sparse shrubs are located at the middle section where many of the dikes are located, and where it is relatively steeper and difficult to plow. Fields at the upper and middle are continuously cropped. Cereal-plow cultivation is the dominant, and most of the cultivated fields are usually planted with tef, wheat, maize, and barley. Finger millet, lupine (particularly, *Lupinus albus*) and grass pea are also the common crops grown in the area.

Figure 2-2: (a) Upper and middle part of the watershed with unsaturated hillsides in the background and runoff plot on the steeper middle part of the watershed in the foreground (b) Lower portion of the sub-watershed at Weir-2 with wet area located in the foreground (pictures taken on 18 Aug 2011)

2.2.2 Data and Methodology

Fieldwork was carried out during the summer of 2010 and 2011 in Debre Mawi watershed. Rainfall was measured in the two summers; runoff discharge was also monitored at five gauging stations (one at the outlet and four at sub-watersheds) during the same period. Infiltration tests were conducted and perched ground water levels were monitored in 2010.

Rainfall measurement*:* The rainfall data were recorded in the watershed at five minute intervals with an automatic tipping bucket rain gauge (with resolution of 0.25 mm) and measured from July 4 to October 11 in 2010 and from June 14 to September 24 in 2011. From continuous readings of the automatic rain gauge, rainfall characteristics like intensity were determined. Because rainfall were not measured in June 2010, precipitation from Adet weather station (Figure 2-3), 10km south of Debre Mawi was used. The rainfall in June of 2010 was two times higher than the same month in 2011.

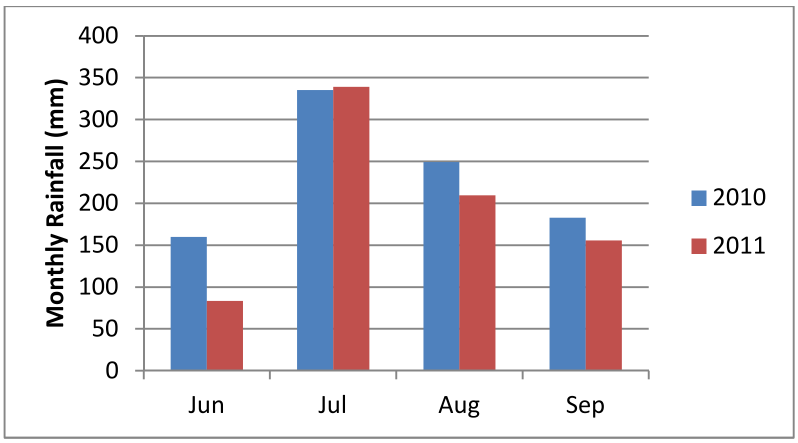

Figure 2-3: Monthly rainfall distribution from the nearby Adet weather station

Sub-watersheds*:* Different level rectangular weir notches (Figure A5-1 in Appendix A5) were constructed from cinderblocks and steel bars at four locations as shown in Figure 2-4 and a masonry weir at the outlet was constructed by Adet Research Center in 2007. Two weirs were constructed upstream of the watershed outlet to monitor upland runoff and the other two were placed at the inlet and outlet of a tributary of a stream that began as gully. These weirs created four sub-watersheds. Sub-watersheds from each weir were defined using GPS tracking in the field. The size of the sub-watersheds areas are 8.8, 10, 6.4 and 10.3 ha at weir 1, 2, 3 and 4, respectively. The area of the sub-watersheds were used to calculate runoff depth at the outlet of each of the watersheds.

The slopes of the sub-watersheds range from 0.6 to 16% with elevation ranging from 2,233 to 2,286 m.a.s.l. All sub-watersheds at the upslope are flat or gently sloping and dominated by agriculture. The main crops were tef, maize, wheat and lupine. The wet bottom area of the sub-watershed at Weir-1 was covered by deep Vertic Nitisol and grass during the two rainy seasons (2010 and 2011). It was saturated during the last part of the rainy phase of the monsoon. This part was not cultivated and used only as grassland because it was too wet for crops. The sub-watershed at Weir-2 was draining storm runoff from part of the main road from Bahir Dar to Adet and developed a relatively small gully upstream and a more substantial gully downstream. The sub-watershed at Weir-4 drained mainly upland runoff from the sub-watershed at Weir-3 and it contained a saturated area upstream of its outlet. The upland areas pertaining to Weir-1, Weir-2 and Weir-3 has lava intrusions at the mid-slope steepest part of the sub-watersheds.

***Storm runoff measurement**:* The discharge for Weirs 1-4 was measured from June 29, 2010 to September 16 2010 and from June 25, 2011 to September 14, 2011 while the outlet was monitored from June 22 to October 1, in 2010 and from June 12 to September 18 in 2011. Runoff in the streams only lasted at most a few days after rainfall events. Approximately, half of these events occurred during night and measurements were even conducted during this time.

Manual measurements of flow depth and velocity started when the water in the stream became turbid. Both water depth and surface water velocity (V, m s^{-1}) at the five weirs were recorded at 10-minute interval until the water became less turbid. The surface velocity was determined with a float that was released 5 to 10 m upstream from the weir's outlet. The time required for the float to reach the weir was recorded. The surface velocities were multiplied by two-third to compute the mean discharge. For each weir a best fit rating curve was developed from all 10-minute flow depths and mean discharge measurements (Figure A6-1 to 5 in Appendix A6). A power equation was employed to develop the relationship between flow depth and storm discharge. When the least square regression for power equation was poor for depth of flow greater than 20 cm, 22 cm and 30 cm at weir-1, weir 2 -4 and weir-5, respectively, 2nd order polynomial function was employed.

Measuring groundwater tables*:* The depths of the perched water from the bottom end of 19 piezometers along 6 transects were measured twice a day from July 17 to November 5, 2010 (Appendix A2). The piezometers were installed in six transects from the top of the hill slope down to the saturated area near the river in six different transects (Figure 2-4). Holes were drilled with an auger to the restricting layer that ranged in depth from 0.58 to 3.9m. The piezometers constructed from 5 cm diameter PVC pipes were inserted all the way to the base of the excavated hole. The bottom 30 cm of the piezometers were perforated and covered with cloth, allowing water to pass but preventing the inflow of sediment. The bottom end (opening) of the pipe was closed with a plastic cap. The above ground opening of the piezometers was capped to protect against the entrance of rainfall. Water table depth from the ground surface was calculated by subtracting the perched water depth from the total depth of the piezometers. Saturated areas were mapped from the water table depth and observations in the watershed. Transect 1 consists of P1, P2, P3; Transect 2 of P4, P5, P6; Transect 3 of P7, P8, P9; Transect 4 of P10, P11, P12 and Transect 5 of P13 to P16 as shown in Figure 2-4. The sixth transect was installed across a gully.

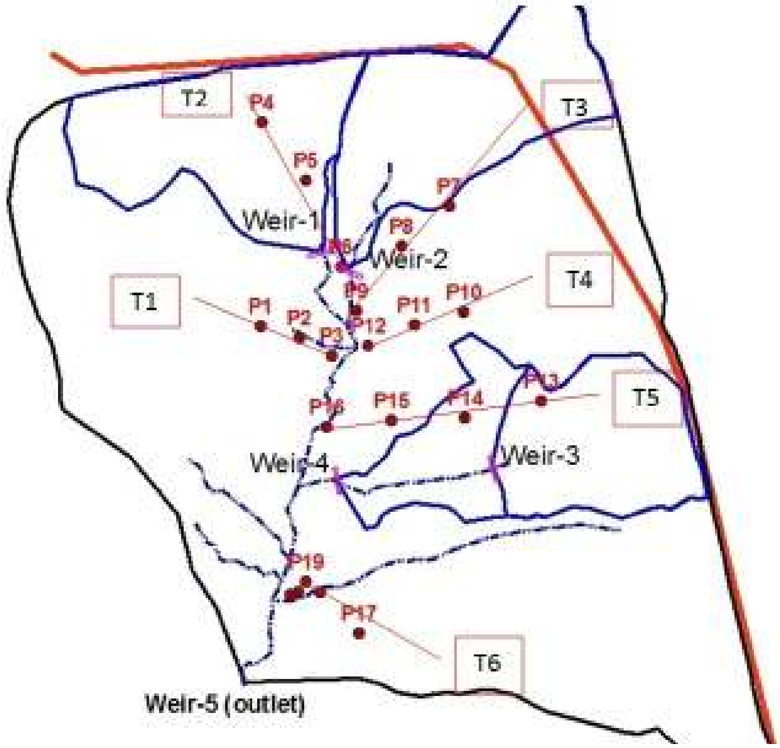

Figure 2-4: Location of piezometer transects. T stands for transects and P stands for piezometers.

Infiltration measurements: Soil infiltration rates were measured at fourteen different locations throughout the watershed using a 25-cm diameter single-ring infiltrometer in August 2010. These locations were on the upslope, midslope and downslope areas of the watershed with different land use (Figure 2-1 and Table A3-3 in Appendix A). Initial infiltration tests on down slope saturated areas showed that the water did not infiltrate and these areas were omitted in any further measurements. After driving the ring to a depth of about 10cm, an average of 28cm of water was added into the ring, and the infiltrated water depth was measured at varying time intervals. A ruler was used to read water depth fluctuations in the infiltrometer throughout the duration of the test. The constant infiltration rate at the end of the test was taken as the infiltration capacity of the test area.

Runoff predictions: The validity of the SCS was tested for predicting the runoff of the watersheds. The SCS runoff equation is

$$Q = \frac{P_r^2}{(P_r + S_e)} \qquad 1$$

Where Q is the runoff; P_r is the effective rainfall after the runoff starts. $P_r = P\text{-}I_a$ where I_a is the initial abstraction and P is the total. S_e, is the effective average available watershed storage after the first runoff until the watershed is completely saturated, Steenhuis et al. (1995) and Schneiderman et al. (2007) showed that the SCS equation represents in principle a saturation excess runoff processes where the fractional area of saturation, A_f, can be found by taking the derivative of the runoff, Q, with respect to the precipitation P, e.g.

$$A_f = 1 - \frac{S_e}{P_e + S_e} \qquad 2$$

To find the effective storage of the watershed, daily effective rainfall and storm runoff data were summed over weekly periods for the 2010 and 2011 summer. Daily effective rainfall is defined as rainfall minus potential evaporation ($P - E$) (Liu et al., 2008). The potential evaporation was obtained from nearby Adet weather station, 10 km south of Debre Mawi. The initial abstraction in a monsoon climate is approximately equal to the water that is lost during the dry phase (Liu et al 2008). Thus the first rains have a distinctly smaller amount of runoff for a given amount of rainfall than rains later in the rainy phase (Liu et al, 2008). For this reason we did not include the June and early July storms in calibrating the S_e values. The value of S_e that provided a best Nash-Sutcliffe efficiency (Nash and Sutcliffe, 1970) and coefficient of determination (R^2) with slope close to one and intercept close to zero was assumed to be the best fit. In the result section, we reported, however, Se values with plus and minus range that provided NSE and R^2 with small change from its optimum values.

In addition, since general knowledge is that infiltration excess is the common runoff mechanisms in the Ethiopian highlands, a linear function that relates storm runoff with two rainfall intensities was tested to see if this would give a better it than the Soil Conservation Service (SCS) runoff equation. In this comparison, the maximum 5-minute rainfall intensity and average rainfall intensity were regressed with the storm runoff at the outlet and sub-watershed outlets. To check the statistical significance of the relationship, the F-test was used at 1% significance level (α).

2.3 Results

2.3.1 Rainfall intensity and infiltration capacity

Two thousand five hundred twenty three recordings of 5-minute interval rainfall intensities with a maximum intensity of 143 mm hr^{-1} were recorded during the period of the study. Large rainfall intensities do not occur frequently (Figure 2-5). Intensities greater than 15 mm hr^{-1} occurred only 9% of the time in 2010 and 12% in 2011. The largest intensities occurred in July. For example in 2011, from 55 events that are greater than 30 mm hr^{-1}, 49% of the events occur in July while 31% is in August and 20% in September. This distribution in 2010 is different with only 39 events greater than 30 mm hr^{-1}. Of this, 46% occurred in July, 21% in August and 33% in September. Table 2-1 shows rainfall intensity distribution for events greater than 15mm hr^{-1} following similar pattern as the rate of 30 mm hr^{-1}.

Table 2-1: Rainfall intensity distribution within three months in 2010 and 2011 rainy period

Month	Number of 5min storm events	Number of storm events >15mm hr^{-1}	percent of time >15mm hr^{-1}
July 2010	528	44	8
Aug 2010	411	37	9
Sep 2010	349	35	10
July 2011	479	57	12
Aug 2011	501	56	11
Sep 2011	255	40	16
Total	2523	269	

In order to compare rainfall intensity with the infiltration capacity, the spatially averaged infiltration capacity of the watershed is compared with the exceedance probability of the rainfall intensity as shown in (Figure 2-5). The steady state infiltration rates ranged from 6 to 360 mm hr^{-1} (Table C1-3 in Appendix C1). In general, infiltration rates were smallest in the downslope areas with the Vertisols and Vertic Nitisols soils and greatest in the upslope position of the landscape with the Nitisols soils (Table A1-3 in Appendix A1). The average infiltration rate from all 14 measurements was 70 mm $hr^{-1}$and the median 33 mm hr^{-1}. As the median is the most meaningful rate to compare with rainfall intensity (Bayabil et al., 2010; Engda et al., 2011), the exceedance plot of rainfall intensities (Figure 2-5) shows that the median infiltration is only exceeded 1.5% in 2010 and 4.4% in 2011. Since the minimum rate was exceeded 30 percent of the time, surface runoff due to infiltration excess occurs in the watershed but as we will see later it infiltrates more down slope in the more permeable soil when not saturated.

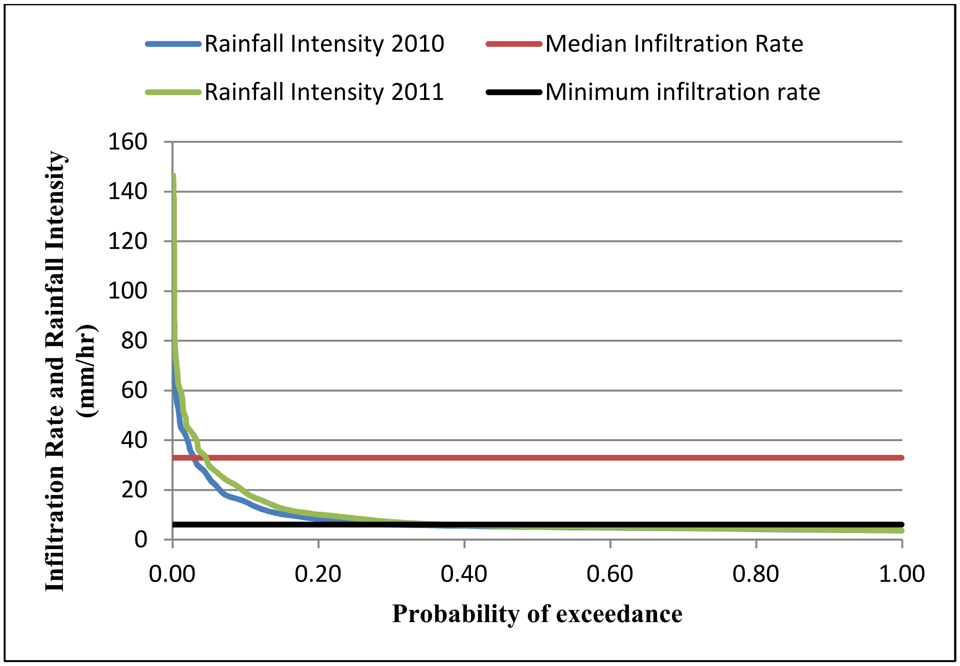

Figure 2-5: The exceedance probability of the average intensities of 2523 storm events and median infiltration rate for the Debra Mawi watershed in 2010 and 2011.

2.3.2 Storm Runoff from 5 weirs

A total of 38, 41, 39, 41, and 46 average storm runoff depth for which both rainfall and runoff amounts were available at Weir-1, Weir-2, Weir-3, Weir-4, and Weir-5, respectively. For similar amounts of storm rainfall, average storm runoff at each weir is less at the beginning of the rainy period (June and early July) compared to the later period of rainy period (August and September; Figure A1-1 and A1-2 in Appendix A1). For example, a 2 hour rainfall event of 14 mm on July 5, 2010 and 17 mm on September 15, 2010 produced average storm runoff depth of 0.8 mm in early July and 7.6 mm in September (Figure 2-6).

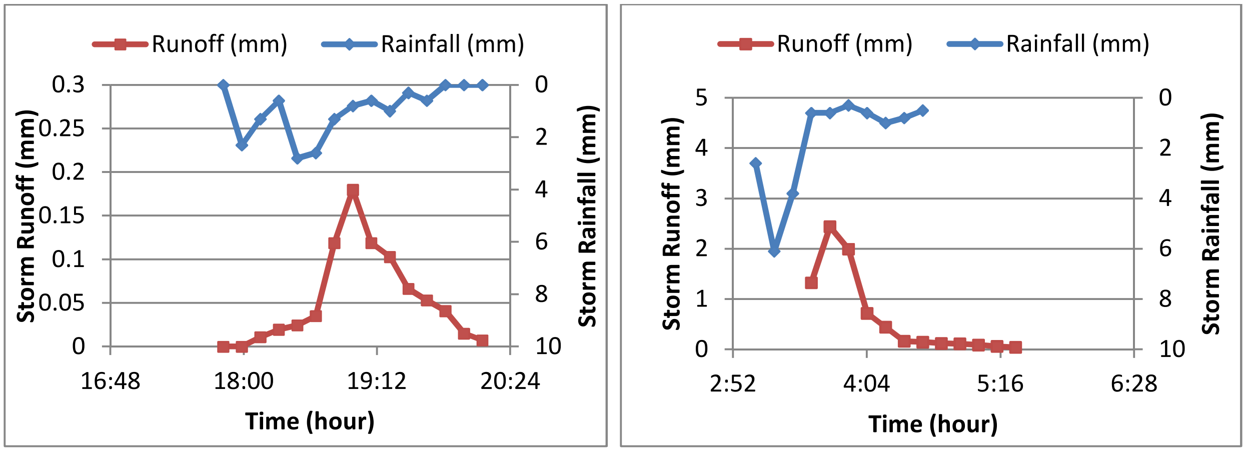

Figure 2-6: Storm runoff response on July 5, 2010 at the left and on September 15, 2010 at the right at the outlet (weir-5) of Debre Mawi watershed. Rainfall and runoff is at 10-minute interval.

In order to easily compare runoff among the sub-watersheds and watershed outlets, a runoff coefficient (defined as the quotient of runoff and rainfall volume) was calculated for each storm and averaged for each month that data was available (Figure 2-7). The results show that it is consistent with the findings of Liu et al (2008). June 2011 has the lowest runoff coefficient indicating that most rain water infiltrated. No data were available for June 2010. The runoff coefficient for the remaining months of 2010 at all weirs were close to 0.45 likely because of the high monthly rainfall in June 2010 (Figure 2-3) filling up the water deficit after the dry phase after which the watershed gets into some kind of equilibrium in which the runoff coefficient becomes constant. In 2011 when June was not as wet, the runoff coefficient for Weir-5 at the outlet increased consistently over the two periods of observation indicating that the area of saturation increased during this time in the bottom part of the watershed since the runoff coefficients for the sub-watersheds (Weirs 1 to 4) did not vary consistently for July, August and September. The increase in saturation is corroborated by the perched groundwater level measurements in the next section.

2.3.3 Perched groundwater water table

Perched water table depths (Appendix A2) were monitored during the rainy phase in 2010 using piezometers to map saturated areas and timing of saturation during the rainy period. Transect 3 (P7, P8 & P9) and 5 (P13, P14, P15 & P16) shown in Figure 2-4 are shown here because they represent the perched water table in the watershed. The water ponded above a low permeable basaltic layer is depicted as depth from the ground surface (Figure 2-8). P7 and P13 are located on the steep mid-slope part of the watershed where no perched water observed due to perhaps during a storm, the water drained quickly as subsurface flow. The water tables near P8 and P9 on the lower slopes of the watershed with grassland reached the surface in the first week of August and became saturated. Likewise within same period, the water table for P14 and P15, which are located on the gentle mid-slopes in the cultivated land, was near to the surface (Figure 2-8). Piezometer P16 at the lower slopes in the area that saturates during the first week of August was situated in close proximity to a deep gully drawing down the water table and hence the water table was deep close to the gully bottom.

After the water tables are rising during the heavy rainfall at the end of July and the beginning of August, Piezometer P14 declines faster than P15. P14 is uphill from P15 and indicates that the water table drains as expected faster at uphill than downhill. A map of the saturated areas in August based on the piezometer reading and physical observation during the rainy period is shown in Figure 2-9. This area is approximately 9 ha (10% of the total watershed area) and exists for approximately a month after the first week of August. The area of saturation decreases as the saturated area recedes in September and October.

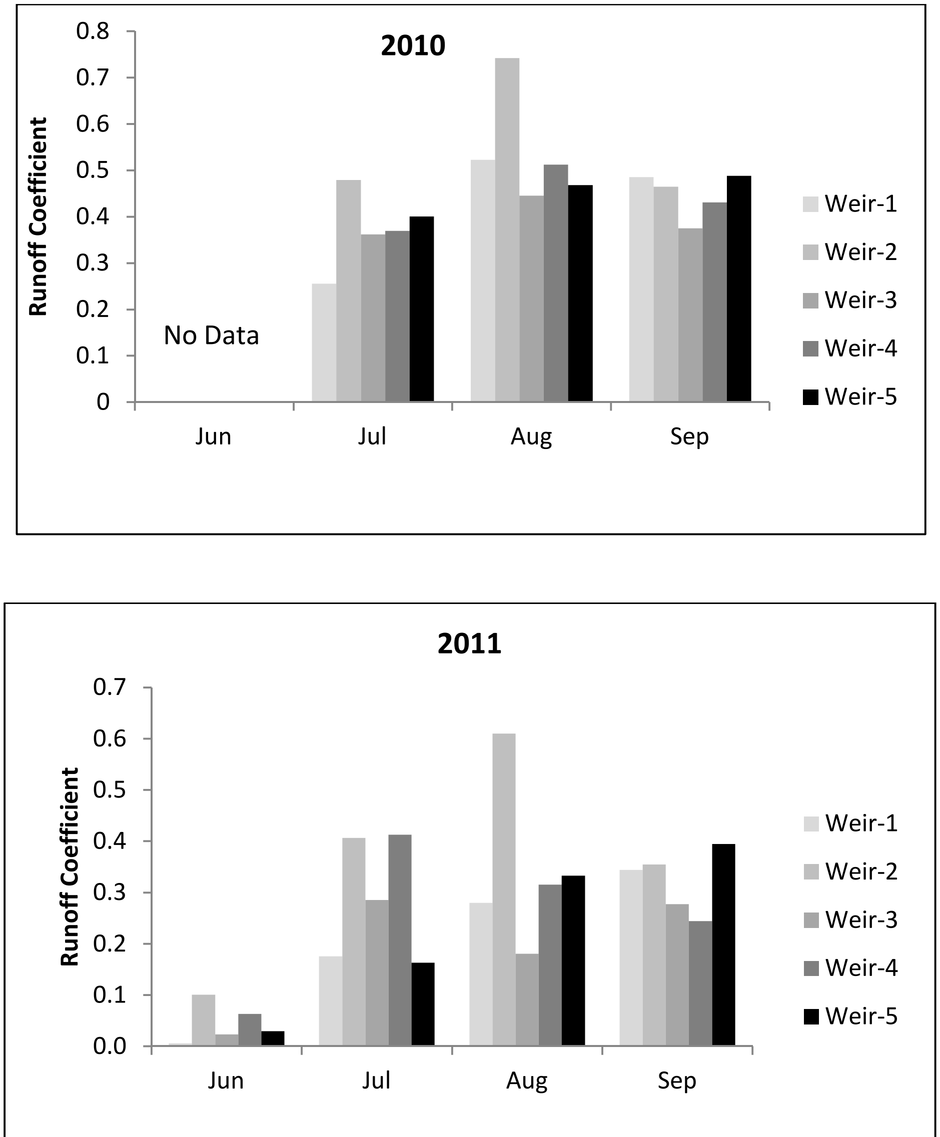

Figure 2-7: Runoff coefficient for four months at each weir for summer 2010 and 2011. (Runoff was not measured in June 2010)

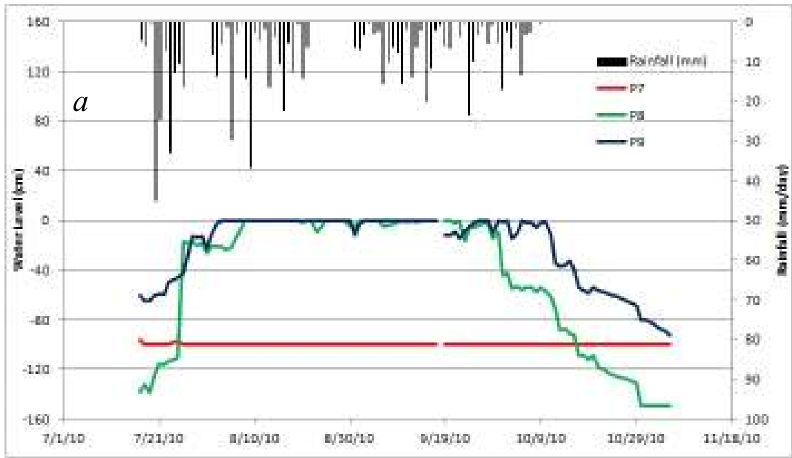

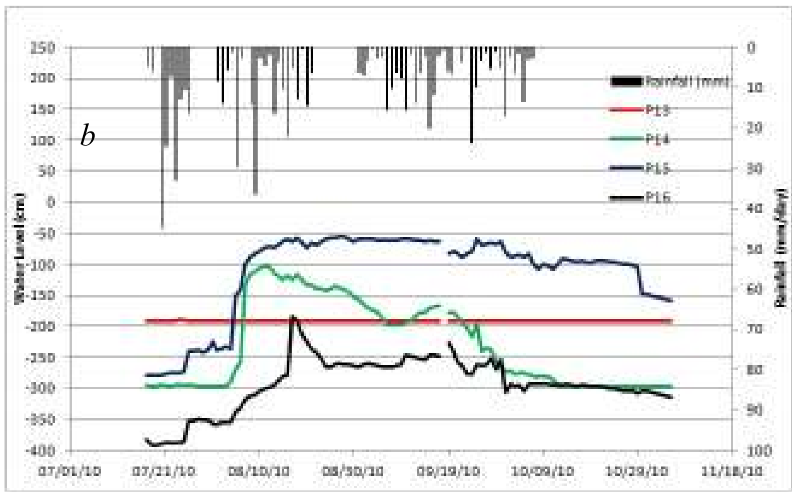

Figure 2-8: (a) transect 3 and (b) transect 5 (in Figure 4-1 and Figure 4-7) in the Debre Mawi watershed where the water level was measured twice a day during the 2010 main rainy season using the ground surface as a reference and rainfall was daily measurement.

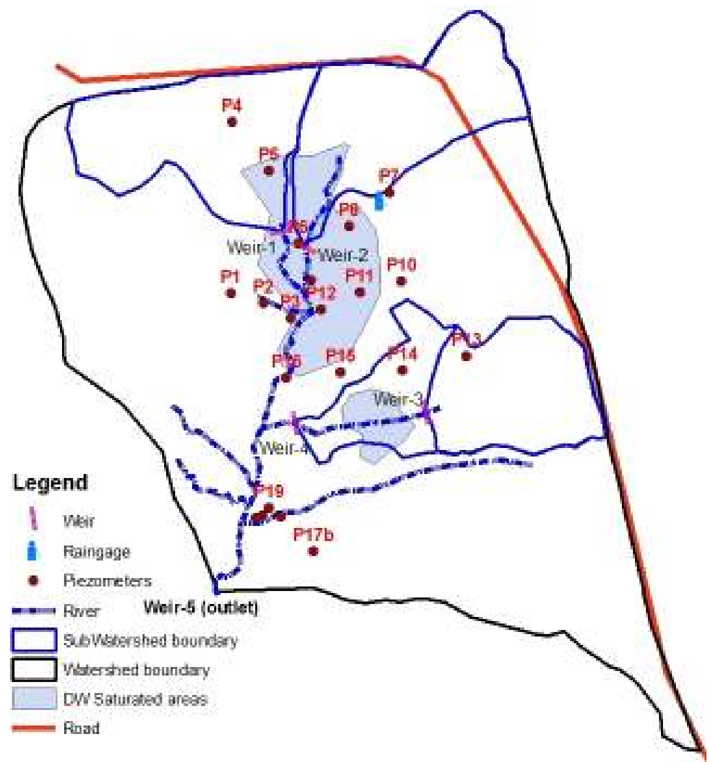

Figure 2-9: Saturated areas mapped from water table reading of piezometers and physical observations

2.3.4 Runoff predictions

In the next section we will test how well the SCS equation (Equation 1) can predict the runoff response, where runoff is produced from land that becomes saturated during the rainfall event. In addition we will test whether runoff is related to rainfall intensity and have the ability to improve runoff predictions.

SCS runoff equation: The storm runoff (without including June and early July runoff) correlated well with the cumulative effective rainfall (Figure 2-11). This correlation is statistically significant at 1% significance level with P-value less than 0.01 at all weirs (number of data, n = 17). The correlation became poor when the June and early July data (Figure A3-2 in Appendix

A3) were included implying that early rains in the rainy monsoon phase infiltrate and fill up the soil storage (Liu et al., 2008).

By fitting the shortened dataset (i.e., removing the June and early July data) of rainfall and average storm runoff depth to the SCS runoff equation (equation 1), we found that the S_e varies from 6 to 22 cm (Figure 2-12) with Nash-Sutcliffe efficiency (NSE) of 0.45 to 0.77 and coefficient of determination (R^2) ranges from 0.52 to 0.8 as shown in Figure 2-13 and this correlation is statistically significant (α = 1%) at all weirs using F-test (P-value <0.01, n = 17). The corresponding saturated area fractions from equation 2 were shown in Figure 2-10.

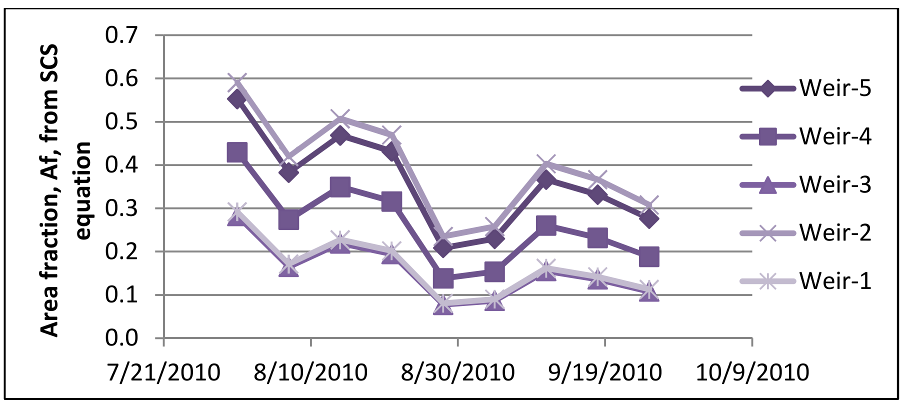

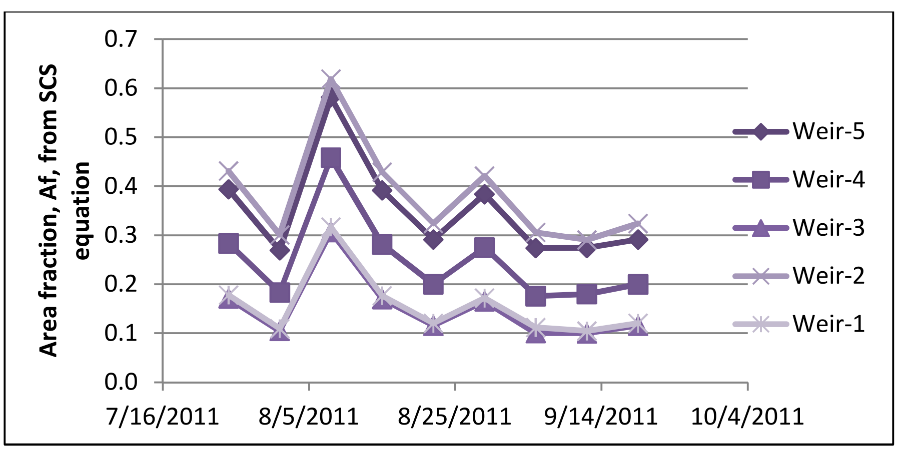

Figure 2-10: Area fraction (A_f) from equation 2 for weekly cumulative effective rainfall

The large range of S_e and A_f values represents the variability in available storage in the watershed. Since the bottom part of watershed becomes saturated, we expect that the available storage (S_e = 7±3 cm) for rainfall to be retained is smaller for the whole watershed (represented by Weir-5) than the average of the sub-watersheds. As Figure 2-10 shows, once the watershed reached equilibrium, the saturated area fraction during rainfall varies according to the prevailed amount of rainfall. The watershed of Weir-2, draining storm runoff from an intersecting road, has a smaller S_e (6±3 cm) than weir-5 and has saturated areas at the bottom with gullies (Figure 2-9b), resulting in larger runoff potential and runoff area fraction. The watershed of weir 1 consists of relatively deep soils at the bottom without lava intrusions and consequently can store a large amount of water before the whole watershed would be saturated and therefore, a high S_e value (21±4 cm) and lower area fraction for all prevailing excess rainfalls were obtained (Figure 2-10). The watershed of weir-3 (S_e = 22±4 cm) has intermediate amounts of lava intrusions while weir 4 has the same lava intrusions as in the watershed of weir-3 and saturated area (Figure 2-9), therefore a relatively small S_e (11.5±3.5 cm) value and large runoff area fractions. The area fractions at the end of the rainy period (Figure 2-10) are lower than the runoff coefficient measurement (Figure 2-7) which is likely due to the contribution of runoff from infiltration excess from high rainfall intensities at the upslope sub-watersheds such as September 16, 2010 in Table A1-1 in Appendix A1.

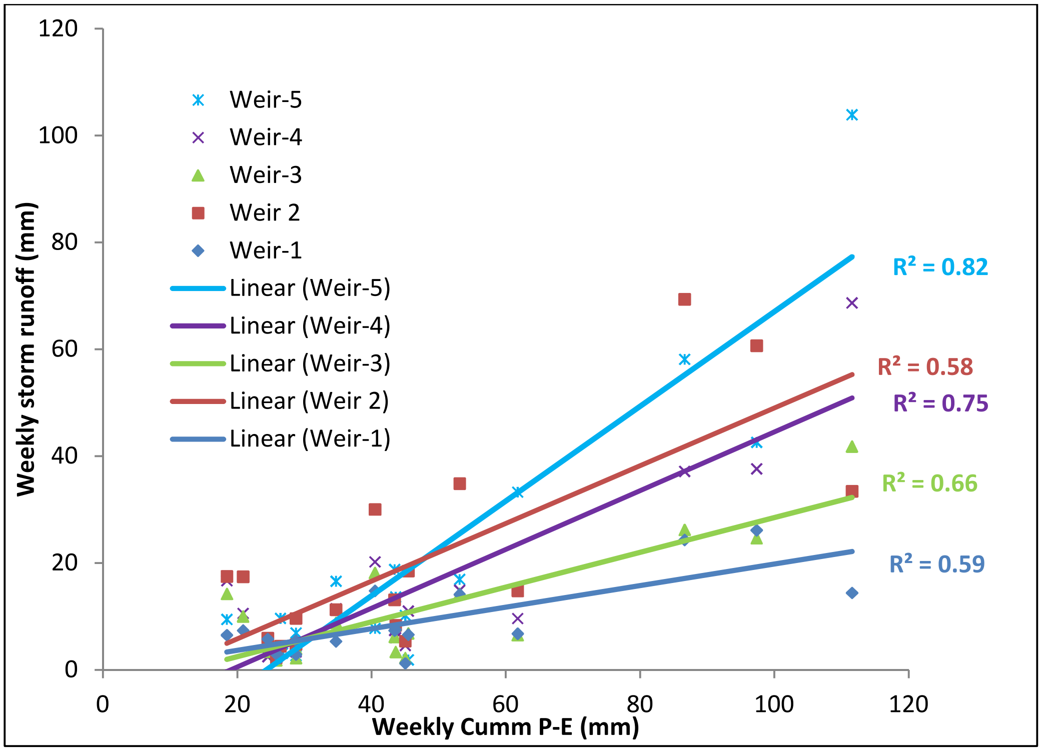

Figure 2-11: Weekly summed effective daily rainfall and storm runoff relationships for Debre Mawi watershed excluding June and early July data. Data are shown in Table C1-2 in Appendix C1.

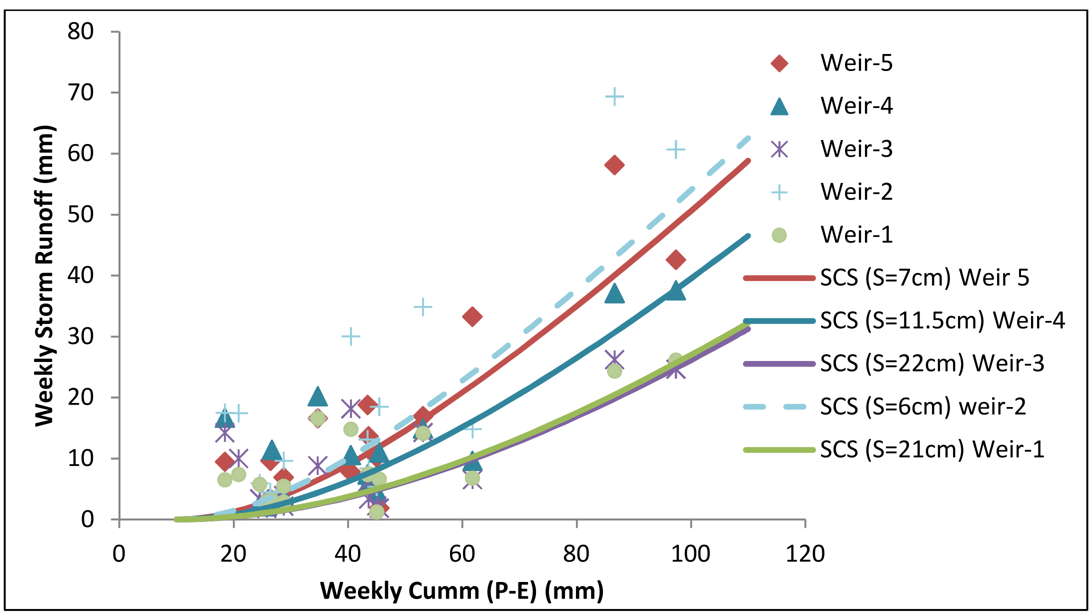

Figure 2-12: Fitting an SCS runoff equation for the different weir in Debre Mawi watershed for a data shown in Table C1-1 in Appendix C1 curtailing June and early July data.

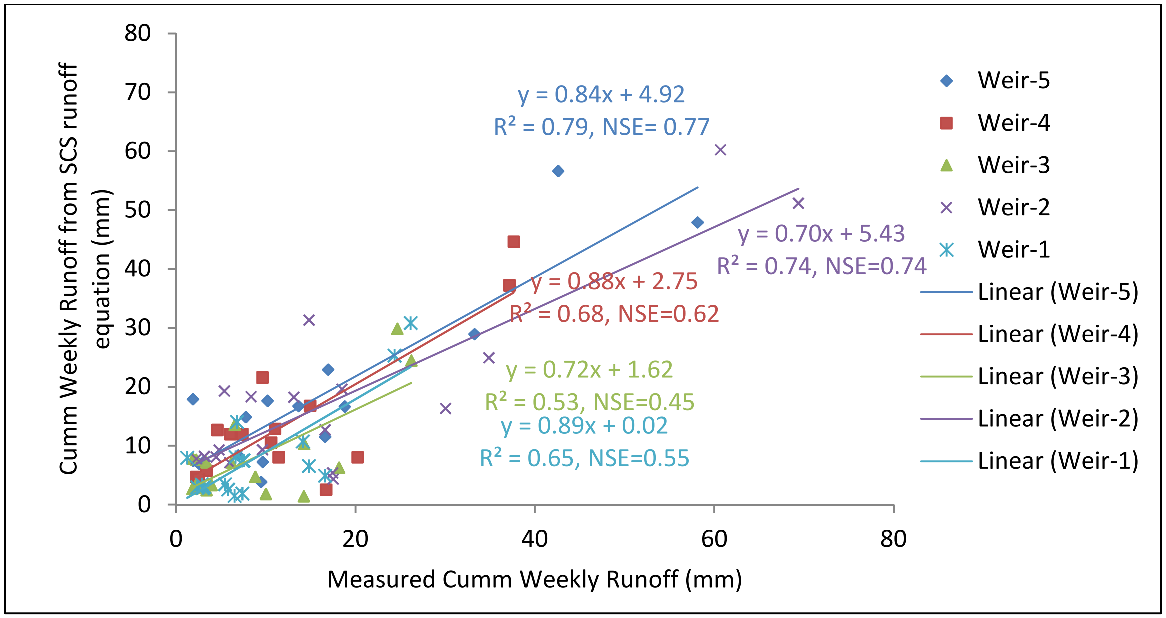

Figure 2-13: Scatter plot for measured and simulated with SCS runoff equation (equation 1) data of cumulative weekly runoff (June and early July data are excluded).

In order to test if infiltration excess could describe the watershed behavior, daily runoff depth was regressed with the 5-minute maximum intensity and average rainfall intensity (data are shown in Figure 2-14, Table A1-1 in Appendix A1 and Figure A3-1 in Appendix A3). The coefficient of determination R2 is 0.32 and less than for the SCS equation that used total amount of storm rainfall as independent variable. The F-test (Table 2-2), however, showed that there is significant correlation between maximum rainfall intensity and storm runoff at 1% significance level for all watersheds except for sub-watershed at Weir-1. The relation between storm runoff and average rainfall intensity was only significant for sub-watersheds at Weir 3 and 4. The significant correlation with maximum rainfall intensity disappeared when the few extreme events are removed as shown in Table 2-1. Since the infiltration rate is exceeded only a few times by rainfall intensity (Figure 2-5), rainfall intensity is not a good predictor for watershed outflow as the correlation is poor (Table 2-2), especially when the few extreme events are removed.

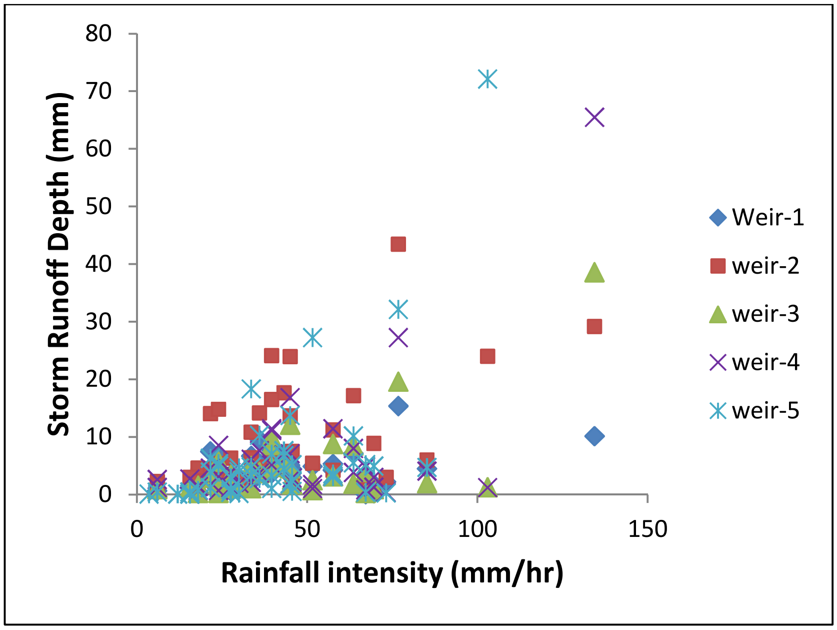

Figure 2-14: Scatter plot of 5-minute maximum rainfall intensity with storm runoff depth at the watershed and subwatershed outlets

Table 2-2: Statistical analysis of average storm runoff with maximum and average rainfall intensity in Debre Mawi watershed

Variables		Average storm runoff (mm) at weir				
		1	2	3	4	5
Maximum rainfall intensity (mm/hr)	R^2	0.14	**0.23**	**0.32**	**0.31**	**0.31**
	n	36	40	38	40	46
	P-value (F-test)	0.022	**0.001**	**0.0002**	**0.0002**	**<0.0001**
Maximum rainfall intensity (mm/hr)*	R^2	0.07	0.08	0.1	0.08	0.14
	n	35	37	35	37	44
	P-value (F-test)	0.14	0.09	0.06	0.09	0.011
Average rainfall intensity (mm/hr)	R^2	0.12	0.13	**0.22**	**0.18**	0.12
	n	36	40	38	40	46
	P-value (F-test)	0.037	0.024	**0.003**	**0.007**	0.017

* excluding maximum rainfall intensity events of July 13, 2010, July 20, 2010 and July 17, 2011; bold numbers indicate the existence of statistical significance.

2.4 Discussion

In temperate humid climates, subsurface storm runoff and saturation excess runoff principles are often found in soils with sufficient organic matter to describe the runoff processes better than the Hortonian infiltration excess overland flow mechanisms (Hewlett and Hibbert, 1963 and Dunne and Black, 1970). Only recently, modeling runoff in the Ethiopian highlands with Hortonian flow processes has been questioned (Liu et al, 2008) and questions raised whether saturated excess runoff mechanisms could provide a better alternative for the infiltration excess runoff.

As we will discuss below based on our observations, we demonstrate that subsurface flow and saturation excess are the dominant processes in the landscape occurring for most of the time but that in portions of the landscape, infiltration excess rainfall might be occurring. .

The importance of saturation excess in producing runoff can be demonstrated by comparing infiltration rates with rainfall intensity (Figure 2-5), where the median steady state infiltration rate (33 mm/hr) was exceeded only 3% of the time. The lowest infiltration rate of 6 mm/hr was exceeded 30% of the time. Runoff from the low infiltration areas can infiltrate more downslope with greater infiltration rates. When the rainfall intensity is equal to the median steady state infiltration rate, half of the watershed area produce runoff and the other half where the infiltration is greater than the median of 33 mm/hr, water will infiltrate. The Andit watershed behaved similarly (Engda et al., 2011) with a median infiltration rate (48 mm/hr) that was only exceeded 3% of the time. This is different from the Maybar watershed where median infiltration rate was greater than any measured rainfall intensity and the minimum infiltration rate of 20mm/hr was only 9% of the time less than the rainfall intensity (Bayabil et al., 2010).

Calculated runoff coefficients corroborate the above findings (Figure 2-6). In all watersheds the runoff coefficients were low early in the rainy monsoon phase and then increased. For the sub-watersheds in Debre Mawi, the runoff coefficients were low in June and then were elevated in the remaining months. In 2010 no data were collected in June. The increase in runoff coefficient for the whole watershed occurred during the whole rainy phase when the watershed became more and more saturated (black bars in Figure 2-6). The increase was faster in 2010 than in 2011, since there was more rain in June in 2010 (Figure 2-3). Thus in all watersheds the water infiltrated first before the runoff became significant. The soils were deeper in the bottom part of the watershed so it took longer for the discharge to increase at Weir-5 at the outlet of the whole watershed. July 2011 (Figure 2-6) shows this most clearly where the runoff coefficient for the whole watershed is less than any of the sub-watersheds meaning that the runoff from the sub-watersheds infiltrated in the lower parts. It is expected that the runoff coefficient remain constant once the watershed is wetted up. This is not the case in 2011 and we expect that the variation is caused by the most intense storms as the number of intense storm events in 2011 is greater than 2010 (Table 2-1). Runoff coefficient and storm runoff from the sub-watershed at weir-2 is much greater during some months because of the contributions of the road drainage.

A direct comparison of perched water tables in piezometers and runoff coefficients is not feasible, because the piezometers represents local conditions and are affected directly by nearby abnormalities in elevation such as the case for P16 (Figures 2-7 and 2-8) that is in a generally saturated area but because of the nearby gully, it has a deep water table. The general trend, however, confirms that the upslope areas are generally unsaturated as shown by Piezometers P7 and P13, (Figures 2-7 and 2-8; Appendix A2) where the horizontal line in the figure for these piezometers is generally at the same depth of the slowly permeable layer and therefore there no saturation in the profile with the exception during the period with heavy rain around July 20, 2010. Although it is difficult to compare individual piezometers with the runoff coefficients, the general trend is correct with low runoff coefficients in the beginning of the rainy phase when perched water tables are deep and high runoff coefficients when the water table at shallow depths (Figure 2-7 and 2-8)

Finally, the fact the SCS equation (based on total effective rainfall and effective storage) for storms after the beginning of July fits the runoff data better than a model with precipitation intensity indicates that saturation excess is more dominant that infiltration excess. Only for the three largest storms with high intensities on July 13, 2010, July 20, 2010 and July 17, 2011 (see Table A1-2 in Appendix A1) infiltration excess could have taken place, because if these storms are included there is a significant correlation of maximum rainfall intensity with storm runoff depth in Table 2-2, but if these storms are not included the relationship becomes weak and statistically insignificant for maximum intensity at all areas. Moreover, under saturation excess conditions short high intensity rainfall burst are associated with high discharges from the runoff source areas that are more likely to reach the outlet than the same amount of rain over a longer period.

2.5 Conclusions

In this chapter, we attempted to identify the dominant storm runoff mechanisms in the 95-ha Debre Mawi watershed by measuring infiltration rates, rainfall intensities, rainfall amounts, perched water tables and discharge for the main watershed and four nested sub-watersheds, In general, rainfall intensities were greater than infiltration capacity of the soil except in some local degraded areas where the subsoil was close to the surface. In addition, since total storm rainfall and total discharge were correlated after the watershed was wetted up, we concluded that saturation excess runoff was the dominant. Contributing runoff source areas ranged from 60% of the total watershed during the high rainfall periods to less than 10% when rainfall amounts decreased. Since the SCS runoff equation is based on saturation excess runoff mechanisms, (e.g., discharge is a function of total rainfall), we found good Nash Sutcliffe efficiencies between predicted and observed weekly discharges using this method. Finally our findings suggest that runoff contributing areas are positioned in landscape specific locations and are likely not altered by changing crop type. This is important knowledge in planning watershed improvements.

References

Abyi, A. Z.: Geological controls in the formations and expansions of gullies over hillslope hydrological processes in the Highlands of Ethiopia, northern Blue Nile region, A Thesis Presented to the Faculty of the Graduate School of Cornell University In Partial Fulfillment of the Requirements for the Degree of Master of Professional Studies, Ithaca, NY, 2009.

Bayabil, H. K., Tilahun, S. A., Collick, A. S., and Steenhuis, T. S.: Are runoff processes ecologically or topographically driven in the Ethiopian Highlands? The case of the Maybar, Ecohydrology, 3(4), 457–466, doi:10.1002/eco.170, 2010.

Bewket, W and Sterk, G.: Farmers' participation in soil and water conservation activities in the Chemoga watershed, Blue Nile Basin, Ethiopia. Land Degradation and Development 13, 189-200, 2002.

Collick, A. S., Easton, Z. M., Ashagrie, T., Biruk, B., Tilahun, S., Adgo, E., Awulachew, S. B., Zeleke, G., and Steenhuis, T. S.: A simple semi distributed water balance model for the Ethiopian Highlands, Hydrol. Process, 23, 3718–3727, 2009.

Dunne T., and Black R. D.: Partial area contributions to storm runoff in a small New England watershed. Water Resources Research 6:1296–1311, 1970.

Easton, Z. M., Fuka, D. R., White, E. D., Collick, A. S., Biruk Ashagre, B., McCartney, M.,Awulachew, S. B., Ahmed, A. A., and Steenhuis, T. S.: A multi basin SWAT model analysis of runoff and sedimentation in the Blue Nile, Ethiopia, Hydrol. Earth Syst. Sci., 14, 1827–1841, doi:10.5194/hess-14-1827-2010, 2010.

Engda, T. A., Bayabil, H. K., Legesse, E. S., Ayana, E. K., Tilahun, S. A., Collick, A. S., Easton, Z. M., Rimmer, A., Awulachew, S. B., and Steenhuis, T. S.: Watershed hydrology of the (semi) humid Ethiopian Highlands, in: Nile River: Hydrology, Climate and Land Use, edited by: Melesse, A., Springer Science Publisher, New York, 2011.

Haregeweyn N and Yohannes F.: Testing and evaluation of the agricultural non-point source pollution model (AGNPS) on Augucho catchment, western Hararghe, Ethiopia. Agriculture Ecosystems & Environment 99: 201-212, 2003.

Herweg K and Ludi E.: The performance of selected soil and water conservation measures- case studies from Ethiopia and Eritrea. Catena (36) 99-114, 1999.

Hewlett, J. D., and Hibbert, A. R.: Moisture and energy conditions within a sloping soil mass during drainage, J. Geophys. Res.,6 8(4), 1081-1087, 1963.

Liu, B. M., Collick, A. S., Zeleke, G., Adgo, E., Easton, Z. M., and Steenhuis, T. S.: Rainfall discharge relationships for a monsoonal climate in the Ethiopian Highlands, Hydrol. Process., 22(7), 1059–1067, 2008.

Mohammed, A., Yohannes, F., and Zeleke, G.: Validation of agricultural non-point source (AGNPS) pollution model in Kori watershed, South Wollo, Ethiopia, Int. J. Appl. Earth Obs., 6, 97–109, 2004.

Nash, J.E., and J.V. Sutcliffe.: River flow forecasting through conceptual models, Part 1 - a discussion of principles. Journal of Hydrology 10: 282–290, 1970.

Schneiderman, E.M., Steenhuis, T.S., Thongs, D.J., Easton, Z.M., Zion, M.S., Mendoza, G.F., Walter, M.T., Neal, A.L.: Incorporating variable source area hydrology into the curve number based generalized watershed loading function model. Hydrol. Process. 21, 3420–3430, 2007

Setegn, S G., Ragahavan S., Bijan D.: Hydrological Modeling in the LakeTana Basin, Ethiopia using SWAT model. The Open Hydrology Journal 2: 49-62, 2008.

Steenhuis T. S., Winchell M., Rossing J., Zollweg J. A., Walter M. F.: SCS runoff equation revisited for variable-source runoff areas. American Society of Civil Engineers, Journal of Irrigation and Drainage Engineering 121: 234–238, 1995.

Steenhuis, T.S., A.S. Collick, Z. M. Easton, E.S. Leggesse, H. K. Bayabil, E. D. White, S.B. Awulachew, E. Adgo5, A.A. Ahmed.: Predicting Discharge and Erosion for the Abay (Blue Nile) with a Simple Model. Hydrological Processes 23: 3728–3737, 2009.

Tesemma, Z. K., Mohamed, Y. A., and Steenhuis, T. S.: Trends in rainfall and runoff in the Blue Nile Basin: 1964–2003, Hydrol. Process., 24(25), 3747–3758, doi:10.1002/hyp.7893, 2010.

Tilahun, S. A., R. Mukundan, B. A. Demisse, C. Guzman, B. C. Tarakegn, T. A. Engda , Z. M. Easton , A. S. Collick, A. D. Zegeye, E. M. Schneiderman, J.Y. Parlange, and T. S. Steenhuis.: A Saturation Excess Erosion Model. In: Proceedings International Symposium on Erosion and Landscape Evolution, ISELE paper number 11061. D.C. Flanagan, J.C. Ascough II, and J.L. Nieber (eds.). St. Joseph, Mich: ASABE, 2011

Tilahun Seifu A., Guzman Christian D., Zegeye Assefa D., Engda Tegenu A., Collick Amy S., Rimmer Alon, and Steenhuis Tammo S.: An efficient semi-distributed hillslope erosion model for the sub humid Ethiopian Highlands. HESSD-9-2121-2012, 2012

White, E. D., Easton, Z. M., Fuka, D. R., Collick, A. S., Adgo, E., McCartney, M., Awulachew, S. B., Selassie, Y., and Steenhuis, T. S.: Development and application of a physically based landscape water balance in the SWAT model, Hydrol. Process., 23, 3728–3737,doi:10.1002/hyp.7876, 2010.

Zegeye, A.D., T.S. Steenhuis, R.W. Blake, S. Kidnau, A.S. Collick and F. Dadgari.: Assessment of Upland Erosion Processes and Farmer Perception of Land Conservation in Debre-Mewi Watershed, near Lake Tana, Ethiopia. Ecohydrologica 10: 297-306, 2010.

Zeleke, G.: Landscape Dynamics and Soil Erosion Process Modeling in the North-western Ethiopian Highlands. African Studies Series A 16, Geographica Bernensia, Berne, 2000.

CHAPTER 3: SOIL EROSION IN THE UPPER BLUE NILE BASIN OF ETHIOPIA: THE DEBRE MAWI WATERSHED

Abstract

Past efforts in predicting erosion was largely unsuccessful due to the limited knowledge of the locations of the watershed runoff and erosion processes (i.e., hotspots) in the Ethiopian highlands. Understanding soil erosion dynamics and identification of hotspot sediment source areas are therefore important for better sediment prediction and soil and water conservation implementation. Debre Mawi, a headwater watershed in Blue Nile basin, was instrumented with automatic rain gauge to measure rainfall and with five broad crested weirs to measure sediment concentration and runoff at five nested locations within the watershed in two summers (2010 and 2011). In addition, rill and gully erosion rates were monitored and estimated from ten selected agricultural fields and four gullies located at saturated areas. The sediment concentration and load measurements in June and July were found to be greater than in August at all weirs because the soil in the watershed was loose after the prolonged dry period and we hypothesized that shear stress became greater than the critical shear stress increasing the entrainment of sediment through newly developed rill network and consequent rill erosion. After saturation, the shear stress of the flux through the rill channel was less than the critical shear stress and hence new rill development ceased and concentration were lowest at the outlet of all sub-watersheds. This hypothesis is however needed further measurements and experiments in future. When soil loss among landscape position and crop type compared from the ten agricultural fields, it was found that erosion between upslope and downslope landscape position showed statistically different soil loss amount than among crop types. When sediment concentration is compared among sub-

watersheds, concentrations from upslope areas were less than at the outlet suggesting that sediment sources were located at down slope part of the landscape. In Debre Mawi, saturated areas were found and confirmed by the piezometer readings and these areas usually had active gullies and wetted agricultural fields producing six and ten times, respectively, more sediment than rill erosion from upslope areas. These results are important in well-vegetated regions where rainfall rates are generally less than the infiltration capacity of the soil not only for reconsideration of the placement of soil and water conservation practices but also for modeling principles that should include local saturated areas.

3.1 Introduction

African mountains and highlands are important resource areas for the African population (Messerli et al, 1988). The East African highlands and mountains above 1.5 km, being the center of major agricultural and economic activities, comprises 43% of Ethiopia and constitute more than half of all the highland areas of Africa (Hurni, 1988). However, soil erosion has been a severe threat to agricultural production for a long time. The highlands have experienced erosion since the early Oligocene Epoch (29Ma) with high, long-term incision rates that have increased exponentially from 0.05 to 0.32 mm/yr (Gani et al., 2007). Currently, this rate has reached approximately 0.5 mm/yr when averaged uniformly over the whole basin (Garzanti et al., 2006). Local erosion rates, however, range from less than 1 t $ha^{-1}year^{-1}$ (Hurni, 1988) to 200t ha^{-1} (14 mm $year^{-1}$) in Lake Tana sub-watersheds (Easton et al., 2010) and it even exceed over 400 t $ha^{-1}year^{-1}$ in some places where gullies are being formed (Tebebu et al., 2010). Gullies became widespread in the highlands during the 20th century when the population pressure increased (Nyssen et al., 2006).

The economy and development of Ethiopia are directly affected by the high erosion rate (Tadesse, 2001; Sutcliffe, 1993; Hurni, 1993). It decreases land productivity leading to greater food shortages (Bewkete & Sterk, 2003) by removing soil nutrients (Mitiku et al., 2006), decreasing water holding capacity and increasing overland flow from shallow eroded soils (Tessema et al, 2010). In addition, erosion causes silting of small ponds for irrigation and water supply and loss of storage capacity of large reservoir systems for hydropower (Tamene et al, 2006).

Erosion research has been carried out on plot, field and watershed scales in Ethiopia in order to help planning of conservation practices and to reduce soil erosion. Field scale studies include measurements of rill erosion from agricultural fields and gully erosion while watershed-scale involves monitoring sediment at the watershed outlet. Plot scale experiments are used to derive parameter values of the Universal Soil Loss Equation (USLE) (Wischmeier and Smith, 1978; Mitiku et al., 2006; Vanmaercke et al., 2011). Zegeye et al (2010), found that values from USLE could predict average annual erosion well, but failed to predict the distribution in the watershed. Moreover, the USLE fails to represent the watershed scale process in which upslope sub-surface flow saturates down-slope areas where gully erosion becomes prominent (Tebebu et al., 2010) or the deposition processes (Bewket and Sterk, 2003;Vanmaercke et al., 2011). Watershed scale studies such as by Soil Research Conservation Program (SCRP) overcome the shortcomings of the USLE (Grunder, 1988). These studies provided an impressive data set on runoff and sediment concentrations both from the runoff plot and at the outlet of watersheds with sizes of 100ha to 500ha but failed to examine the distribution of erosion and sedimentation within the watersheds.

While on-going research has contributed to our understanding of the physical processes underlying soil erosion on field scale, further research is therefore needed on watershed scale to understand the sediment dynamics. In Ethiopia, sediment concentration in the rivers uniquely decreases at the time the stream flow discharge become peak during the first week of August (Awulachew et al., 2008). And this dynamics is explained by different researchers differentially. Some are relating this phenomena with sediment depletion (Vanmaercke et al., 2010), or vegetation cover improvement (Descheemaeker et al., 2006; Awulachew et al., 2008; Vanmaercke et al., 2010) or dilution of sediment by subsurface flow (Tilahun et al., 2012) while as shown in the result and discussion section in this study, we argued that the decrease is associated with soil moisture increase. Soils are dry at the end of the dry phase of the monsoon in Ethiopia and then during the rainy phase, it wets up either to field capacity or to saturation depending on the landscape position. As moisture content is directly related to shear strength of the soil (Freduland et al., 1995) and transport capacity of overland flow is related with shear stress of the flux (Hofer et al., 2012, we hypothesized that sediment concentration decreases in the river because shear stress become lower and shear strength of the soil become higher at the beginning of saturation on the Ethiopian highland.

Therefore, the objective of this paper is to investigate the sediment dynamics and identify sediment sources temporally and spatially in a watershed by conducting measurements at field and watershed scales. The Debre Mawi watershed located near Bahir Dar was selected as the study area because of our previous research in the watershed (Tebebu et al., 2010; Zegeye et al., 2010).

3.2 Material and Methods

In this study, sediment sources and erosion processes from upslope and downslope areas are investigated through fieldwork that was carried out during 2010 and 2011 rainy period. In addition to measurements mentioned in chapter 2, sediment concentration was monitored at five gauging stations (one at the outlet and four at sub-watersheds). Grain size distribution for soil samples were conducted in 2010. Rill erosion from agricultural fields and gully expansions were measured and monitored in 2011.

3.2.1 Site Description

The Debre Mawi watershed research site, named after the Keble Debre Mawi in Yilmana-Densa Woreda (district), covers a total area of 523 ha. It is situated 30 km south of Bahir Dar adjacent to the Bahir Dar-Adet road at 37°22' East and 11°18' North (Figure 3-1) in the western plateau of the Ethiopian highlands at the northern source region of the Blue Nile River. A sub-watershed of approximately 95ha was selected for this study which is located in the upstream portion of the whole watershed. Its slope ranges from 1 to 30% and topography ranges from 2,212 m above sea level (m.a.s.l.) near the outlet to 2,306 m.a.s.l. in the south east.

The watershed is underlain by shallow, highly weathered and fractured basalt overlain by dark brown compacted clay, followed by light brown wet and sticky clay soil and at the surface finally a black clay and organic rich soil sequences (Abiy, 2009). The fractures are highly interconnected with limited clay infillings. Lava intrusion dikes in the western upper part of the watershed disrupt the fractures forcing the subsurface flowing water to the surface. The dominant soil types in the watershed are Nitisols, Vertisols and Vertic Nitisols: Nitisols (locally, *Dewel*) are found in the upper part of the watershed. This is a very deep, well-drained red clay loam soil and is considered the most productive. This is a very deep, volcanic derived well-drained red clay loam soil and is considered the most productive and permeable soil. The Vertisols (locally called *Walka*) is black and cover the lower slope positions. This soil forms deep wide crack during dry period and, it swells and develop stickiness during rainy period. Vertic Nitisols (locally known as *Silehana*) are located at midslope between the Vertisols and Nitisols. It is reddish-brown and has properties of draining water when it is excess and hold water when it is low. When it is dry, it forms cracks similar to Vertisols. It is especially suitable for tef production.

Seventy percent of the watershed is cropland with the remaining area in grassland, bush or fallow that is either too dry or too wet for crop production (Mekonnen and Melesse, 2011). The lower part of the watershed with slopes of 0 to 6% is saturated near the end of the rainy monsoon phase and is covered with grass with actively expanding gullies (Figure 3-2). These areas of the watershed serve as grazing land. Sparse shrubs are located at the middle (slope of 6 to 27%), in areas that are difficult to plow. Fields at the upper (slope of 0 to 6%) and middle are continuously cropped. Cereal-plow cultivation is the dominant system with fields are usually planted with tef, wheat, maize, barley and to a lesser extent with finger millet, lupine (particularly, *Lupinus albus*) and grass pea.

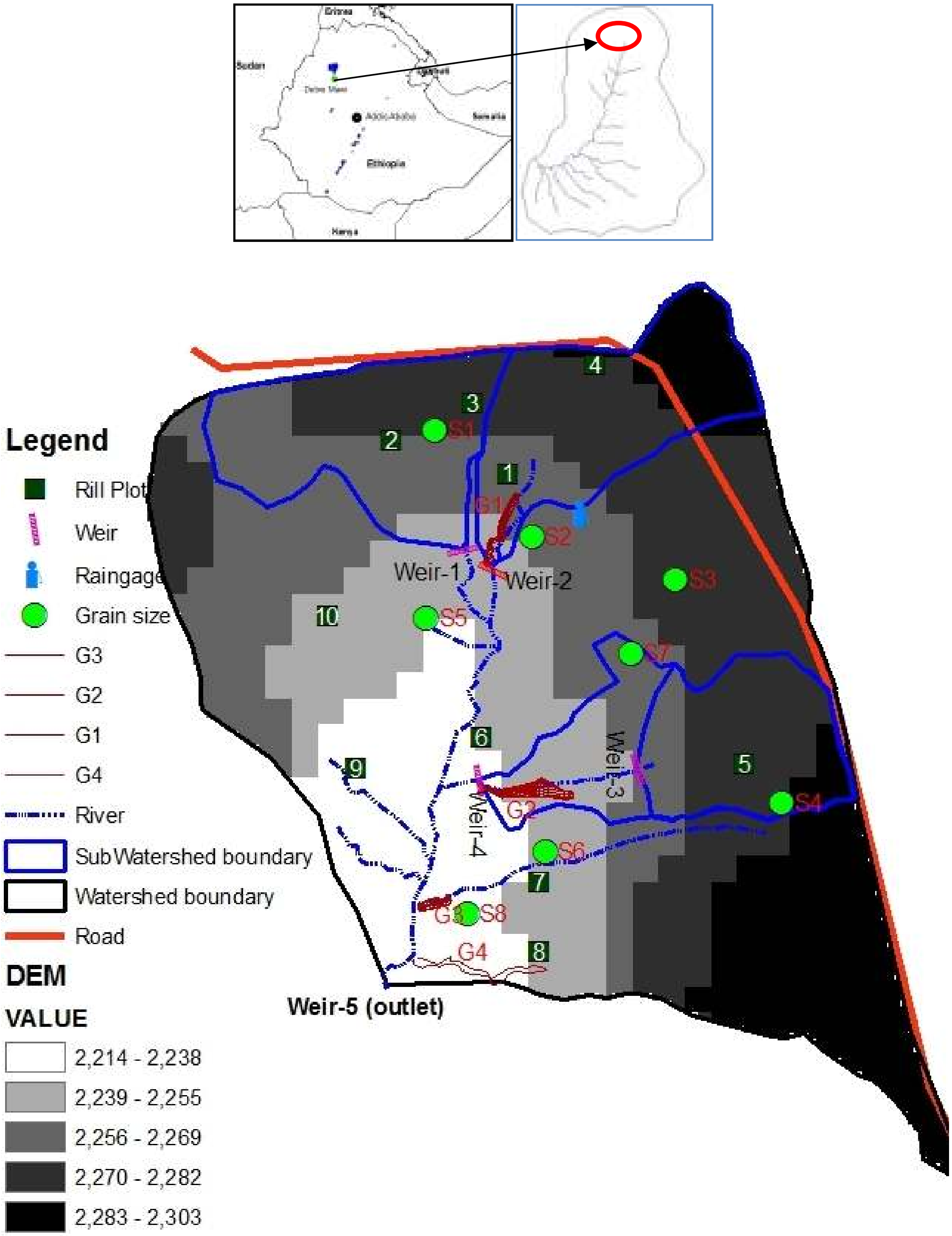

Figure 3-1: Location, boundary and drainage map of Debre Mawi sediment concentration monitoring sites (Weirs), field plots and gullies within the watershed (G stands for Gully; S stands for sampling location of grain size distribution)

Figure 3-2: (a) Lower portion of the sub-watershed 2 in dry period of April 2010 (b) Lower portion of the sub-watershed 2 with unsaturated hillsides at the background and with wet gully (G1) area located in the foreground in August 2010.

3.2.2 Data and Methodology

Fieldwork was carried out during the summer of 2010 and 2011 in the upper part of the Debre Mawi. Daily rainfall was measured during the two summers, and suspended sediment concentrations were monitored at five gauging stations by defining four sub-watersheds during the two summers. Grain size distribution analysis was conducted in 2010, while rill erosion from field plots in 2011 and gully erosion in 2010 and 2011was measured.

Sediment concentration measurements: Different level rectangular weir notches were constructed in 2010 from cinderblocks and steel bars at four locations as shown in Figure 3-1, and the weir at the outlet was constructed by Adet Research Center in 2007. Water samples (1 L volume) were taken at 10 minute intervals at the gauging stations (Weirs) for sediment concentration from June 29, 2010 to September 16, 2010 and from June 25, 2011 to September 14, 2011 at the four monitoring sites (Weir 1 to 4) while at the outlet, water was sampled from June 22, 2010 to October 1, 2010 and from June 12, 2011 to September 18, 2011. Sampling during storm period started when storm floods developed and when the water from the storms at each gauging station looked turbid (brown), and the sampling continued at ten-minute intervals. Storm period is defined as a time length that measurement was conducted from the beginning of runoff to its end at the event of considerable runoff and sediment transport in the stream. Each sample was filtered using Whatman filter papers with a pore opening of 2.5 μm, oven dried and weighed to allow determination of dry soil losses. Due to strong floods, it was often impossible to sample sediment from the entire water column. However, since the flow was very turbulent during these floods, a good mixing of the sediments was expected, reducing errors to an acceptable level. In addition, because of the quick rise of flood depths, there were challenges to sample sediments from the rising limb of the flood for all events, especially events occurring at night. Floods destroyed two of the cinderblock weirs and resulted in missing data for sediment concentration on 20 July, 2010 for weir-1, on June 29, and July 4 and July 5, 2010 for weir-3. A maximum number of 18 samples were collected during each storm periods for Weir-5, while as many as 13 samples were collected at each of the remaining weirs. The rate of flow obtained from rating equation (chapter 2) was multiplied by the sediment concentration to determine sediment load at each 10-minute interval during storm period for all weirs. Sediment concentrations for storm events were determined by dividing the total sediment load by the total storm runoff during that storm period. A total of 44 storm event sediment concentrations for weir-1 and -3, 47 for weir-2 and -4 and 63 for weir-5 were determined.

Grain size distribution: Eight sites (Figure 3-1) were selected to sample soil from the top surface that is readily available to be eroded by overland flow on 21 Sep 2010. This was conducted to determine and compare the clay and sand content of the soil at the ground surface in order to verify the hypothesis suggested in the discussion section that shielding the soil surface with sand at the end of the rainy period to prevent splash erosion (Hairsine and Rose, 1991; Heilig et al., 2001; Gao et al., 2005; Walker et al., 2007). Soil sample with a mass of greater than 100g was then taken from a depth of less than 0.5cm at each of the eight sampling ground surface. All the necessary sample preparation work was done before the hydrometer analyses in the laboratory. The pre-laboratory analyses sample preparation process included preparing a soil sample mass of 65g soil from each site, dispersing the soil samples using deflocculating agent (i.e., solution of sodium hexametaphosphate), and sieving so as to remove stones and other large organic materials. From the hydrometer analysis, clay, silt and sand content of eight sites were determined. This is compared with the soil texture determination from a soil depth profile of 15cm by Adet Research Center in 2008 from six locations in the watershed (Zegeye, 2009). The average values from the six sites were 43% sand, 29% silt and 27% sand.

***Rill erosion*:** Ten representative fields were selected from the 95-ha Debre Mawi watershed, and the erosion rates from rills in these fields were determined after 9 storm events between the periods of July 14, 2011 to September 15, 2011. The total area of the 10 fields was 2.6 ha (almost 3% of the watershed area, Table 3-2). These fields were selected at different slope positions in the watershed: upslope, mid-slope and down-slope fields (Figure 3-1). Fields 1 and 6 were in maize; Field 5 in fava-bean; Fields 7 and 10 in finger millet and on the remainder of the Fields (2, 3, 4, 8 and 9), tef was grown. The method of rill erosion was conducted similarly as in Zegeye et al, (2010) and Beweket and Sterk (2003). Agricultural fields were divided into a number of transects where the number of rills, average depth, average width, and average length was computed. The total volume of soil loss was obtained simply by summing the volumes of all homogenous rill segments. The total soil loss (t ha^{-1}) was computed by multiplying the calculated volume by the measured bulk density (1.24kg m^{-3}) and then dividing by the area of the agricultural land. In addition, rill density was calculated by dividing the total rill lengths obtained by summing up the length measurements of all the rills by the total area of the agricultural fields.

Gully erosion: The volume was determined for four gullies that depicted in Figure 3-1 named as G1, G2, G3 and G4. G1 is located in sub-watershed near Weir-2: G2 is in sub-watershed near Weir-4; G3 and G4 are located close to the outlet of the watershed near at Weir-5. All gullies' volumes were measured on June 30, 2011 and August 11, 2011 while gully 3 was, in addition, measured on June 26, 2010 and September 5, 2010. Volumes were measured from the cross sectional area and length of segment between cross-sections (Appendix B3). Cross-sections were selected at abrupt changes along the length of the gully. The length of each segment between two cross-sections, the top width of the cross-sections and depth of gullies at the cross-sections were measured using a 30m long surveyor's tape in 2010 and leveling instrument in 2011. The depth at the cross-sections was measured at 1m intervals and corresponding depths were measured at locations where the gully cross-sections changed abruptly. Based on these measurements an average gully volume of each segment was estimated. Gully erosion rates (t ha^{-1} yr^{-1}) were calculated using the estimated volume of the gully, the average soil bulk density (1.24kg m^{-3}) obtained from measurement and the contributing watershed area of the gully. The evolution of G3 with time was also monitored using a Google earth images since 2005. Surface area of this particular gully was estimated in 2005, 2010 and 2011 and compared with the field measurements in 2010 and 2011.

3.3 Results

3.3.1 Sediment concentration and load from 5 weir

Sediment concentrations were up to 3% by weight in June and July and then decreased in August and September to values of less than 0.1% (Figure 3-3; Figure B1-1 and B1-2 in Appendix-B). Sediment concentration in June and July at the outlet were approximately twice that of the sub-watersheds (Figure 3-3; Figure 3-4 and B1-3 in Appendix B1). The decreasing trend in the sediment concentration is opposite of increasing runoff coefficient shown in Chapter 2. The differences in the cumulative frequency distribution of both concentration and load at the outlet (Weir-5) and the upslope sub-watershed outlets (Figure 3-5) will be discussed later in reference to other researchers such as Descheemaeker et al. (2006) and Vanmaercke et al. (2010).

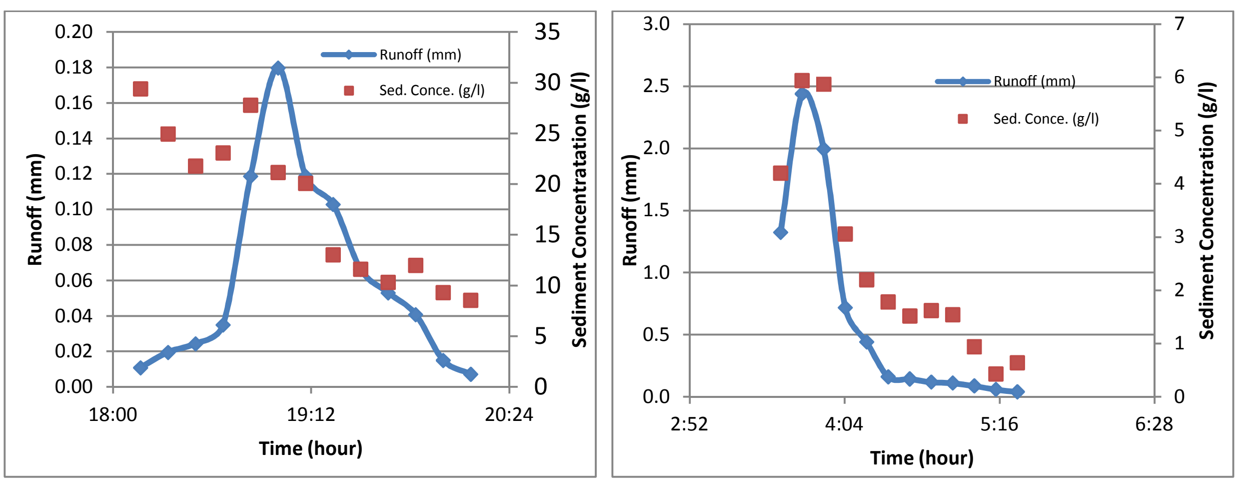

Figure 3-3: Sediment concentration and storm runoff rate at 10-minutes interval during storm period on 5 Jul 2010 at the left and on 15 Sep 2010 at the right at the outlet (weir-5) of Debre Mawi watershed.

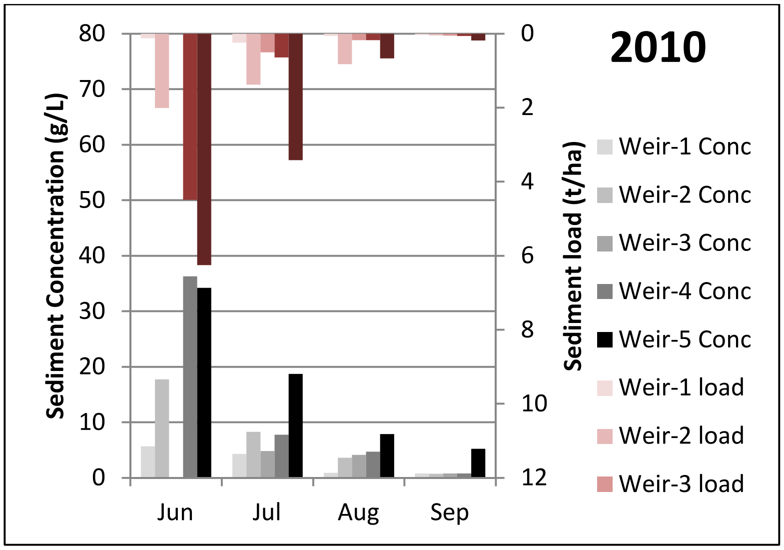

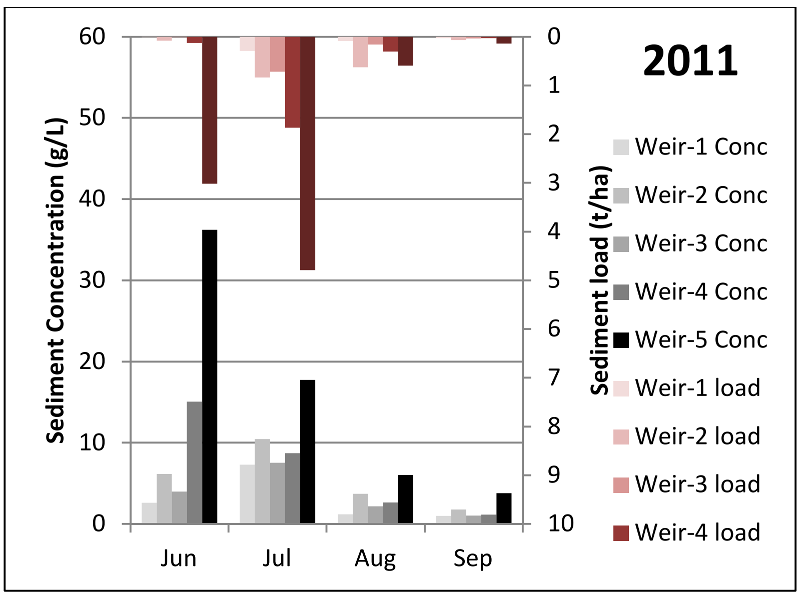

Figure 3-4: Monthly average sediment concentrations and the corresponding sediment load at each weir for rainy phases of the monsoon in 2010 and 2011 for the Debra Mawi watershed. It is calculated for all data points from Table F1

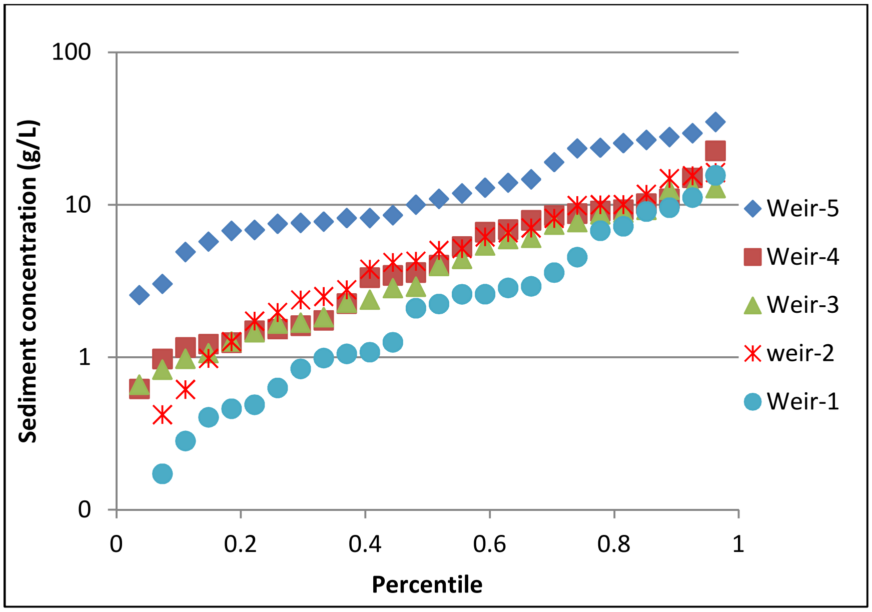

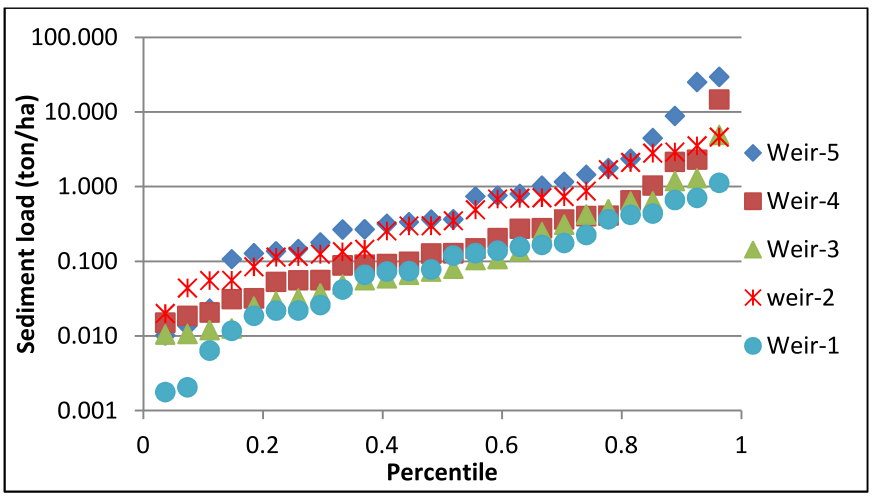

Figure 3-5: Cumulative frequency distribution of sediment concentration and sediment load values at each weir for both summer using data from similar dates at all weirs.

3.3.2 Grain size distribution

Table 3-1 shows the clay-silt-sand content of the soil sample from eight different locations sampled from a depth of 0.5cm within the watershed. All sites in Table 3-1 show approximately similar percentage of clay-silt-sand content and the average from eight sites is 54% clay, 22% silt and 24% sand which is similar with the average values from the six sites (43% clay, 29% silt and

27% sand) that were obtained from 15cm depth soil profile conducted in 2008 by Adet Research Center (Zegeye, 2009). Except at locations of S2 and S8 which are close to gully 1 and gully 3, all locations shows a clay content of more than 50% at the end of rainy period. These two locations have also showed a higher sand content because of likely the erosion of fine sediment. Location at S5 shows higher clay content because of the domination of Vertisol type of soil. The result generally confirms that the watershed is covered by fine soil that can be transported by overland flow at the end of the rainy period in contrary to the suggestion that sources of readily available sediment to be transported is diminished at the end of rainy period (Vanmaercke et al., 2010; Hairsine and Rose, 1991).

Table 3-1: Grain size distribution from eight locations (Figure 3-1) using hydrometer analysis

Sampling location	S1	S2	S3	S4	S5	S6	S7	S8
Clay (%)	0.51	0.45	0.58	0.50	0.77	0.53	0.49	0.44
Silt (%)	0.23	0.28	0.25	0.18	0.18	0.18	0.26	0.23
Sand (%)	0.26	0.27	0.17	0.32	0.06	0.29	0.25	0.33

3.3.3 Rill erosion

Spatially averaged cumulative soil loss (as indicated by the volume in the rills) and the rill density from 10 agricultural fields (locations are shown in Figure 3-1) increase from July 14, 2011 to the first week of August (Figure 3-6). There was an apparent decrease in cumulative soil loss and number of rills after August 6, 2011 until the end of September when the rain stopped, and when rills were filled up by soil from the inter-rill areas. Therefore we will use the rate of soil loss on August 6 as the amount of soil lost. This is reasonable as the sediment concentrations in the stream (Figure B1-1 and B1-2 in Appendix-B) indicate that soil losses are small after this time. In average, the cumulative soil loss rate from rills in the watershed is 60 t/ha (Figure 3-6). But this rate varies in the landscape as the sediment concentration varied among the weirs. Field

3, 8 and 9 had values of zero soil loss for days at the beginning of observations because the field was not plowed (Table 3-2). Fields such as 1, 6 and 9 which are close to the valley bottom had an average cumulative soil loss of 200 t/ha while the upslope fields such as 2, 3, 4 and 5 were only 17 t/ha. This deference between upslope and downslope is statistically significant at 1% significance level using F-test (Table 3-3). Fields 1, 6, and 9 are delivering sediment to Weir-5 which is all the time higher than upslope weirs (Figure 3-5) in which these areas were supplied by agricultural plots of 2, 3 and 5 (Figure 3-1). The difference of soil losses among fields with different crop types (Table 3-3) are not statistically different indicating that the landscape position of fields makes the difference than crop types.

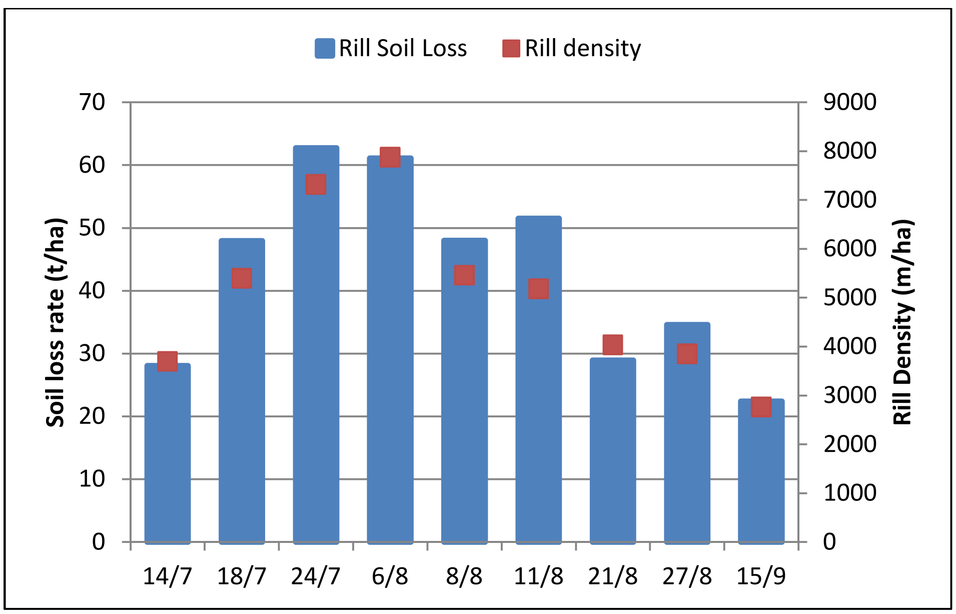

Figure 3-6: Average cumulative soil loss and rill density for the agricultural fields measured in summer of 2011(x-axis shows date with format of day/month)

Table 3-2: Soil loss rate from agricultural fields monitored in 2011

Field ID	Field size (ha)	Type of Crop	Cumulative Soil Loss (t/ha)								
			Jul 14	Jul 18	Jul 24	Aug 6	Aug 8	Aug 11	Aug 21	Aug 27	Sep 15
1	0.34	Maize	144.3	221.2	174.4	171.1	62.1	110.9	23.1	58.5	53.4
2	0.098	Tef	14.9	31.8	44.7	24.9	10.9	12.5	7.6	8.80	0.63
3	0.481	Tef	0.00	0.00	10.1	17.1	20.9	17.2	10.4	5.7	4.1
4	0.27	Tef	16.5	37.9	42.1	22.4	5.3	5.1	1.5	0.53	0.10
5	0.27	Favabean	0.78	3.1	4.3	5.1	2.3	1.9	0.00	0.00	
6	0.16	Maize	77.6	231.2	105.4	277.3	91.5	87.4	51.6	48.5	29.7
7	0.336	Finger Millet	10.9	12.4	3.5	7.9	7.0	2.3	2.8	1.9	0.43
8	0.17	Tef	0.00	0.00	35.9	77.8	88.70	95.5	41.1	64.5	21.8
9	0.356	Tef	0.00	153.0	201.1	153.0	190.2	180.2	149.7	214.8	113.2
10	0.148	Finger Millet	15.6	10.00	5.4	6.9	1.2	1.4	0.85	1.1	0.46

Table 3-3: Comparisons to show significant differences of variables among landscape position and crop cover types using F-test at 1%significance level (Data is from Table 3-2**)**

	Landscape position	Crop type		
Variables	Upslope vs. downslope	Tef vs. Maize	Tef vs. Finger millet	Maize vs. Finger millet
P-value	0.0025	0.024	0.28	0.055

3.3.4 Gully erosion

Gullies 1, 2 and 4 that were monitored during 2011 expanded slightly (Table 3-4) while Gully 3 measured during two years expanded rapidly (Table 3-4, Figure 3-7 and Figure B3-2). The Google Earth image (Figure 3-7) delineation of gully 3 indicated that the planimetric area of the gully was 81m^2 in 2005, 321m^2 in 2010 and 625m^2 in 2011 while the measurement of the same gully on the field in 2010 resulted in 325 m^2 in June and 520m^2 in September (Table 3-4). The gully has enlarged almost seven times since six years ago and five times since five years ago.

According to Nyssen et al. (2006), new gully formation is initially slow and then goes into an exponentially expanding phase and then growth rate decrease at the end. Gully 2 and 3 are in its exponentially growing phase when gully 1 is just starting, and gully 4 are stopped expanding

(Table 3-5). Gully 2 is treated with biological conservation practices covering the banks with grasses and bushes (Figure B3-3) but is active at the top and gully 4 is geometrically V-shape indicating that the gully has stooped expanding (Tebebu et al., 2010).

Table 3-4: Surface area (m^2) of gullies during measurement time

Gully	26-Jun-10	5-Sep-10	4-Jul-11	12-Aug-11	% increase
G1			1285.8	1463.2	13
G2			2296.5	2473.4	7
G3	325.06	520.8	697.68	828.2	60 in 2010 and 18.7 in 2011
G4			701.7	706.5	0.6

The estimated average soil loss rate due to gully erosion in the watershed is approximately 50t ha^{-1} yr^{-1} (Table 3-5). This rate is 50 times higher than area specific gully erosion rate reported in Northern part of Ethiopia (Nyssen et al., 2006). Gully 3 had shown a decrease in volume during the monitoring period in 2011 which is likely because of collapse of banks of gully that is not transported enough during the last measurements on August 12, 2011. There was no sufficient storm between August 8 and August 14, 2011 in which the measurement was conducted (Table B1-1 in Appendix B1). The erosion rate in 2010 was 120 t ha^{-1} yr^{-1} which is likely the actual erosion rate of this particular gully as it is in its expansion stage (Figure 3-10b). The soil loss from the next active gully-2 is 60t ha^{-1} yr^{-1} (Figure B3-3 in Appendix B3).

Table 3-5: Soil loss and summarized dimension of gullies in Debre Mawi Watershed

Gully	Year	Contributing areas (ha)	Length (m)	Max Depth (m)	First measurement Volume (m^3)	Second measurement Volume (m^3)	Soil loss (ton/ha)
G1	2011	11	124	2.2	631.8	741.5	12.2
G2	2011	12.4	160	3.8	1637.1	2241.4	59.5
G3	2010	8.5	30	5.2	924.7	1744.9	117.7
G3	2011	8.5	54	6.2	2061.8	1985.1	-11.0
G4	2011	6.2	82	3.3	701.3	727.7	5.2

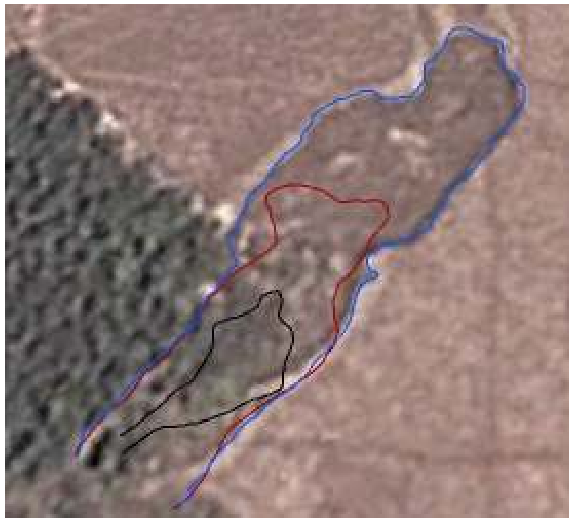

Figure 3-7: Gully 3 evolution with time since 2005 showing the surface area by digitizing from Google earth image (black solid line indicates 2005; red indicates 2010 and blue indicates 2011)

3.4 Discussion

Two trends can be found from the results and collected data presented in the result section: a decrease of the sediment concentration with effective cumulative rainfall during the rainy phase of the monsoon (Figure 3.9) and an increase of erosion and sediment sources with landscape position (Table 3-3, Figure 3-4, Figure 3-5). These trends will be discussed in this section separately although they are not quite independent.

Sediment concentration decrease with cumulative rainfall

In the plot of the weekly average sediment concentration with cumulative effective rainfall (P-E) (Figure 3.9), the sub-watershed areas at weirs that include active gullying (Weir 4 and 5) and at the weirs that have no active gullying (Weir 1 and 3) have slightly different behavior. The concentration decreased linearly for sub-watershed at Weir-4 and the whole watershed (weir 5) during the whole rainy phase. For sub-watersheds at Weir-1 and -3, the concentration decreased linearly in both years to the cumulative effective rainfall of about 400 mm and then it remains low. Watershed 2 had some gullying and is in between these two trends.

Several researchers have argued to the underlying reason of the decrease in erosion with time as plant cover (Descheemaeker et al., 2006; Awulachew et al., 2008; Vanmaercke et al., 2010). Crops in Debre Mawi watershed were planted at different times during the rainy period (Zegeye et al., 2010). Tef is sown from early July to early August, finger millet from late May to late June, and maize from late April to mid June. Both rill measurements and sediment concentrations decreased with time in the rainy period for all crop types while there was difference in sowing and corresponding plant cover. For example tef was just sown around August 8, 2011 (Table 3-2) and was maize 10 cm high when the sediment concentration decreased in the sub-watersheds at Weir-1 and -3 (in which active gullying did not occur) at the end of July. Though one would expect to find a statistical difference of soil loss from agricultural fields with different crop type, but Table 3-3 clearly showed that this is not the case. Our field measurement of rill erosion in 2011 showed that independent of crop type, the rill density and soil loss stopped after the storm on July 24, 2011 (Table 3.1 and Figure 3.6). Other researchers have made similar observations where the average rill density network at the watershed outlet (Figure 3-6) increased during and after the beginning of the rainy period and decreased around the beginning of August by Zegeye et al (2010) in the same watershed in 2008 and by Bewkete and Sterk (2003) in Chemoga Mountain 40km south of Debre Mawi.

Since plant cover was not responsible for the decrease in erosion, we formulated based on the existing literature two possible hypotheses for the observed decrease in sediment concentration in time. These were: 1) armoring the soil surface with sand preventing splash erosion (Hairsine and Rose, 1991; Heilig et al., 2001; Gao et al., 2005; Walker et al., 2007) and 2) shear stress becomes smaller than the critical shear stress reducing entrainment of sediment by the flowing water (Yalin, 1963).

Armoring of the surface occurs by washing out the fines and leaving the sand behind because of the greater fall velocity in the water (Heilig et al., 2001). This sand prevents any further splash erosion. We tested this hypothesis by comparing the clay and sand content of soil sample that shields the ground surface in September 2010 of the monsoonal period. Table 3-1 showed that the clay content was greater than 50% during the end of the rainy period and there was also no difference in sand content between this measurement and measurements conducted from 15cm soil depth in 2008 (Zegeye, 2009). Thus the first hypothesis was invalid.

The second hypothesis in which erosion occurs when the shear stress is less than the critical shear strength is more difficult to prove (or reject) experimentally since it was only formulated after the field work was completed. The shear stress is a function of flow depth of the overland water and therefore of the flux in the rill. Critical sheer stress is a function of particle size distribution and moisture content and it is thus directly related to the cohesion between particles of the soil and will be smallest when the soil is saturated and air dry (Fredlund et al., 1996). The critical shear strength has its maximum value near field capacity when the capillary forces keep the particles together. Thus critical shear stresses increase during the rainy season when the soil reached its field capacity at the end of July.

In order to accept or reject hypothesis based on the experimental data, let us consider the observed change in active rill erosion for 10 fields in 2011. In Table 3-2 and more clearly depicted in the summarized data of Figure 3-6, we see that before July 24, 2011 the rills were actively being formed and after that date, rill formation nearly stopped. Since theoretically rill erosion occurs when the shear stress of the overland flow is greater than the critical sheer stress of the soil (Hofer et al., 2012), it was around July 24 that the relative magnitude of sheer stress of the runoff and critical shear stress reverse. In this period, the shear stress becomes less than critical shear stress. In order to understand the switch we need to understand how the rill network is formed.

In this regard, Hofer et al. (2012) shows that rill networks initially form slowly, and more rills form when more rain falls. Once the rill network is established, it will remain the same. In the Debre Mawi watershed, plowing erased previous rill networks and it loosens up the soil by decreasing the critical sheer stress that results in a new set of rills. We observed that the rill network in the watershed was developed (Figure 3-6) at the time when the sediment concentration in the river was high (Figure B1-2, Figure 3-3 and Figure 3-4). This was mainly associated with the loose erodible sediment on the plowed land. In June, the storms are relatively small as most water infiltrates. These storms had a low runoff coefficient as explained in chapter 2 but in July, the lateral flow will concentrate in rills and all runoff will carry as much soil as the transport capacity allows. If the next storm is larger (such as July 17, 2011 in Table B1-1 in Appendix B1), the runoff will need additional rills to carry off the lateral flow and will erode few additional rills. The runoff on July 17, 2011 was associated with a large soil loss of 29 t ha^{-1}(Table D1-1) at the outlet of the watershed that originated from the newly formed rills, and it established the maximum extent of the rill network (Figure 3-6).

Figure 3-8: Agricultural land with maize at the forefront, saturated area and tef field at the middle and bush land with scattered forest at the background on the steepest portion of the watershed (Picture taken on 8 Aug 2010)

Thus at the end of July both the maximum extent of the rill network was formed and the critical shear strength had reached its maximum value. Moreover after July 17, 2011 any runoff was smaller and no additional rills were formed. In other words, the earlier established network could not carry the flow at the flux that were less than the July 17 storm and the imposed shear stress by the flux was smaller than the critical shear strength and hence the sediment concentration were lower at the outlet of the two watersheds (Weir-1 and Weir-3) which are without gullies.

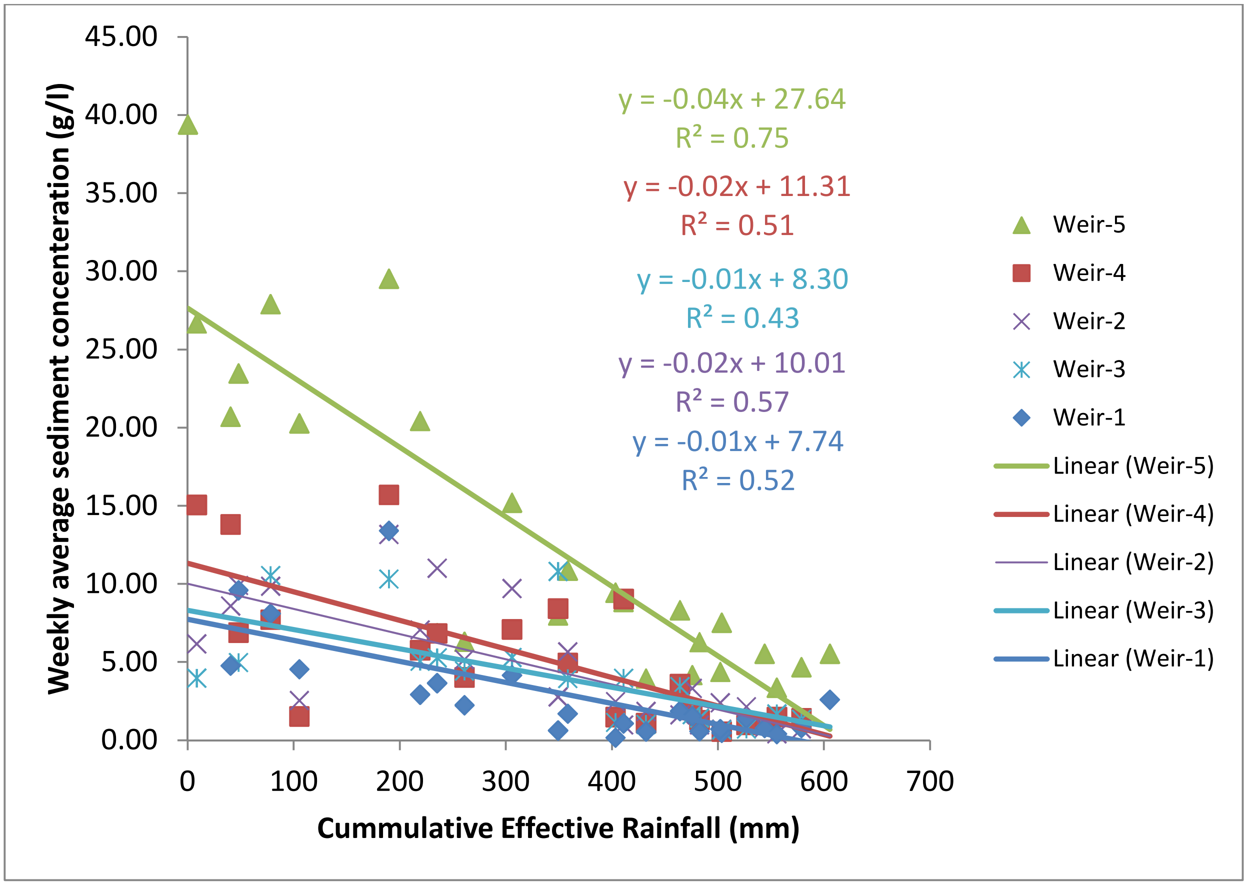

Figure 3-9: linear regression between cumulative effective rainfall (P-E) and weekly average sediment concentration at the watershed and sub-watershed outlets

We did not discuss yet the fact that there was no erosion of the tef plots before plowing occurred. On these fields the original rill system from the year before was still in place and water was carried off through the original rill network with little erosion since the critical shear stress was high because of the compaction of the field by grazing animals during the dry phases of the monsoon.

Finally sub-watersheds at Weir-4 and -5 with active gullying (Table 3-5) had always greater concentrations (after July 17, 2011) than the watersheds 1 and 3 without gullying. These gullies were located in areas that are saturated and bank failures are common due to slippage (Tebebu et al., 2010). These slips dump loose soil in the bottom of gullies that is being eroded by the flowing water during the storm.

Increase of erosion and sediment sources with landscape position

When the sediment concentration and loads from the different weirs are compared to each other (Figure 3-4), the sediment concentration and load at the outlet of Weir-5 and Weir-4 were always higher than the concentrations at the outlets located upstream (Weir-1 and Weir-3). This indicates that there are hotspot sediment source areas close to the river channel and at the outlet in contrast to the upslope areas reported by Mekonnen and Melesse (2011) in the same watershed. These differences are due to higher soil loss through rill erosion from agricultural fields located at downslope than upslope and additional sources from active gullying from downslope saturated areas.

Increase of soil loss from agricultural fields varied with landscape position (Table 3-3) in Debre Mawi watershed that is more related to wetness than run-on flux from upstream fields since farmers usually drain away the water from these areas through waterways of field ditch. The overland runoff flux is greater at downhill than uphill because the soil is wetter and less water can infiltrate and more runoff is generated. The shear stress due to high runoff then exceed the critical shear stress and transport more sediment to the outlet of the watershed at Weir-4 and -5 in which their sediment concentration (Figure 3-4 and Figure 3-5) are greater than upslope (Weir-1 and -3). The soil loss from agricultural areas located at the downslope areas (200tha^{-1}) is for example ten times higher than agricultural fields from upslope (17tha^{-1}) as described in Table 3-2.

In addition to sediment sources from rill, these sub-watersheds (Weir-4 and Weir-5) have seasonally saturated active gully incisions as shown in Figure 3-10 and Figure B3-3 in Appendix B3. In the saturated area, the overland flow is highest and exceeds the critical shear stress as explained above. The available loose sediment at the gully bottom due to bank collapse will be easily transported that made the sediment concentration at down slope outlets greater than upslope outlets. Such gully incisions are many in number located along the main river channel where it is seasonally saturated (Figure 3-10 and Figure B3-3). The soil loss from gullies located in such areas were estimated 120 t ha^{-1} from gully 3 and 60 t ha^{-1} from gully 2 which are two times or more higher than the average cumulative rill erosion from upslope (17 t ha^{-1}) indicating that gullies are major sediment source to river outlets. In the other part of the same watershed, Tebebu et al. (2010) measured gully soil loss of 500 t ha^{-1}. Sediment sources at down-slope areas are also reported in the Mediterranean region by Vanmaercke et al. (2011) suggesting that gully and channel erosion is the important sediment sources.

Figure 3-10: (a) Initiation of gully erosion in saturated area downstream of the outlet at Weir-2 and (b) gully-3 monitored in this study for two season close to the outlet at Weir-5

Our hypothesis that the decrease of shear stress at the end of July limited the sediment transport and hence decreased sediment concentration in the river need further experiments and researches in future while our finding that soil erosion was related to wetness through landscape position and not directly to crop type is proved by both rill and gully measurements in conjunction with sediment concentration at different landscape. The later is contrary to models that are based on infiltration excess in which runoff (and erosion) is directly related to the crop and soil type. The finding of major sediment source areas at down slope areas in this watershed is in line with the modeling approach by Steenhuis et al. (2009), Tilahun et al. (2011) and Tilahun et al. (2012) that will be explained in the next chapter.

3.5 Conclusion

The investigation of sediment concentrations at five nested location at spatially different locations in Debre Mawi watershed showed that the concentration at the watershed outlet and sub-watershed outlet decreased with similar trend after the end of July. We hypothesized that the most likely reason for decrease of sediment concentration at this time is that shear stress became smaller than the critical shear stress reducing entrainment of sediment by the flowing water after the month of July. We argued that the decrease of rill density and erosion from observations of 10-agricultural fields after the heavy storm at the end of July led to the formation maximum rill density and then any storm after this event produced lower runoff that decreased the shear stress of the flow to pick up sediment and transport it to the outlet of the sub-watersheds. This hypothesis is however needed further field measurements and experiments in the future. On the other hand, it is observed that soil loss from agricultural fields located at downslope is different significantly from upslopes irrespective of crop type and all the time the sediment concentrations at the outlet is higher than sub-watersheds from upslope indicating downslope part of the landscape was the major sources of sediment in the watershed. The sources of sediment for the outlet were located as rills from wetted agricultural fields or gullies from local saturated areas from field measurements. The erosion rates from both rills and gullies located in the down slope areas were more than six times from the upslope upland areas, which are traditionally described as hotspot erosion areas and targeted for soil and water conservation practices. Both the watershed and field measurements approaches indicated that soil conservation practices should target small areas such as saturated areas with gullies and wetted agricultural fields at downslope landscape portion of a watershed. In addition, erosion modeling practices should consider local saturated areas for better prediction and then planning of soil and water conservations.

References

Abyi, A. Z.: Geological controls in the formations and expansions of gullies over hillslope hydrological processes in the Highlands of Ethiopia, northern Blue Nile region, A Thesis Presented to the Faculty of the Graduate School of Cornell University In Partial Fulfillment of the Requirements for the Degree of Master of Professional Studies, Ithaca, NY, 2009.

Zegeye, A. D.: Assessment of upland erosion processes and farmer's perception of land conservation in Debre-Mewi watershed near Lake Tana, Northern Highland of Ethiopia. A Thesis Presented to the Faculty of the Graduate School Of Cornell University In Partial Fulfillment of the Requirements for the Degree of Master of Professional Studies, Ithaca, NY, 2009.

Awulachew, S. B.; McCartney, M.; Steenhuis, T. S; Ahmed, A. A.: A review of hydrology, sediment and water resource use in the Blue Nile Basin. Colombo, Sri Lanka: International Water Management Institute, IWMI Working Paper 131, 87p, 2008.

Bewket, W. and Sterk, G.: Assessment of soil erosion in cultivated fields using a survey methodology for rills in Chemoga watershed, Ethiopia. Agriculture, Ecosystem and Environment, 97, 81-93, 2003.

Easton, Z. M., Fuka, D. R., White, E. D., Collick, A. S., Biruk A., B., McCartney, M., Awulachew, S. B., Ahmed, A. A., and Steenhuis, T. S.: A multi basin SWAT model analysis of runoff and sedimentation in the Blue Nile, Ethiopia, Hydrol. Earth Syst. Sci., 14, 1827–1841, doi: 10.5194/hess-14-1827-2010, 2010.

Fredlund, D.G., Xing, A., Fredlund, M.D., and Barbour, S.L.: The relationship of the unsaturated soil shear strength function to the soil-water characteristic curve. Canadian Geotechnical Journal, 32, 40-448, 1995.

Gani, N. D. Gani, M. R. and Abdelsalam, M. G.: Blue Nile incision on the Ethiopian Plateau: Pulsed plateau growth, Pliocene uplift, and hominin evolution, GSA Today, v. 17, p. 4-11, 2007.

Gao, B., Walter, M.T., Steenhuis, T.S., Parlange, J.-Y., Richards, B.K., Hogarth, W.L., and Rose, C.W.: Investigating raindrop effects on transport of sediment and non-sorbed chemicals from soil to surface runoff. Journal of Hydrology, 308 313–320, 2005.

Garzanti, E., Ando, S., Vezzoli, G., Ali Abdel Megid, A., and El Kammar, A.: Petrology of Nile River sands (Ethiopia and Sudan): sediment budgets and erosion patterns, Earth Planet. Sc. Lett., 252(3–4), 327–341, 2006.

Grunder, M.: Soil conservation research in Ethiopia. Mountain Research and Development, 8(2/3): 145-151, 1988.

Haregeweyn, N. and Yohannes, F.: Testing and evaluation of the agricultural non-point source pollution model (AGNPS) on Augucho catchment, western Hararghe, Ethiopia. Agriculture Ecosystems & Environment 99: 201-212, 2003.

Hairsine, P. B. and Rose, C. W.: Rainfall Detachment and Deposition: Sediment Transport in the Absence of Flow-Driven Processes. Soil Sci. Am. J. 55: 320-324, 1991.

Hairsine, P. B. and Rose, C. W.: Modeling water erosion due to overland flow using physical principles 1. Sheet flow. Water resources research, 28(1): 237-243, 1992.

Heilig, A., Debruyn, D., Walter, M.T., Rose, C.W., Parlange, J.Y., Sander, G.C., Hairsine, P.B., Hogarth, W.L., Walker, L.P., Steenhuis, T.S.: Testing a mechanistic soil erosion model with a simple experiment. J. Hydrol. 244 (1–2), 9–16, 2001.

Hofer, M., Lehmann, P., Stähli, M., Seifert, S., and Krafczyk, M.: Two approaches to modeling the initiation and development of rills in a man-made catchment. Water Resources Research, 48, W01531, doi: 10.1029/2011WR010719, 2012

Hurni, H.: Soil Erosion and Soil Formation in Agricultural Ecosystems: Ethiopia and Northern Thailand. Mountain Research and Development, 3(2): 131-142, 1983.

Hurni, H.: Degradation and Conservation of the Resources in the Ethiopian highlands. Mountain Research and Development 8(2/3): 123-130, 1988.

Hurni, H.: Land degradation, famine, and land resource scenarios in Ethiopia. In: Pimentel, D. (Ed.), World Soil Erosion and Conservation. Cambridge University Press, Cambridge, pp. 27–62, 1993

Mekonnen, M. and Melesse, M.: Soil erosion mapping and hotspots area identification using GIS and Remote Sensing in Northwest Ethiopian Highlands, near Lake Tana. in: Nile River: Hydrology, Climate and Land Use, edited by: Melesse, A., Springer Science Publisher, New York, 2011.

Messerli, B., Hurni, H., Wolde-Semayat, B., Tedla, S., Ives, J. D. and Wolde-Mariam, M.: African mountains and highlands, Mountain Research and Development, Vol 2/3, 93-100, 1988.

Mitiku, H., Herweg, K., Stillhardt, B.: Sustainable land management –A new approach to soil and water conservation in Ethiopia. Mekelle, Ethiopia: Land Resource Management and Environmental Protection Department, Mekelle university; Bern, Switzerland: Center for Development and Environment (CDE), University of Bern and Swiss National Center of Competence in Research (NCCR) North-South, 269pp, 2006.

Mohammed, A., Yohannes, F., and Zeleke, G.: Validation of agricultural non-point source (AGNPS) pollution model in Kori watershed, South Wollo, Ethiopia, Int. J. Appl. Earth Obs., 6, 97–109, 2004.

Nyssen, J., Poesen, J., Veyret-Picot, M., Moeyersons, J., Haile, M., Deckers J., Dewit, J., Naudts, J., Teka, K., Govers, G.: Assessment of gully erosion rates through interviews and measurements: a case study from northern Ethiopia. Earth Surface Processes and Landforms 31, 167-185, 2006.

Setegn, S G., Ragahavan S., Bijan D.: Hydrological Modeling in the LakeTana Basin, Ethiopia using SWAT model. The Open Hydrology Journal 2: 49-62, 2008.

Steenhuis, T.S., A.S. Collick, Z. M. Easton, E.S. Leggesse, H. K. Bayabil, E. D. White, S.B. Awulachew, E. Adgo5, A.A. Ahmed.: Predicting Discharge and Erosion for the Abay (Blue Nile) with a Simple Model. Hydrological Processes 23: 3728–3737, 2009.

Sutcliffe, J.P.: Economic Assessment of Land Degradation in the Ethiopian Highlands: A Case Study. National Conservation Strategy Secretariat, Ministry of Planning and Economic Development, Addis Ababa, Ethiopia, 1993.

Tadesse, G.: Land degradation: a challenge to Ethiopia. Environmental Management 27, 815-824, 2001

Tamene, L., Park, S. J., Dikau R., P.L.G. Vlek.: Analysis of factors determining sediment yield variability in the highlands of northern Ethiopia. Gemprphology 76: 76-91, 2006.

Tesemma, Z. K., Mohamed, Y. A., and Steenhuis, T. S.: Trends in rainfall and runoff in the Blue Nile Basin: 1964–2003, Hydrol. Process., 24(25), 3747–3758, doi:10.1002/hyp.7893, 2010.

Tilahun, S. A., R. Mukundan, B. A. Demisse, C. Guzman, B. C. Tarakegn, T. A. Engda , Z. M. Easton , A. S. Collick, A. D. Zegeye, E. M. Schneiderman, J.Y. Parlange, and T. S. Steenhuis.: A Saturation Excess Erosion Model. In: Proceedings International Symposium on Erosion and Landscape Evolution, ISELE paper number 11061. D.C. Flanagan, J.C. Ascough II, and J.L. Nieber (eds.). St. Joseph, Mich: ASABE, 2011

Tilahun S. A., Guzman C. D., Zegeye A. D., Engda T. A., Collick A. S., Rimmer A., and Steenhuis T. S.: An efficient semi-distributed hillslope erosion model for the sub humid Ethiopian Highlands. HESSD-9-2121-2012, 2012

Vanmaercke, M., Zenebe, A., Poesen, J., Nyssen, J., Vertstraeten, G., and Deckers, J.: Sediment dynamics and the role of flash floods in sediment export from medium-sized catchments: a case study from the semi-arid tropical highlands in Northern Ethiopia, J. Soil Sediment., 10(4), 611–627, 2010.

Vanmaercke, M., Poesen, J., Maetens, W., Vente, J., and Verstraeten, G.: Sediment yield as a desertification risk indicator. Science of the Total Environment, 409, 1715-1725, doi:10.1016/j.scitotenv. 2011.01.034, 2011.

Wischmeier, W.H., and Smith, D.D.. Predicting rainfall erosion losses—a guide to conservation planning. USDA Agric. Handbook 537, 58 p, 1978.

Yalin, M.S.: An expression for bed-load transportation. ASCE, Journal of the Hydraulics Division 89 (HY3), 221–250, 1963.

Zegeye, A.D., T.S. Steenhuis, R.W. Blake, S. Kidnau, A.S. Collick and F. Dadgari.: Assessment of Upland Erosion Processes and Farmer Perception of Land Conservation in Debre-Mewi Watershed, near Lake Tana, Ethiopia. Ecohydrologica 10: 297-306, 2010.

Zeleke, G.: Landscape Dynamics and Soil Erosion Process Modeling in the North-western Ethiopian Highlands. African Studies Series A 16, Geographica Bernensia, Berne, 2000.

CHAPTER 4: AN EFFICIENT SEMI-DISTRIBUTED HILLSLOPE EROSION MODEL FOR THE SUB HUMID ETHIOPIAN HIGHLANDS

Abstract

Erosion modeling has been generally scaling up from plot scale but not based on landscape topographic position, which is a main variable in saturation excess runoff. In addition, predicting sediment loss in Africa has been hampered by using models that have been developed in western countries and do not perform as well in the monsoon climate prevailing in most of the continent. The objective of this paper is to develop a hillslope erosion model that can be used in the Ethiopian highlands in Africa. We base our sediment prediction on a semi-distributed water balance hydrology model that predicts surface runoff from severely degraded lands and from bottom lands that become saturated during the rainy season and estimates interflow and base flow from the remaining portions of the landscape. By developing an equation that relates surface runoff to sediment concentration generated from runoff source areas, assuming that base flow and interflow are sediment free, we were able to predict daily sediment concentrations from the Anjeni watershed with a Nash Sutcliffe efficiency ranging from 0.64 to 0.77 using only two calibrated sediment parameters. Anjeni is a 113 ha watershed in the 17.4 million ha Blue Nile Basin in the Ethiopian Highlands. The daily flows were predicted with Nash Sutcliffe efficiency values ranging from 0.80 to 0.93 if degraded areas were assumed the major sediment source areas and covered 14% of the Anjeni watershed and 20% of the Blue Nile basin. The analysis suggests that identifying the runoff source areas and predicting the surface runoff correctly is an important step in predicting the sediment concentration.

4.1 Introduction

In the African highlands, erosion has occurred for a long time (Lal, 1985; Nyssen et al., 2004). In colonial times, the devastating effects of soil loss from newly developed agricultural lands was noted and the need to combat it was expressed (Champion, 1933). However, despite large investments in soil and water conservation practices, sediment yields have been increasing in Africa (Lal, 1985; Fleitmann et al., 2007). The reasons mentioned for increased soil loss were greater population pressure and consequently more intensive cultivation (Fleitmann et al., 2007). In addition, most of the soil and water conservation practices were imported from the US without considerations of their appropriateness for the monsoon climate (Hudson, 1987). These imported practices were usually placed on steep slopes to reduce soil loss based on research recommendations at the plot scale (Wischmeier and Smith, 1978; EI-Swaify et al., 1982; Hudson, 1957, 1983) rather than the watershed scale. In Ethiopia, Mituku et al. (2006) reported that 40% of all erosion is caused by the wrong installation of soil and water conservation (SWC) practices.

For the Blue Nile basin, a part of the Ethiopian highlands, reported soil losses varying from 1 to over 400 t $ha^{-1}year^{-1}$ (Hurni, 1988; Mitiku et al., 2006; Tebebu et al., 2010) with an average of 7 t ha^{-1}, or equivalent to a depth 0.5 mm (Garzanti et al., 2006). At the same time several large dams are planned in the Blue Nile Basin; therefore, these future developments urgently need better ways to reduce soil loss in order to sustain the efficient operation of the dams well into the future.

In the coming decades, models will play an important role in erosion control of this basin, especially by prioritizing the location for erosion control. However, this is problematic because most erosion modeling (just as with evaluation of soil and water conservation practices) is based on plot scale research (Wischmeier and Smith, 1978; Vanmaercke et al., 2011). Although Hurni (1985) adapted the empirical plot scale USLE for Ethiopian conditions, Eweg et al. (1998) and Zegeye et al. (2011) showed that the modified USLE can be used to estimate average annual soil losses but reliable predictions of the spatial and temporal distributions were questionable.

Agricultural Non-Point Source Pollution (AGNPS) model (Haregeweyn and Yohannes, 2003; Mohammed et al., 2004), and the Soil and Water Assessment Tool (SWAT) (Setegn et al., 2008) where USLE scaled up to watershed scale were applied in the Ethiopian highlands. These models that use both the curve number (infiltration excess runoff) for the hydrology and the USLE for erosion predictions do not perform satisfactorily even on a monthly basis. The modified SWAT Water Balance (WB) model (Easton et al., 2010; White et al., 2010) with saturation excess gave better results in Ethiopia, while the Water Erosion Prediction Project (WEPP) (Zeleke, 2000), which has a more advanced erosion prediction tool but still used infiltration excess for runoff, performed below average.

Scaling up plot scale soil estimates to watershed or basin scale invariably leads to overestimation or underestimation at the outlet (Vanmaercke et al., 2011). Discussions of scaling up from plot scale is not only limited to erosion. For example, for discharge predictions Savenije (2010) writes "physically based small scale basic principles (such as the Darcy, Richards, and Navier-Stokes equations) with detailed distributed modeling, leads to equifinality and high predictive uncertainty, mostly because these methods ill account for heterogeneity, preferential pathways and structural patterns on and under the surface". Other researchers are not as pessimistic and argue that Darcy's and Richards' law apply and can predict with a reasonable degree of accuracy the moisture contents and leaching patterns after some calibration of the parameters (Kung et al., 2000; Kim et al, 2005; Zehe et al, 2010; Klaus and Zehe, 2011). Although, due to lack of fine and detailed information, the best way of finding the regularity in the "calibration" parameters is being intensively researched, there is agreement that there exists some measure of organized complexity at intermediate and larger scales (Dooge 1986, 2005; Savenije, 2010; He et al, 2011).

The objective of this study is therefore to develop a hillslope erosion model and goes beyond scaling up plot prediction tools for erosion prediction by using a reasonably accurate hydrology model of Steenhuis et al. (2009) to improve sediment concentration predictions in the Ethiopian highlands at several scales. Our conceptual model will use the patterns of self-organization introduced by Savenije (2010) to model the discharge and the sediment concentration of two watersheds in the Ethiopian highlands varying greatly in size. The use of relatively simple watershed models utilizes the realm of the organized complexity implicit in naturally formed catchments and river basins (Dooge, 1986, 2005 and Savenije, 2010). Our experience confirms that in (semi) humid Ethiopian highlands and in the Catskill mountain (New York State) watersheds with saturated excess runoff, simple catchment-scale models can make use successfully of emerging patterns of self-organization because these watersheds always wet up similarly (Bayabil et al., 2011).

In the new approach, we combined (and tested further at smaller scales) the hydrology model of Steenhuis et al. (2009) and Tesemma et al. (2010) with the simplified erosion models from the Rose and Hairsine group in Australia and test both the hydrology and erosion models at small and large scales. The erosion model closely follows the model of Hairsine and Rose (1992a, b) as developed by Rose (1993) and that of Ciesiolka et al. (1995) and Yu et al. (1997) assuming that a linear relationship between sediment concentration and velocity from runoff producing areas. It also assumes dilution with interflow similar to the Steenhuis et al. (2009) sediment concentration prediction approach. The Harisine and Rose model predicted sediment concentrations successfully in the monsoon climate of the Philippines, Thailand and Malaysia using observed stream flows (Rose, 2001). In the foot hills of Nepal, WEPP predicted soil erosion the best from USLE type plots followed by the Griffith University Erosion System Template (GUEST) Technology and European Soil Erosion Model (EUSROSEM) (Kandel et al., 2001).

Sediment concentration data are available for a few watersheds in Ethiopia. These watersheds were established by the Soil Conservation Research Program (SCRP) initiated in 1981 in order to support and monitor SWC efforts in the highlands of Ethiopia by the Governments of Ethiopia and Switzerland. In this paper, we used the data of one of these experimental watersheds located in the Ethiopian Highlands, Anjeni, and the Ethiopian Blue Nile basin at the Ethiopian–Sudan border.

4.2 Material and Methods

4.2.1 Model development:

4.2.1.1 Conceptual model

The model predicts daily sediment concentrations. A daily time step was chosen for predicting discharge because the data for rainfall distribution within a day was generally not available. The prediction of daily sediment concentration is based on the concept that erosion is produced in areas with surface runoff. Thus, in our hydrology model that simulates surface runoff from saturated and degraded hillside areas, erosion is simulated only from these runoff producing source areas. Practically, saturated areas are identified in the watershed during most times of the year as green areas with flat or gentle slopes while degraded lands are defined here as those lands that are shallow and store only small amounts of rainwater, and therefore, produce runoff and support very little vegetation. Erosion is negligible from the non-degraded hillsides because almost all water infiltrates (Bayabil et al., 2010; Engda et al., 2011). Erosion rates are greater from the more heavily degraded areas without plant cover than from the saturated source areas with natural vegetation. The only exception could be in the beginning of the rainy season in cases where these soils were used for growing a crop during the dry season. This is not simulated since we do not have this information.

The other concept is that baseflow and interflow play an important role in the conversion of event-based sediment concentration to daily sediment concentration. This directly affects how the sediment concentrations are simulated. To demonstrate this, two storms are depicted one in the beginning of the short rainy season (24 April 1992, Figure 4-1a) and one later in the main rainy season (19 July 1992, Figure 4-1b) when more than 500 mm of cumulative effective rainfall had fallen since the beginning of the main rainy season for the Anjeni watershed which will be discussed later in more detail. At this time, the watershed had wetted up and interflow occurred (Liu et al., 2008). The surface runoff for both events is similar with peak runoff at 400–500 L s^{-1} above the flow recorded prior to the beginning of the storm. The duration of the runoff event was approximately 2 h. The peak sediment concentrations were nearly the same around 30–35 g L^{-1}. Base flow discharge is low during the beginning of the rainy season (around 10 L s^{-1} for April or equivalent to 0.8 mm day^{-1} over the whole watershed). Baseflow increases during the rainy season. It is approximately 50 L s^{-1} (equivalent to 4 mm day^{-1}) in July. Despite the similar surface runoff characteristics, the April discharge was 2.4×10^3 m^3 day^{-1} and for July was 6.5×10^3 m^3 day^{-1}. The average daily sediment concentrations can be obtained by dividing the load by the total flow resulting in concentrations of 11.3 g L^{-1} for the April storm and 4.4 g L^{-1} for the July storm. What is important to note is that in calculating the average daily stream flow data, the peak flows occur less than 10% of the time, thus the baseflow contributions when averaged over a day is a significant portion of the daily flow for the July storm when the watershed is in equilibrium. In essence, the baseflow dilutes the peak storm concentration when simulated on a daily basis later in the rainy season. It is therefore important to incorporate the contribution of baseflow in the prediction of sediment concentration.

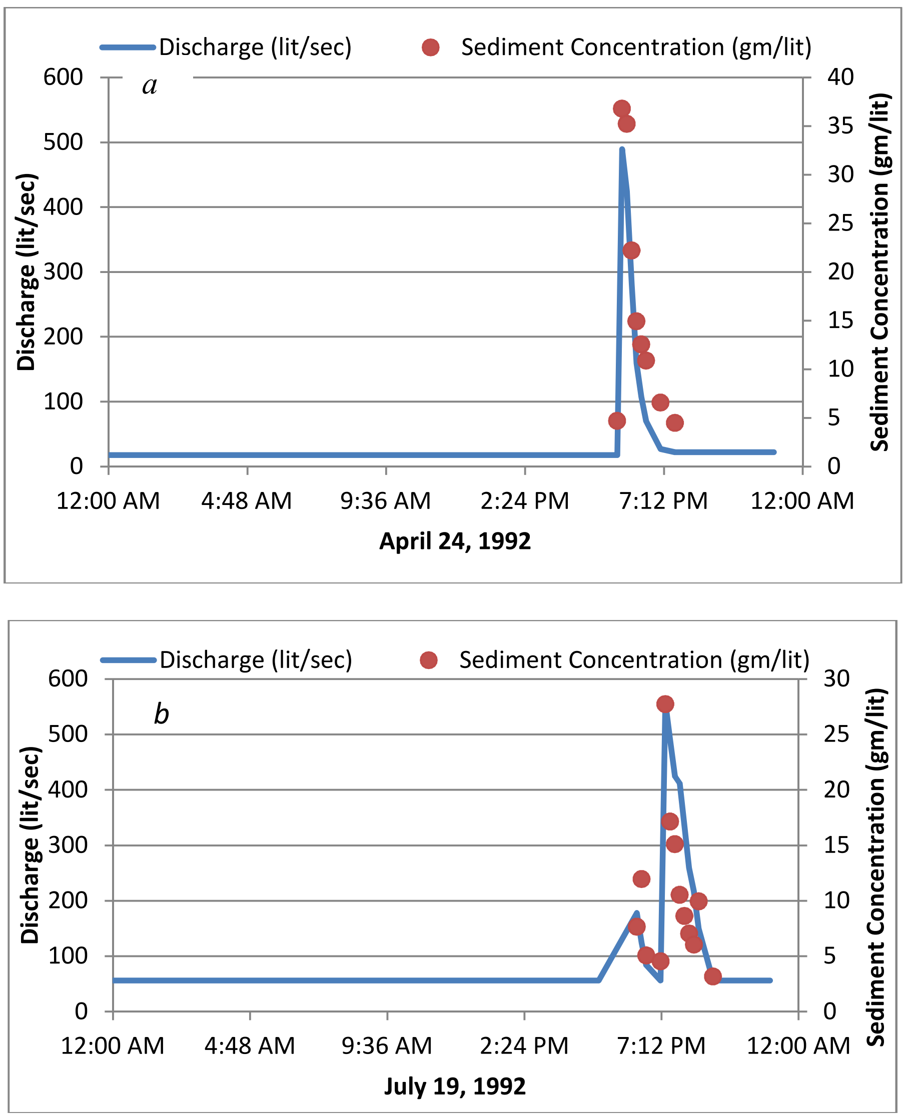

Figure 4-1: Measured discharge (LS^{-1}) and sediment concentration ($g\ L^{-1}$) during (a) 24 April 1992 and (b) 19 July 1992 for Anjeni watershed.

4.2.1.2 Hydrology model

The watershed is divided into three regions (Figure 4-2): two surface runoff source areas consisting of areas near the river that become saturated during the wet monsoon period and the degraded hillsides with little or no soil cover. The remaining hillsides are the third zone where the rainwater infiltrates and becomes either interflow (zero order reservoir) or base flow (first order reservoir) depending on its path to the stream. Rainwater on the hillside infiltrates and becomes either interflow or baseflow depending on its path to the stream. A daily water balance is kept for each of the regions using the Thornthwaite-Mather procedure (Thornthwaite and Mather, 1955; Steenhuis and van der Molen, 1986) for calculating the actual evaporation. Overland flow is simulated when the soil is at saturation for the potentially saturated areas and the degraded hillsides (Figure 4-2). Since the soil in the degraded areas is shallow, only minor amounts of rainfall are required before the soil saturates and runoff is produced. When the soil on the hillsides reaches field capacity, additional rainfall is released to the first order base flow reservoir and a linear interflow reservoir (Figure 4-2). More detail on the daily water balance and subsurface flow equations derivations are given in Steenhuis et al. (2009) and Tesemma et al. (2010) where the model was applied to the whole Blue Nile Basin using a Microsoft Excel spreadsheet.

Inputs to the model are daily rainfall and potential evaporation. Calibrated parameters of the model are the extent of the three areas in the watershed, the amount of storage in the soil between witling point and saturation for the runoff producing areas, and wilting point and field capacity for the hillside. In addition, there are three more subsurface parameters: a maximum storage and half-life for the first order groundwater reservoir, and the time it takes for a hill slope to drain after a rain storm for the linear interflow reservoir.

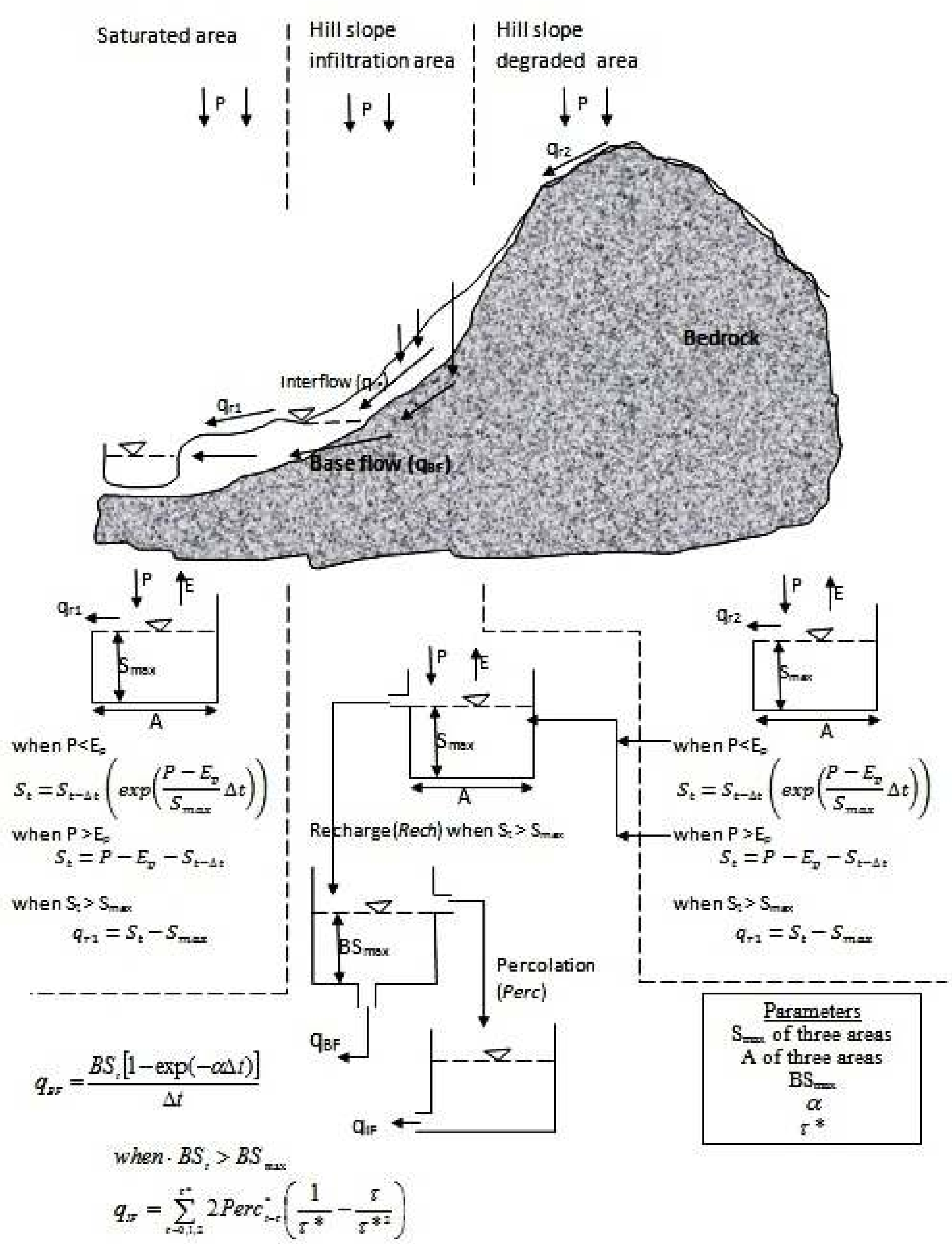

Figure 4-2: Conceptual hydrology model *(P is precipitation; E_p is potential evaporation; A is area fraction for components of 1-saturated area, 2-degarded area and 3-infiltration areas; S_{max} is maximum water storage capacity of the three areas; BS_{max} is maximum base flow storage of linear reservoir; $t_{½}$ (=0.69/α) is the time it takes in days to reduce the volume of the base flow reservoir by a factor of two under no recharge condition;, τ* is the duration of the period after a single rainstorm until interflow ceases).*

4.2.1.3 Sediment model

In the sediment model, we assume for simplicity that the erosion process is transport limiting. Then for the two source areas, the mean suspended sediment concentration C (kg/m^3) is a function of flow rate and a coefficient dependent on landscape and sediment characteristics (Hairsine and Rose, 1992a, b; Rose et al., 1993; Siepel et al., 2002; Ciesiolka et al., 1995 and Yu et al., 1997). The derivation of equation 1 is shown in Appendix C3.

$$C = a\, q^{n} \qquad (1)$$

where q is the runoff rate per unit area from each source areas (m/day), a is a constant which is a function of the slope, Manning's roughness coefficient, slope length, and the effective depositability (Yu et al., 1997) and n is the exponent that takes a value of 0.4 assuming a linear relationship between sediment concentration and velocity and wide channel on the runoff producing areas (Ciesiolka et al., 1995 and Yu et al., 1997). As water depth increases, *a,* essentially becomes independent of the runoff rate and can be taken as a constant such as in this application where we are interested in sediment concentration at the outlet of watersheds of over 100 ha (Lisle et al., 1996).

Sediment yield (tons/day/ha) Y_i, for each of the two runoff source areas, i, then becomes

$$Y_i = q_i \times q_i^{0.4} \times a \qquad (2)$$

To calculate the suspended sediment concentration at the watershed outlet, we note that the discharge Q_T can be written in terms of the contributions of the three areas delineated in the watershed.

$$q_{T_t} = A_1 q_{r1_t} + A_2 q_{r2_t} + A_3\left(q_{BF_t} + q_{IF_t}\right) \qquad 3$$

Where q_{r1} and q_{r2} are the runoff rates expressed in depths units for contributing area A_1 is the fractional saturated area and A_2 is the fractional degraded area. A_3 is the fractional contributing area for baseflow, q_{BFt} and interflow, q_{IFt}.

Sediment yield in the stream depends on the amount of suspended sediment delivered by each component of the stream flow. The daily sediment yield equation in its most general form is:

$$Y_t = A_1 q_{r1_t} C_{1_t} + A_2 q_{r2_t} C_{2_t} + A_3\left(q_{BF_t} C_{BF_t} + q_{IF_t} C_{IF_t}\right) \qquad 4$$

Where C_1 and C_2 and C_3 are the sediment concentration in runoff from the saturated area, and degraded area respectively C_{BF_t} is the sediment concentration in the baseflow and C_{IF_t} the concentration in interflow. Recalling that sediments concentration, C, is related to the discharge as shown in Eq. 1, Eq. 4 can be rewritten as:

$$Y_t = a_1 A_1 q_{r1_t}^{n+1} + a_2 A_2 q_{r2_t}^{n+1} + A_3\left(a_{BF} q_{BF_t}^{n+1} + a_{IF} q_{IF_t}^{n+1}\right) \qquad 5$$

Which simplifies to a relationship between sediment yield and discharge for n =0.4

$$Y_t = a_1 A_1 q_{1_t}^{1.4} + a_2 A_2 q_{2_t}^{1.4} + A_3\left(a_{BF} q_{BF_t}^{1.4} + a_{IF} q_{IF_t}^{1.4}\right) \qquad 6$$

The superscript of q in Eq. 6 is within the range from 0.5 to 2 in the most common sediment transport capacity models (Prosser and Rustomji, 2000). By dividing Eq.6 by the total discharge (Eq. 4.) and taking the sediment concentration in the base and interflow as zero (i.e., a_{BF}=0 and a_{IF}=0), the sediment concentration can be found as:

$$C_t = \frac{a_1 A_1 q_{r1_t}^{1.4} + a_2 A_2 q_{r2_t}^{1.4}}{A_1 q_{r1_t} + A_2 q_{r2_t} + A_3\left(q_{BF_t} + q_{IF_t}\right)} \qquad 7$$

All parameters in Eq. 7 can be obtained from the hydrologic simulation with the exception of a_1 and a_2 that need to be calibrated with existing field data.

4.2.2 Description of Anjeni watershed and Blue Nile Basin

Anjeni is one of the seven experimental watersheds that were in operation in June 1984 as part of the Soil Conservation Research Program (SCRP), a collaborative project of the University of Berne, Switzerland, and the Ministry of Agriculture, Ethiopia. This watershed is in the Ethiopian Highlands and drains into the Blue Nile Basin.

The Anjeni watershed (Figure 4-3 and Table 4-1) covers an area of 113.4 ha with elevations ranging between 2405 and 2507m. It is located approximately at the center of the Blue Nile Basin that covers 17,400,000 ha. Anjeni is sub-humid in climate while the Blue Nile flows from humid to semi-arid climates on the way to the Ethiopian Sudan border. The annual rainfall of the basin ranges from approximately 2000mm in the southeast to nearly 1000 in the northeast and 1690 mm at Anjeni. The rainfall at Anjeni is unimodal which lasts from the middle of May to the middle of October. Mean daily temperature ranges from approximately 6^0C to 25^0C in the basin as well as in the Anjeni Watershed.

The basin has a rugged topography and considerable variation in altitude ranging from 480 m to 4260 m highly incised by Blue Nile River and its tributaries in the northwest direction. The highlands of the basin are mainly basaltic rock and the lower part is predominantly basement complex rocks. The Anjeni watershed at the highland of the basin is oriented north-south and flanked on three sides by plateau ridges. Most of the watershed is on slopes ranging from 8 to 30%. The geological formation of this watershed area belongs to the basaltic Trap series of the Tertiary volcanic eruptions, and the topography of the area is typical of Tertiary volcanic landscapes deeply incised by streams (Zeleke, 2000). There is high gully formation at the upper part of the watershed where a perennial spring is located at the head of the gully and becomes a source for a river called Minchet.

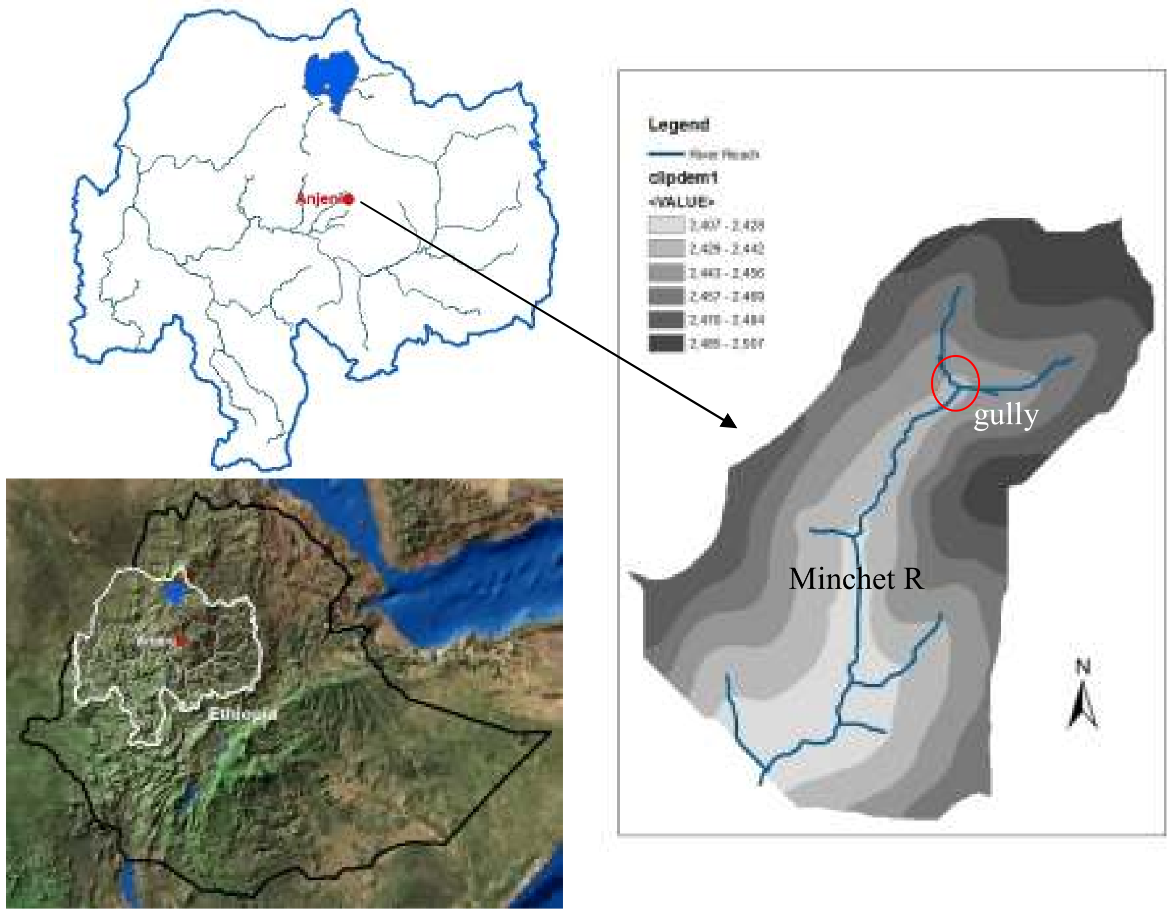

Figure 4-3: Location, watershed boundary and drainage map of Anjeni Watershed and Blue Nile Basin

Table 4-1: Location, description, and data used in the model for the Anjeni sites (SCRP, 2000)

Area Description	
• Size of the area (ha)	113.4
• Location	37°31’E and 10°40’N
• Elevation (m a.s.l)	2405-2507
• Mean Annual Rainfall (mm)	1690
Length of Data	
1. Precipitation (mm/day)	1988 - 1997
2. Potential evaporation (mm/day)	1988-1997 (1995-1996 incomplete)
3. Stream flow (mm/day)	1988-1997
4. Sediment concentration (g/l)	1988-1997 (1988, 1994 and 1997 incomplete)
Periods regarding conservation practices	
5. No conservation	1984-1985
6. Fanya Juu conservation implementation	1986
7. Full terraces developed	1992

Alisols and Leptosols (21%), Nitisols (16%) and Vertisols (15%) are the dominant soil types in the basin with shallow and permeable soil underlain by bedrock on the highlands and deeper soil at the lower reaches of the basin and its tributaries (Betrie et al., 2011). The soils of Anjeni have developed on the basalt and volcanic ash of the plateau. The southern part of the watershed with valley floors and the depressions of the foothill land consist of deep and highly conductive Humic Alisols and Haplic Nitisols, while moderately deep Cambisols cover the middle area and the shallow Haplic Alisols and Humic Nitisols cover the hillsides indicating land degradation processes (Zeleke, 2000). The very shallow Regosols and Leptosols soils covered 12% the hillsides (Leggesse, 2009).

Before 1986, no management activities existed in the Anjeni watershed and were monitored without any SWC (SCRP, 2000). Fanya juu (SWC structure comprised of a bund above and a drainage ditch below the bund (Thomas and Biamah, 1991)) were then constructed in early 1986 throughout the watershed and by 1992 had generally developed into terraces (Figure 4-4, Hanggi, 1997).

Figure 4-4: Flank portion of the Anjeni watershed which was developed to full terraces from Fanya juu conservation practices

4.2.3 Data

Since the establishment of the micro-watersheds by the Soil Conservation Research Project (SCRP) in 1984, fine resolution data on climate, hydrology, and suspended sediment from both river and test plots have been collected. In addition, an expansive data base has been established that serves as a data source to carry out hydrological, soil erosion, and conservation research activities at regional, national, and international levels. This watershed provided the most comprehensive data of daily rainfall, potential evaporation, stream flow, and sediment concentrations (Mitiku et al., 2006).

Stream flow and sediment concentration were measured at a station located at the outlet of each watershed by SCRP. The depth of water was taken with float-actuated recorders. The water level in the stream was measured daily at 08:00 a.m. In case of peak stream flow events, water level measurements and sediment samples were usually taken at ten-minute intervals during the event and every 30 minutes when water level decreased. Discharge was evaluated using the relation between the water level and stream discharge (Bossahart, 1997). The river stage-discharge relationship was determined using salt-dilution and current-meter methods.

One liter samples were taken from the river at the gauging station during the storm to determine the sediment concentration. Sampling started once the water in the gauging station looked turbid (brown), and the sampling continued at ten-minute intervals. When the runoff became clearer, the sampling interval was extended to thirty minutes and sampling continued until the runoff was visibly sediment free. The collected water samples were filtered using filter paper, sundried, and finally oven dried and weighed and net dry soil loss was calculated. Event-based sediment yields were summed over a daily period to determine daily sediment load. Daily sediment concentration was determined by dividing the daily sediment load by the total discharge during that day. These were then compared to the daily predicted sediment concentrations.

4.2.4 Model calibration and validation

4.2.4.1 Data

We calibrated first daily discharge values with the water balance model and subsequently the sediment concentrations with the sediment model of Eq. (7). The data used in the model is summarized in Table 4-1. In Anjeni, the period from 1988 to 1997 was used as data source for daily rainfall, potential evaporation and stream flow in this study. For calibration of the water balance model in Anjeni (Table 4-2), the data of year 1988 and 1990 were used and 1989, 1991–1994 and 1997 were used for validation. The climate data for the years 1995 and 1996 were incomplete and excluded from model development processes.

Table 4-2: Input parameters for daily and 10-days stream flow and sediment concentration modeling in the Anjeni watershed and Blue Nile Basin, respectively.

Components	Description	parameters	Unit	Calibrated values	
				Anjeni	Blue Nile
Hydrology	Saturated area	Area A_1	%	2	20
		S_{max} in A_1	mm	200	200
	Degraded area	Area A_2	%	14	20
		S_{max} in A_2	mm	10	10
	Hill side	Area A_3	%	50	60
		S_{max} in A_3	mm	100	300
	Subsurface flow parameters	BS_{max}	mm	100	20
		$t_{½}$	days	70	35
		τ*	days	10	140
Sediment	Subsurface flow	a_{BF}	$(g/l)(mm/day)^{-0.4}$	0	0
		a_{IF}	$(g/l)(mm/day)^{-0.4}$	0	0
	Saturated area	a_1	$(g/l)(mm/day)^{-0.4}$	0.2	0.2
	Degraded area	a_2	$(g/l)(mm/day)^{-0.4}$	3.40	1.2

A_i is area fraction for components of 1-saturated area, 2-degarded area and 3-infiltration zone; S_{max} is maximum water storage capacity; $t_{½}$ is the time it takes in days to reduce the volume of the base flow reservoir by a factor of two under no recharge condition;, BS_{max} is maximum base flow storage of linear reservoir; τ is the duration of the period after a single rainstorm until interflow ceases; a_i is calibrated parameter in sediment concentration model for components of base flow (BF), interflow(IF), saturated area (1) and degraded area (2).*

The sediment concentration data for the same years, except 1988, was excluded because of very low sediment concentration measurements. The low concentration might have been caused by bunds installed (Fanya juu) in the watershed in 1986 that captured all sediment effectively. Equilibrium was likely established in 1990, when the terraces were formed behind the bunds in the runoff source area. In the non-source area terrace were established in 1992 (Hanggi, 1997). Consequently, the year 1990 was used for calibration and the period 1991-1993 was used for validation in the sediment modeling.

The years with sediment concentrations data for the Blue Nile at the Sudan border was limited to three years 1993, 2003 and 2004. The period of 1993 was used to calibrate both hydrology and sediment models in the Blue Nile basin while the other two years 2003 and 2004 were used for validation.

4.2.4.2 Methods of calibration and validation

All the nine parameters (Figure 4-2) were calibrated for the hydrology model (Table 4-2). Initial values for calibrating parameters were based on Steenhuis et al. (2009) and Collick et al. (2009). These initial values were changed manually through randomly varying parameters in order that the best "closeness" or "goodness-of-fit" was achieved between simulated and observed subsurface and overland flow in the watershed. For partitioning the rainfall into surface runoff and recharge for sub-surface reservoirs, they consisted of the size (A) and the maximum storage capacity (S_{max}) for the three areas, and for the subsurface they involved the half-life ($t_{1/2}$) and maximum storage capacity (BS_{max}) of a linear aquifer and the drainage time of the zero order reservoir(τ^*).

In the sediment model, daily sediment load was first computed and then divided by the total daily stream flow using Eq.(7) to compute the daily sediment concentration. In the equation, there are two calibration parameters consisting of the constants for each of the two runoff source areas a_1 and a_2. These constants are changed manually in order to get a best fit between measured and simulated daily sediment concentration.

During model calibration and validation period, the Nash-Sutcliffe coefficient (NSE) (equation 8), coefficient of determination (R^2) with least square linear regression and the Root Mean Squared Error (RMSE) (equation 9) were used to evaluate the performance.

$$NSE = 1 - \frac{\sum_{i=1}^{n}\left(q_{obs(i)} - q_{sim(i)}\right)^2}{\sum_{i=1}^{n}\left(q_{obs(i)} - q_{obs(ave)}\right)^2} \qquad 8$$

$$RMSE = \sqrt{\frac{\sum_{i=1}^{n}\left(q_{obs(i)} - q_{sim(i)}\right)^2}{n-1}} \qquad 9$$

Where NSE is Nash-Sutcliffe efficiency, $q_{sim(i)}$ is simulated storm flow, $q_{obs(i)}$ is observed storm flow and $q_{obs(ave)}$ is average observed flow. The simulated storm flow is the sum of q_{r1}, q_{r2}, q_{BF} and q_{IF}. The NSE coefficient for the sediment concentration can be obtained similarly by replacing the "*q*" by "*C*". Coefficient of determination (R^2) describe the degree of collinearity between simulated and measured data while NSE determines the relative magnitude of the residual variance compared to the measured data variance (Moriasi et al., 2007). During calibration, parameters are optimized and searched for that resulted in R^2 values close to 1, a slope of 1 and y intercept of zero, and NSE to 1, and RMSE to zero.

4.3 Results and Discussion

The calibrated parameters are shown in Table 4-2 and the goodness of fit Nash-Sutcliffe coefficient (NSE), coefficient of determination R^2 and root mean squared error (RMSE) for the hydrology and sediment model are presented in Table 4-3. A comparison of predicted and observed daily stream flow for the Anjeni watershed is shown in Figure 4-5 and Appendix C1 Figure C1-1 and for sediment concentrations in Figure 4-6 and Appendix C1 Figure C1-2. For the Blue Nile Basin, Figure 4-7 shows both predicted and observed 10-day stream flow and 10-days average sediment concentration were shown in Figure 4-8.

Table 4-3: Runoff (q) and Sediment concentration (C) simulation efficiency as evaluated by statistical measures for daily time step in Anjeni watershed and Blue Nile Basin

Site			**Stream flow (mm)**		**Sediment Concentration (g/l)**	
			Calibration	**Validation**	**Calibration**	**Validation**
	Year		**1988 &1990**	**1989, 1991-1997**	**1990**	**1991-1993**
Anjeni	Mean	Observed	2.1	1.9	0.72	0.67
		Predicted	2.3	1.9	0.65	0.65
	Standard Deviation	Observed	3.2	2.7	2.24	2.19
		Predicted	3.6	2.8	1.94	1.78
	Statistical Parameters	NSE	0.86	0.80	0.78	0.64
		R^2	0.88	0.82	0.80	0.67
		RMSE	1.6	1.5	1.66	1.32
Blue Nile Basin	Year		**1993**	**2003-2004**	**1993**	**2003-2004**
	Mean	Observed	9.7	9.4	0.85	1.28
		Predicted	9.5	9.2	1.26	0.92
	Standard Deviation	Observed	9.9	9.9	1.51	2.32
		Predicted	11.8	9.2	1.98	1.87
	Statistical Parameters	NSE	0.93	0.92	0.76	0.76
		R^2	0.97	0.93	0.88	0.80
		RMSE	2.6	2.7	0.73	1.89

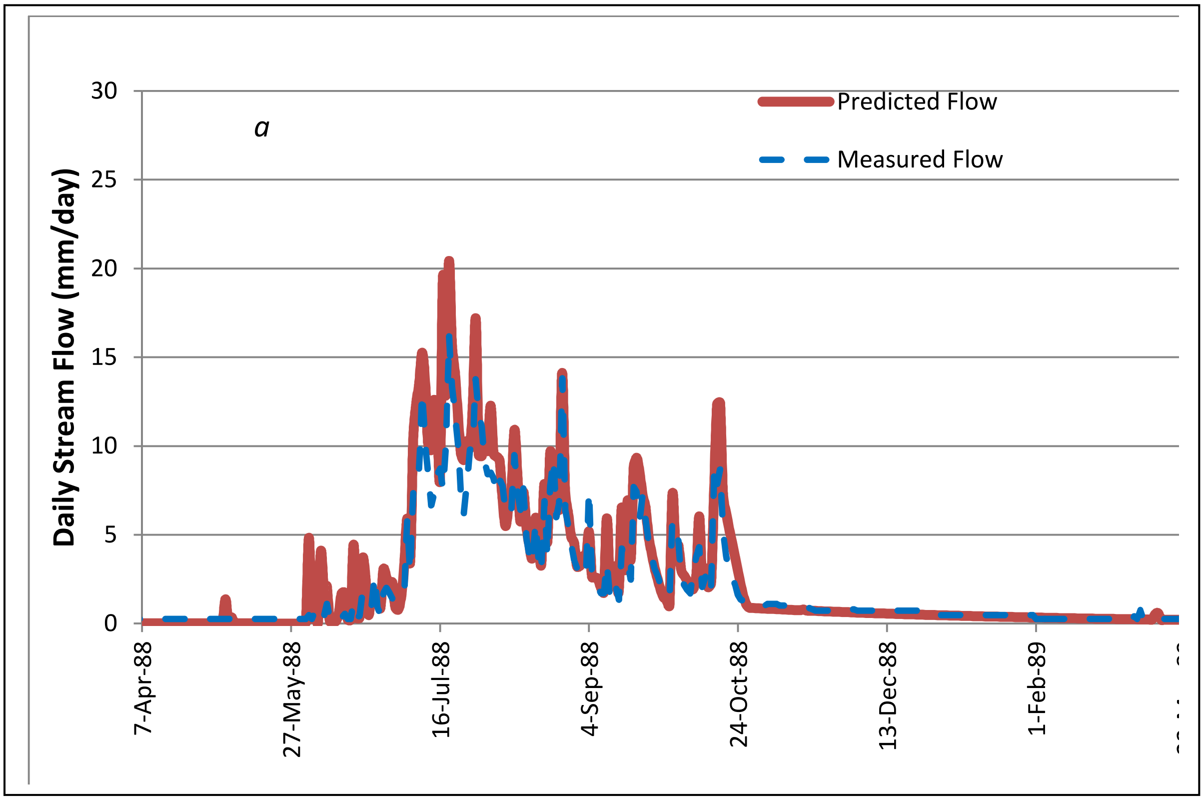
a
Predicted Flow
Measured Flow
Daily Stream Flow (mm/day)
30
25
20
15
10
5
0
7-Apr-88
27-May-88
16-Jul-88
4-Sep-88
24-Oct-88
13-Dec-88
1-Feb-89

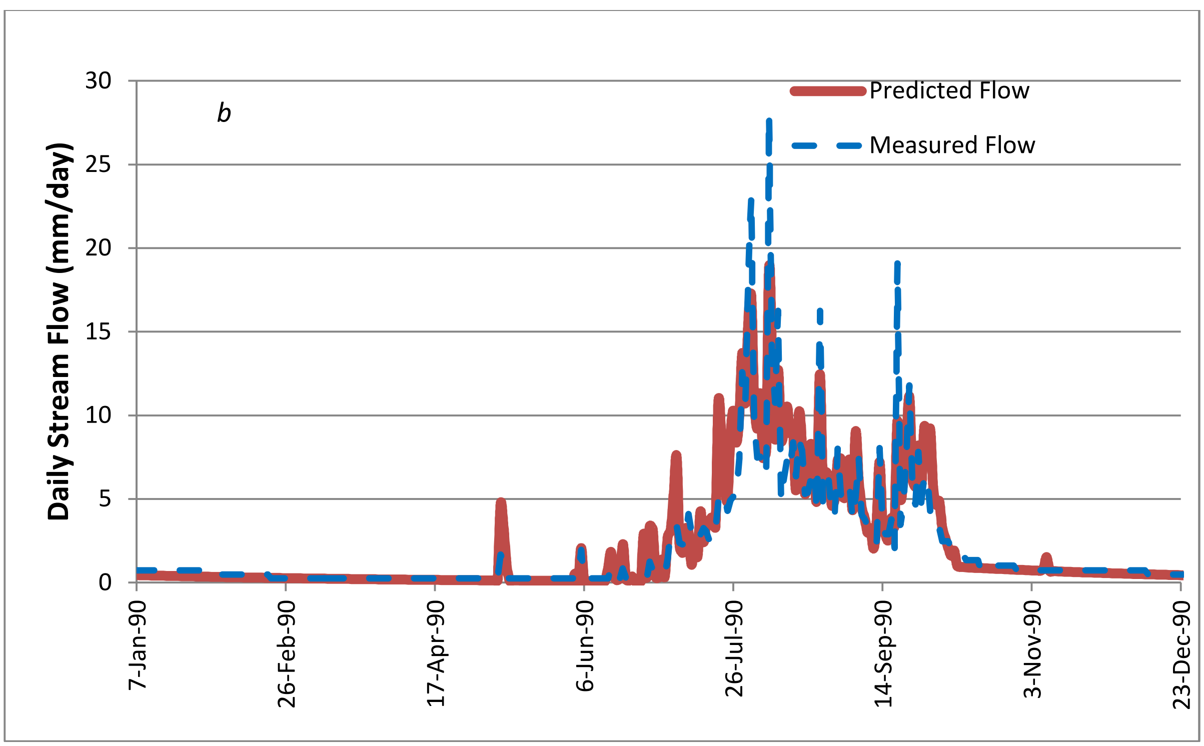
b
Predicted Flow
Measured Flow
Daily Stream Flow (mm/day)
30
25
20
15
10
5
0
7-Jan-90
26-Feb-90
17-Apr-90
6-Jun-90
26-Jul-90
14-Sep-90
3-Nov-90
23-Dec-90

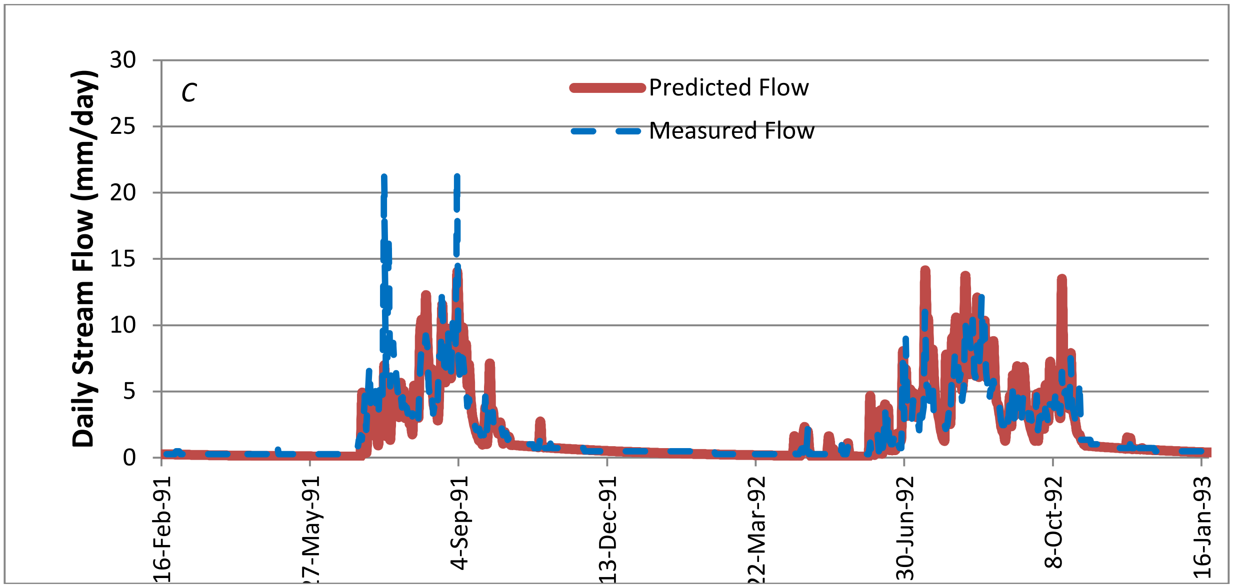

Figure 4-5: Predicted and observed daily stream flow for Anjeni watershed (a) and (b) calibrated discharge using 1988 and 1990 daily data (c) Validated discharge (shown only 1991 and 1992).

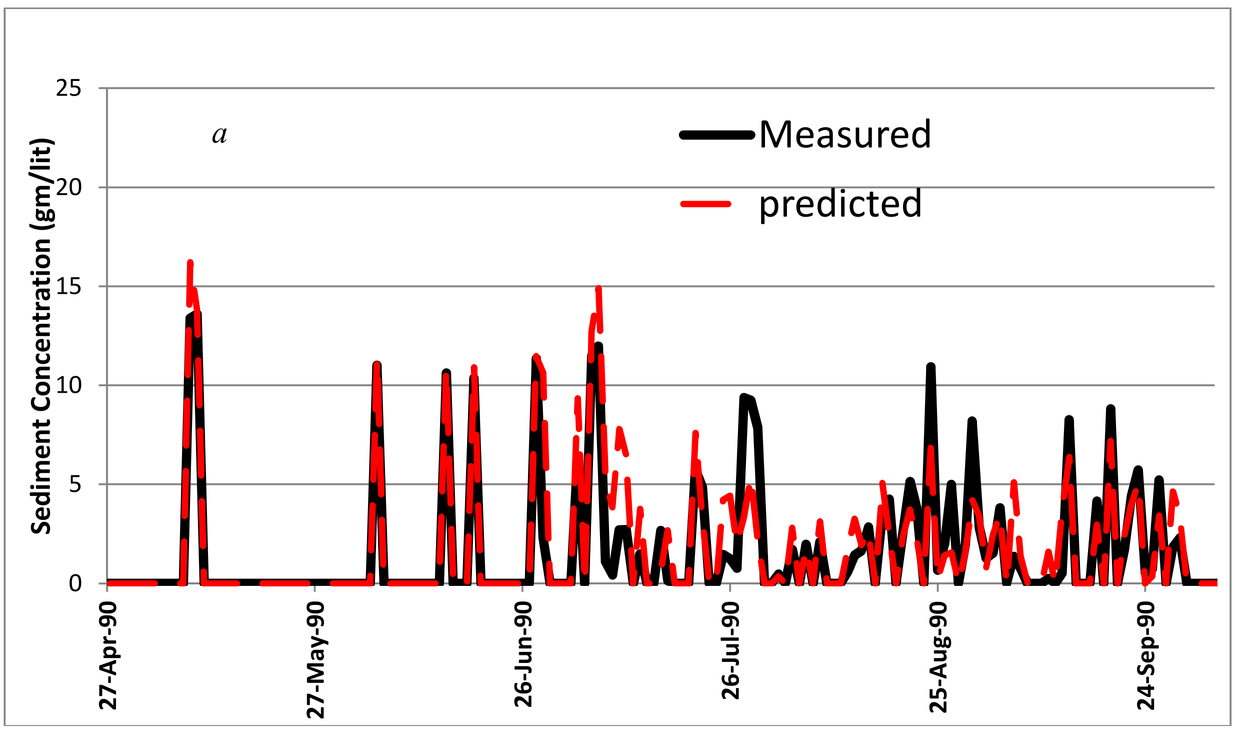

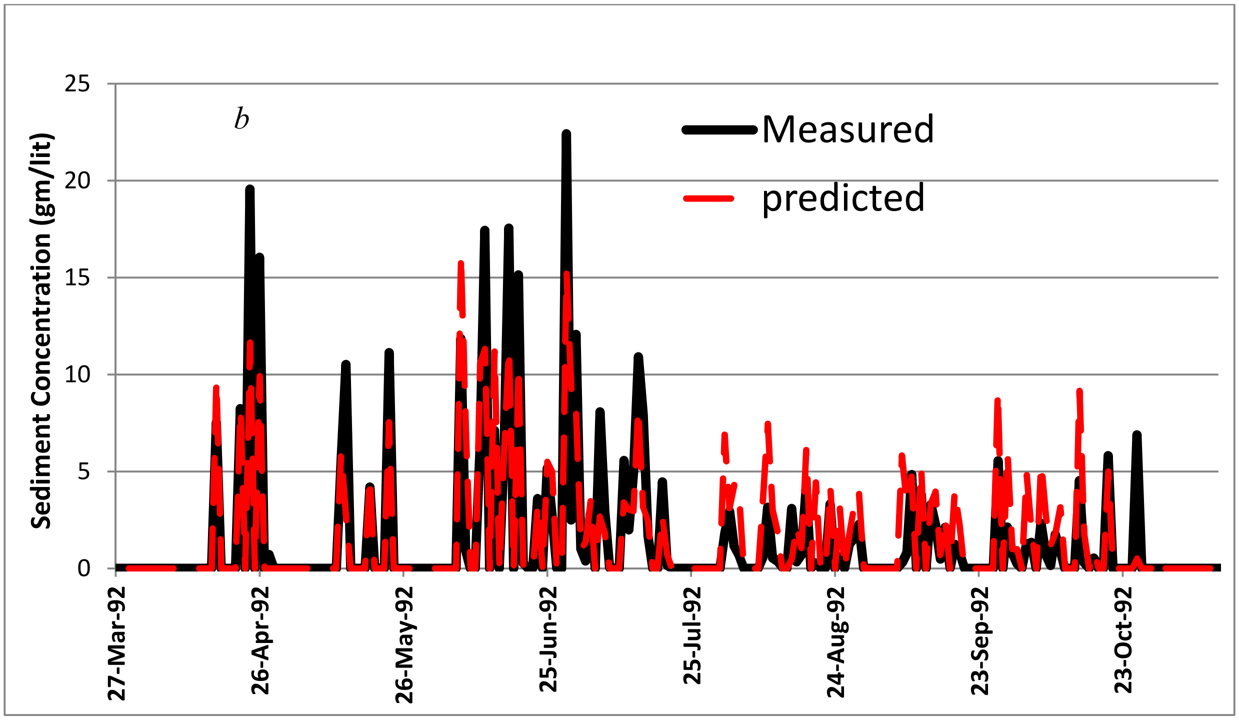

Figure 4-6: Predicted and observed daily sediments concentration for the Anjeni watershed (a) calibrated 1990 and (b) validated period (shown only 1992).

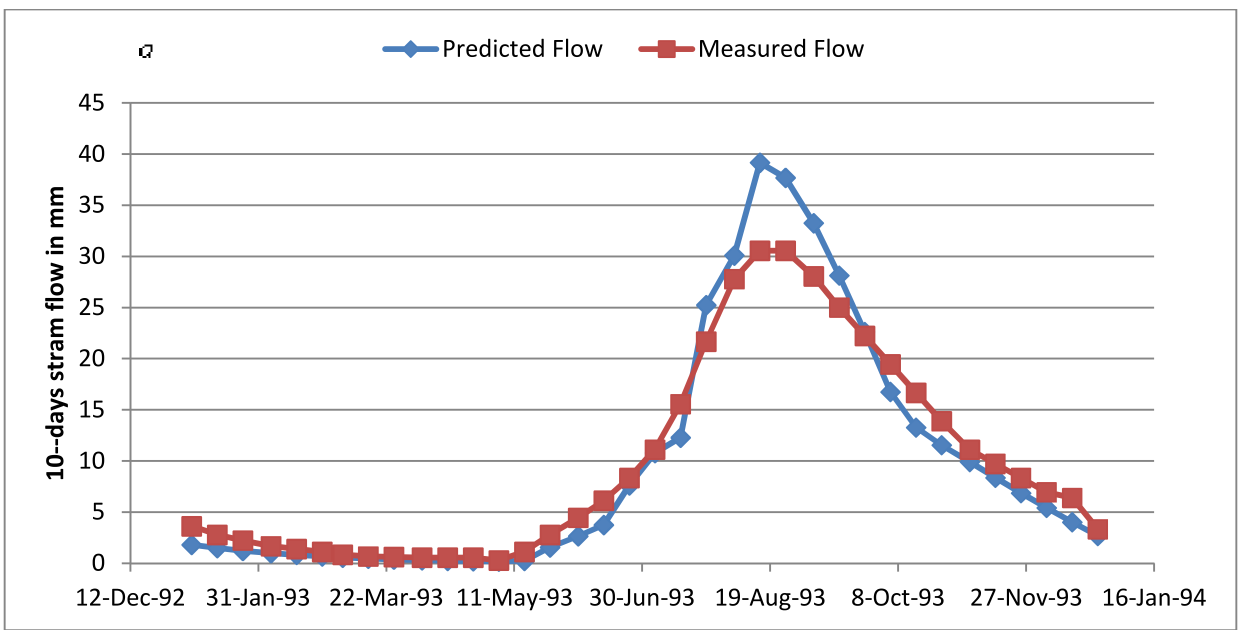

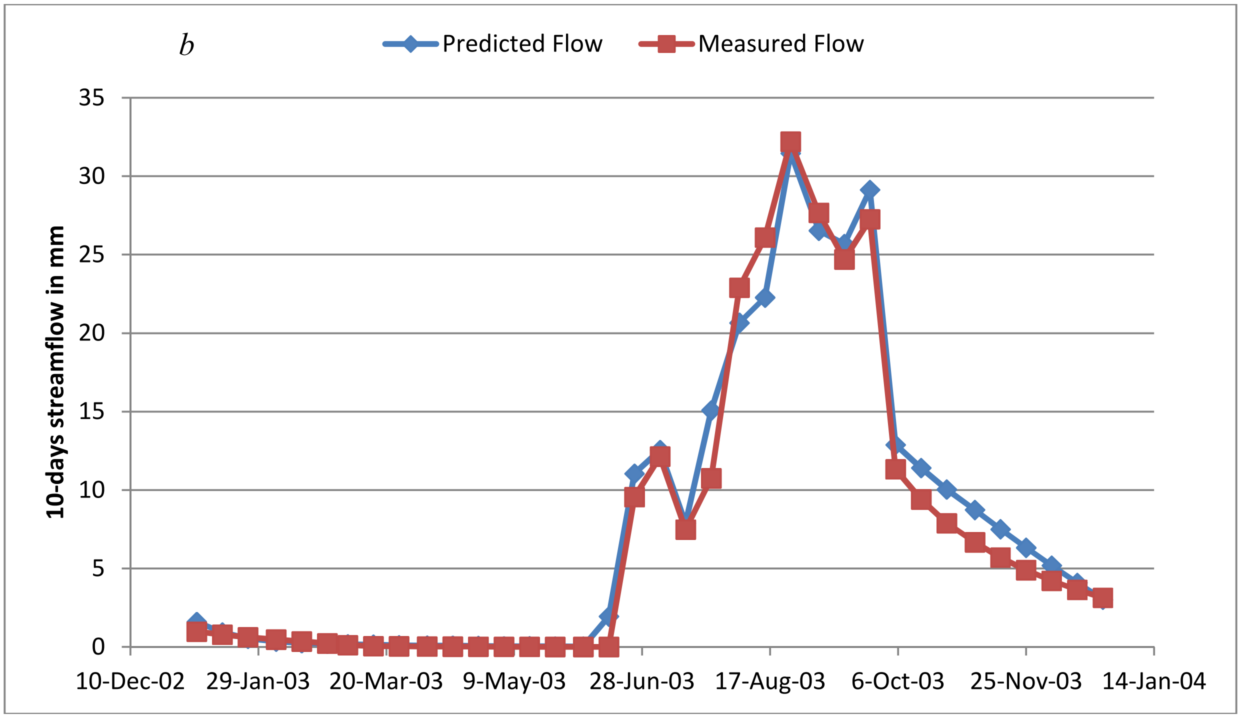

Figure 4-7: Observed and predicted 10-day stream flow (mm/10-day) for the Blue Nile basin and (a) Calibration and (b) validation

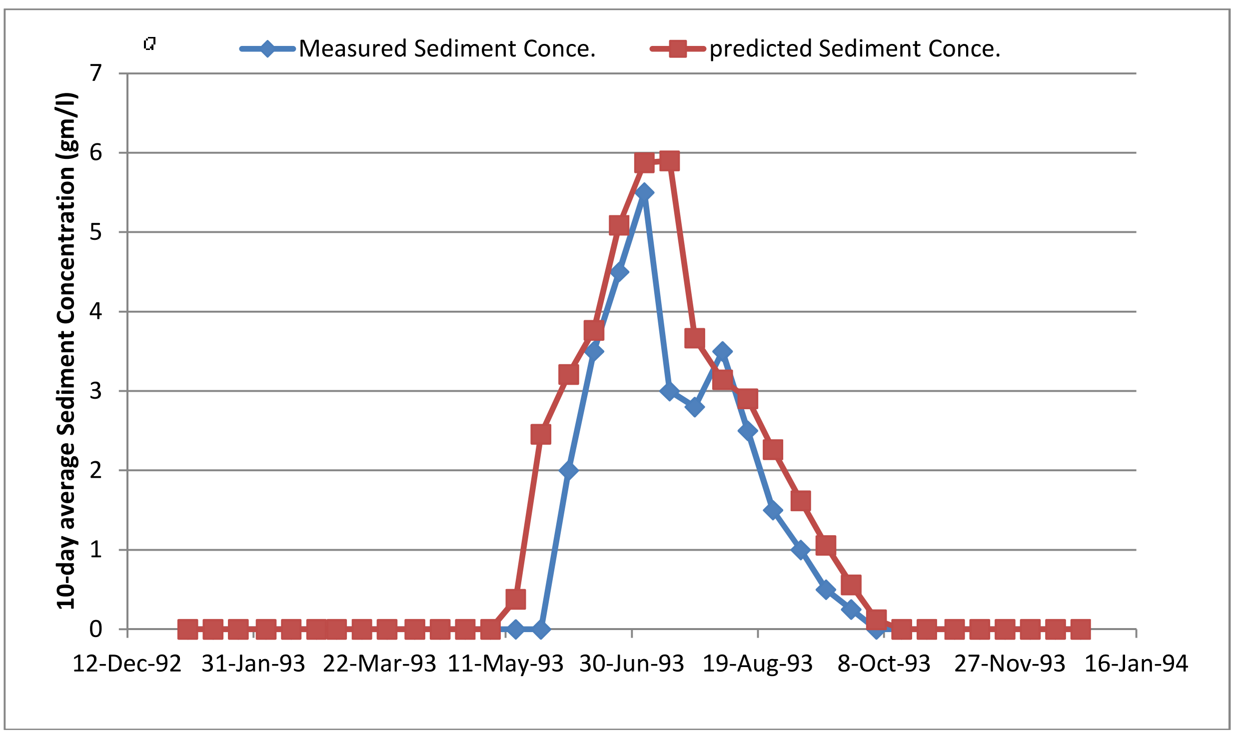

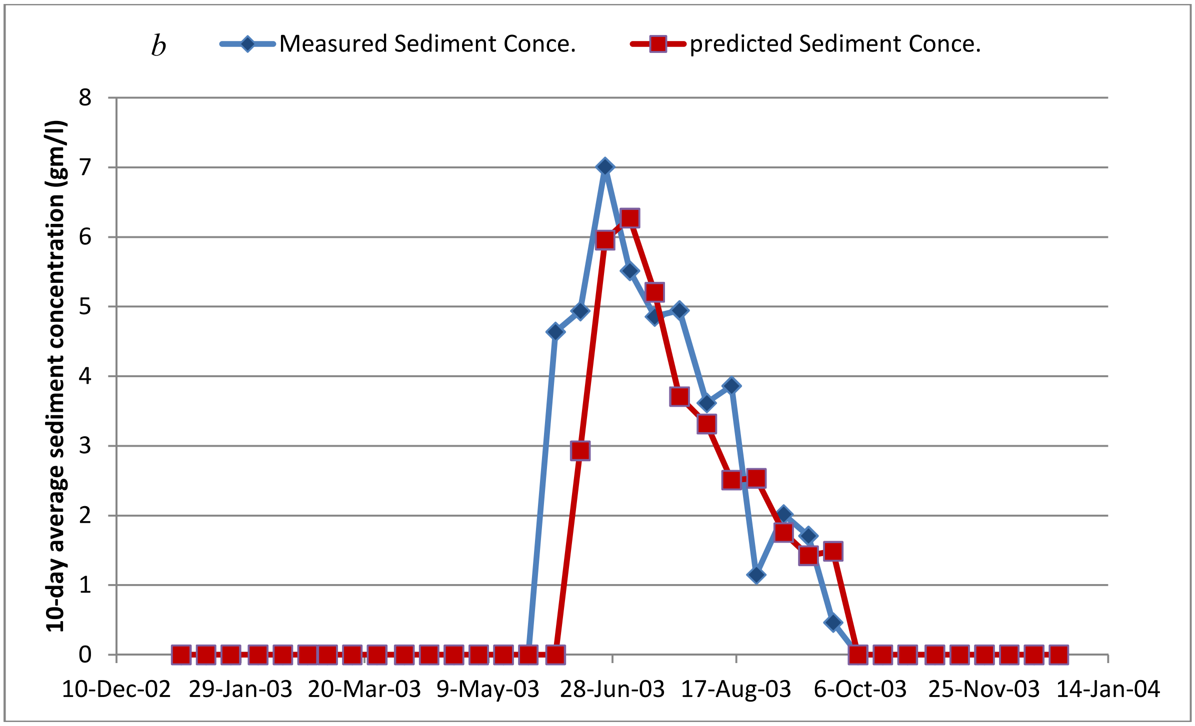

Figure 4-8: 10-day average sediment concentration (g/l) (shown in b) at the Blue Nile Basin: (a) calibration and (b) validation

4.3.1 Hydrology model

The hydrology model performed quite well (Table 4-2) for both the Anjeni watershed (Figure 4-5) and the Blue Nile Basin (Figure 4-7). The model calibration suggests (Table 4-2) that 14% of the Anjeni watershed and 20% of the Blue Nile Basin areas consists of degraded area with shallow soil or exposed hardpan, which requires only a little rain to generate direct runoff (i.e., S_{max} = 10 mm) and approximately 2% of Anjeni and 20% of Blue Nile Basin are of saturated bottom lands that needed 70 mm and 200mm, respectively, of effective precipitation to generate runoff (i.e., S_{max} = 70 mm and 200mm). The hillside or the infiltration (recharge) areas in Anjeni and Blue Nile Basin represent 50% and 60%, respectively, of the total area and require 100 mm and 300mm of effective precipitation to reach field capacity. The remaining thirty four percent of the discharge in the Anjeni watershed is not accounted for and leaves the watershed as deep regional flow while this cannot be (and is not) the case for the Blue Nile Basin.

In the Anjeni watershed, the small proportion of saturated area is consistent with the piezometer readings of Leggesse (2009) that showed a deep water table throughout the uniformly steep watershed except in very close proximity to the stream (Figure 4-4). This is unlike the Maybar (Bayabil et al., 2010) and Andit Tid (Engda et al., 2011) watersheds where large flat areas near the river usually saturate during the rainy season with annual precipitation over 500 mm (Liu et al., 2008). In the Anjeni watershed where the soils are deep at the middle and lower part and there are no flat areas, all the water that otherwise would have saturated the soil drains directly into the stream. Similarly, the 14% degraded area is at least consistent with the very shallow soil 12% coverage in the watershed (Leggesse, 2009). The maximum baseflow storage (BS_{max}) was calibrated to be 100 mm and τ^* was 10 days for the watershed. The half-life for the baseflow storage was set to be 70 days.

The good fit in Figure 4-5, Figure 4-7 and in the supplementary material Appendix C1 Figures A1-1 and A1-2 was confirmed by the performance statistics. The R^2, NSE and RMSE values for Anjeni (Table 4-3) were 0.88, 0.84 and 1.29mm, respectively for calibration and 0.82, 0.80 and 1.19 mm for validation indicating that the model has reasonably captured the watershed response to rainfall. For the case of the Blue Nile, the R^2, NSE and RMSE values were 0.97, 0.93 and 2.59mm for calibration and 0.93, 0.92 and 2.73 mm for validation, respectively.

Despite the good statistics, the model over-predicted low flows and under-predicted flows of greater than 20 mm day^{-1} during the calibration period for Anjeni (Figure 4-5a, b and Figure 4-7a). The same is true for the Blue Nile Basin where the peak flows during August were underestimated during the calibration period, 1993 (Figure 4-7a). During validation (Figure 4-5c and Figure 4-7b), there is a reasonable agreement between observed and predicted low flows especially for the Blue Nile Basin in year 2003, even though there is under prediction for flows greater than 20 mm day^{-1} for Anjeni. The under prediction of peak flows is likely caused by an expansion of runoff producing areas during heavy storms of longer duration. This expansion is not captured because our model fixes the fraction of the runoff-generating areas. The overestimation of low flows early in the period of 1988–1990 for Anjeni is likely due to the impact of the implementation of Fanya juu (SWC with bunds and drainage ditches) in the watershed in 1986. Initially water could be stored behind the bunds (decreasing discharge), but by 1990 the storages behind the bunds were filled up with sediment (Bosshart, 1997) and runoff increased thereafter.

In Appendix C, we show that the hydrology model was only sensitive to fractional areas and one can assume that the fitted values in Table 4-2 are reasonably close to the optimum values. For the other model parameters a wide range of values exists that give the same NSE.

In summary, the hillslope model was able to simulate the discharge patterns quite well in the small 113 ha watershed and large 17.4 million ha Blue Nile basin watershed with area fractions that were approximately similar. The R^2 and NSE values obtained were equal or better than the simulation of Easton (2010) for the SWAT-WB model, indicating that the concept of patterns of self-organization on a watershed scale is realistic. This pattern suggest that the initial rains following the dry season first need to replace the water that has been lost due to evaporation during the dry season before the watershed discharge can begin to respond to precipitation (Liu et al., 2008) from less than 1/3 of the watershed. The remaining watershed is the source of the base and interflow.

4.3.2 Sediment model

According to the hydrology model, there are two surface runoff source areas in the watershed. We assume that these runoff source areas are sources of sediment in our modeling. The simulation results fit quite well (Figure 4-6 and Figure 4-8, Table 4-3). The calibration results in Table 4-2 show that the degraded runoff source areas (represented by a constant a_2) generate most of the erosion. Because of the low proportion of level lands in the Anjeni watershed and the low coefficient value of a_1, sediment transported by runoff from saturated source areas was relatively low. The assumption that no sediment concentration is generated from interflow and base flow seems to be reasonable as the agreement between observed and predicted sediment concentration deteriorates rapidly in the trial of increasing the coefficients a_{IF} and a_{BF} from zero. In Appendix C, we showed that the sediment model was sensitive to the a_2 coefficient and one can assume that the fitted values in Table 4-2 are reasonably close to the optimum values.

The finding that a small portion of the watershed (14% for Anjeni and 20% for Blue Nile Basin) delivers most of the sediment is also shown by the study of Easton et al. (2010) for multi-watersheds in the Blue Nile Basin. The coefficient a_2 for degraded areas in Anjeni is three times higher than Blue Nile Basin (Table 4-2). This was expected because the Anjeni watershed has a much greater slope than the Blue Nile Basin. In Anjeni, these areas are located on the fields in which the farmers have traditional small drainage (or cultural) ditches on shallow and slowly permeable soils (Leggesse, 2009) while in the Blue Nile Basin, the degraded areas are located at Mount Choke in East and West Gojam where Anjeni is located, Lake Tana sub basin, Jema sub basin in Wolo and Abay Gorge in East Wollega (Hydrosult Inc. et al., 2006).

The coefficient of determination, R^2, values of 0.9 and 0.7 were found between measured and modeled daily suspended sediment concentration during calibration and validation periods, respectively (Table 4-3). The Nash-Sutcliffe efficiencies were also relatively better; 0.77 for calibration and 0.64 for validation. These results are comparable with the work of Easton et al. (2010) in which the modified SWAT-WB for monsoonal climates was used and that of Zeleke (2000) which used WEPP. Our model uses only two parameters whereas SWAT and WEPP models incorporate more calibration parameters, such as plant cover, slope, soil and water management or soil type. Since such factors interact to affect soil erosion at a spot, sediment data homogenization is a very challenging task. This makes sediment modeling very difficult. Therefore, getting these relatively high coefficients of determination and NSE for daily data using only two calibration parameters is highly valuable.

Despite the good fit, the model under-predicted sediment concentrations during high measurements and overestimates during low measurements in Anjeni (Figure 4-6 and Figure 4-8). This occurred during the validation period specifically in 1992 and 1993. This is due to, first, the under and over-estimations in the hydrology model being propagated to the simulation of sediment concentration. Secondly, it is reported in Bosshart (1997), that poor maintenance of SWC in the watershed during these years resulted in higher sediment concentrations.

The integration of base flow and interflow in the model as shown in equation 7 helps to capture the lower sediment concentration after July for Anjeni Watershed Figure 4-6 and Figure 4-8. The drop and subsequent low sediment concentration at the end of the rainy season is also reported in Tigray, in the northern part of Ethiopia by Vanmaercke et al. (2010). They argued that lower concentrations of sediment are due to sediment depletion. Others (Descheemaeker et al., 2006; Bewket and Sterk, 2003) suggested that the lower sediment concentrations are a result of the increased plant cover. Although this effect could exist, Tebebu et al. (2010) showed that such a relationship does not exist for the Debre Mawi watershed. In the Blue Nile Basin, it seems that base flow and interflow play an important role in diluting the sediment after July and decreasing the sediment concentration.

The low sediment concentration measurements in 1989 due to SWC were difficult to capture using the model and hence excluded from the data set. This justifies that incorporating more calibration parameters, such as SWC management for the different runoff areas, might improve the sediment concentration prediction.

4.4 Conclusions

A simplified watershed erosion model coupled with a hydrology model was developed and used to simulate sediment concentrations and runoff at two widely varying scales. Such simplified models that require very few calibration parameters to simulate runoff and sediment transport are important in the data limiting environment. Using these models, it was possible to identify the proportion of runoff source areas which are also sources of sediment. The analysis showed that the model could capture the variability in discharge and sediment concentrations quite well with parameters that were not greatly different between the scales. The model basically assumes in its simplest form that a watershed in a monsoon climate wets up after the dry season and produces increasing amounts of inter- and base flow as the rainy season progresses. At the same time this dilutes the sediment in the rivers that originates mainly from relatively small portions of degraded hillsides. More research is needed into how the model parameters vary between scales and watershed characteristics.

References

Bayabil, H. K., Tilahun, S. A., Collick, A. S., and Steenhuis, T. S.: Are runoff processes ecologically or topographically driven in the Ethiopian Highlands? The case of the Maybar, Ecohydrology, 3(4), 457–466, doi:10.1002/eco.170, 2010.

Beasley, D. B., Huggins, L. F., and Monke, E. J.: ANSWERS: a model for watershed planning, in: Transactions of the ASAE, ASABE, St. Joseph, Michigan, 23(4), 938–944, 1980.

Betrie, G. D., Mohamed, Y. A. A., Griensven, van, and Srinivasan R.: Sediment management modeling in the Blue Nile Basin using SWAT model. Hydrol. Earth Syst. Sci., 15, 807–818, doi:10.5194/hess-15-807-2011, 2011

Bewket, W. and Sterk, G.: Assessment of soil erosion in cultivated fields using a survey methodology for rills in Chemoga watershed, Ethiopia, Agr. Ecosyst. Environ., 97, 81–93, 2003.

Bosshart, U.: Catchment Discharge and Suspended Sediment Transport as Indicators of Physical Soil and Water Conservation in the Minchet Catchment, Anjeni Research Unit, Soil Conservation Research Report 40, University of Berne, Berne, Switzerland, 1997.

Ciesiolka, C. A. A., Coughlan, K. J., Rose, C. W., Escalante, M. C., Hashim, G. M., Paningbatan Jr., E. P., and Sombatpanit, S.: Methodology for a multi-country study of soil erosion management, Soil Technol., 8, 179–192, 1995.

Champion, A.M.: Soil Erosion in Africa. The Geographical Journal 82: 131-139, 1933.

Collick, A. S., Easton, Z. M., Ashagrie, T., Biruk, B., Tilahun, S., Adgo, E., Awulachew, S. B., Zeleke, G., and Steenhuis, T. S.: A simple semi distributed water balance model for the Ethiopian Highlands, Hydrol. Process., 23, 3718–3727, 2009.

Descheemaeker, K., Nyssen, J., Rossi, J., Poesen, J., Haile, M., Raes, D., Muys, B., Moeyersons, J., and Deckers, S.: Sediment deposition and pedogenesis in exclosures in the Tigray Highlands, Ethiopia, Geoderma, 132, 291–314, 2006.

Dooge, J. C. I.: Looking for Hydrologic Laws, Water Resour. Res., 22(9), S46–S58, 1986.

Dooge, J. C. I.: Bringing it all together, Hydrol. Earth Syst. Sci., 9, 3–14, doi:10.5194/hess-9-3-2005, 2005.

Easton, Z. M., Fuka, D. R., Walter, M. T., Cowan, D. M., Schneiderman, E. M., and Steenhuis, T. S.: Re-conceptualizing the soil and water assessment tool (SWAT) model to predict runoff from variable source areas, J. Hydrol., 348(3–4), 279–291, 2008.

Easton, Z. M., Fuka, D. R., White, E. D., Collick, A. S., Ashagre, B., McCartney, M., Awulachew, S. B., Ahmed, A. A., and Steenhuis, T. S.: A multi basin SWAT model analysis of runoff and sedimentation in the Blue Nile, Ethiopia, Hydrol. Earth Syst. Sci., 14, 1827–1841, doi:10.5194/hess-14-1827-2010, 2010.

EI-Swaify, S. A., Dangler E. W. and Armstrong C. L. Soil erosion by water in the tropics. Research Extension series 24 University of Hawaii Honolulu, Hawaii. 1982 http://pdf.usaid.gov/pdf_docs/PNAAR134.pdf

Engda, T. A., Bayabil, H. K., Legesse, E. S., Ayana, E. K., Tilahun, S. A., Collick, A. S., Easton, Z. M., Rimmer, A., Awulachew, S. B., and Steenhuis, T. S.: Watershed hydrology of the (semi) humid Ethiopian Highlands, in: Nile River: Hydrology, Climate and Land Use, edited by: Melesse, A., Springer Science Publisher, New York, 2011.

Eweg, H. P. A., Van Lammeren, R., Deurloo, H., and Woldu, Z.: Analyzing degradation and rehabilitation for sustainable land management in the highlands of Ethiopia, Land Degrad. Develop. 9, 529–542, 1998.

Fleitmann, D., Dunbar, R. B., McCulloch, M., Mudelsee, M., Vuille, M., McClanahan, T. R., Cole, J. E. and Eggins S.: East African soil erosion recorded in a 300 year old coral colony from Kenya, Geophys. Res. Lett., 34, L04401, doi:10.1029/2006GL028525, 2007.

Garzanti, E., Ando, S., Vezzoli, G., Ali Abdel Megid, A., and El Kammar, A.: Petrology of Nile River sands (Ethiopia and Sudan): sediment budgets and erosion patterns, Earth Planet. Sc. Lett., 252(3–4), 327–341, 2006.

Hanggi, F.: Temporal and spatial variations of soil erosion in the Research Units Anjeni and Andit Tid: case studies of test plot soil erosion in the north western and central highlands of Ethiopia, SCRP research report 37, University of Berne, Berne, Switzerland, 1997.

Hairsine, P. B. and Rose, C. W.: Modeling water erosion due to overland flow using physical principles 1. Sheet flow, Water Resour. Res., 28(1), 237–243, 1992a.

Hairsine, P. B. and Rose, C. W.: Modeling water erosion due to overland flow using physical principles 2. Rill flow, Water Resour. Res., 28(1), 245–250, 1992b.

Haregeweyn, N. and Yohannes F.: Testing and evaluation of the agricultural non-point source pollution model (AGNPS) on Augucho catchment, Western Hararghe, Ethiopia, Agr. Ecosyst. Environ., 99, 201–212, 2003.

He, Y., Bàrdossy A., and Zehe,E. A catchment classification scheme using local variance reduction method. J Hydrology 411:140-154. 2011

Hudson, N. W.:, Erosion control research. Progress report on experiments at Henderson Research Station, 1953-1956. Rhodesia Agric. Jour. 54(4):297-323 , 1957.

Hudson, N. W., Raindrop size distribution in high intensity storms. Rhodesian Jour. of Agric.Res. 1: 6-11, 1963

Hudson N. W. Soil and Water conservation in semi-arid areas. Soil Resources, Management and Conservation Service, FAO Land and Water Development Division, Food and Agriculture Organization of the United Nations, Rome, 1987.

Hurni H.: An ecosystem approach to soil conservation, in: Soil Erosion and Conservation, edited by: El-Swaify, S. A., Moldenhauer, W. C., and Lo, A., Soil Conservation Society of America, Ankey, Iowa, 759–771, 1985.

Hurni, H.: Degradation and conservation of the resources in the Ethiopian Highlands, Mt. Res. Dev., 8(2/3), 123–130,1988.

Hydrosult Inc; Techsult; DHV; and their Associates Nile Consult, Comatex Nilotica; and T and A Consulting. Trans-Boundary Analysis: Abay – Blue Nile Sub-basin. NBI-ENTRO (Nile Basin Initiative-Eastern Nile Technical Regional Organization), 2006.

Kandel, D., Western, A., Grayson, R., and Turral, H.: Testing current generation soil erosion models at two minute and daily scales using plot scale data from a mid-hill catchment of Nepal, in: Integrating Models for Natural Resources Management Across Disciplines, Issues and Scales, edited by: Ghassemi, F., Post, D., Sivapalan, M., and Vertessy, R., Proceedings of the International Congress on Modeling and Simulation (MODSIM 2001), Volume 1: Natural Systems Modeling and Simulation Society of Australia and New Zealand Inc., Australian National University, Canberra, Australia, 365–370, 2001.

Kim, Y.-J., Darnault, C.J.G., Bailey, N.O., Parlange, J.-Y., and Steenhuis, T.S. Equation for describing solute transport in field soils with preferential flow paths. Soil Sci. Soc. of Amer. J. 69:291-300, 2005.

Klaus, J. and Zehe E., A novel explicit approach to model bromide and pesticide transport in connected soil structures. Hydrol. Earth. Sys. Sci. 15, 2127-2144, 2011

Kung, K.-J.S., Steenhuis, T.S., Kladivko, E.J., Gish, T.J., Bubenzer, G., and Helling, C.S.. Impact of Preferential Flow on the Transport of Adsorbing and Non-Adsorbing Tracers. Soil Sci. Soc. Am. J. 64:1290-1296, 2000.

Lal R.: Soil erosion and transport research in tropical Africa. Hydrological Sciences 30, 1985

Legesse, E. S.: Modeling Rainfall-Runoff Relationships for the Anjeni watershed in the Blue Nile Basin, A Thesis Presented to the Faculty of the Graduate School of Cornell University In Partial Fulfillment of the Requirements for the Degree of Master of Professional Studies, Ithaca, NY, 2009.

Lisle, I. G., Coughlan, K. J., and Rose, C. W.: GUPRO 3.1: A program for calculating particle size and settling characteristics, ENSWorking Paper 7/96. Faculty of Environmental Sciences, Griffith University, Brisbane, 1996.

Liu, B. M., Collick, A. S., Zeleke, G., Adgo, E., Easton, Z. M., and Steenhuis, T. S.: Rainfall discharge relationships for a monsoonal climate in the Ethiopian Highlands, Hydrol. Process., 22(7), 1059–1067, 2008.

Mitiku, H., Herweg, K., and Stillhardt, B.: Sustainable land management – a new approach to soil and water conservation in Ethiopia, Land Resource Management and Environmental Protection Department, Mekelle University, Mekelle, Ethiopia, Center for Development and Environment (CDE), University of Bern and Swiss National Center of Competence in Research (NCCR) North-South, Bern, Switzerland, 269 pp., 2006.

Mohammed, A., Yohannes, F., and Zeleke, G.: Validation of agricultural non-point source (AGNPS) pollution model in Kori watershed, South Wollo, Ethiopia, Int. J. Appl. Earth Obs., 6, 97–109, 2004.

Moriasi, D.N., Arnold, J.G., Van Liew, M.W., Bingner, R.L., Harmel, R.D., Veith, T.L.: Model evaluation guidelines for systematic quantification of accuracy in watershed simulations. Transactions of the ASABE. 50(3):885-900, 2007

Morgan, R. P. C., Quinton, J. N., Smith, R. E., Govers, G., Poesen, J. W. A., Auerswald, K., Chisci, G., Torri, D., and Styczen, M. E.: The European soil erosion model (EUROSEM): a dynamic approach for predicting sediment transport from fields and small catchments, Earth Surf. Proc. Land., 23, 527–544, 1998.

Nyssen, J., Poesen, J., Moeyersons, J., Haile, M., Deckers, J., and Lang, A.: Human impacts on the environment in the Ethiopian and Eritrean Highlands – a states of the art, Earth Sci. Rev., 64, 270–320, 2004.

Prosser, I. P. and Rustomji, P.: Sediment transport capacity relations for overland flow, Prog. Phys. Geog., 24(2), 179–193, 2000.

Rose, C. W.: Erosion and sedimentation, in: Hydrology and Water Management in the Humid Tropics-Hydrological Research Issues and Strategies for Water Management, edited by: Bonnell, M., Hufschmidt, M. M., and Gladwell, J. S., Cambridge University Press, Cambridge, 301–343, 1993.

Rose, C. W.: Soil erosion models and implications for conservation of sloping tropical lands, in: Sustaining the Global Farm- Selected papers from the 10th International Soil Conservation Organization Meeting, 24–29 May 1999, West Lafayette, IN, International Soil Conservation Organization in cooperation with the USDA and Purdue University, West Lafayette, edited by: Stott, D. E., Mohtar, R. H., and Steinardt, G. C., CD-ROM available from the USDA-ARS National Soil Erosion Laboratory, West Lafayette, 852–859, 2001.

Savenije, H. H. G.: HESS Opinions "Topography driven conceptual modeling (FLEX-Topo)", Hydrol. Earth Syst. Sci., 14, 2681–2692, doi:10.5194/hess-14-2681-2010, 2010.

SCRP: Area of Anjeni, Gojam, Ethiopia: long-term monitoring of the agricultural environment 1984–1994, Soil erosion and conservation database, Soil Conservation Research Programme (SCRP), Centre for Development and Environment and the Ministry of Agriculture, Ethiopia, University of Berne, Berne, Switzerland, 89 pp., 2000.

Setegn, S. G., Ragahavan, S., and Bijan, D.: Hydrological modeling in the Lake Tana Basin, Ethiopia using SWAT model, Open Hydrol. J., 2, 49–62, 2008.

Siepel, A. C., Steenhuis, T. S., Rose, C. W., Parlange, J.-Y., and McIsaac, G. F.: A simplified hillslope erosion model with vegetation elements for practical applications, J. Hydrol., 258, 111–121, 2002.

Steenhuis, T. S. and van der Molen, W. H.: The Thornthwaite-Mather procedure as a simple engineering method to predict recharge, J. Hydrol., 84(3–4), 221–229, 1986.

Steenhuis, T. S., Collick, A. S., Easton, Z. M., Leggesse, E. S., Bayabil, H. K., White, E. D., Awulachew, S. B., Adgo, E., and Ahmed, A. A.: Predicting discharge and erosion for the Abay (Blue Nile) with a simple model, Hydrol. Process., 23, 3728–3737, 2009.

Tebebu, T. Y., Abiy, A. Z., Zegeye, A. D., Dahlke, H. E., Easton, Z. M., Tilahun, S. A., Collick, A. S., Kidnau, S., Moges, S., Dadgari, F., and Steenhuis, T. S.: Surface and subsurface flow effect on permanent gully formation and upland erosion near Lake Tana in the northern highlands of Ethiopia, Hydrol. Earth Syst. Sci., 14, 2207–2217, doi:10.5194/hess-14-2207- 2010, 2010.

Tesemma, Z. K., Mohamed, Y. A., and Steenhuis, T. S.: Trends in rainfall and runoff in the Blue Nile Basin: 1964–2003, Hydrol. Process., 24(25), 3747–3758, doi:10.1002/hyp.7893, 2010.

Thomas, D.B., and Biamah, E.K. Origin, application and design of fanya juu terrace, in: Development of Conservation Farming on Hillslopes, edited by Moldenhauer W.C., Hudson N.W., Sheng T.C., and Lee S.W., Soil and Water Conservation Society, Ankeny, Iowa, pp. 185–194, 1991.

Thornthwaite, C. W. and Mather, J. R.: The water balance, Publ. Climatol., 8(1), 1–104, 1955.

Vanmaercke, M., Poesen, J., Maetens, W., Vente, J., and Verstraeten, G.: Sediment yield as a desertification risk indicator. Science of the Total Environment, 409, 1715-1725, doi:10.1016/j.scitotenv. 2011.01.034, 2011.

Wischmeier, W.H., and Smith, D.D.. Predicting rainfall erosion losses—a guide to conservation planning. USDA Agric. Handbook 537, 58 p, 1978.

White, E. D., Easton, Z. M., Fuka, D. R., Collick, A. S., Adgo, E., McCartney, M., Awulachew, S. B., Selassie, Y., and Steenhuis, T. S.: Development and application of a physically based landscape water balance in the SWAT model, Hydrol. Process., 23, 3728–3737,doi:10.1002/hyp.7876, 2010.

Yalin, M. S.: An expression for bed-load transportation, ASCE J. Hydraul. Div., 89(HY3), 221–250, 1963.

Yu, B., Rose, C. W., Ciesiolka, B. C. A. A., Coughlan, K. J., and Fentie, B.: Toward a framework for runoff and soil loss prediction using GUEST technology, Aust. J. Soil Res., 35, 1191-1212,1997.

Zehe, E., Graeff ,T., Morgner, M., Bauer, A., and Bronstert, A. Plot and filed scale soil moisture dynamics and subsurface wetness control on runoff generation in a headwater in the Ore Mountains. Hydrol. Earth Syst. Sci 14: 873-889, 2010

Zeleke, G.: Landscape Dynamics and Soil Erosion Process Modeling in the North-Western Ethiopian Highlands, African Studies Series A 16, Geographica Bernensia, Berne, Switzerland, 2000.

CHAPTER 5: A SATURATION EXCESS EROSION MODEL

Abstract

Scaling up sediment transport has been problematic because most sediment loss models (e.g., the Universal Soil Loss Equation) are developed using data from small plots where runoff is generated by infiltration excess. However, in most watersheds, runoff is produced by saturation excess processes. In this paper we improve an earlier saturation excess erosion model in which runoff and erosion originated from periodically saturated and severely degraded areas and apply it to three watersheds over a wider geographical area. This earlier model was only tested on a limited basis. The model is based on semi-distributed saturation excess hydrology model, which calculates surface runoff, interflow, and baseflow. To obtain the sediment concentrations, we assume that during surface runoff, there is a linear relationship between runoff velocity and sediment concentration, but baseflow and interflow are sediment free. Initially during the rainy season in Ethiopia, when the fields are being plowed the sediment is transport limits later in the season the concentration becomes source limited. To show the general applicability of the Saturation Excess Erosion Model (SEEModel), the model was tested for watersheds located 10,000 km apart, in the United States and in Ethiopia. In the Ethiopia highlands, we simulated the 113 ha Anjeni watershed, the 477 ha Andit Tid watershed, the 400 ha Enkulal watershed and the 17.4 million ha the Blue Nile basin. In the Catskill Mountains in New York State, the sediment concentrations were simulated in the upper 493 km^2 Esopus Creek watershed. Daily discharge and sediment concentration were well simulated over the range of scales with comparable parameter sets. The Nash Sutcliffe values for the daily stream discharge were greater than 0.80 and the daily sediment concentrations had Nash Sutcliffe values of 0.65 using only two

calibrated sediment parameters and the subsurface and surface runoff discharges calculated by the hydrology model. The model results suggest that correctly predicting both amount of surface runoff and subsurface flow is an important step in simulating the sediment concentrations.

5.1 Introduction

The success of soil and water conservation practices depend on the understanding of the processes involved in the generation and transport of sediment (Ciesiolka et al., 1995). Most of existing models use the Universal Soil Loss Equation for predicting sediment loads, which assumes that rainfall intensity is one of the main driving forces for causing erosion. Although this might be a reasonable assumption for areas with limited infiltration capacity and/or extremely high intensity storms, it is not applicable for humid climates, where soils are well structured and rainfall intensities are usually less than the infiltration capacity of the soil (Bayabil et al., 2011; Engda et al., 2011). Models that bases on USLE also assumes that runoff and sediment sources are from all part of the Watershed with a hotspots of steep slope while in humid areas runoff is generated from saturated and degraded areas of the landscape and the amount of runoff is a function of cumulative precipitation depth and available soil storage (Liu et al., 2008; Steenhuis et al., 2009; Tilahun et al., 2012). Because of such limitation, existing models which are applied on Ethiopian humid highland are only able to simulate the monthly and annual sediment load and have difficulty indicating the process of erosion and scheduling of erosion control (Tilahun et al., 2012).

The limitation of USLE urged modelers to come up with an alternative hill-slope erosion model which are less complex than physically based models but applicable to monsoon climates. One of such attempt is the work of Rose et al. (1983) and Hairsine and Rose (1992). The former defined a mathematical model of sediment transport from a sloping plain by determining sediment concentration as a function of overland flow while the latter developed a new model to determine sediment concentration based on physical principle that depends on the overland flow rate and a coefficient dependent on landscape and sediment characteristics. Models based on Hairsine and Rose (1992a, b) such as Griffith University Erosion System Template (GUEST) Technology have been found to be suitable for monsoonal climates (Kandel et al., 2001; Rose, 2001). Tilahun et al., (2012) developed a hill-slope erosion model for monsoonal humid climate that bases on the Hairsine and Rose (1992). In this hill-slope erosion model, it is assumed that the erosion process is transport limiting for simplicity throughout the simulation period and the models performs reasonably well in simulating sediment concentration in Anjeni Watershed (113ha) and Blue Nile Basin (17.4 million ha).

In reality, however, sediment concentration will reduce to the sediment source limit as sediment sources declines after a certain time of the rainy period (Ciesiolka et al., 1995). On the Ethiopian highland, this phenomenon is well documented by Tebebu et al (2010) and Vanmaercke et al. (2010). Here, the objective of this paper is therefore to develop a modified hill-slope model for humid monsoonal climates and test if this method also applies to the Anjeni and Blue Nile Basin and other two additional watersheds (Andit Tid and Enkulal) in Ethiopia and one watershed in humid temperate climate, USA.

5.2 Saturated Excess Erosion Model (SEEModel) development

In this section, the amount of erosion is predicted as a function of the (daily) amounts of surface runoff, interflow, and baseflow. These fluxes are obtained from a relatively simple hydrology model (Steenhuis et al., 2009; Tesemma et al., 2011). In this water balance hydrology model, the watershed is divided into three zones: two surface runoff zones consisting of areas, one that becomes saturated during the wet monsoon period and the other the degraded hillsides. The remaining hillsides are the third zone where the rainwater infiltrates and becomes either interflow (zero order reservoir) or base flow (first order reservoir) depending on its path to the stream. A daily water balance is kept for each of the zones using the Thornthwaite Mather procedure where actual evaporation has a linear relationship with the available water storage in the root zone. At maximum storage, S_{max}, actual evaporation is equal to the potential evaporation (Steenhuis and van der Molen, 1986). More information about the hydrology model can be found in Steenhuis et al. (2009) and Tesemma et al. (2011). Erosion originates from the runoff producing zones. Erosion is negligible from the non-degraded hillsides because almost all water infiltrates before it would reach the stream.

In calculating the erosion from runoff producing area, we are assuming that rate of erosion depends on the stream power per unit area. The maximum concentration of sediment that a stream can carry (called the transport limiting capacity C_t *(g/L)*) can be derived from the stream power function as shown by Hairsine and Rose (1992), Siepel et al. (2002), Ciesiolka et al. (1995) and Yu et al. (1997).

$$C_t = a_t {q_r}^n \qquad 1$$

where q_r (mm/day) is the runoff rate per unit area from each runoff producing region, a_t (g L mm^{-n}day^n) is a variable derived from the stream power. The variable a_t is a function of the slope, manning's roughness coefficient, slope length, and the effective depositability (Yu et al., 1997). As water depth increases a_t essentially becomes independent of the runoff rate per unit area and can be taken as a constant (Yu et al., 1997). The exponential, n, that takes a value of 0.4

assuming both a wide channel and a linear relationship between sediment concentration and velocity (Ciesiolka et al., 1995 and Yu et al., 1997). In this paper where the smallest watershed considered is 113 ha, the water in the channel is sufficiently deep so that a_t is constant.

For erosion of cohesive soils, the sediment concentration will not always reach the transport limit. Only in cases where, for example, the rills are formed in newly plowed soils, the transport capacity will be met. Tebebu et al (2010) found that once the rill network has been fully established, no further erosion will take place and the sediment source becomes limited and, the concentration, C, will fall below the transport limit. For the cases when the sediment concentration becomes lower than the transport limit, C_t, Ciesiolka et al. (1995) found based on the work of Hairsine and Rose (1992) that the sediment concentration will not decline below the "source limit", C_s (g/L):

$$C_s = a_s q_r{}^n \qquad 2$$

where a_s is the source limit and is assumed to be independent on the flow rate for a particular watershed (as compared to plots). Introducing a new variable, H, defined as the fraction of the runoff producing area with active rill formation, the concentration of sediment from the runoff producing area can then be written as:

$$C_r = C_s + H(C_t - C_s) \qquad 3$$

Combining Eq. 3 with Eqs. 1 and 2, the concentration from the runoff producing area becomes

$$C_r = [a_s + H(a_t - a_s)]q_r{}^n \qquad 4$$

Finally, in the calculation of the daily concentration, baseflow and interflow play an important role. In a monsoon climate, baseflow at the end of the rainy season can be a significant portion of the total flow. Thus, in the last part of the rainy season the subsurface flow dilutes the peak storm sediment concentration from the runoff producing zones when simulated on a daily basis. It is therefore important to incorporate the contribution of baseflow in the prediction of sediment concentration.

Next we will calculate the concentration of the sediment yield in the stream. Since the interflow and baseflow are sediment free the sediment load per unit watershed area, Y (g m^{-2}day^{-1}), can be obtained by multiplying C_r in Eq. 4 by the relative area and the flux per unit area, e.g.,

$$Y = A_1 q_{r_1}\left[a_{s_1} + H\left(a_{t_1} - a_{s_1}\right)\right]{q_{r_1}}^{n} + A_2 q_{r_2}\left[a_{s_2} + H\left(a_{t_2} - a_{s_2}\right)\right]{q_{r_2}}^{n} \qquad 5$$

where q_{r1} and q_{r2} are the runoff rates expressed in depth units for contributing area A_1 (fractional saturated area) and A_2 (fractional degraded area), respectively. Assuming that the saturated and the degraded zones have the same values for transport and source limiting capacities, the concentration of sediment in the stream can be obtained by dividing the load Y (Eq. 5) by the total watershed discharge.

$$C = \frac{\left(A_1 {q_{r_1}}^{n+1} + A_2 {q_{r_2}}^{n+1}\right)\left[a_s + H(a_t - a_s)\right]}{A_1 q_{r_1} + A_2 q_{r_2} + A_3 (q_b + q_i)} \qquad 6$$

Where q_b (mm/day) is the base flow and q_i (mm/day) is the interflow per unit area of the non-degraded hillside, A_3 where the water is being recharged to the subsurface (baseflow) reservoir.

These equations are only as good as the experimental data. Therefore Eq. 6 is tested in four watersheds in the Ethiopian highlands and one in New York State The watersheds (Anjeni, Enkulal, Andit Tid, Esopus Creek and the entire the Blue Nile Basin in Ethiopia) range in size from 113 ha to 174,000 km^2.

5.3 Watershed descriptions

The Anjeni watershed (Figure 5-1) covers an area of 113 ha with elevations ranging between 2405 and 2507m and is cropped. It is located in the sub-humid northwestern part of Ethiopia near Debre Markos 370 km NW of Addis Ababa. The mean annual rainfall is 1690 mm, which lasts from the middle of May to the middle of October. 90% of the watershed is cultivated land (Guzman, 2011). There is a large active gully in the upper part of the watershed. Both discharge and sediment concentrations were measured during storm events. Daily average discharge and sediment concentrations were calculated. Rainfall, potential evaporation, stream discharge and sediment concentrations were collected from 1988 to 1997. In 1986 soil and water conservation practices were installed resulting in a decrease in soil loss for two years (Bosshart, 1997). Periods in which there is incomplete data were excluded. The model was calibrated for the years 1988 and 1990 for discharge, and was validated for the years 1989, 1991-1993 and 1997. Only four years were available for sediment concentration: The year 1990 was used for calibration and 1991 to 1993 for validation.

The Andit Tid watershed (Figure 5-1) covers an area of 477.3 ha. It is situated 180 km NE of Addis Ababa in North Shewa Administrative Zone adjacent to the Debre Birhan-Mekelle Highway. The catchment has a relatively high bimodal rainfall pattern with annual rainfall of 1400 mm. Hill slopes were very steep and degraded, with altitudinal range from 3040-3548 m a.s.l. Only 15% of the watershed is cultivated land (Guzman, 2011). Like Anjeni, Both discharge and sediment concentrations were measured during storm events. Daily average discharge and sediment concentrations were calculated. Rainfall, potential evaporation, stream discharge and sediment concentrations were collected from 1986 to 1994. Bosshart (1997) pointed out the stream gauging site of this watershed changed in 1997 because of high bank erosion. The model was calibrated 1986, 1988 and 1988 for discharge, and was validated for the years from 1990 to 1994. The model for erosion was calibrated for years 1986 and 1988 while the years from 1989 to 1993 except 1990 were used for validation.

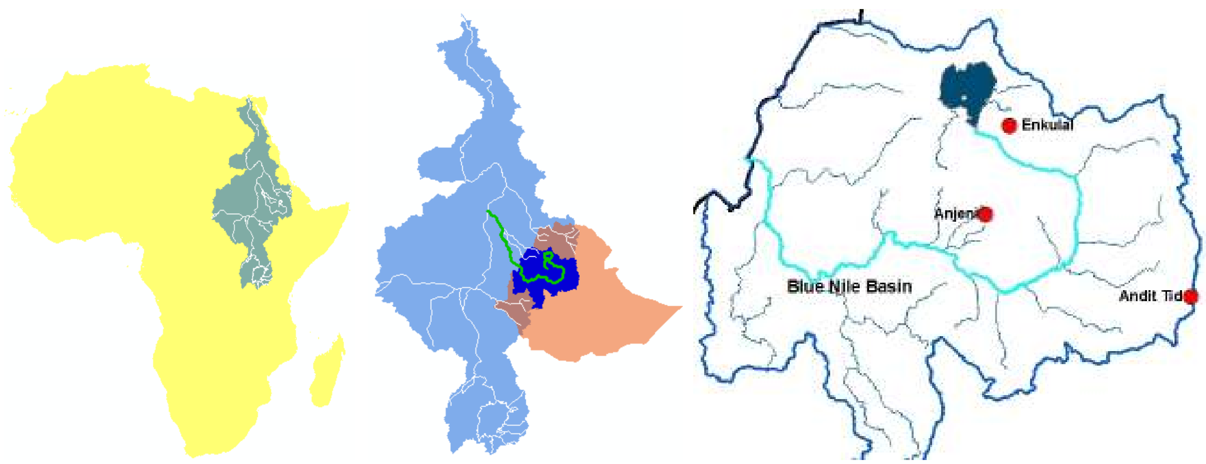

Figure 5-1: Location map of Nile, Blue Nile and three watersheds (Anjeni, Andit Tid and Enkulal) in Blue Nile Basin, respectively, from left to right.

The Enkulal catchment (Figure 5-1) is a small tributary of Gumara watershed, located approximately 80 km northeast of Bahir Dar. The Enkulal watershed covers an area of 400 ha. Elevation ranges from 2306 to 2528 m. The average annual rainfall is 1577 mm. Most of the rainfall is concentrated from June to September. More than three quarter of the watershed is in low yielding oxen-plowed agriculture. Discharge and sediment concentration data were available twice a day at 6 a.m. and 6 p.m. for the year 2010. Especially at the end of the rainy season many storms occurred at night and the peak flows were not recorded. The rivers in the watershed are stable and in the lower part run over bedrock.

The last watershed modeled in Ethiopia is the entire Blue Nile Basin in Ethiopia. It is 174, 000 km^2 and encompasses the Anjeni, Andit Tid and the Enkulal watersheds. It is said that the source of the Blue Nile is a spring located about 100 km south of Lake Tana at an elevation of 2,900 m. This spring is the beginning of the Gilgil Abbay, which flows into Lake Tana. After Lake Tana the Nile flows through a 1 km deep gorge to the Sudanese border mostly over bedrock. The Blue Nile leaves the highlands near the western border of Ethiopia, and enters the Sudan at an elevation of 490 m. The annual rainfall varies from less than 1000 mm near the Sudanese border to over 1800 mm in the highlands south of Lake Tana. Three years of discharge and sediment data were available at the Sudanese border (1997, 2003 and 2004). The year 1997 was used for calibration and 2003 and 2004 for validation. Tesemma et al. (2010) found that the degraded soils had increased by 10% during a 25 year time span. For that reason the degraded hillslope area was increased by 3% from 1997 to 2003 and 2004.

The final watershed is The Esopus Creek watershed located in the Catskill region of New York State drains 493 km^2 and is dominated by forests, which occupy more than 90 % of the watershed area. The elevation of the watershed ranges from 194 m near the watershed outlet at Coldbrook to 1275 m at the headwaters. Widespread stream channel erosion of glacial clay deposits has been identified as the primary cause of high levels of turbidity. For the Esopus Creek watershed, measured daily stream discharge from the USGS gauging station at the watershed outlet near Coldbrook was used. Turbidity measurements were taken at intervals between 15 min and 1 hr using an YSI water quality sonde from which flow-weighted average daily values were calculated. The measured stream discharge was separated into base flow and surface runoff components using a base flow filter program (Arnold and Allen, 1999). The values for surface runoff region (A1 and A2) and hillside recharge region (A3) were derived as the long-term (1931-2011) mean proportions of runoff and base flow to total stream flow. Observed daily turbidity and daily stream discharge from the March 2003 to March 2004 period were used for calibration of the sediment of the SEEModel and data from March 2007- 2008 period were employed for validation. The Esopus Creek is at times fed by a diversion tunnel operated from the nearby Schoharie reservoir that contributes to stream discharge. Therefore all calculations were confined to days when the tunnel contribution of stream discharge was insignificant.

5.4 Results and Discussions

The model calibration over a wide range of scales has some remarkable similarities (Table 5-1). Especially the fraction of surface runoff zones in the three watersheds, which is between 0.3 to 0.4. Only in the Anjeni watershed the surface runoff area is equal to 15% of the watershed. The size of permeable hillside increases with watershed size. The small watersheds are located in the top of the watershed and some of the subsurface water passes under the gaging station and provides water for springs below. The hillside area is especially small for the Enkulal watershed, which is in accordance with the data from piezometers readings that indicated that the top part of the watershed contributed mainly to baseflow (Demisse, 2011). The maximum storage of water in the root zone (S_{max}) and shallow aquifer (BS_{max}) varies among the watersheds. However, the model is relatively insensitive to the S_{max} and BS_{max} values since it only affects the amount of surface runoff in the beginning of the rainfall season (Tilahun et al, 2012). Variations in these values between watersheds are therefore not significant with the exception of the maximum storage for the hillside and saturated area of the whole Blue Nile Basin that is larger.

Table 5-1: Calibrated model parameters and model efficiencies for the five watersheds.

Component	Description	Parameters	Unit	Calibrated Values				
				Anjeni (113ha)	Andit Tid (477ha)	Enkulal (400ha)	Blue Nile ($17.4x10^6$ ha)	Esopus ($49.3x10^3$ ha)
Hydrology	Saturated area	Area A_1	fraction	0.02	0.1	0.1	0.2	-
		S_{max} in A_1	mm	200	70	50	200	-
	Degraded area	Area A_2	fraction	0.14	0.15	0.2	0.2	0.32
		S_{max} in A_2	mm	10	10	10	10	-
	Hillside	Area A_3	fraction	0.5	0.75	0.3	0.6	0.68
		S_{max} in A_3	mm	100	80	50	300	-
	Subsurface	BS_{max}	mm	100	100	500	20	
		$t_{½}$	days	70	100	120	35	-
		τ*	days	10	10	100	140	-
Sediment transport limit		a_t	see text	4	2.2	17	1.2	-
Sediment Source limit		a_s	see text	3	0.8	5	0.5	0.63
Nash Sutcliffe Efficiencies (NSE)*	Time step		days	1	7	7	10	1
	Hydrology	calibration	none	0.84	0.91	0.75	0.93	-
		validation	none	0.80	0.78		0.92	-
	Erosion	calibration	none	0.77	0.71	0.76	0.84	0.63
		validation	none	0.68	0.60		0.81	0.66

*Nash and Sutcliffe (1970)

There are two parameters that determine the subsurface flow: interflow and baseflow. While the baseflow contribution to streamflow decreases slowly depending on the amount of water in the aquifer, the interflow remains constant for a particular storm and stops after a time, τ*. As expected τ* increases with watershed size, because more deep flow paths are intercepted by the river. The larger than expected τ* for the Enkulal watershed is likely a consequence of missing most of the peak flows especially later in the rainy season (due to the sample collection timing). The half-life, $t_{½}$, for the aquifer system is almost independent of watershed size, indicating that there is not a large aquifer. With the Nile flowing over bedrock this should not be a surprise. Finally, the hydrology model could not be fitted very well to the Esopus Creek watershed discharge data, because in a temperate climate the snowmelt requires another subroutine and with the large height differences in the watershed, the snowmelt is spatial variable. The proportion of surface runoff zone and permeable hillsides were derived statistically from the discharge data. The SEEM model was able to simulate the discharge pattern quite well in the watersheds (Figure D1-1, D1-3, and D1-5 in Appendix D).

The Nash Sutcliffe efficiencies in Table 5-1 for validation for the daily discharge data in the Anjeni watershed was 0.80 (Table 5-1), for the 7-day average discharge in Andit Tid was similarly 0.8 and for the 10-day average discharge in the entire Blue Nile in Ethiopia was 0.92. The SEEModel was able to simulate the discharge pattern quite well in the watersheds. The predicted and observed discharge for 1989 validation year for the Anjeni watershed and for 1990 validation year for Andit Tid are shown in Figure 5-2a. In Anjeni the peak daily flows were underestimated likely because saturated areas were forming near the river for the high flows and they were not included in the model. The fit for Andit Tid during calibration was successful as shown from NSE in Table 5-1. During validation, it is found that the watershed produced less runoff peaks as shown for validation of 1993 in Figure 5-2b which might be due to the problem with gauging site. The data for the Enkulal watershed was only collected in 2010 and weekly running averaged discharge in 2010 is simulated in Figure 5-2c. The fit is not great and is partly caused by the uncertainty of the peak flows. The Blue Nile validation is shown for the year 2003 in Figure 5-2d. The NSE values were improved over the Collick et al. (2009) spreadsheet model and comparable to the SWAT-WB model in Easton et al. (2010) for Anjeni and the entire Ethiopian Blue Nile basin. The good fit of the hydrology model is a consequence that the model recognizes that before the watershed discharge can respond to precipitation after the dry season, the soils need to be filled to field capacity or saturation.

In simulating the sediment losses, we first define the form of the function of H, indicating the fraction of plowed land with active rill formation. Tebebu et al. (2010) and Zegeye et al. (2010) found that the erosion is the greatest just after plowing and stopped after rills were formed in the field. Cultivation begins after the first rainfall and then continues for approximately a three to four week period. Therefore, in the model we assume that the concentration from the runoff areas is at the transport limit (i.e., H=1) for the first four weeks after the first rainfall event. Then for another month a few more fields are being prepared and the H decreases from 1 to zero. Around August 1 the sediment concentration from the runoff areas is at the source limit except for the Esopus Creek watershed where the sediment remains at its transport limit due to the unstable banks.

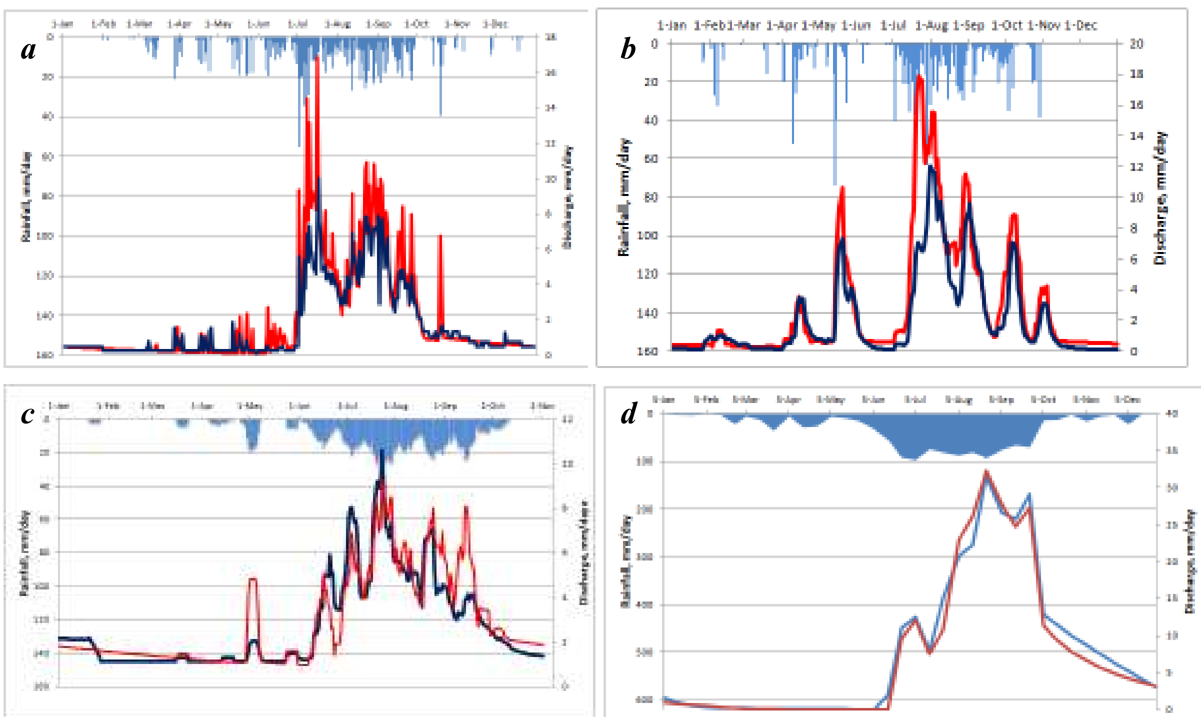

Figure 5-2: Predicted (red line) and observed (blue line) discharge data for a) Anjeni validation for daily discharge in 1989; b) Andit Tid validation for weekly average discharge in 1990. c) Enkulal calibration running weekly average discharge in 2010; d) Validation for the Blue Nile at the Ethiopian-Sudan border in 2003. Rainfall amounts expressed in mm/day is the solid blue area chart hanging from the top of each figure.

The sediment concentration shown in Figure 5-3 are calculated according to Equation 6 by using the H values as specified above and the discharges predicted by the hydrology model. The value for n was 0.4 as it theoretically should be for a wide field (Tilahun et al., 2012). This modeling approach has resulted in a better simulation (Figure D2-1, D2-3 and D2-5 in Appendix D) than that of the first attempt using only transport limiting by Tilahun et al. (2012). For validation period in Anjeni and Blue Nile Basin, the NSF improved reasonably. The coefficients a_t and a_s in Table 5-1 were calibrated for first year of data and then validated with the remaining years of data. The observed and predicted values for the validation of three watersheds with multiple years of data fit well (Table 5-1; Figure 5-3a, b and d). The transport limiting concentration, a_t for Andit Tid and the Blue Nile is surprisingly similar (Table 5-1). The transport limiting capacity, a_t, for Anjeni and Enkulal watershed is greater than the other two likely because both watersheds have more cultivated land and the soils in Enqulal watershed are sandier than the remaining watersheds. The source limits for all three watersheds spanning a range of scales in Ethiopia are similar. We could not use the model employed for Ethiopia for the Esopus Creek because of the inability to simulate snow melt accurately. Therefore, based on the long-term statistical analysis the average area contributing to base and interflow (A3 in Equation 6) was found to be 0.68 and therefore ($A_1 + A_2$) was 0.32. The H value was kept constant at 0. We left the exponential term n=0.4 and calibrated the value of the transport limiting capacity, as 0.63 (Figure 5-4). This was much lower than in the Nile basin, likely because the watershed was completely forested. The Nash Sutcliffe efficiency was 0.61 for calibration. However, during the validation period, the model (Equation 6) performed better (NS efficiency of 0.66) than the calibration. The SEEModel was able to capture the variability in stream discharge-turbidity relationship to a certain extent (Figure 5-3).

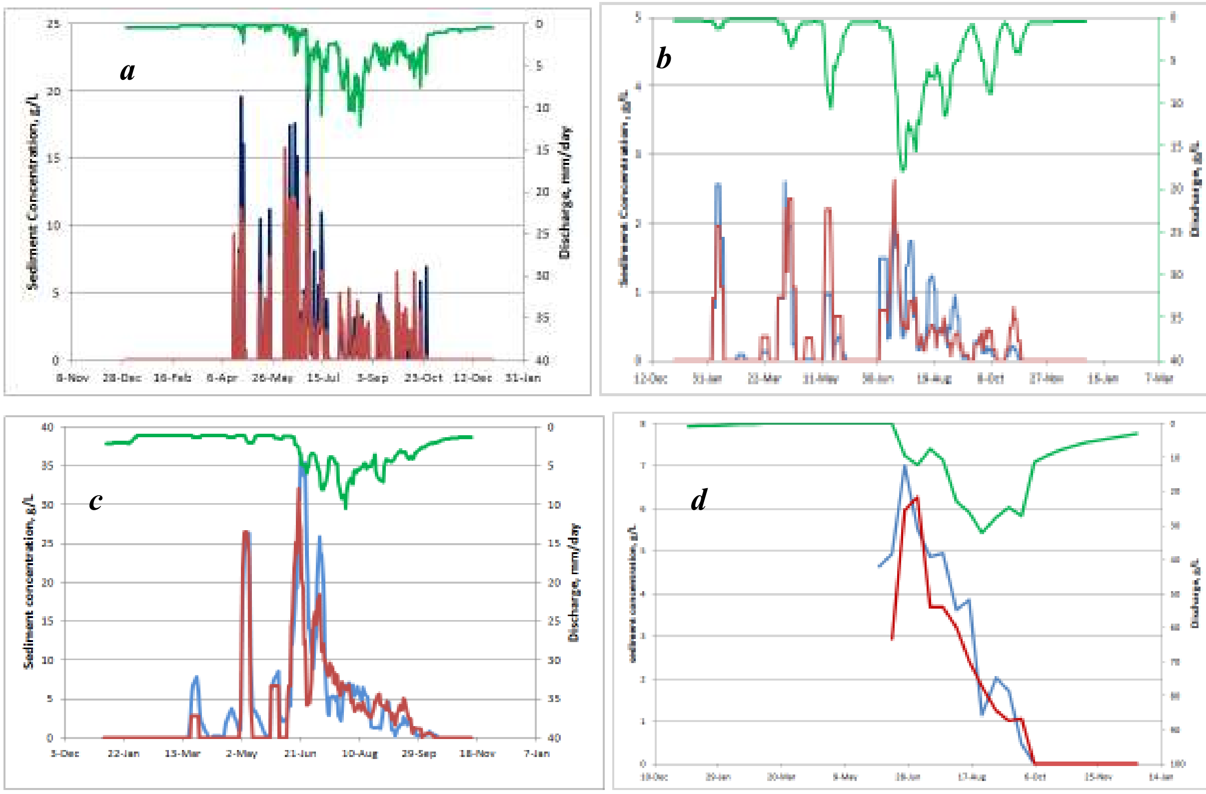

Figure 5-3: Predicted (red line) and observed (blue line) sediment concentration for a) Anjeni validation for daily concentrations in 1992; b)Andit Tid validation for weekly concentration in 1993; c)Enkulale calibration running weekly average concentration in 2010; d) validation for 10-days average of the Blue Nile at Ethiopian-Sudan border in 2003. Discharge expressed in mm/day is the solid green area chart hanging from top of figure.

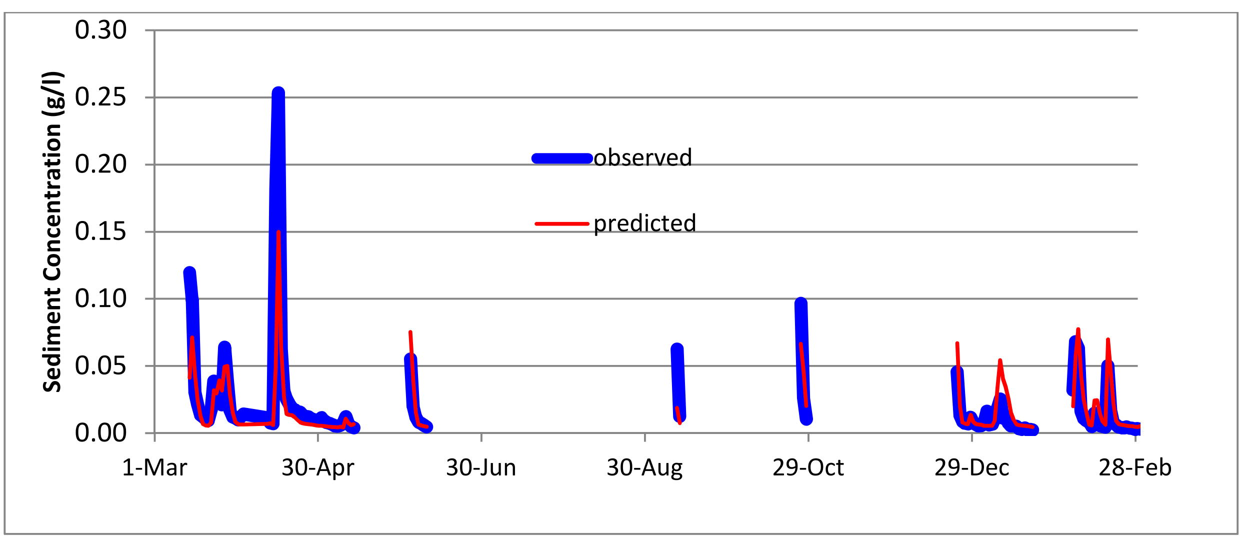

Figure 5-4: Esopus creek watershed 2007-2008 validation.

5.5 Conclusions

Sediment concentrations in the stream were monitored in four watersheds. The SEEModel was developed by assuming that the concentration in the stream was the transport limiting capacity at the time the fields were plowed and then became equal the source limit once the rill network in the field were fully developed. The Nash Sutcliffe efficiencies are remarkably good for such a hillslope erosion model over such a wide range of scales and better than most values reported in the literature for the Blue Nile Basin. Although the hydrology model could not be used in temperate climate where most runoff is produced during snowmelt, the sediment relationships seemed to apply as well.

References

Arnold, J. G. and P. M. Allen.: Methods for estimating baseflow and groundwater recharge from stream flow. Journal of the American Water Resources Association 35(2): 411-424, 1999.

Bayabil, H. K., Tilahun, S. A., Collick, A. S., and Steenhuis, T. S.: Are runoff processes ecologically or topographically driven in the Ethiopian Highlands? The case of the maybar, Ecohydrology, 3(4), 457–466, doi:10.1002/eco.170, 2010.

Ciesiolka, C. A. A., K.J. Coughlan,C.W. Rose, M.C. Escalante, G.M. Hashim, E.P. Paningbatan Jr. and S. Sombatpanit.: Methodology for a multi-country study of soil erosion management, Soil Technol., 8, 179–192, 1995.

Collick, A. S., Z.M. Easton, T. Ashagrie, B. Biruk, S. Tilahun, E. Adgo, S.B. Awulachew, G. Zeleke, and T.S. Steenhuis.: A simple semidistributed water balance model for the Ethiopian Highlands, Hydrol. Process., 23, 3718–3727, 2009.

Demisse, B.A.: Discharge and sediment yield modeling in enkulal Watershed, Lake Tana region, Ethiopia. A Thesis Presented to the Faculty of the Graduate School of Cornell University In Partial Fulfillment of the Requirements for the Degree of Master of Professional Studies, Ithaca, NY, 2011

Easton, Z. M., D.R. Fuka, E.D. White, A.S. Collick, B. Biruk B, Ashagre, M. McCartney, S.B. Awulachew, A.A. Ahmed, and T.S. Steenhuis.: A multi basin SWAT model analysis of runoff and sedimentation in the Blue Nile, Ethiopia, Hydrol. Earth Syst. Sci., 14, 1827–1841, doi:10.5194/hess-14-1827-2010, 2010.

Engda, T. A., Bayabil, H. K., Legesse, E. S., Ayana, E. K., Tilahun, S. A., Collick, A. S., Easton, Z. M., Rimmer, A., Awulachew, S. B., and Steenhuis, T. S.: Watershed hydrology of the (semi) humid Ethiopian Highlands, in: Nile River: Hydrology, Climate and Land Use, edited by: Melesse, A., Springer Science Publisher, New York, 2011.

Guzman, C.D.: Suspended sediment concentration and discharge relationships in the Ethiopian highlands. A Thesis Presented to the Faculty of the Graduate School of Cornell University In Partial Fulfillment of the Requirements for the Degree of Master of Science, Ithaca, NY, 2011

Hairsine, P. B. and C.W. Rose.: Modeling water erosion due to overland flow using physical principles 2. Rill flow, Water Resour. Res., 28(1), 245–250, 1992.

Kandel, D., Western, A., Grayson, R., and Turral, H.: Testing current generation soil erosion models at two minute and daily scales using plot scale data from a mid-hill catchment of Nepal, in: Integrating Models for Natural Resources Management Across Disciplines, Issues and Scales, edited by: Ghassemi, F., Post, D., Sivapalan, M., and Vertessy, R., Proceedings of the International Congress on Modeling and Simulation (MODSIM 2001), Volume 1: Natural Systems Modeling and Simulation Society of Australia and New Zealand Inc., Australian National University, Canberra, Australia, 365–370, 2001

Liu, B. M., Collick, A. S., Zeleke, G., Adgo, E., Easton, Z. M., and Steenhuis, T. S.: Rainfall discharge relationships for a monsoonal climate in the Ethiopian Highlands, Hydrol. Process., 22(7), 1059–1067, 2008.

Nash, J.E., and J.V. Sutcliffe.: River flow forecasting through conceptual models, Part 1 - a discussion of principles. Journal of Hydrology 10: 282–290, 1970.

Rose, C. W.: Soil erosion models and implications for conservation of sloping tropical lands, in: Sustaining the Global Farm- Selected papers from the 10th International Soil Conservation Organization Meeting, 24–29 May 1999, West Lafayette, IN, International Soil Conservation Organization in cooperation with the USDA and Purdue University, West Lafayette, edited by: Stott, D. E., Mohtar, R. H., and Steinardt, G. C., CD-ROM available from the USDA-ARS National Soil Erosion Laboratory, West Lafayette, 852–859, 2001.

Rose, C.W., Williams, J.R., Sander, G.C., Barry, D.A.: A mathematical model of soil erosion and deposition processes: I. Theory for a plane land element. Soil Sci. Soc.Am. J. 47, 991– 995, 1983.

Siepel, A. C., T.S. Steenhuis, C.W. Rose, J.-Y. Parlange, and G.F. McIsaac.: A simplified hillslope erosion model with vegetation elements for practical applications, J. Hydrol., 258, 111–121, 2002.

Steenhuis, T. S. and W.H. van der Molen,: The Thornthwaite-Mather procedure as a simple engineering method to predict recharge, J. Hydrol., 84(3–4), 221–229, 1986.

Steenhuis, T. S., A.S. Collick, Z.M. Easton, E.S. Leggesse, H.K. Bayabil, E.D. White, S.B. Awulachew, E. Adgo and A. A. Ahmed. Predicting discharge and erosion for the Abay (Blue Nile) with a simple model, Hydrol. Process., 23, 3728–3737, 2009.

Tebebu, T.Y., A.Z. Abiy, A.D. Zegeye, H.E. Dahlke, Z.M. Easton, S.A. Tilahun, A.S. Collick. S. Kidnau, S. Moges, F. Dadgari and T. S. Steenhuis. Surface and subsurface flow effect on permanent gully formation and upland erosion near Lake Tana Ethiopia. HESS 14: 2207-2217, 2010.

Tesemma, Z. K., Y. A. Mohamed and T.S. Steenhuis.: Trends in rainfall and runoff in the Blue Nile Basin: 1964–2003, Hydrol. Process., 24(25), 3747–3758, doi:10.1002/hyp.7893, 2010.

Tilahun,S.A., Guzman, C.D., Zegeye, A.D., Engda, T.A., Collick, A.S., Rimmer, A., and Steenhuis, T.S.: An efficient semi-distributed hillslope erosion model: The Anjeni in the sub humid Ethiopian highlands. Hydrol. Earth Syst. Sci. Discuss., 9, 2121-2155, 2012.

Vanmaercke, M., Zenebe, A., Poesen, J., Nyssen, J., Vertstraeten, G., and Deckers, J.: Sediment dynamics and the role of flash floods in sediment export from medium-sized catchments: a case study from the semi-arid tropical highlands in Northern Ethiopia, J. Soil Sediment., 10(4), 611–627, 2010.

Yu, B., C.W. Rose, B.C. Ciesiolka, K.J. Coughlan and B. Fentie.: Toward a framework for runoff and soil loss prediction using GUEST technology, Aust. J. Soil Res., 35, 1191-1212, 1997.

Zegeye, A.D., T.S. Steenhuis, R.W. Blake, S. Kidnau, A.S. Collick and F. Dadgari.: Assessment of Upland Erosion Processes and Farmer Perception of Land Conservation in Debre-Mewi Watershed, near Lake Tana, Ethiopia. Ecohydrologica 10: 297-306, 2010.

CHAPTER 6: PERFORMANCE OF SATURATION EXCESS HYDROLOGY AND EROSION MODELS FOR THE NESTED DEBRE MAWI WATERSHEDS IN THE SEMI HUMID ETHIOPIAN HIGHLANDS

Abstract

Erosion by saturation excess runoff is common in the Ethiopian highlands. In earlier chapters, we developed semi-distributed conceptual models that can simulate water and sediment fluxes in these landscapes, but these models were only tested for concentrations at the outlet of the watershed and not on the distribution of runoff and erosion within the watershed. In this paper we tested this saturation excess erosion model on a 95 ha Debre Mawi watershed and three of its nested sub-watersheds. The hydrology and erosion models are based on dividing the watershed into two potentially runoff (and erosion) generating areas where either the water table or slowly permeable horizon is close to the surface and in the remaining part of the watershed, the rainwater infiltrates and becomes baseflow or interflow. Daily storm runoff and sediment concentration were measured at the outlet (Weir-5) and its sub-watershed outlet (Weir-1, -3 and -4) in the 2010 and 2011 rainy phase and are used to validate the hydrology and erosion model. Model input consisted of climate data of daily rainfall and potential evaporation; hydrology parameters of area fraction and maximum water storage of the three areas and three parameters describing subsurface flow. Furthermore erosion parameters were used that describe transport and source limited conditions with an H value to represent the fraction of runoff producing area with active rill erosion. Daily storm runoff and sediment concentration were well simulated with realistic fractional areas for surface and subsurface flow and with close similarity of the remaining hydrology and erosion parameter values except with the distinctly greater transport

limited parameter for the actively gullying watersheds. The Nash Sutcliffe efficiency values for the daily storm runoff were greater than 0.66 and the daily sediment concentrations had Nash Sutcliffe values greater than 0.78. The results suggest that the model can simulate the spatially distributed runoff and sediment concentration within a watershed.

6.1 Introduction

There is an urgent need for effective and better erosion control in the Blue Nile Basin since past efforts have been less than successful in reducing soil loss. One of the reasons is that most erosion control practices were constructed with food for work (Osman and Sauerborn, 2001) since 1970's throughout watersheds without a good plan for selecting the most appropriate locations. For proper planning of soil and water conservation practices, realistic erosion models are needed. Since saturation excess runoff mechanisms are prevalent in the (sub) humid Ethiopia highlands (Steenhuis et al., 2009), the challenge is to develop and test models that represent the spatial nature of these runoff processes.

Most models applied in the Ethiopia highlands such as the Agricultural Non-Point Source Pollution (AGNPS) model (Haregeweyn and Yohannes, 2003; Mohammed et al., 2004) and the Soil and Water Assessment Tool (SWAT) (Setegn et al., 2008) had limitation because the underlying runoff mechanism in these models is infiltration excess runoff mechanism and with additional limitation of using Universal Soil Loss Equation (USLE) to estimate soil loss, while runoff mechanism are topographically driven through saturation excess on soil with either shallow hardpan or high water table (Liu et al., 2008; Steenhuis et al., 2009, Bayabil et al., 2010; Engda et al, 2011). The Water Erosion Prediction Project (WEPP) (Zeleke, 2000) was another model applied in the highland, which has physically based erosion routines but prediction precision is also hampered by infiltration excess based runoff simulations.

On the contrary, the modified SWAT-Water Balance (WB) model (Easton et al., 2010) has realistic predictions of runoff and sediment source locations because of its consideration of the correct runoff mechanisms and therefore erosion predictions were improved. In addition, a hill-slope erosion model based on a simplification of the Hairsine and Rose model (1992) (Tilahun et al., 2012) and a saturation excess erosion model (Tilahun et al., 2012) was developed and performed well in three small watershed and the entire Blue Nile Basin. Further validation of this hillslope model in additional watersheds is however needed and particularly its calibration at sub-watershed outlets for it to be used with confidence in the prediction of watershed scale soil loss for improved planning of soil and water conservation.

The objective of this paper is therefore to test and check the applicability of the saturation excess erosion model and its underlying hydrology model developed by Tilahun et al. (2011) in the Debre Mawi watershed at its outlet and its nested sub-watersheds.

6.2 Material and Methods

6.2.1 Site Description

The Debre Mawi watershed research site, named after the Keble Debre Mawi in Yilmana-Densa Woreda (district), covers a total area of 523 ha. It is situated 30 km south of Bahir Dar adjacent to the Bahir Dar-Adet road at 37°22’ East and 11°18’ North (Figure 6-1) in the western plateau of the Ethiopian highlands at the northern source region of the Blue Nile River. A sub-watershed of approximately 95ha was selected for this study which is located in the upstream portion of the whole watershed. Its slope ranges from 1 to 30% and topography ranges from 2,212 meters above sea level (m.a.s.l.) near the outlet to 2,306 m.a.s.l. in the south east.

The watershed is underlain by shallow, highly weathered and fractured basalt overlain by dark brown compacted clay, then by light brown wet and sticky clay soil and then finally by black clay and organic rich soil sequences (Abiy, 2009). The fractures are highly interconnected with limited clay infillings. Lava intrusion dikes block the fractures at several location in the watershed as will be discussed later. The dominant soil types in the watershed are Nitisols, Vertisols and Vertic Nitisols: Nitisols (locally referred to as, *Dewel*) are found in the upper part of the watershed. This is a very deep, volcanic derived well-drained red clay loam soil and is considered the most productive and permeable soil. The Vertisols (locally referred to as *Walka*) is black and cover the lower slope positions. This soil forms deep wide cracks during the dry period and, it swells and develops stickiness during rainy period. Vertic Nitisols (locally known as *Silehana*) are located midslope between the Vertisols and Nitisols. It is reddish-brown and has properties of draining water when it is in excess and holding water when it is low. When it is dry, it has similar cracking properties as Vertisols. It is especially suitable for tef production.

Seventy percent of the watershed is cropland with the remaining as grassland, bush or fallow that is either too dry or too wet for crop production (Mekonnen and Melesse, 2011). Most of the upper (slope of 0 to 6%) and middle area (slope of 6 to 27%) of the sub-watershed is used for cultivation. The lower part of the watershed with slopes of 0 to 6% is usually saturated during the rainy season and covered with grass and gullies. These areas of the watershed serve as grazing land. Sparse shrubs are located at the middle, which is relatively steeper and difficult to plough. Fields at the upper and middle are continuously cropped. Cereal-plough cultivation is the dominant cultivation system in the area, and most of the cultivated fields are usually planted with tef, wheat, maize, and barley. Finger millet, lupine (particularly, Lupinus albus) and grass pea are also common crops grown in the area.

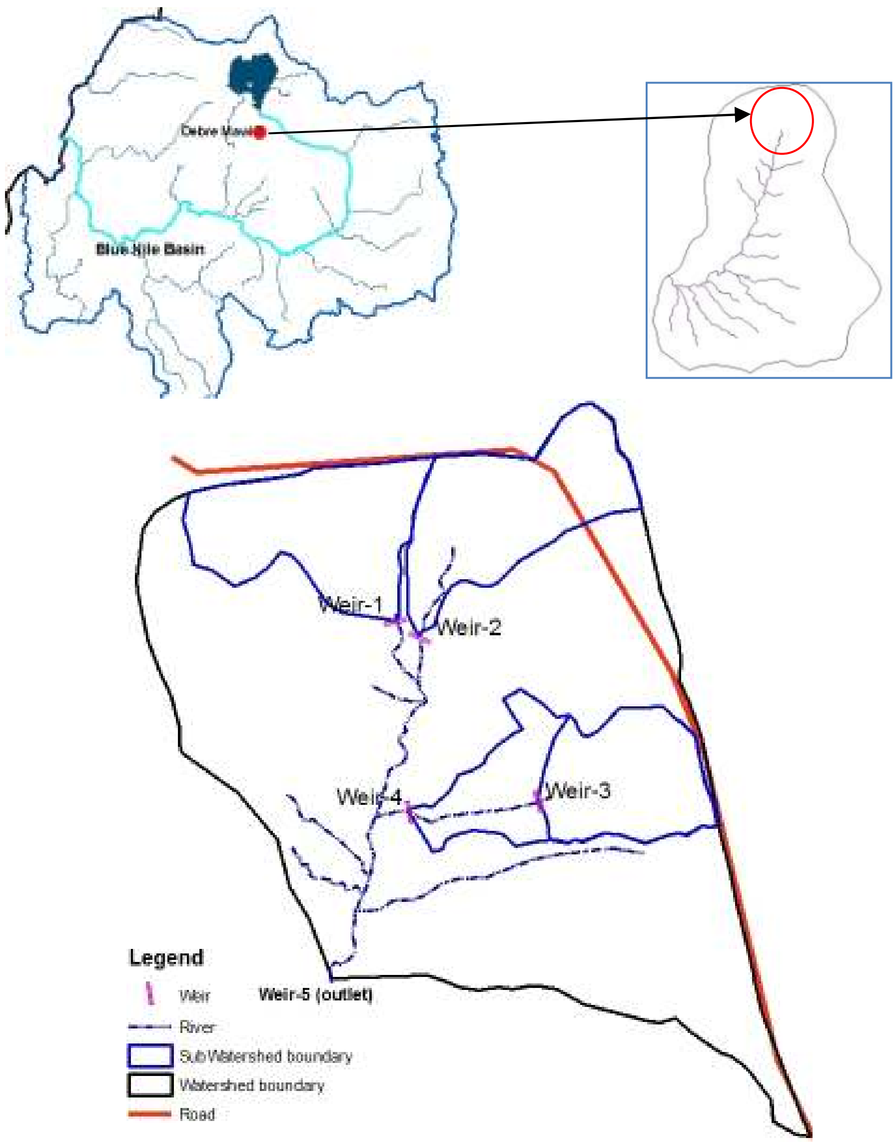

Figure 6-1: Location, boundary and drainage map of Debre Mawi storm runoff monitoring sites (Weirs), perched water table sampling and infiltration test sites within the watershed (P stands for piezometer, and I stands for infiltration)

Four sub-watersheds, within the 95 ha Debre Mawi watershed, were established and included in this study. Sub-watersheds from each weir (Figure 6-1) were defined using GPS tracking on the field. The size of the sub-watershed areas are 8.8, 10, 6.4 and 10.3 ha at Weir- 1, 2, 3 and 4, respectively. The slope of the sub-watersheds ranges from 0.6 to 16%. All sub-watersheds at the upslope are covered by Nitisols soils, flat or gently sloping and dominated by agriculture. The main crops were tef, maize, wheat and lupine. The wet bottom area of the sub-watershed at Weir-1 was covered by grass during the two rainy seasons (2010 and 2011). It was saturated during the last part of the rainy phase of the monsoon. This part was not cultivated and used only as grassland because it was too wet for crops. The sub-watershed at Weir-2 received storm runoff from part of the main road from Bahir Dar to Adet and developed a relatively small gully upstream and a more substantial gully downstream. Since the unpredictability of the runoff from this watershed is high due to road runoff, this watershed is excluded from validation of the model. The sub-watershed of Weir-4 drained mainly upland runoff from the sub-watershed at Weir-3 and it contains a saturated area upstream of its outlet. The watersheds of Weir-1, Weir-2 and Weir-3 has lava intrusions that interrupt the continuity of flow to the outlet of the weirs and are associated with springs that are located in the river bed approximately 50 m below weir 1 and 2 (

Figure 6-2) and saturated area below Weir-3. Weir 4 is located below the lava intrusion dikes at the steepest middle part of the sub-watershed.

Figure 6-2: Spring downstream of Weir-1 at a distance of 50m (picture taken in Jun, 2012)

6.2.2 Data

Storm runoff and corresponding sediment concentration were measured at the outlet and its four sub-watershed outlet in Debre Mawi for 2010 and 2011 rainy period. The measurements were conducted from June 29, 2010 to September 16, 2010 and from June 25, 2011 to September 14, 2011 at the four monitoring sites (Weir 1 to 4) of the sub-watersheds while at the outlet, measurements were conducted from June 22, 2010 to October 1, 2010 and from June 12, 2011 to September 18, 2011 as described in Chapter 2 and 3. Rainfall, total discharge and average sediment concentration were recorded for each storm period during the day and night. A storm period is defined as the period from the beginning of runoff to its end when the water became clear of sediment. Rainfall was recorded at five minute intervals with an automatic tipping bucket (with resolution of 0.25 mm) installed near the center of the watershed. Flow rate was estimated each ten minutes using the water depth at the weir and a rating equation (Chapter 2). The stage-discharge rating equation was calculated by the product of cross-sectional area and the average velocity that was determined by releasing a float in the stream. Sediment samples were taken using a 1L plastic bottle at 10 minute intervals during runoff event. Ten minute runoff rate and loads (product of storm runoff and sediment concentration) were summed up over a storm period to determine total storm runoff and sediment load. Daily sediment concentration was determined by dividing the total sediment load by the total storm runoff during that day. Finally, daily potential evaporation for 2010 and 2011 was obtained from Adet weather station, 10km south of Debre Mawi. Both rainfall and potential evaporations were input to the model that is described below.

6.2.3 Methodology

We calibrated first the daily storm runoff values during the storm periods in the rainy period of 2010 and 2011 with the semi-distributed conceptual water balance model developed by Steenhuis et al. (2009) and subsequently the corresponding daily sediment concentrations (during storm period) with the sediment model developed by Tilahun et al.(2011) at the outlet (Weir-5) of the watershed and three sub-watershed at Weir-1, Weir-3 and Weir-4. Sub-watershed at Weir-2 is excluded as it was affected by the runoff from road.

Semi-distributed water balance hydrology model: The water balance conceptual model that takes into account saturation excess runoff principles (Steenhuis et al., 2009; Tessema et al., 2010; Tilahun et al., 2011, Tilahun et al., 2012) is depicted in Figure 6-3. The watershed is divided into three zones: two surface runoff zones -- one that becomes saturated during the wet monsoon phase and the other is the degraded hillsides with the slowly permeable sub-horizon with shallow soil depth. In the third zone (consisting of the remaining the hillsides), the rainwater infiltrates and becomes either interflow (zero order reservoirs) or base flow (first order reservoir).

Climatic input to the model consists of rainfall and potential evaporation. We used total storm rainfall for days on which storm runoff was measured for calculating total storm runoff and daily rainfall for the remaining days for updating the water balance. The model has nine parameters (Figure 6-3) including the area fraction (A) and the maximum storage capacity (S_{max}) for the three zones and three subsurface parameters: half life ($t_{1/2}$) and maximum storage capacity (BS_{max}) for a linear aquifer and the drainage time of the zero order reservoir (τ^*). The initial values of the area fractions of these zones were derived from map of saturated areas and computed runoff coefficients in chapter 2. The initial values of the remaining six parameters were obtained from the calibration and validation of the model in Anjeni and Blue Nile Basin by Tilahun et al.(2012). Although the baseflow was not measured, the baseflow was simulated because during the storm events, baseflow is an additional component especially in August and September when the subsurface flow continues for a few days after the runoff event.

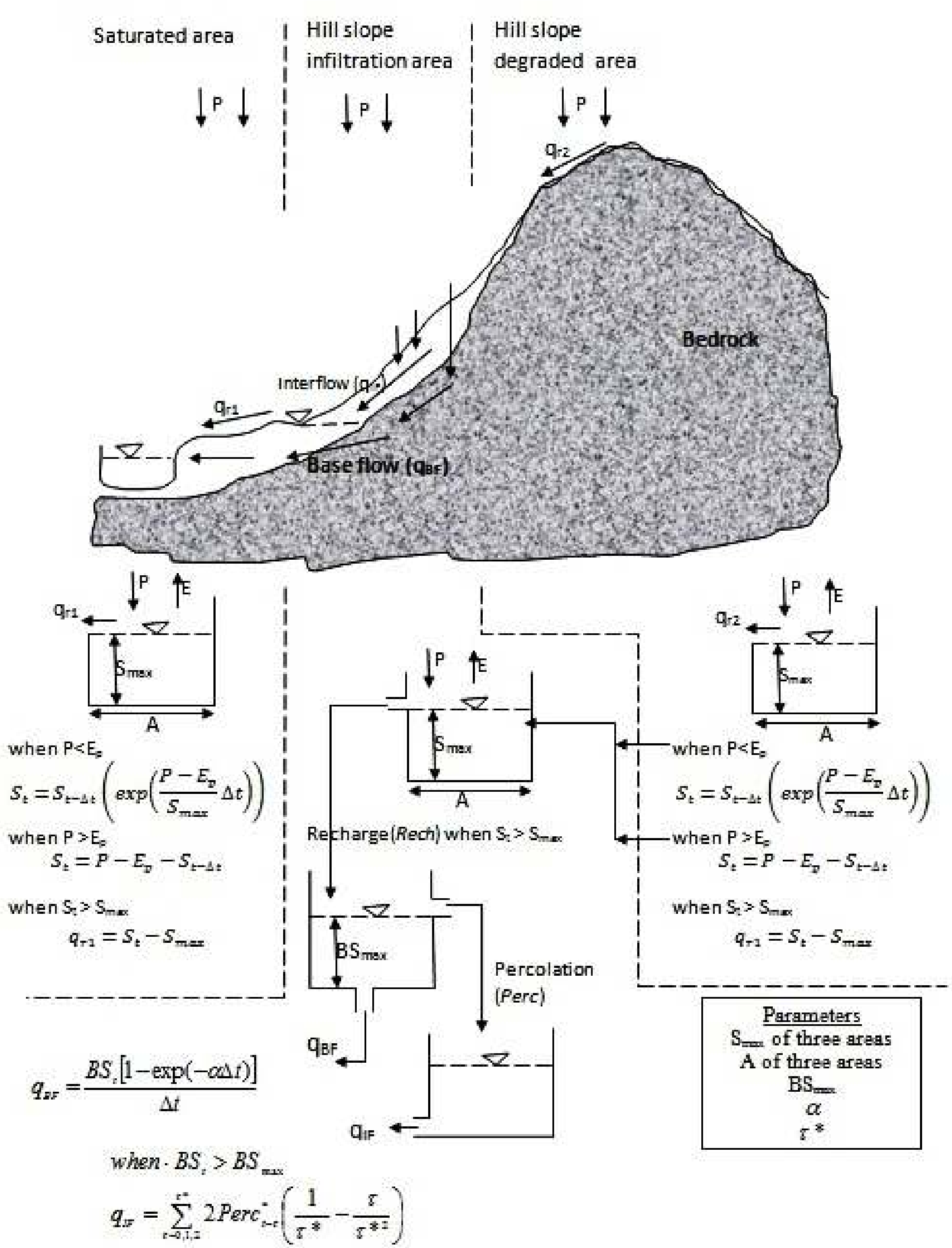

Figure 6-3: Conceptual hydrology model *(P is precipitation; Ep is potential evaporation; A is area fraction for components of 1-saturated area, 2-degarded area and 3-infiltration areas; Smax is maximum water storage capacity of the three areas; BSmax is maximum base flow storage of linear reservoir; t½ (=0.69/α) is the time it takes in days to reduce the volume of the base flow reservoir by a factor of two under no recharge condition;, τ* is the duration of the period after a single rainstorm until interflow ceases).*

Saturation excess erosion model: In the saturation excess erosion model (Tilahun et al, 2011), erosion only takes place from two surface runoff zones that produces surface runoff: surface flow from one that becomes saturated during the wet monsoon period, q_{r_1} , and the other, surface flow from the degraded hillsides, q_{r_2} (Figure 6-3). Moreover an assumption is made that the erosion rate is proportional to the average overland flow water velocity (Hairsine and Rose model, 1992). In addition, it is assumed that the sediment is at the transport limit early in the rainy phase and at the source limit at the end of the rainy phase. Finally, base flow q_b and interflow q_i dilutes the sediment concentration from the source areas. Based on these assumptions, Tilanhun et al. (2011) derived the following equation for sediment concentration.

$$C = \frac{\left(A_1 {q_{r_1}}^{1.4}[a_{s1}+H(a_{t1}-a_{s1})]+A_2 {q_{r_2}}^{1.4}[a_{s2}+H(a_{t2}-a_{s2})]\right)}{A_1 q_{r_1}+A_2 q_{r_2}+A_3(q_b+q_i)} \qquad 1$$

The four soil related parameters a_{t1}, a_{t2}, a_{s1} and a_{s2} are coefficients where the subscripts indicate the saturated (1) and degraded areas (2) for transport limiting (t) and source limiting (s). The variable H in the model was used as explained in Chapter 5 but we modified here the values based on the observations and measurements of rill erosion in 2011. H (Figure 6-4) is defined as the fraction of the runoff producing area with active rill formation. Fields are plowed from the beginning of rainy period in June to beginning of August where rill network and erosion were active. For the last two weeks of June and the beginning two week of July, H is assigned as 1 indicating transport limit in which rill erosion started developing. After the first two week of July, the H value drops to 0.5. Then, H drops to 0.25 in August as rill development stopped and then zero (indicating source limit) after August. The flows q and the areas A were obtained from the hydrology model.

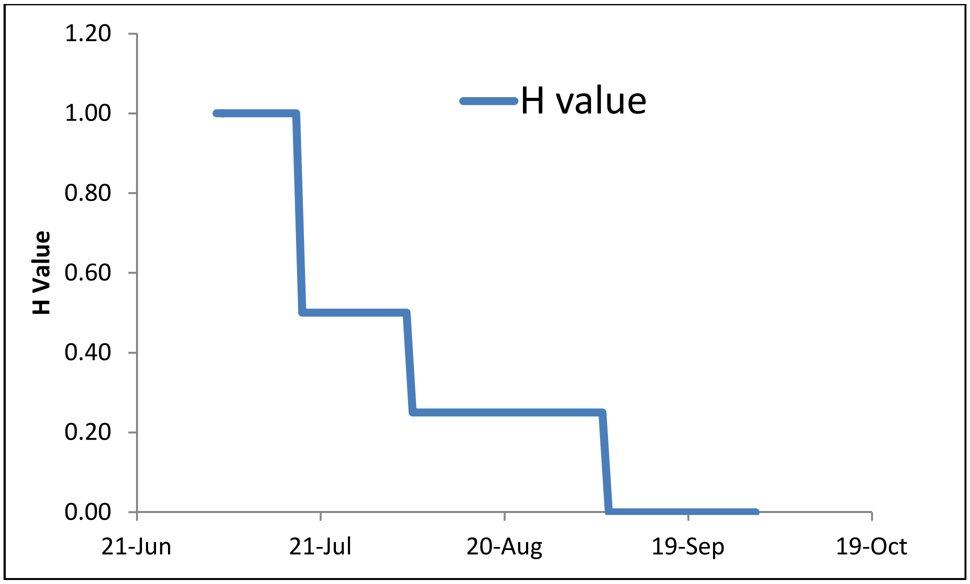

Figure 6-4: The temporal variation of H defined for Debre Mawi watershed. H is a fraction of area with rill erosion during the rainy period.

6.2.4 Calibration

All the nine hydrology parameters were calibrated (Figure 6-3). We first fitted the parameters for the main watershed and then we tried to adjust the fractional areas for the three zones while keeping all six other parameters constant. Initial values for calibrating parameters such as area fraction were based from field measurements described in chapter 2 and other parameters were obtained from watershed modeling experiences in chapter 4. These initial values were changed manually through randomly varying input parameters in order that the best "closeness" or "goodness-of-fit" was achieved between simulated and observed storm runoff at the outlet and its sub-watersheds.

In the sediment model, there are four calibration parameters consisting of the constants for each of the two runoff source areas a_{1t} , a_{2t} , a_{1s} and a_{2s}. The initial values of these coefficients were obtained from the calibration and validation of the model in Anjeni and Blue Nile Basin by

Tilahun et al. (2011) assuming that the watersheds in the basin behave similarly. These constants are then changed manually in order to get a best fit between measured and simulated daily sediment concentration during the storm period.

Model evaluation to calibrate the parameters of both hydrology and erosion model was based on the Nash-Sutcliffe efficiency coefficient (NSE), and coefficient of determination (R^2) with least square linear regression. The Nash Sutcliffe efficiency for the predicted and observed discharge can be calculated as

$$NSE = 1 - \frac{\sum_{i=1}^{n}\left(Q_{obs(i)} - Q_{sim(i)}\right)^2}{\sum_{i=1}^{n}\left(Q_{obs(i)} - Q_{obs(ave)}\right)^2} \qquad 2$$

Where NSE is Nash-Sutcliffe efficiency, $Q_{sim(i)}$ is simulated storm flow, $Q_{obs(i)}$ is observed storm flow and $Q_{obs(ave)}$ is average observed flow. The simulated storm flow is the sum of q_{r1}, q_{r2}, q_b and q_i. The NSE coefficient for the sediment concentration can be obtained similarly by replacing the "Q" by "C". Coefficient of determination (R^2) describe the degree of collinearity between simulated and measured data while NSE determines the relative magnitude of the residual variance compared to the measured data variance (Moriasi et al., 2007). During calibration, parameters are optimized and searched for that resulted in R^2 values close to 1, a slope of 1 and y intercept of zero, and NSE to 1.

6.3 Result and Discussion

We will fist present the hydrology simulation results followed by the predictions of the sediment concentrations. For hydrology, we calibrated the semi distributed model for the whole 95 ha watershed (Weir 5) first. According to Chapter 4, the hydrology model is sensitive to the fractional areas but less sensitive to the other 6 input parameters. Thus to fit the three remaining nested sub-watersheds, we only changed the fractional areas and try to leave the other 6 parameters constant.

The semi-distributed conceptual hydrology model fitted the daily storm runoff at the outlet of the 95 ha watershed (Weir-5) well with a NSE of 0.82 (Table 6.1) and R^2 of 0.79 (Figure 6-6a, and E1-1). The fractional areas added up to one as shown in Table 6-1 meaning that all rainfall minus what evaporated was accounted for at weir 5 (Figure 6-6a). The calibrated 15% saturated area is approximately equivalent to the observed 10% of the saturated area in Chapter 2. Thirty percent of the area was calibrated as degraded soils and is likely represented by the area where the weathered lava rock outcrop and pyroclastic fall is very close to surface. The latter became obvious when in 2012 terraces were build and the weathered rock was close the surface in many parts of the upper watershed (Figure 6-5). These degraded area fractions are slightly greater than other watersheds (Anjeni, Andit Tid; Steenhuis et al., 2009; Tilahun et al., 2011) in Blue Nile basin because of the lava intrusions, but otherwise the Debre Mawi watershed responded similar to these watersheds of the same or larger sizes indicating that many watersheds highland respond similar.

Figure 6-5: (a) Shallow soil over deeply weathered pyroclastic fall (picture taken in June 2012) b) exposed weathered rock outcrop (picture taken in July 2010)

For the sub-watersheds, we found that the degraded area fractional areas were similar to the large watersheds with 30% for sub-watersheds at Weir-3 and 4 and 20% for sub-watershed at Weir-1 (Table 6.1). The saturated areas varied around the 15% of Weir-5. It was larger (20%) for the watershed at Weir-4 that had a large saturated area in its watershed (Figure 2-9 in chapter 2) and less for sub-watershed at Weir-3 with 5% saturated area where indeed no saturated area were observed and 8% for watershed at Weir-1. The main difference between sub-watersheds and the main watershed was the total area that contributed flow to the weir (Table 6-1). This was 75 % for sub-watershed at Weir-4, 50% for sub-watershed at Weir-3 and 68% for sub-watershed at Weir-1. This is supported by our observation of the watershed. The sub-watershed at Weir-1 and -3 are located upstream of the major lava intrusions and have a relatively deep soil. Springs are found below the weir but above the lava intrusions (

Figure 6-2). The water in the spring is coming from the watershed above and is thus the unaccounted water in our model. Finally, our model fitted well for the sub-watershed as well with NSE ranging in value from 0.66 to 0.83 and reasonable R^2 ranging from 0.61 to 0.83 at the sub-watersheds outlets (Figure 6-6 and Figure E1-2 to Figure E1-4).

The other parameter such as S_{max} (the maximum soil water storage) in each area, BS_{max} (maximum storage for base flow linear reservoir), $t_{1/2}$ (half life of the linear reservoir) and τ^* (the time to complete drainage of water from zero order reservoir) in the model were not sensitive since it only affects the amount of surface runoff in the beginning of the rainfall season (Tilahun et al., 2012) and are similar among the sub-watersheds. The sub-surface interflow flow parameters τ^* are slightly different from values in Anjeni and Andit Tid since the streams in this watershed are only flowing due to storms.

Table 6-1: Parameters value optimized in the hydrology model to simulate the storm runoff at the outlet of the watershed and its sub-watershed

	Weir	5	4	3	1
	Unit				
Area	(ha)	95	10.3	6.4	8.8
Area A_1	%	15	20	5	8
S_{max} in A_1	mm	80	80	80	80
Area A_2	%	30	30	30	20
S_{max} in A_2	mm	30	30	30	30
Area A_3	%	55	25	15	40
S_{max} in A_3	mm	60	60	60	60
BS_{max}	mm	80	80	80	80
$t_{½}$	days	70	70	70	70
τ^*	days	5	5	5	5
Total area	%	100	75	50	68
NSE*		0.82	0.8	0.83	0.66

*Nash-Sutcliffe efficiency coefficient

The performance of the model to capture the storm runoff process is very good compared to the simple linear rainfall intensity described in Chapter 2. This is because runoff was produced when the soil moisture reached saturation at the valley bottom area of the watershed and the maximum available water at the hillside after a prolonged dry period (Bayabil et al., 2010). The conceptual hydrology model simulated the runoff processes that were spatially distributed among the sub-watershed implying that the model could be applied in ungaged watersheds for the watersheds where there is no subsurface under the gage.

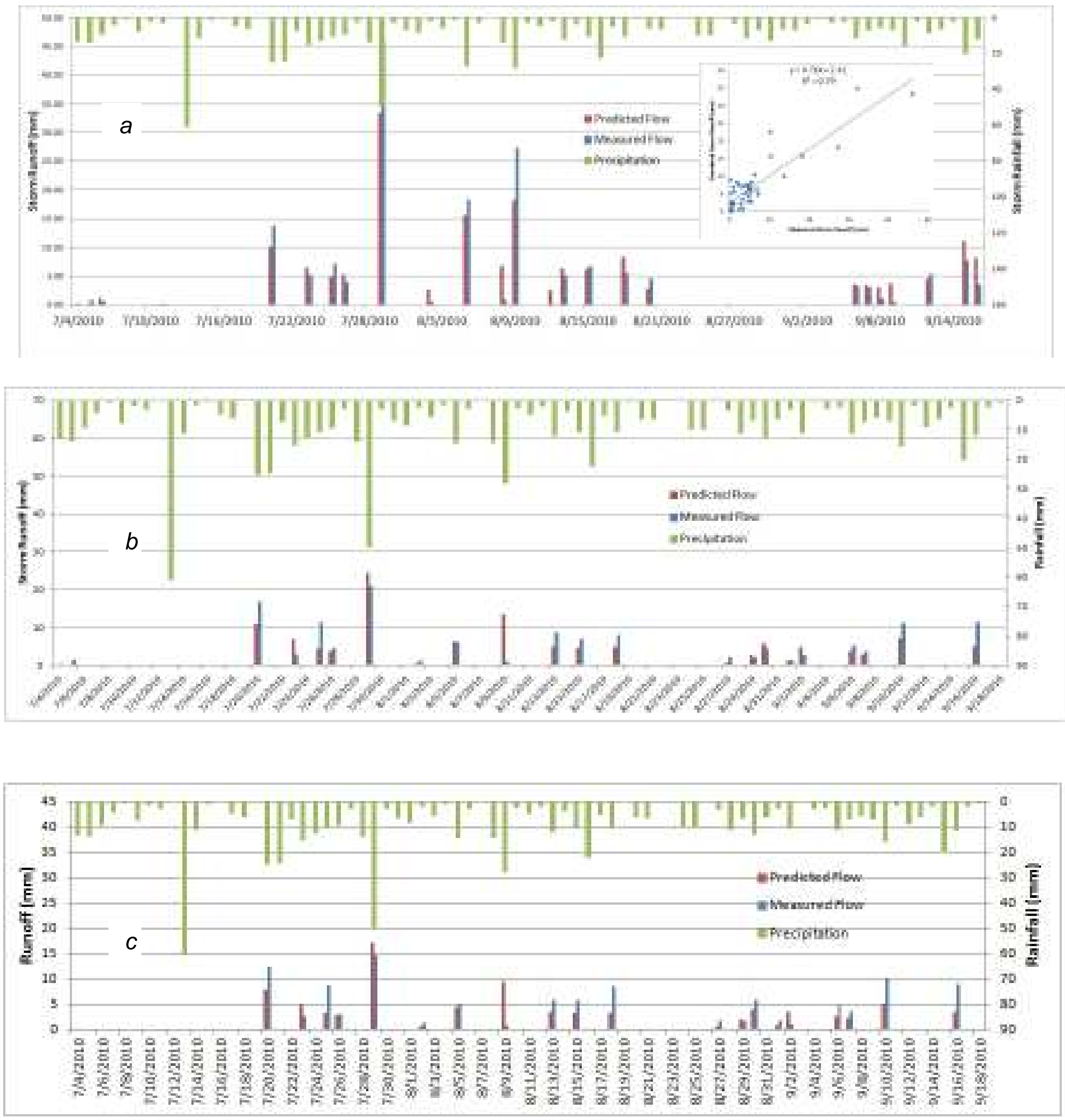

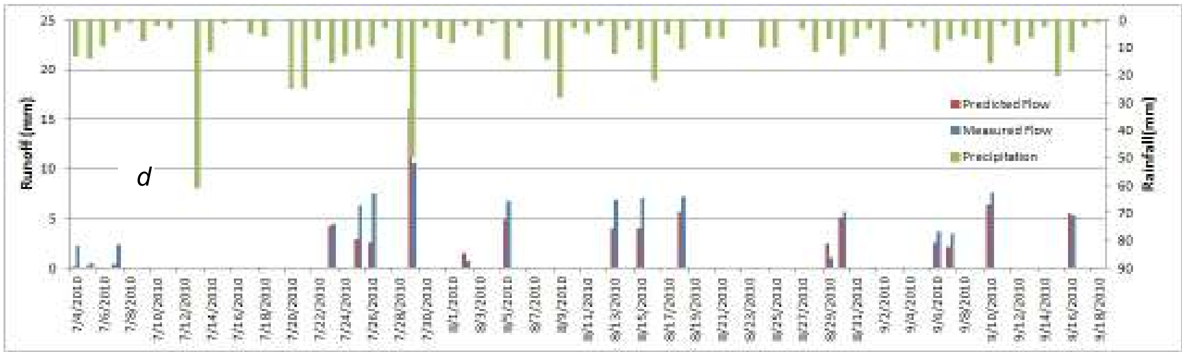

Figure 6-6: Measured and simulated storm runoff (a)at the outlet of Debre Mawi watershed (b) at Weir-4 (c) at Weir-3 and (d) at Weir-1 for summer 2010 and the scatter plot at the outlet (Weir-5) is for the 2010 & 2011 rainy season.

In simulating the sediment transport in the Debre Mawi watershed and its sub-watersheds (Figure 6-7 and Figures E2-1to E2-4 in Appendix E), we first defined the form of the function of H in equation 1 (Figure 6-4), and then calibrated the four parameters. The area proportions (A_1, A_2 and A_3), the surface runoff (q_{r1}, runoff from saturated areas and, q_{r2} runoff from degraded areas) and the sub-surface runoff (q_b, baseflow and q_i, interflow) were obtained from the hydrology model (Table 6-1). The simulation resulted in coefficient of determination R^2 values ranging from 0.65 to 0.74 while the NSE ranges between 0.78 and 0.82 (Figure 6-7 and Figure E2-1 to Figure E2-4 in Appendix E).

Table 6-2 indicated that the upslope sub-watersheds at weir-1, weir-3 and weir-4 have similar coefficients except for the transport limiting coefficient (a_{1t}) from saturated areas. This similarity is due to similarity of slope and soil type (Nitisols) of the hill slope degraded areas in these sub-watersheds. The difference of a_{1t} between Weir-4 and the other weirs (1 and 3) is due to the existence of saturated areas described in Chapter 2.

Table 6-2: Calibrated sediment model parameters

	Coefficients	Weir-5	Weir-4	Weir-3	Weir-1
Sediment transport limit	a_{1t}	6	6	1	1
	a_{2t}	14	6	6	6
Sediment Source limit	a_{1s}	3	0.5	0.5	0.5
	a_{2s}	3	0.5	0.5	0.5
	NSE*	0.75	0.8	0.78	0.8

* Nash-Sutcliffe efficiency coefficient

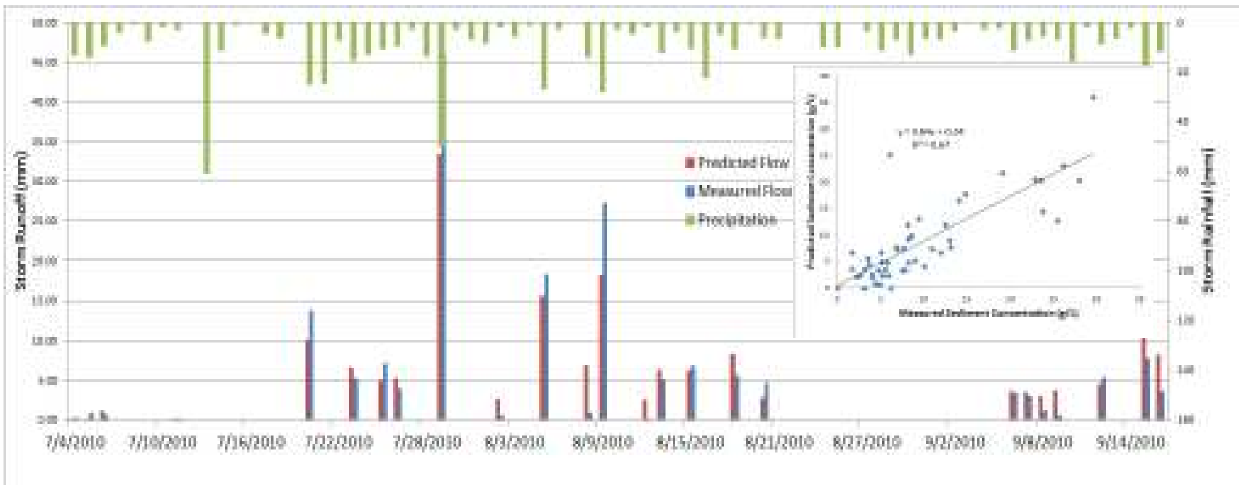

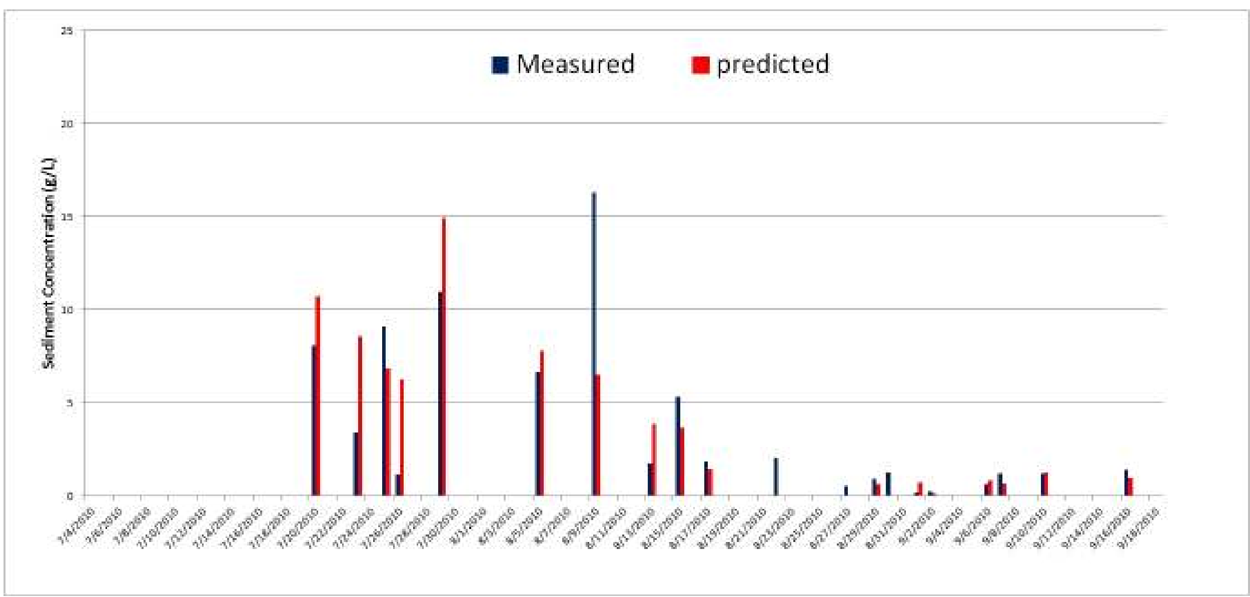

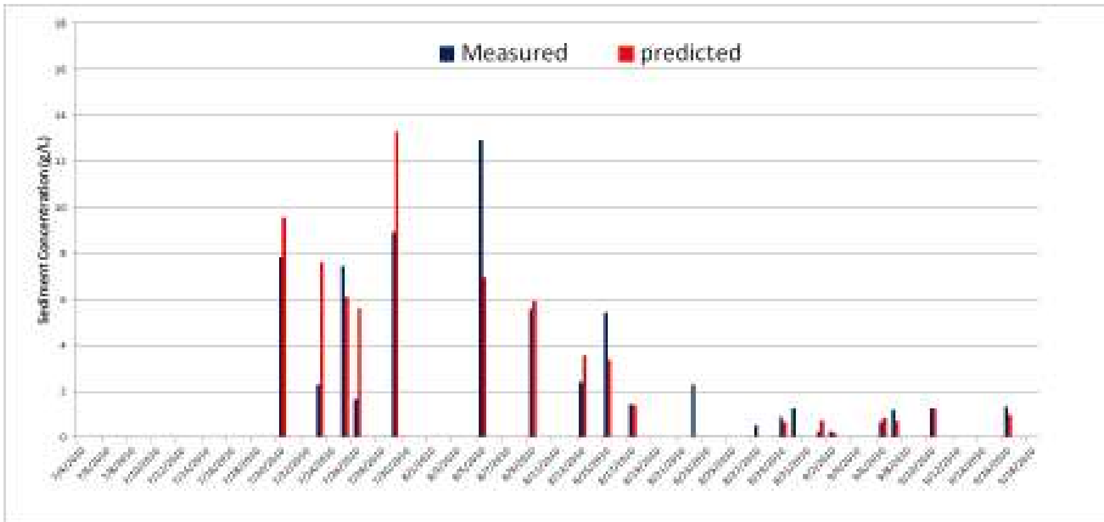

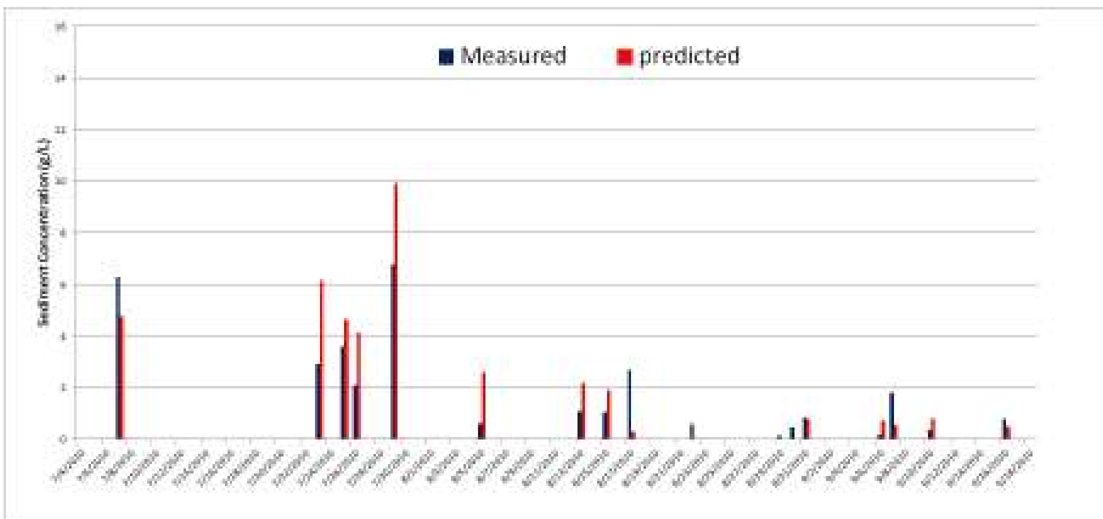

Figure 6-7: Measured and simulated sediment concentration (a)at the outlet of Debre Mawi watershed (b) at Weir-4 (c) at Weir-3 and (d) at Weir-1 for summer 2010 and the scatter plot at the outlet (Weir-5) is for the 2010 & 2011 rainy season.

The simulation at weir-5 resulted in higher transport limited coefficient (a_{2t}). The transport limiting coefficient (a_{2t} = 14) in Table 6-2, at the outlet of the whole watershed, is much higher than the sub-watersheds (a_{2t} = 6) in Table 6-2 and other watersheds such as Anjeni (a_t = 4) and Andit Tid (a_t = 2.2) shown in Chapter 5. The coefficient *a* holds the property of the watershed as explained in Tilahun et al. (2011) and the watershed at Weir-5 have a maximum slope of 30% while the sub-watershed has a maximum of 16%. The transport limiting capacity, a_{2t}, for Debre

Mawi at the outlet is therefore greater than for the sub-watersheds likely either because it is steeper than the sub-watersheds or because it has more cultivated land on the degraded part of the watershed.

The source limiting capacity coefficient (a_t = 3) at the outlet (Weir-5) in Table 6-2 is also greater than coefficients at the sub-watersheds but similar with Anjeni watershed (refer chapter 5), while the sub-watersheds' source limiting coefficients (a_s = 0.5) in Table 6-2 are similar with the Andit Tid watershed shown in Chapter 5. The higher coefficient at the outlet of Debre Mawi and Anjeni during August and September is likely due to the potential sediment sources from active gullying existing in the watersheds. These gullies in Debre Mawi were located in areas that are saturated and where bank failures are common due to slippage (Tebebu et al.,2010) and in Anjeni, it is located at the source of the river where water from the sub-surface come to the surface as a spring.

An attempt to test this saturation excess erosion model in the watershed and sub-watersheds shows the applicability of the model to sediment concentration prediction on the Ethiopian highland (Figure 6-7 and Figure E2-1 to E2-4 in Appendix E). The model was generally able to capture the variability of sediment concentrations measured during storm periods. In addition, it has shown similarity of erosion parameters among the sub-watersheds within Debre Mawi and with other different watersheds (Anjeni and Andit Tid) in Blue Nile Basin. Such similarity existed because the watersheds behave similarly when they dry out and wet up. In addition to dilution effect reported by Tilahun et al. (2012) after the first week of August, we hypothesized that shear stress of flow rate in the rill channel become lower than the shear strength of the soil at the beginning of saturation. After the beginning of August, the upland watersheds developed the maximum rill density and any flux after this time is carried off below full capacity of the rill channel and hence the applied shear stress on the soil is smaller than the critical shear strength of the soil that increased when the field capacity of the watersheds reached. Sediment concentration had therefore decreased similarly at a similar time in all upland watersheds in the basin. The difference in the sediment model parameters observed within Debre Mawi and among other watersheds in Blue Nile Basin is likely associated with difference in slope, the existence of active gullies at saturated areas and extent of agricultural activities. Finding the relationship of the erosion model parameters with watershed characteristics needs further investigation and could be future research areas.

6.4 Conclusion

Storm runoff rate and sediment concentrations monitored in 2010 and 2011 at the outlet and three sub-watershed outlet of Debre Mawi were used to test the saturation excess hydrology and erosion models. The semi-distributed conceptual hydrology model calculates surface runoff from the saturated and degraded zones of the watershed, and interflow and baseflow from the infiltration zone of the hillside. The erosion model that is coupled with the hydrology model is based on the assumption that only the surface runoff producing areas are sediment sources and that the concentration in the stream are at transport limiting capacity at the time the fields are plowed and then become equal to the source limit once the rill network in the field of runoff producing areas were fully developed. The model captured the pattern of measured storm runoff and sediment concentration with Nash Sutcliffe efficiencies greater than 0.66. The parameters are similar among the sub-watersheds but different with the outlet of the watershed likely due to the difference in slope, agricultural activities and active gullies. The modeling of the watershed and its sub-watersheds with a saturation excess erosion model showed that the model is applicable to predict the spatially distributed sediment concentration within a watershed.

References

Abyi, A. Z.: Geological controls in the formations and expansions of gullies over hillslope hydrological processes in the Highlands of Ethiopia, northern Blue Nile region, A Thesis Presented to the Faculty of the Graduate School of Cornell University In Partial Fulfillment of the Requirements for the Degree of Master of Professional Studies, Ithaca, NY, 2009.

Easton, Z. M., Fuka, D. R., White, E. D., Collick, A. S., Biruk A., B., McCartney, M., Awulachew, S. B., Ahmed, A. A., and Steenhuis, T. S.: A multi basin SWAT model analysis of runoff and sedimentation in the Blue Nile, Ethiopia, Hydrol. Earth Syst. Sci., 14, 1827–1841, doi: 10.5194/hess-14-1827-2010, 2010.

Engda, T. A., Bayabil, H. K., Legesse, E. S., Ayana, E. K., Tilahun, S. A., Collick, A. S., Easton, Z. M., Rimmer, A., Awulachew, S. B., and Steenhuis, T. S.: Watershed hydrology of the (semi) humid Ethiopian Highlands, in: Nile River: Hydrology, Climate and Land Use, edited by: Melesse, A., Springer Science Publisher, New York, 2011.

Haregeweyn, N. and Yohannes, F.: Testing and evaluation of the agricultural non-point source pollution model (AGNPS) on Augucho catchment, western Hararghe, Ethiopia. Agriculture Ecosystems & Environment 99: 201-212, 2003.

Hairsine, P. B. and Rose, C. W.: Modeling water erosion due to overland flow using physical principles 1. Sheet flow. Water resources research, 28(1): 237-243, 1992.

Liu, B. M., Collick, A. S., Zeleke, G., Adgo, E., Easton, Z. M., and Steenhuis, T. S.: Rainfall discharge relationships for a monsoonal climate in the Ethiopian Highlands, Hydrol. Process., 22(7), 1059–1067, 2008.

Mekonnen, M. and Melesse, M.: Soil erosion mapping and hotspots area identification using GIS and Remote Sensing in Northwest Ethiopian Highlands, near Lake Tana. in: Nile River: Hydrology, Climate and Land Use, edited by: Melesse, A., Springer Science Publisher, New York, 2011.

Mohammed, A., Yohannes, F., and Zeleke, G.: Validation of agricultural non-point source (AGNPS) pollution model in Kori watershed, South Wollo, Ethiopia, Int. J. Appl. Earth Obs., 6, 97–109, 2004.

Moriasi, D.N., Arnold, J.G., Van Liew, M.W., Bingner, R.L., Harmel, R.D., Veith, T.L.: Model evaluation guidelines for systematic quantification of accuracy in watershed simulations. Transactions of the ASABE. 50(3):885-900, 2007.

Osman, M. and Sauerborn, P.: Soil and Water Conservation in Ethiopia: Experiences and Lessons. J Soils & Sediments, 1 (2), 117 - 123, 2001.

Setegn, S G., Ragahavan S., Bijan D.: Hydrological Modeling in the LakeTana Basin, Ethiopia using SWAT model. The Open Hydrology Journal 2: 49-62, 2008.

Steenhuis, T.S., A.S. Collick, Z. M. Easton, E.S. Leggesse, H. K. Bayabil, E. D. White, S.B. Awulachew, E. Adgo5, A.A. Ahmed.: Predicting Discharge and Erosion for the Abay (Blue Nile) with a Simple Model. Hydrological Processes 23: 3728–3737, 2009.

Tadesse, G.: Land degradation: a challenge to Ethiopia. Environmental Management 27, 815-824, 2001

Tesemma, Z. K., Mohamed, Y. A., and Steenhuis, T. S.: Trends in rainfall and runoff in the Blue Nile Basin: 1964–2003, Hydrol. Process., 24(25), 3747–3758, doi:10.1002/hyp.7893, 2010.

Tilahun, S. A., R. Mukundan, B. A. Demisse, C. Guzman, B. C. Tarakegn, T. A. Engda , Z. M. Easton , A. S. Collick, A. D. Zegeye, E. M. Schneiderman, J.Y. Parlange, and T. S. Steenhuis.: A Saturation Excess Erosion Model. In: Proceedings International Symposium on Erosion and Landscape Evolution, ISELE paper number 11061. D.C. Flanagan, J.C. Ascough II, and J.L. Nieber (eds.). St. Joseph, Mich: ASABE, 2011

Tilahun S. A., Guzman C. D., Zegeye A. D., Engda T. A., Collick A. S., Rimmer A., and Steenhuis T. S.: An efficient semi-distributed hillslope erosion model for the sub humid Ethiopian Highlands. HESSD-9-2121-2012, 2012

Zeleke, G.: Landscape Dynamics and Soil Erosion Process Modeling in the North-western Ethiopian Highlands. African Studies Series A 16, Geographica Bernensia, Berne, 2000.

APPENDIX A: CHAPTER TWO

Appendix A1: Time series plot of measured storm runoff in Debre Mawi watershed

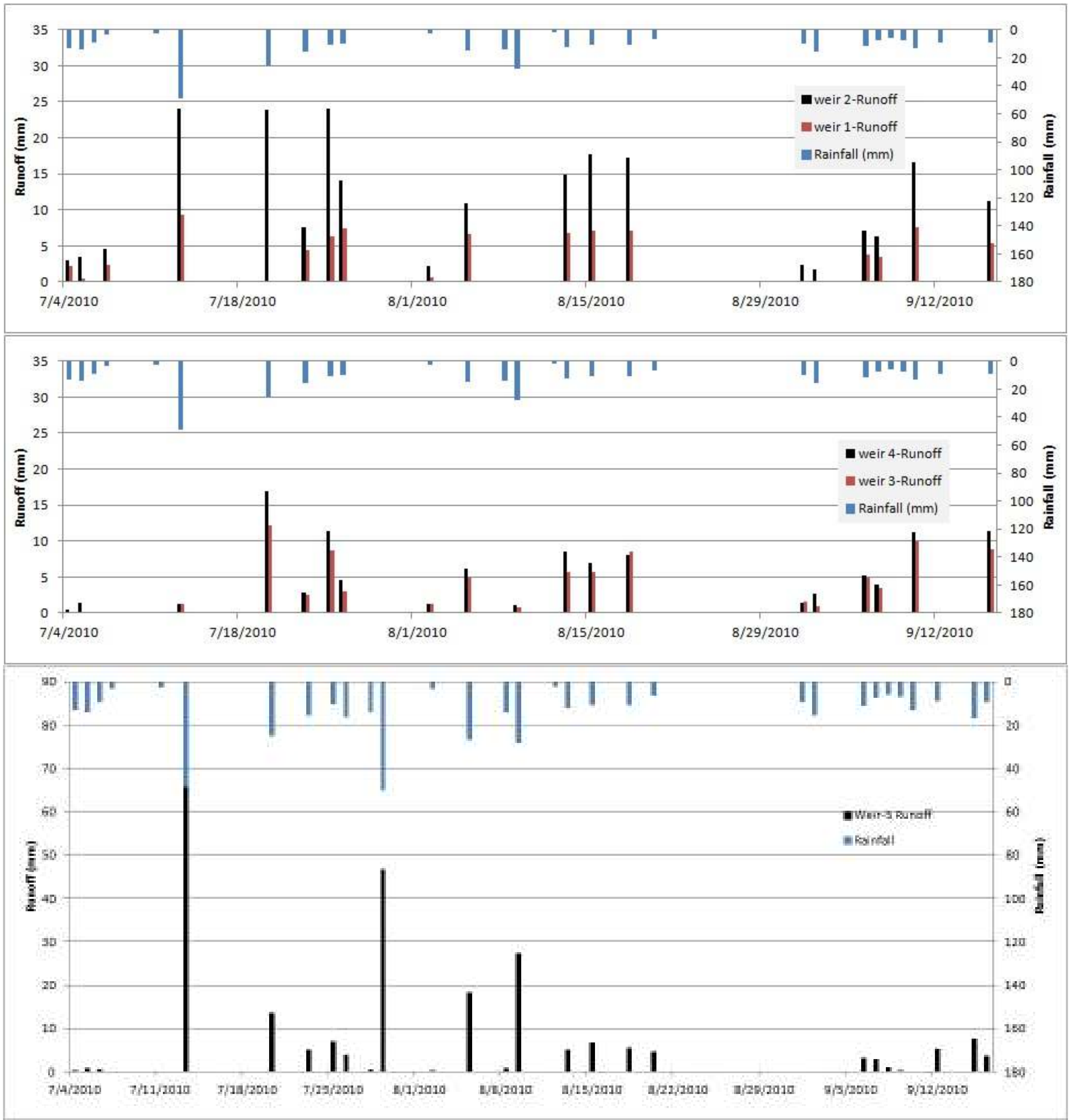

Figure A1-1: Storm runoff depth vs. time with the corresponding storm rainfall depth at each weir for 2010 summer

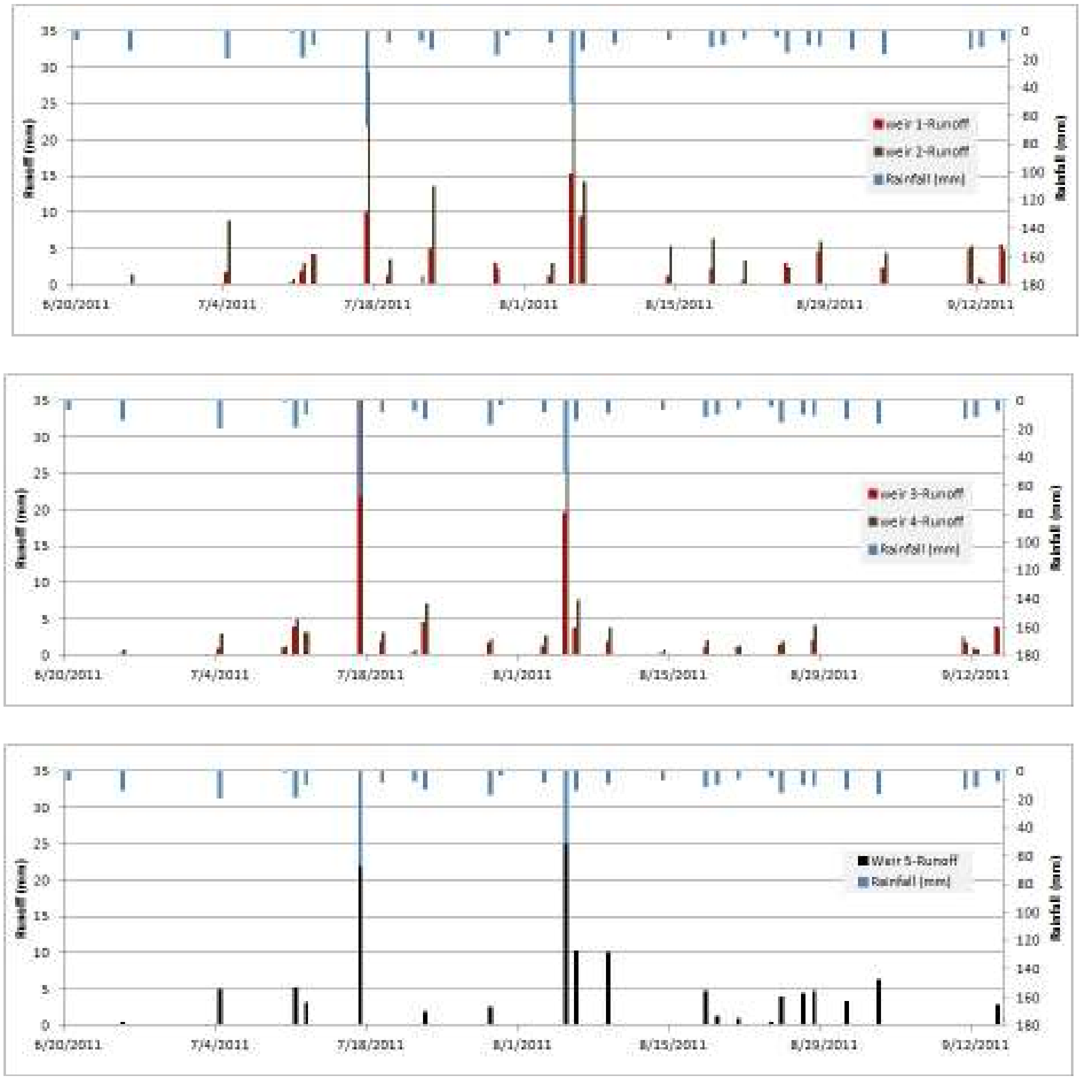

Figure A1-2: Storm runoff depth vs. time with the corresponding storm rainfall depth at each weir for 2011 summer

Table A1-1: Data of 5-min maximum rainfall intensity (mm/hr) with the corresponding runoff depth (mm) at each weir

Date	5-minute Max rainfall intensity (mm/hr)	Average rainfall intensity (mm/hr)	weir 1-Runoff (mm)	weir 2-Runoff (mm)	weir 3-Runoff (mm)	weir 4-Runoff (mm)	Weir 5-Runoff (mm)
7/4/2010	73.2	26.8	2.23	3.00	-	0.41	0.31
7/5/2010	18	7.8	0.47	3.40	-	1.48	0.79
7/6/2010	45.6	6.3	-	-	-	-	0.56
7/7/2010	18	6.2	2.39	4.62	-	-	
7/11/2010	15.6	9.6	-	-	-	-	0.09
7/13/2010	103	30.84	9.29	24.03	1.295	1.23	72.15
7/20/2010	45	8.5	-	23.96	12.167	16.86	13.74
7/23/2010	45.6	14.5	4.43	7.53	2.602	2.89	5.20
7/25/2010	39.6	21	6.32	24.12	8.634	11.44	7.05
7/26/2010	21.6	7.2	7.48	14.05	2.964	4.61	3.91
8/2/2010	6	4	0.67	2.28	1.203	1.25	0.45
8/5/2010	33.6	9.5	6.70	10.84	4.972	6.14	18.34
8/9/2010	51.6	20.57	-	-	0.776	1.07	27.26
8/12/2010	12	4.2	-	-	-	-	0.11
8/13/2010	24	6.5	6.80	14.82	5.753	8.57	5.00
8/15/2010	43.2	25.9	7.07	17.66	5.757	6.89	6.77
8/18/2010	63.6	18.7	7.16	17.21	8.514	8.04	5.53
8/20/2010	30	15.36	-	-	-	-	4.65
9/1/2010	18	12.9	-	2.41	1.563	1.39	-
9/2/2010	6	3.6	-	1.73	0.969	2.63	-
9/6/2010	39.6	14.04	3.72	7.19	4.830	5.18	3.29
9/7/2010	27.6	14.6	3.42	6.32	3.426	3.88	2.94
9/8/2010	39.6	23.6	-	-	-	-	1.07
9/9/2010	15.6	5.8	-	-	-	-	0.47
9/10/2010	39.6	15.72	7.66	16.53	9.909	11.17	-
9/12/2010	24	18.2					5.38
9/15/2010	43.2	10.7					7.64
9/16/2010	57.6	17.8	5.33	11.26	8.832	11.43	3.59
6/20/2011	30	10.8					0.21
6/25/2011	67.2	12.6	0.08	1.38	0.319	0.86	0.40
7/4/2011	69.6	14	1.74	8.88	0.942	3.00	4.98
7/10/2011	69.6	10.8	0.25	0.76	1.028	1.31	-
7/11/2011	67.2	15.36	1.96	3.00	3.996	4.84	5.23
7/12/2011	57.6	24.5	4.27	4.22	3.208	3.20	3.15
7/17/2011	134.4	38	10.15	29.21	38.624	65.50	-

Date	5-minute Max rainfall intensity (mm/hr)	Average rainfall intensity (mm/hr)	weir 1-Runoff (mm)	weir 2-Runoff (mm)	weir 3-Runoff (mm)	weir 4-Runoff (mm)	Weir 5-Runoff (mm)
7/19/2011	24	9.3	1.32	3.48	1.939	3.18	-
7/22/2011	18	7.7	0.20	1.34	0.319	0.73	-
7/23/2011	45	12	5.09	13.68	4.588	7.12	1.88
7/29/2011	45.6	20.76	2.97	2.27	1.810	2.21	2.45
7/30/2011	3.6	3.6	-	-	-	-	0.11
8/3/2011	15.6	11.7	1.20	3.03	1.319	2.73	0.12
8/5/2011	76.8	15.7	15.38	43.46	19.620	27.27	32.16
8/6/2011	36	8.6	9.57	14.19	3.724	7.64	10.31
8/9/2011	63.6	12	-	-	1.905	3.85	10.20
8/14/2011	24	11.5	1.24	5.38	0.319	0.73	-
8/18/2011	33.6	21.8	2.24	6.39	1.131	2.13	4.80
8/19/2011	21.6	6.6	-	-	-	-	1.21
8/21/2011	27.6	13.2	0.63	3.24	1.077	1.25	0.92
8/24/2011	27.6	16.4	-	-	-	-	0.42
8/25/2011	30	9.6	3.02	2.34	1.365	1.95	4.01
8/27/2011	43.2	30.6	-	-	-	-	4.48
8/28/2011	85.2	25.9	4.51	6.02	2.009	4.09	4.73
8/31/2011	33.6	9.8	-	-	-	-	3.35
9/3/2011	21.6	10.8	2.36	4.46	-	-	6.31
9/11/2011	51.6	21.9	4.91	5.45	2.520	1.75	-
9/14/2011	36	21.3	5.46	4.78	3.950	3.76	2.80

- indicates that no measurement was conducted

Table A1-2: Weekly cumulative effective rainfall (mm) data and storm runoff (mm) data in Debre Mawi watershed in 2010 and 2011 rainy period.

Date	P-E (mm)	Storm Runoff (mm)				
		weir-5	Weir-4	weir-3	Weir-2	Weir-1
7/10/2010	40.5	1.66	1.90	-	11.02	5.1
7/17/2010	64.8	72.27	1.23	1.30	25.99	9.3
7/24/2010	113.9	18.94	19.75	14.77	31.49	4.4
7/31/2010	86.6	58.14	37.15	26.23	69.37	24.3
8/7/2010	43.4	18.80	7.39	6.18	13.12	7.4
8/14/2010	61.8	33.28	9.63	6.53	14.82	6.8
8/21/2010	53.1	16.95	14.92	14.27	34.87	14.1
8/28/2010	18.5	9.47	16.71	14.24	17.51	6.5
9/4/2010	20.9	10	10.58	10.00	17.44	7.4
9/11/2010	40.5	7.78	20.23	18.17	30.04	14.8
9/18/2010	34.7	16.60	11.43	8.83	11.26	5.3
9/25/2010	26.7	3.15	-	-	-	-
6/20/2011	0.2	0.20	-	-	-	-
6/27/2011	8.4	0.40	0.86	0.32	1.38	0.1
7/4/2011	39.4	4.98	3.0	0.94	8.88	1.7
7/11/2011	30.3	5.23	6.15	5.02	3.76	2.2
7/18/2011	111.6	103.90	68.70	41.83	33.43	14.4
7/25/2011	45.5	1.88	11.02	6.85	18.50	6.6
8/1/2011	25.8	2.56	2.21	1.81	2.27	3.0
8/8/2011	97.4	42.60	37.64	24.66	60.68	26.1
8/15/2011	45.0	10.20	4.58	2.22	5.38	1.2
8/22/2011	28.8	6.93	3.37	2.21	9.63	2.9
8/29/2011	43.6	13.65	6.04	3.37	8.35	7.5
9/5/2011	26.4	9.66	-	-	4.46	2.4
9/12/2011	24.55	-	2.49	3.39	5.96	5.8
9/19/2011	28.8	2.67	3.76	3.95	4.78	5.5

Table A1-3: Infiltration capacity from infiltration test conducted in Debre Mawi Watershed August 2010

ID No	Infiltration Capacity (mm/hr)	Land cover	Slope (%)	landscape position
I1	12	cultivated land (tef)	7	Up-slope
I2	30	cultivated land (tef & Bean)	6	Up-slope
I3	44	bush & grass land	10	Mid-slope
I4	102	bush land	8	Mid-slope
I5	22.5	grass land close to saturation	14	Down-slope
I6	12	cultivated land	12.3	Down-slope
I7	6	cultivated land	14.2	Down-slope
I8	36	grass land close to saturation	9.8	Down-slope
I9	42	grass land	11	Mid-slope
I10	78	grass land	13.8	Mid-slope
I11	216	cultivated land	8	Up-slope
I12	360	cultivated land	7.3	Up-slope
I13	18	cultivated land	7.4	Up-slope
I14	16	cultivated land	5.9	Up-slope

Appendix A2: Perched water table depth (in cm) below the ground surface for piezometers installed in 2010 summer

	P1	P2	P3	P4	P5	P6	P7	P8	P9	P10	P11	P12	P13	P14	P15	P16
Depth of P	116	292	294	95	174	352	100	149	280	58	255	300	191	296	280	392
7/17/2010	115	285.5	262.5	89.25	82.5	191	96	138	60	58	238	182.5	191	295.6	279	382.5
7/18/2010	114.5	288	261.2	81.5	75.25	196.5	100	132.5	64.5	57.5	243.5	184.5	191	296	280	389.5
7/19/2010	116	274.5	261	84.5	68.5	196.5	100	138	65	58	244	190	191	296	280	391.5
7/20/2010	115	279.5	256.7	71.5	52.5	188.5	100	125	60	58	241.5	175	191	295.5	278.5	390
7/21/2010	115	268.5	257.5	62.5	47.25	185	100	116.2	59.5	58	242.5	157.5	191	295	277.5	388
7/22/2010	115	270	258.2	61.5	47.5	186	100	116	59.5	58	243.5	155.5	191	296	276	388
7/23/2010	113	264.5	255	56	43.5	183	99.5	113	50	58	238	146.5	191	294.5	275	389
7/24/2010	111.5	261	250	53.5	44	183	98	112.5	47.5	58	234	146	190.5	294.5	275.5	387.5
7/25/2010	112	258.5	249.5	52	41.5	183.5	97	110.5	46	58	232	143	190	294	274	386.5
7/26/2010	81	152	207.5	14.5	37	182	100	17	42	58	217.5	52	191	294	240	353.7
7/27/2010	83.5	138	190.5	12.5	39	187	100	18.5	28.5	58	221	52	191	294.5	241	353.5
7/28/2010	83	121	172	10	34	190.5	100	17.5	12.5	58	222	51.5	191	296	238.5	348.5
7/29/2010	86	123.5	162	15.5	37.5	194	100	20	14	58	225	56	191	296	242.5	351
7/30/2010	82	123	162	15.5	32	192.5	100	18.5	12.5	58	221.5	53	191	296	238.5	351
7/31/2010	87	129.5	163.5	15	56	68.5	100	26	22.5	58	100.5	61	191	296	225.5	357
8/1/2010	80	121.5	160	13.5	78	63.5	100	21	11.5	58	99.5	57.5	191	296	238.5	359
8/2/2010	76.5	119.5	159	10	74	128	100	20.5	3	58	97	52	191	296	235.5	355
8/3/2010	73.5	115.5	155	6.5	73	66	100	21	0	58	96	54	191	296	233.5	355.5
8/4/2010	80	124.5	155.5	45.5	74	107.5	100	24	0	58	72	56.5	191	289.5	237	354.5
8/5/2010	79	123	142.5	27.5	64.5	75	100	21.5	0	58	75	53	191	269	151	338.5
8/6/2010	81.5	115.5	139	53	58.5	86.5	100	15	0	58	66	48	191	257.5	141	332.5
8/7/2010	79	112	136.5	59	53	93	100	8	0	58	56	45.5	191	133	100	318.5
8/8/2010	80	109	136	76.5	47	112.5	100	0	0	58	35.5	44	191	116.5	88.5	312.5
8/9/2010	76.5	105	134	82	44	118.5	100	0	0	58	21	41.5	191	112.5	82.5	309.5
8/10/2010	116	103.5	133	88	41	125.5	100	0	0	58	16	38	191	106.5	78	305
8/11/2010	116	103	132	91.5	38	130	100	0	0	58	12	33	191	104.5	73.5	301.5
8/12/2010	116	100.5	129	91.5	33	118	100	0	0	58	12	30.5	191	104	71	298
8/13/2010	116	100	131	91	35.5	102	100	0	0	58	18.5	32.5	191	113.5	74	294.5
8/14/2010	116	105	133.5	91	33.5	89.5	100	0	0	58	22	37.5	191	117	68.5	289
8/15/2010	116	109	133.5	95	10	78.5	100	0	0	58	33.5	47.5	191	125	63	280.5
8/16/2010	116	103	124	94	3	70.5	100	0	0	58	35	40.5	191	118.5	59	279
8/17/2010	114	108	126	95	6	75.5	100	0	0	58	49	43	191	125	63	183
8/18/2010	113.5	100.5	119.5	93	3	92	100	0	0	58	22.5	36	191	116	58	192
8/19/2010	116	98.5	105.5	95	34.5	98	100	0	0	58	12.5	25.5	191	126	65	213.5
8/20/2010	116	103	109	95	42	99	100	0	1.5	58	21.5	34	191	132.5	72.5	224
8/21/2010	113.5	99.5	113	95	36.5	114.5	100	0	0	58	13.5	23.5	191	134	64.5	235.5

8/22/2010	115	102	116	95	39.5	112.5	100	0	0	58	20	31.5	191	140	70	243
8/23/2010	112.5	91.5	105	91	30	111.5	100	9	0	58	10	20.5	191	140	62.5	252
8/24/2010	110.5	92	121	89	33.5	131	100	4.5	0	58	10	26	191	142.5	59.5	266
8/25/2010	109.5	92	102.5	85	30	63.5	100	0	0	58	7.5	19	191	140	58	265.5
8/26/2010	107	88.5	120.5	85	35.5	67	100	0	0	58	15.5	26.5	191	136	57	261
8/27/2010	106.5	90	122.5	85.5	34.5	70	100	0	0	58	15	25	191	137	56	260.5
8/28/2010	109	88.5	107.5	86.5	34	70.5	100	0	0	58	12	22	191	141.5	56.5	262
8/29/2010	112	88.5	108	90.5	35	72	100	0	0	58	12.5	22	191	145	58.5	262
8/30/2010	111.5	91	109.5	89	34.5	102	100	5	0	58	18.5	37.5	191	153	63	263
8/31/2010	111	91.5	111	91	33.5	115.5	100	5.5	12	58	17.5	30	191	157	59.5	265.5
9/1/2010	112	91.5	110.5	90	36	102.5	100	0	3	58	15	29.5	191	164	59	262
9/2/2010	111.5	91.5	112	90	35.5	82	100	0	0	58	15	27.5	191	170.5	59.5	260.5
9/3/2010	113	91.5	131.5	90	37.5	86.5	100	0	0	58	23.5	35	191	174	59.5	262
9/4/2010	113.5	93.5	136	90	37.5	82.5	100	0	0	58	28	36.5	191	178	61	264.5
9/5/2010	114	97.5	141.5	90	37.5	84	100	0.5	0	58	30.5	40	191	187.5	61.5	265
9/6/2010	113	101	144.5	89	38	84	100	5	0	58	34.5	43.5	191	197.5	62	266.5
9/7/2010	113	101.5	142.5	86.5	37	83.5	100	4	0	58	36	41.5	191	198	61.5	265
9/8/2010	113.5	101	134.5	89.5	36.5	81	100	3	0	58	35.5	40	191	197	60.5	264
9/9/2010	114	102	121	90	36.5	81.5	100	1.5	0	58	29.5	32	191	197	59	262
9/10/2010	114	101.5	114	90.5	36	78.5	100	0	0	58	26.5	28.5	191	194.5	59.5	246.5
9/11/2010	113	102	110	90	35.5	84.5	100	1	0	58	29	26.5	191	191	60	249
9/12/2010	112.5	104	109	90	35.5	98.5	100	0	0	58	29	27	191	184	60.5	251
9/13/2010	113.5	113.5	123	89	36	87	100	1.5	0	58	31	34.5	191	179	62	252.5
9/14/2010	113.5	109.5	122.5	90.5	34.5	82.5	100	0	0	58	29	33	191	177.5	63	254
9/15/2010	112	96	113	90	34	79	100	0	0	58	15	31	191	171	60.5	247
9/16/2010	112	96	113	89.5	33	84.5	100	0	0	58	26.5	29	191	168	62.5	246
9/17/2010	111.5	97	123.5	91	33	87.5	100	0	0	58	29.5	32	191	166	63	249
9/18/2010																
9/19/2010	107.5	107	146.5	85.5	40.5	116	100	0	12	58	44	67	191	178.5	83.5	226
9/20/2010	111.5	104.5	141.5	86	27.5	120.5	100	0	12	58	57.5	66.5	191	178.5	78	243
9/21/2010	111	123	135.5	92.5	23	126	100	2	9	58	53.5	59.5	191	183	82	258
9/22/2010	116	142	139.5	95	47	128	100	1.5	15	58	55	83.5	191	194	88.5	264.5
9/23/2010	116	119.5	152.5	95	14	131	100	16.5	8	58	66.5	66.5	191	203	82	277
9/24/2010	116	113.5	139	95	23	132	100	5.5	4.5	58	57	64.5	191	217.5	78	277
9/25/2010	116	118	141	95	64	138	100	6	2	58	55	62	191	196	60	262
9/26/2010	111	122	142	90	54	136	100	4	0	58	42	47	191	240	70	263
9/27/2010	109	102	107	87	48	134	100	2	0	58	39	45	191	235	67	262
9/28/2010	108	98	118	95	54	140	100	4	0	58	40	45	191	238	66	252
9/29/2010	116	165	145	95	74	146	100	15	10	58	43	60	191	256	67	269
9/30/2010	116	132	124	95	44	144	100	9	0	58	35	45	191	261	63	254
10/1/2010	116	146	140	95	62	167	100	44	1	58	55	57	191	274	80	307
10/2/2010	116	133	134	95	60	162	100	42	0	58	55	54	191	271	88	292
10/3/2010	116	132	142	95	64	162	100	55	15	58	85	77	191	277	87	296

10/4/2010	116	128	149	95	63	160	100	53	10	58	63	63	191	276	85	294
10/5/2010	116	146	149	95	64	155	100	56	0	58	60	67	191	276	88	305
10/6/2010	116	134	141	95	63	152	100	54	2	58	8	59	191	277	82	292
10/7/2010	116	138	144	95	64	162	100	54	2	58	63	62	191	281	100	292
10/8/2010	116	140	149	95	69	161	100	58	6	58	65	70	191	282	108	292
10/9/2010	116	138	144	95	64	162	100	54	2	58	63	62	191	281	100	292
10/10/2010	116	140	144	95	55	172	100	57	1	58	65	64	191	281	103	292
10/11/2010	116	152	156	95	72	170	100	61	11	58	71	72	191	286	108	295
10/12/2010	116	151	173	95	71	157	100	71	34	58	72	79	191	296	101	292
10/13/2010	116	151	192	95	73	159	100	88	37	58	78	79	191	296	90	294
10/14/2010	116	153	174	95	71	157	100	87	36	58	79	80	191	296	92	292
10/15/2010	116	155	176	95	74	161	100	91	33	58	82	82	191	296	95	294
10/16/2010	116	156	178	95	77	162	100	93	40	58	83	85	191	296	97	296
10/17/2010	116	176	177	95	79	165	100	109	54	58	105	101	191	296	95	294
10/18/2010	116	176	178	95	81	166	100	109	57	58	110	103	191	296	96	295
10/19/2010	116	177	177	95	82	167	100	112	59	58	112	104	191	296	98	297
10/20/2010	116	177	177	95	84	164	100	109	54	58	105	103	191	296	94	296
10/21/2010	116	178	188	95	84	157	100	119	57	58	110	102	191	296	95	297
10/22/2010	116	179	189	95	85	158	100	120	58	58	112	103	191	296	94	299
10/23/2010	116	180	191	95	77	160	100	122	59	58	113	105	191	296	96	301
10/24/2010	116	181	191	95	88	161	100	124	60	58	114	106	191	296	97	301
10/25/2010	116	182	192	95	89	160	100	126	61	58	114	107	191	296	99	302
10/26/2010	116	183	193	95	91	162	100	127	63	58	115	108	191	296	100	304
10/27/2010	116	183	194	95	93	164	100	128	65	58	117	110	191	296	101	304
10/28/2010	116	185	196	95	94	166	100	129	67	58	119	112	191	296	103	305
10/29/2010	116	187	197	95	99	167	100	131	68	58	121	113	191	296	105	308
10/30/2010	116	292	194	95	110	212	100	149	80	58	164	147	191	296	148	304
10/31/2010	116	292	194	95	111	212	100	149	80	58	165	148	191	296	149	305
11/1/2010	116	292	195	95	112	214	100	149	82	58	167	149	191	296	150	307
11/2/2010	116	292	197	95	114	218	100	149	85	58	169	150	191	296	153	309
11/3/2010	116	292	199	95	117	220	100	149	87	58	171	152	191	296	155	311
11/4/2010	116	292	201	95	121	221	100	149	89	58	173	154	191	296	157	312
11/5/2010	116	292	203	95	124	223	100	149	93	58	175	157	191	296	159	315

Appendix A3: Scatter plot of storm runoff with rainfall intensity and 7-days effective rainfall

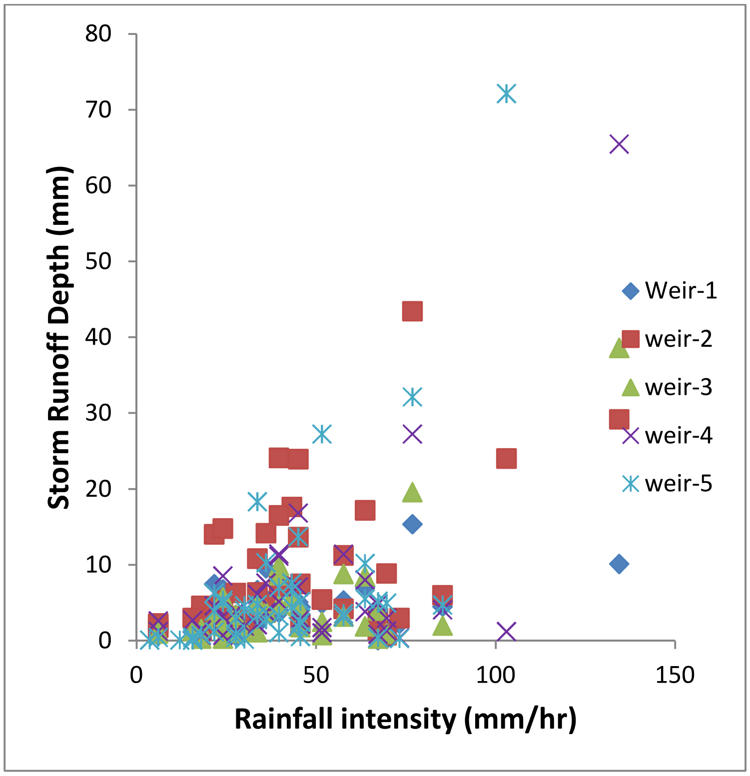

Figure A3-1: Linear regression between 5-minute maximum rainfall intensity with storm runoff depth at each weir by excluding data from July 13, 2010, July 20, 2010 and July 17, 2011

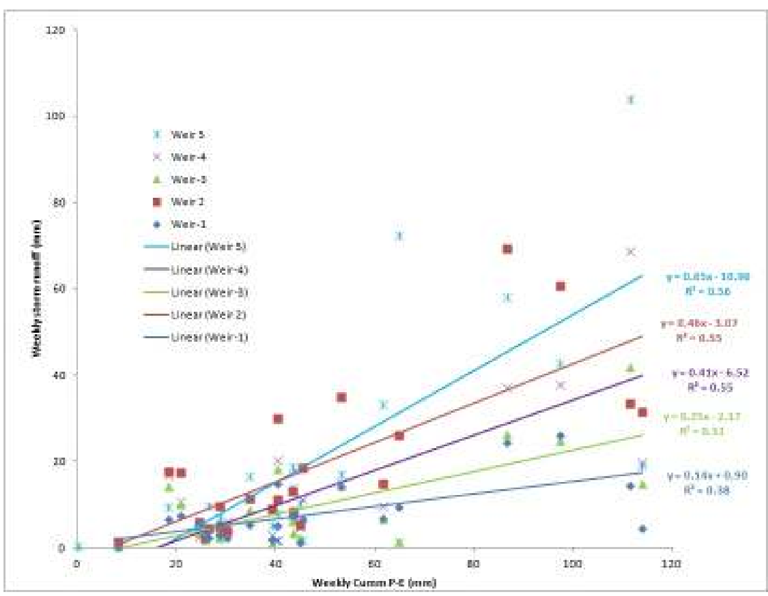

Figure A3-2: weekly summed effective daily rainfall and storm runoff relationships for Debre Mawi Watershed for all measured data. Data are shown in Table A2 in Appendix A.

Appendix A4: Comparison of measured runoff and SCS-CN simulated runoff

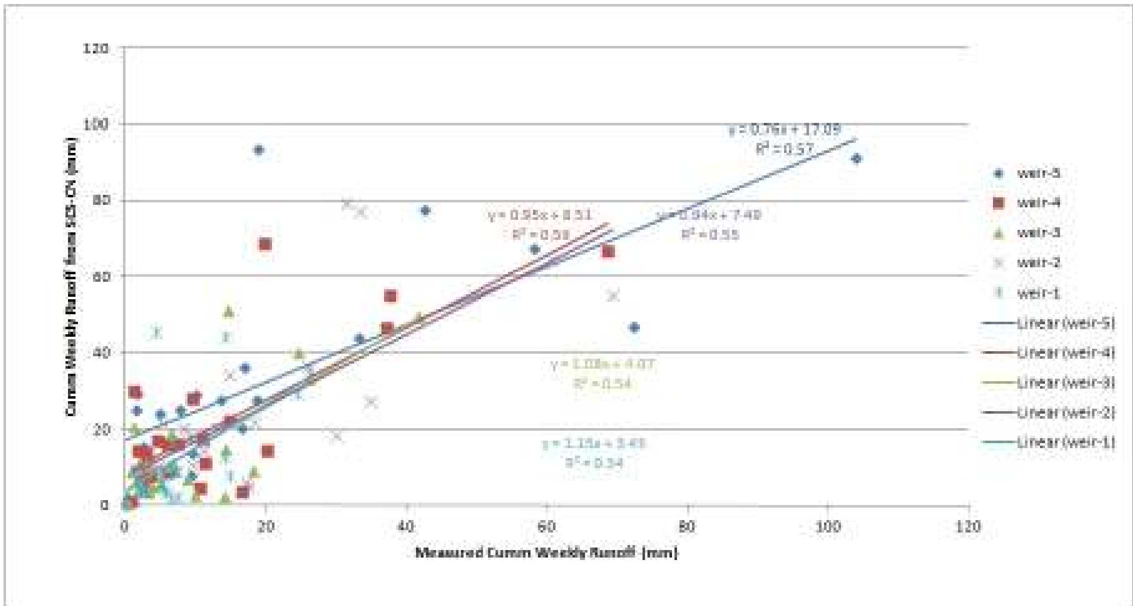

Figure A4-1: Scatter plot for measured and simulated with SCS runoff equation (equation 1) data of cumulative weekly runoff.

Appendix A5: Photographs of the weirs situated throughout Debre Mawi Watershed

Figure A5-1: Photos of (a) Weir-1 (b) Weir-2 (c) Weir-3 (d) Weir-4 and (e) Weir-5 installed in Debre Mawi watershed

Appendix A6: Stage discharge relationship at each weir in Debre Mawi Watershed

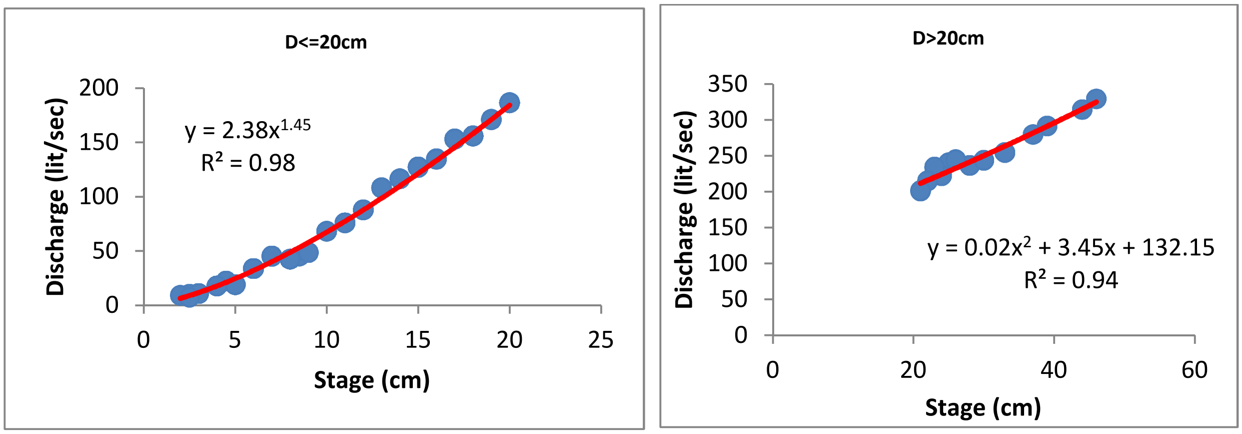

Figure A6-1: Stage discharge relationship at Weir-1 (D indicates depth of flow at the weir)

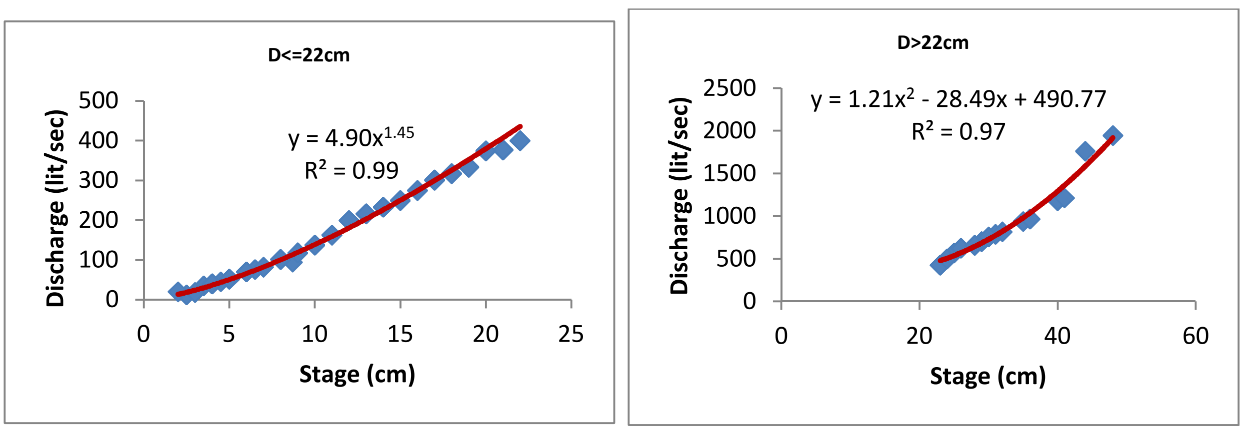

Figure A6-2: Stage discharge relationship at Weir-2 (D indiactes depth of flow at the weir)

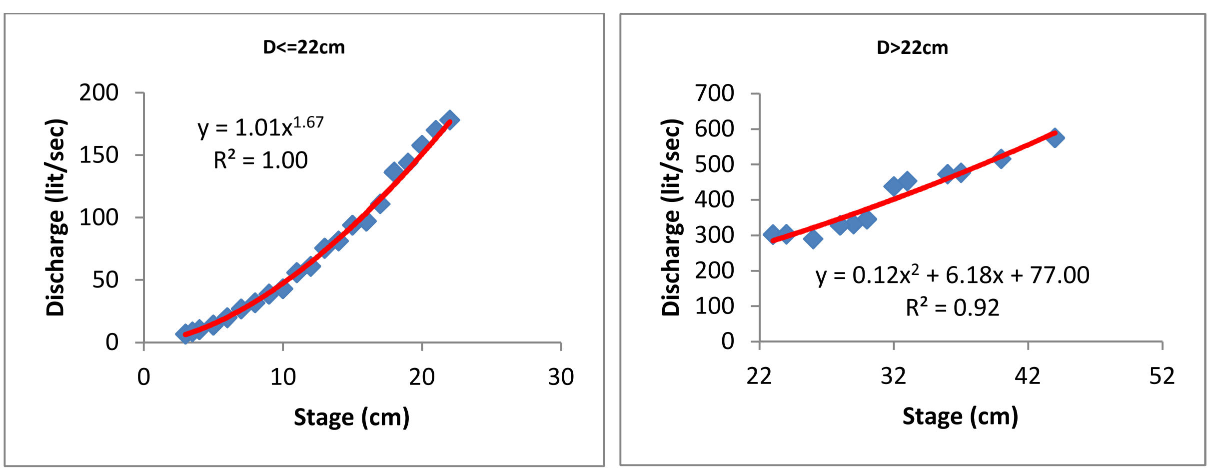

Figure A6-3: Stage discharge relationship at Weir-3 (D indiactes depth of flow at the weir)

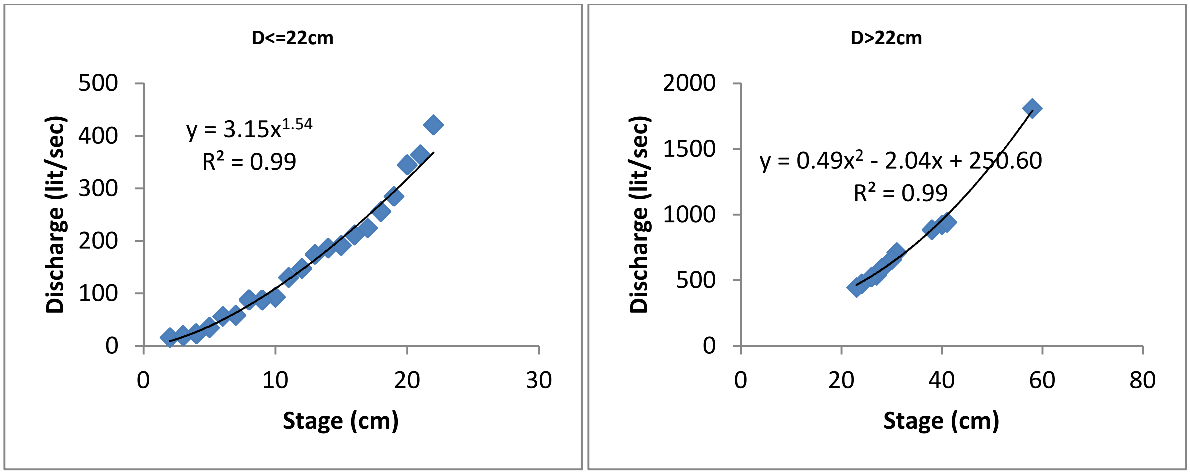

Figure A6-4: Stage discharge relationship at Weir-4 (D indiactes depth of flow at the weir)

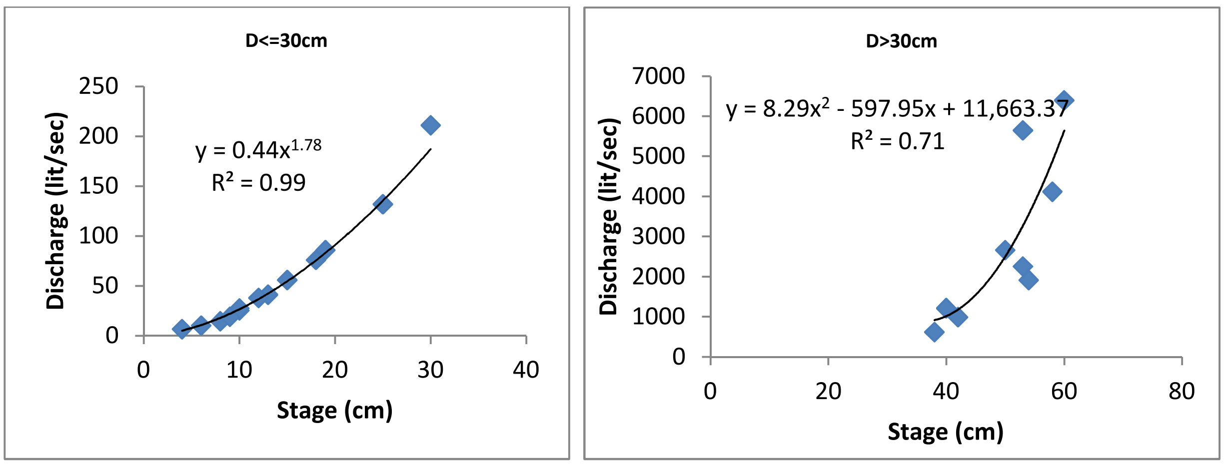

Figure A6-5: Stage discharge relationship at Weir-5 (D indiactes depth of flow at the weir)

APPENDIX B: CHAPTER THREE

Appendix B1: Sediment data in Debre Mawi watershed

Table B1-1: Measured sediment concentration and runoff and calculated sediment load at the watershed outlet and sub-watershed outlets in Debre Mawi

	Weir-1			Weir-2			Weir-3			Weir-4			Weir-5		
Date	Q (mm)	C (g/l)	SY (t/ha)	Q (mm)	C (g/l)	SY (t/ha)	Q (mm)	C (g/l)	SY (t/ha)	Q (mm)	C (g/l)	SY (t/ha)	Q (mm)	C (g/l)	SY (t/ha)
6/22/2010	-	-	-	-	-	-	-	-	-	-	-	-	4.74	32.93	1.56
6/27/2010	-	-	-	-	-	-	-	-	-	-	-	-	5.14	28.09	1.44
6/29/2010	5.85	6.93	0.41	11.34	17.73	2.01	-	-	-	12.38	36.27	4.49	37.88	41.62	15.76
7/4/2010	2.23	5.72	0.13	3.00	7.53	0.23	-	-	-	0.41	15.75	0.07	0.31	20.42	0.06
7/5/2010	0.47	2.32	0.01	3.40	9.20	0.31				1.48	11.88	0.18	0.79	18.92	0.15
7/6/2010	-	-	-	-	-	-	-	-	-	-	-	-	0.56	22.78	0.13
7/7/2010	2.39	6.29	0.15	4.62	9.05	0.42	-	-	-	-	-	-	-	-	-
7/11/2010	-	-	-	-	-	-	-	-	-	-	-	-	0.09	19.73	0.02
7/13/2010	9.29	4.55	0.42	24.03	7.06	1.70	1.30	0.83	0.01	1.23	1.53	0.02	72.15	35.05	25.29
7/20/2010	-	-	-	23.96	11.54	2.76	12.17	7.84	0.95	16.86	8.08	1.36	13.74	26.13	3.59
7/23/2010	4.43	2.93	0.13	7.53	6.57	0.49	2.60	2.29	0.06	2.89	3.45	0.10	5.20	14.74	0.77
7/25/2010	6.32	3.60	0.23	24.12	11.75	2.84	8.63	7.43	0.64	11.44	9.13	1.04	7.05	25.41	1.79
7/26/2010	7.48	2.10	0.16	14.05	2.51	0.35	2.96	1.67	0.05	4.61	1.16	0.05	3.91	8.21	0.32
7/28/2010	-	-	-	-	-	-	-	-	-	-	-	-	0.53	8.11	0.04
7/29/2010	10.54	6.78	0.71	31.20	14.89	4.65	14.63	8.93	1.31	21.10	10.99	2.32	46.65	19.08	8.90
8/2/2010	0.67	0.00	0.14	2.28	0.00	0.70	1.20	8.70	0.10	1.25	10.21	0.13	0.45	3.04	0.01
8/5/2010	6.70	0.63	0.04	10.84	2.78	0.30	4.97	12.92	0.64	6.14	6.64	0.41	18.34	12.96	2.38
8/8/2010	-	-	-	-	-	-	-	-	-	-	-	-	0.90	13.11	0.12
8/9/2010	-	-	-	-	-	-	0.78	5.56	0.04	1.07	16.34	0.17	27.26	12.44	3.39

8/12/2010	-	-	-	-	-	-	-	-	-	-	-	-	0.11	3.13	0.00
8/13/2010	6.80	1.08	0.07	14.82	0.99	0.15	5.75	2.39	0.14	8.57	1.75	0.15	5.00	6.77	0.34
8/15/2010	7.07	1.06	0.07	17.66	4.20	0.74	5.76	5.42	0.31	6.89	5.33	0.37	6.77	11.92	0.81
8/18/2010	-	-	-	-	-	-	8.51	1.46	0.12	8.04	1.86	0.15	5.53	8.99	0.50
8/20/2010	-	-	-	-	-	-	-	-	-	-	-	-	4.65	4.05	0.19
8/22/2010	6.52	0.58	0.04	16.15	1.55	0.25	12.67	2.33	0.30	14.68	2.07	0.30	-	-	-
8/23/2010	-	-	-	-	-	-	-	-	-	-	-	-	8.12	8.31	0.67
8/25/2010	-	-	-	-	-	-	-	-	-	-	-	-	0.72	4.35	0.03
8/27/2010	-	-	-	1.36	0.41	0.01	1.57	0.52	0.01	2.03	0.52	0.01	0.63	6.20	0.04
8/29/2010	1.02	0.15	0.00	2.63	0.49	0.01	1.70	0.89	0.02	2.05	0.91	0.02	-	-	-
8/30/2010	5.69	0.46	0.03	10.68	1.27	0.14	5.77	1.27	0.07	4.51	1.25	0.06	2.39	7.53	0.18
8/31/2010	0.68	0.83	0.01	10.68	1.27	0.14	-	-	-	-	-	-	-	-	-
9/1/2010	-	-	-	2.41	0.54	0.01	1.56	0.23	0.00	1.39	0.17	0.00	-	-	-
9/2/2010	-	-	-	1.73	0.58	0.01	0.97	0.25	0.00	2.63	0.26	0.01	-	-	-
9/6/2010	3.72	0.17	0.01	7.19	0.62	0.04	4.83	0.66	0.03	5.18	0.62	0.03	3.29	8.21	0.27
9/7/2010	-	-	-	6.32	1.50	0.09	3.43	1.20	0.04	3.88	1.23	0.05	2.94	4.78	0.14
9/8/2010	-	-	-	6.32	1.50	0.09	-	-	-	-	-	-	1.07	5.22	0.06
9/9/2010	-	-	-	6.32	1.50	0.09	-	-	-	-	-	-	0.47	3.95	0.02
9/10/2010	7.66	0.36	0.03	16.53	0.36	0.06	9.91	1.25	0.12	11.17	1.21	0.13	-	-	-
9/12/2010	-	-	-	16.53	0.36	0.06	-	-	-	-	-	-	5.38	5.87	0.32
9/15/2010	-	-	-	16.53	0.36	0.06	-	-	-	-	-	-	3.59	3.49	0.13
9/16/2010	5.33	0.78	0.04	11.26	0.73	0.08	8.83	1.35	0.12	11.43	1.42	0.16	-	-	-
9/25/2010	-	-	-	-	-	-	-	-	-	-	-	-	3.15	5.54	0.17
10/1/2010	-	-	-	-	-	-	-	-	-	-	-	-	1.29	5.01	0.06
6/12/2011	-	-	-	-	-	-	-	-	-	-	-	-	19.39	56.30	10.91
6/13/2011	-	-	-	-	-	-	-	-	-	-	-	-	3.20	30.77	0.98
6/20/2011	-	-	-	-	-	-	-	-	-	-	-	-	0.21	31.15	0.07
6/25/2011	0.08	2.60	0.00	1.38	6.18	0.09	0.32	3.98	0.01	0.86	15.06	0.13	0.40	26.68	0.11
7/4/2011	1.74	9.60	0.17	8.88	9.91	0.88	0.94	5.98	0.06	3.00	6.89	0.21	4.98	23.48	1.17
7/10/2011	0.25	7.16	0.02	0.76	9.67	0.07	1.03	8.51	0.09	1.31	6.91	0.09	-	-	-

7/11/2011	1.96	9.06	0.18	3.00	10.05	0.30	4.00	12.58	0.50	4.84	8.53	0.41	5.23	27.91	1.46
7/12/2011	4.27	15.65	0.67	4.22	16.32	0.69	3.21	7.73	0.25	3.20	8.77	0.28	3.15	23.72	0.75
7/17/2011	10.15	11.18	1.13	29.21	10.03	2.93	38.62	12.91	4.99	65.50	22.64	14.83	100.75	29.54	29.76
7/19/2011	1.32	2.85	0.04	3.48	9.51	0.33	1.94	4.06	0.08	3.18	7.50	0.24	-	-	-
7/22/2011	0.20	0.88	0.00	1.34	7.99	0.11	0.32	2.48	0.01	0.73	3.72	0.03	-	-	-
7/23/2011	5.09	7.25	0.37	13.68	15.53	2.13	4.59	9.30	0.43	7.12	9.30	0.66	1.88	6.87	0.13
7/29/2011	2.97	2.24	0.07	2.27	5.18	0.12	1.81	4.44	0.08	2.21	4.03	0.09	2.45	10.95	0.27
7/30/2011	-	-	-	-	-	-	-	-	-	-	-	-	0.11	1.67	0.00
8/3/2011	1.20	0.99	0.01	3.03	3.79	0.11	1.32	2.85	0.04	2.73	3.34	0.09	0.12	8.56	0.01
8/5/2011	15.38	2.86	0.44	43.46	8.17	3.55	19.62	6.10	1.20	27.27	7.93	2.16	32.16	13.99	4.50
8/6/2011	9.57	1.26	0.12	14.19	5.03	0.71	3.72	2.92	0.11	7.64	3.61	0.28	10.31	10.03	1.03
8/9/2011	-	-	-	-	-	-	1.90	1.50	0.03	3.85	2.01	0.08	10.20	9.45	0.96
8/14/2011	1.24	0.17	0.00	5.38	2.48	0.13	0.32	0.80	0.00	0.73	0.97	0.01	-	-	-
8/18/2011	2.24	0.84	0.02	6.39	1.97	0.13	1.13	1.07	0.01	2.13	0.98	0.02	4.80	7.63	0.37
8/19/2011	-	-	-	-	-	-	-	-	-	-	-	-	1.21	1.68	0.02
8/21/2011	0.63	0.28	0.00	3.24	1.73	0.06	1.08	0.98	0.01	1.25	1.22	0.02	0.92	2.56	0.02
8/24/2011										1.25	1.22	0.02	0.42	2.21	0.01
8/25/2011	3.02	2.60	0.08	2.34	2.39	0.06	1.36	1.84	0.03	1.95	1.62	0.03	2.57	5.75	0.15
8/27/2011	-	-	-	-	-	-	-	-	-	-	-	-	4.48	3.10	0.14
8/28/2011	4.51	0.49	0.02	6.02	4.27	0.26	2.01	1.46	0.03	4.09	2.26	0.09	4.73	7.77	0.37
8/31/2011	-	-	-	-	-	-	-	-	-	-	-	-	3.35	3.65	0.12
9/3/2011	2.36	0.72	0.02	4.46	2.41	0.11	-	-	-	-	-	-	6.31	5.11	0.32
9/11/2011	4.91	1.19	0.06	5.45	2.67	0.15	2.52	1.20	0.03	1.75	1.59	0.03	-	-	-
9/12/2011	0.87	1.60	0.01	0.51	1.63	0.01	0.87	0.23	0.00	0.75	0.38	0.00	-	-	-
9/14/2011	5.46	0.41	0.02	4.78	0.42	0.02	3.95	1.69	0.07	3.76	1.50	0.06	2.80	4.92	0.14
9/17/2011	-	-	-	-	-	-	-	-	-	-	-	-	2.42	3.88	0.09
9/18/2011	-	-	-	-	-	-	-	-	-	-	-	-	0.25	1.32	0.00

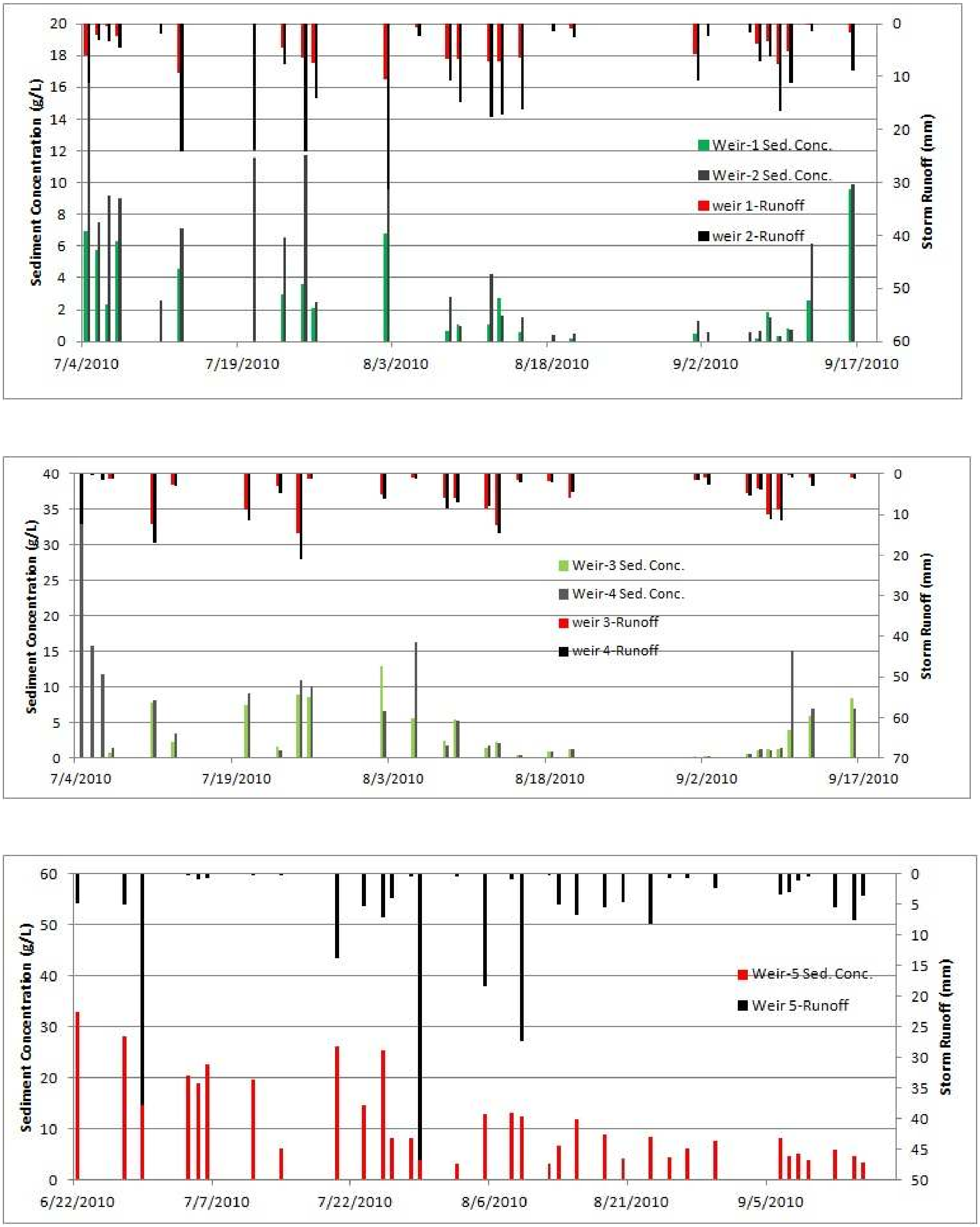

Figure B1-1: Sediment concentration vs. time with the corresponding storm runoff depth at each weir for 2010 summer

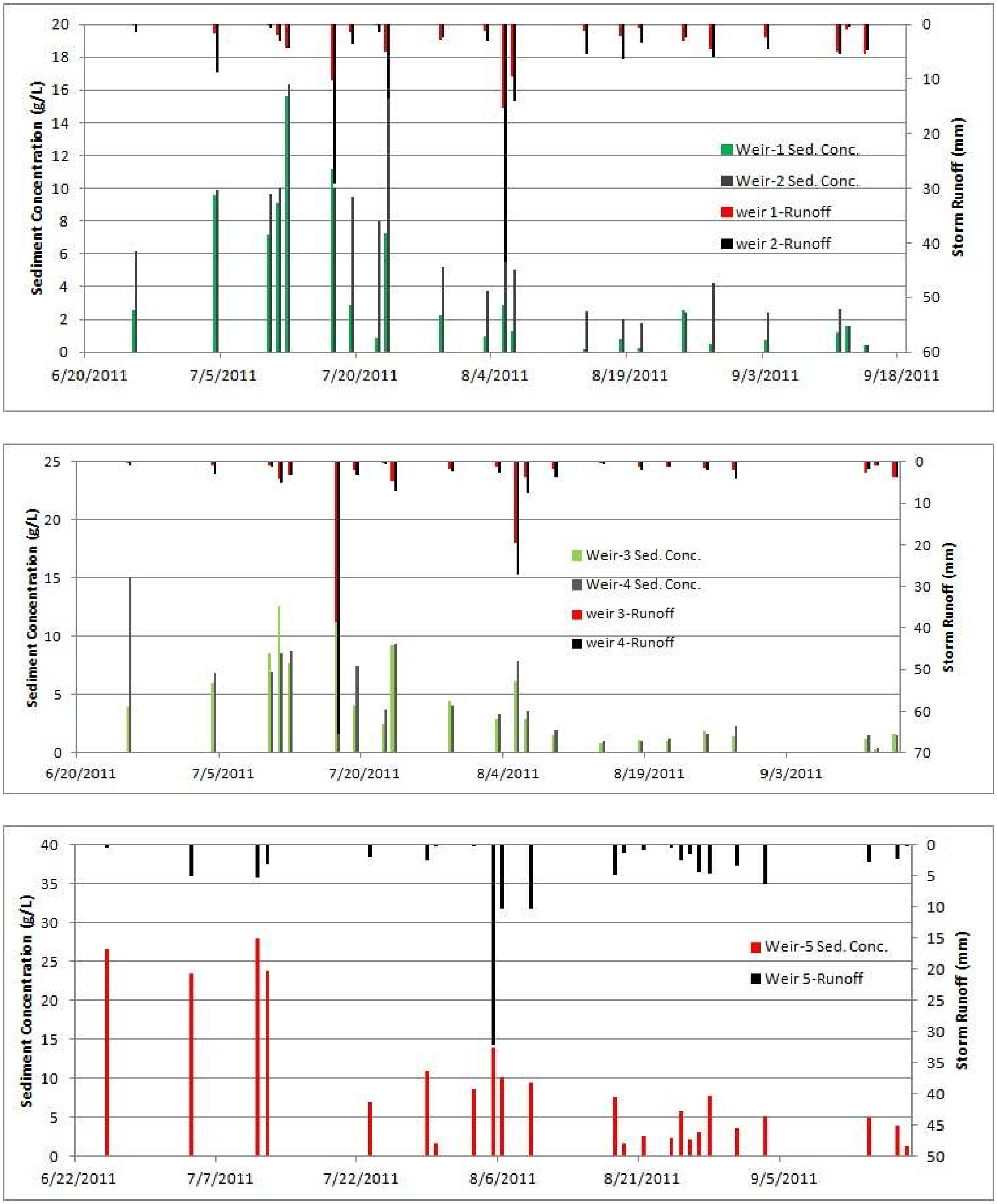

Figure B1-2: Sediment concentration vs. time with the corresponding storm runoff depth at each weir for 2011 summer

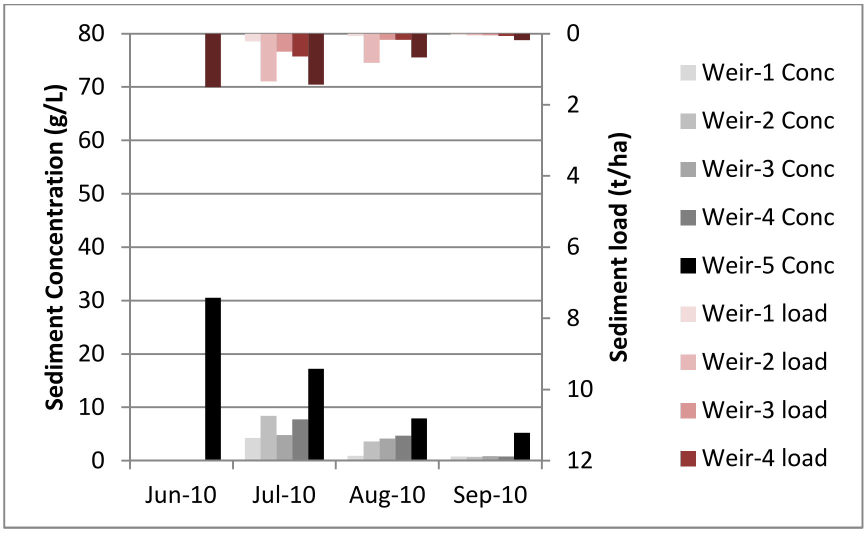

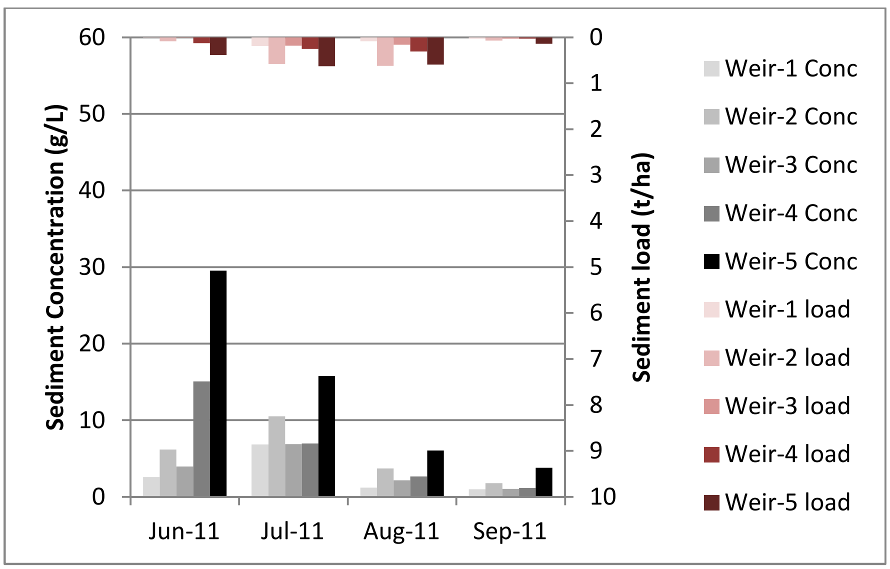

Figure B1-3: monthly average sediment concentrations and the corresponding sediment load at each weir for rainy phase of the monsoon in 2010 and 2011 for the Debra Mawi watershed. It is calculated excluding data of 22 Jun 2010, 13 Jul 2010, 12 June 2011, and 17 Jul 2011 which have high rainfall intensity

Appendix B2: Sediment concentration estimation in the soil mechanics laboratory of Bahir Dar University

Figure B2-1: Filtering sediment using Whiteman filter paper to determine sediment concentration from 1-liter sample of plastic bottles

Appendix B3: Picture of Gully 3 (G3) in 2010 and 2011 with example of gully soil loss estimation by field measurement

Figure B3-1: Picture of Gully-3 taken on 17 April 2010

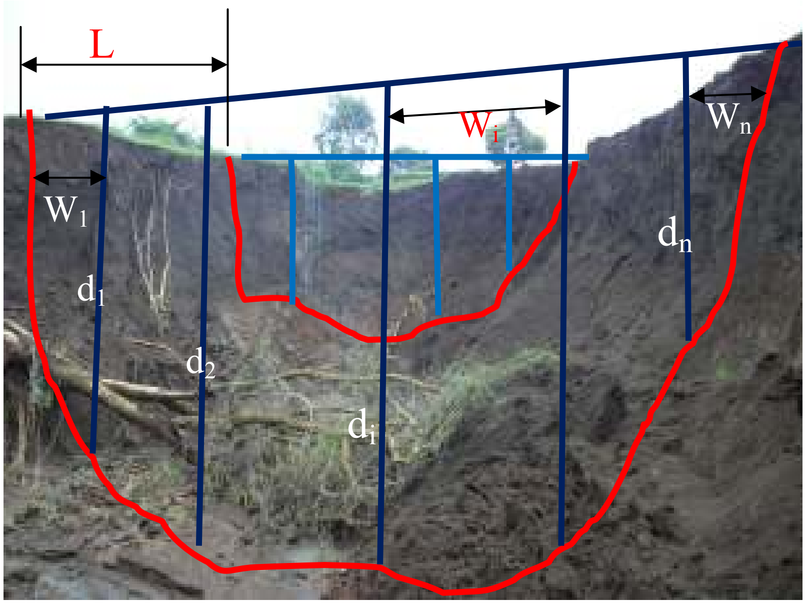

Figure B3-2: Picture of Gully-3 taken on 17 Aug 2010

Cross-sectional areas were first calculated for each cross-section:

$$A_i = \frac{W_1 d_1}{2} + \sum_{i=2}^{i=n-1} (d_i + d_{i+1}) W_i + \frac{W_n d_n}{2}$$

Total volume of the gully was determined as

$$V_T = \sum_{i=1}^{n} L_i \frac{(A_i + A_{i+1})}{2}$$

Gully erosion rates (R_L) in ton ha^{-1}yr^{-1} during the monitoring period were calculated using the equation:

$$R_L = \frac{V_T \rho_d}{A_w}$$

Where,

V_T= estimated current volume of the gully (m^3)

ρ_d= average bulk density of soils in the watershed

A_w= the watershed area in hectares

Figure B3-3: Picture of gully-2 at downstream taken on 10 Jun 2010 (left) and upstream part of the gully taken on 18 Aug 2011

APPENDIX C: CHAPTER FOUR

Appendix C1: Scatter plot runoff and sediment concentration for Anjeni

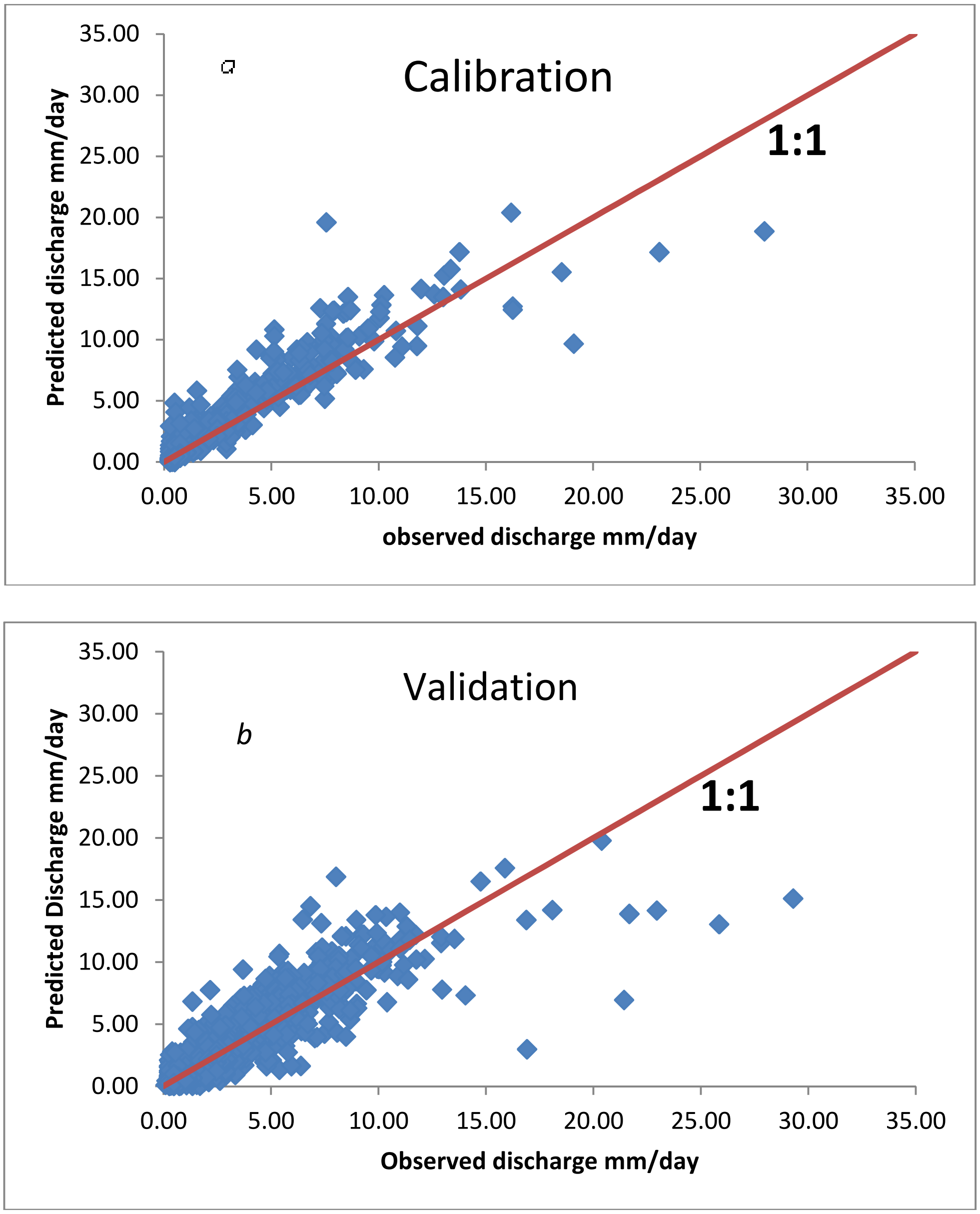

Figure C1-1 Comparison of predicted and observed daily stream flow with the 1:1 line (a) for calibration period (b) for validation period

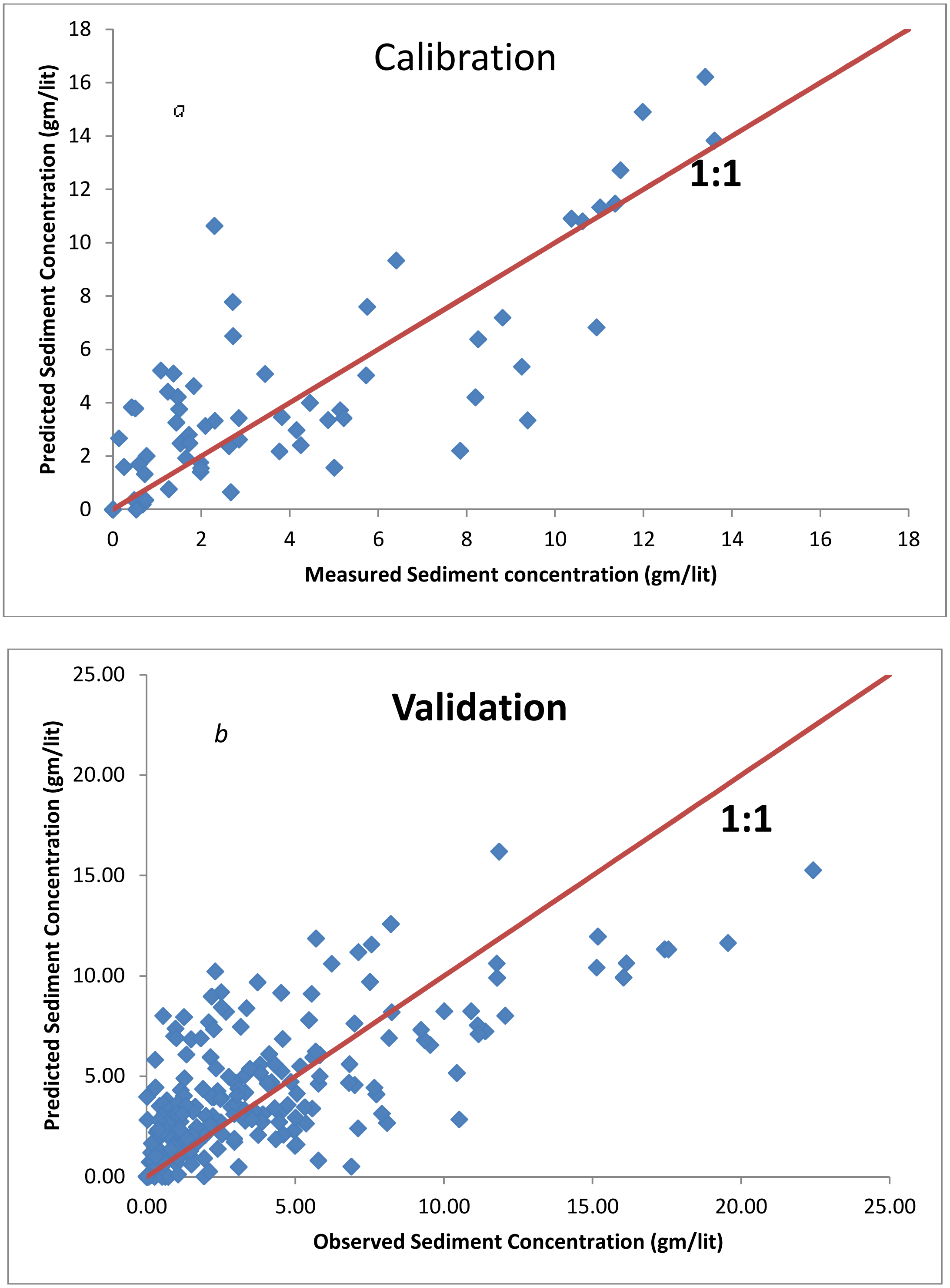

Figure C1-2 Comparison of predicted and observed daily sediment concentration with the 1:1 line (a) for calibration period (b) for validation period

Appendix C2: Sensitivity analysis for Anjeni

The model was fitted visually and not according to any particular statistics. The most sensitive parameter is the fractional areas that produce runoff and recharge. Increasing the recharge area by 30% (or 15 % of the total area), the NS efficiency decreases from 0.8 to 0.63. For a 30% decrease of the recharge area, the NSE efficiency remained the same, i.e., 0.8. A 15% increase in saturated runoff area resulted in a NS efficiency of 0.46, and a 50% increase of degraded areas from the total area resulted in a NS efficiency of 0.07. The reason for the sensitivity is that the overall water balance is not met. Moreover changing recharge areas to runoff areas resulted in peak runoff occurring earlier (Tesemma et al., 2010). As expected the N-S efficiency is insensitive to variation in the amount of water that can be stored in the root zone because the magnitude of the storage affects only the first runoff events after the rains have started. Since it rains often during the rainy season, the watershed soils remain near full capacity, and the total size of the storage affects the amount of recharge or runoff only minimally. This will not be the case for temperate climates where large storms are more infrequent. Finally, the model is not greatly dependent on the subsurface flow parameters. Testing has shown that when changing the parameters by a factor of two the baseflow tail is affected. Since the deviations are small the N-S efficiency stays the same but the relative mean square error and the visual appearance is affected.

Table A2-1: Sensitivity analysis of hydrologic parameters

Parameters	Values	NSF	Parameters	Values	NSF
A1	0.02	0.8	**Smax in A3**	100	0.8
A1 +10%	0.022	0.8	**Smax in A3 +10%**	110	0.8
A1+20%	0.024	0.8	**Smax in A3+20%**	120	0.8
A1+30%	0.026	0.8	**Smax in A3+30%**	130	0.8
A1-10%	0.018	0.8	**Smax in A3-10%**	90.91	0.8
A1-20%	0.017	0.8	**Smax in A3-20%**	83.33	0.8
A1-30%	0.015	0.81	**Smax in A3-30%**	76.92	0.8
A2	0.14	0.8	**IF**	10	0.8
A2 +10%	0.154	0.8	**τ* +10%**	11	0.81
A2+20%	0.168	0.77	**τ* +20%**	12	0.81
A2+30%	0.182	0.76	**τ* +30%**	13	0.81
A2-10%	0.127	0.81	**τ* -10%**	9.091	0.8
A2-20%	0.117	0.81	**τ* -20%**	8.333	0.79
A2-30%	0.108	0.82	**τ* -30%**	7.692	0.78
A3	0.5	0.8	$t_{½}$	70	0.8
A3 +10%	0.55	0.77	**t½ +10%**	77	0.8
A3+20%	0.6	0.71	**t½ +20%**	84	0.8
A3+30%	0.65	0.63	**t½ +30%**	91	0.8
A3-10%	0.45	0.81	**t½ -10%**	63.64	0.8
A3-20%	0.42	0.81	**t½ -20%**	58.33	0.81
A3-30%	0.38	0.8	**t½ -30%**	53.85	0.81
Smax in A1	200	0.8	**BSmax**	100	0.8
Smax in A1 +10%	220	0.8	**BSmax+10%**	110	0.8
Smax in A1+20%	240	0.8	**BSmax+20%**	120	0.8
Smax in A1+30%	260	0.8	**BSmax+30%**	130	0.8
Smax in A1-10%	181.8	0.8	**BSmax-10%**	90.91	0.8
Smax in A1-20%	166.7	0.8	**BSmax-20%**	83.33	0.8
Smax in A1-30%	153.8	0.8	**BSmax-30%**	76.92	0.8
Smax in A2	10	0.8	$\mathbf{a_2}$	3.4	0.64
Smax in A2 +10%	11	0.8	$\mathbf{a_2}$ **+ 10%**	3.74	0.63
Smax in A2+20%	12	0.8	$\mathbf{a_2}$ **+ 20%**	4.08	0.61
Smax in A2+30%	13	0.8	$\mathbf{a_2}$ **+ 30%**	4.42	0.57
Smax in A2-10%	9.09	0.8	$\mathbf{a_2}$ **– 10%**	3.091	0.63
Smax in A2-20%	8.33	0.8	$\mathbf{a_2}$ **– 20%**	2.833	0.62
Smax in A2-30%	7.69	0.8	$\mathbf{a_2}$ **– 30%**	2.615	0.59

Appendix C3: The relationship between sediment concentration, C and Surface runoff q

The mean suspended sediment concentration C described as a function of surface runoff in chapter 2 follows the Harisine and Rose model (1992a) modeling approach. The derivation is shown below by following the approach of Ciesiolka et al. (1997). It is shown that, for sheet flow, the sediment concentration (kg/m^3) at the transport limit, c_t, can be expressed in

$$C_t = \frac{F\sigma SV}{\left(\frac{\sigma}{\rho-1}\right)\varphi_e} \qquad 1$$

F is the fraction of the stream power effective in erosive processes, S (m/m) is the slope of the land surface, *V* (m/s) is mean overland flow velocity, φ_e (m/s) is the effective sediment depositability and σ (Kg/m^3) and ρ (Kg/m^3) are sediment and water density, respectively.

Runoff per unit width, **Q (m^2/s)**, from a sloping plane surface with later inflow, q **(m/s)**

$$Q = DV = qL \qquad 2$$

Assuming kinematic flow approximation and flow to be turbulent

$$Q = KD^{5/3} \qquad 3$$

Where K=1/n*S$^{1/2}$

$$qL = K(qL/V)^{5/3} \qquad 4$$

L (m) is the slope length. Rearranging for V:

$$V\alpha q^{2/5} \qquad 5$$

If we substitute equation 5 in the sediment concentration equation 1

$$C_t = Kq^{0.4} \qquad 6$$

$$K = \frac{F\sigma S L^{2/5}}{\left(\frac{\sigma}{\rho-1}\right)\varphi_e}\left(\frac{\sqrt{S}}{n}\right)^{3/5} \qquad 7$$

In our simplified equation, ***a*** is similar with K. Therefore ***a*** is a function of sediment and watershed characteristics. For each runoff area, ***a*** will vary accordingly and it is assumed constant.

For Sediment load per unit area Y_t :

$$Y_t = C_t{*}q = a{*}A{*}q^{1.4} \qquad 8$$

APPENDIX D: CHAPTER FIVE

Appendix D1: Stream flow time series plot and scatter plot

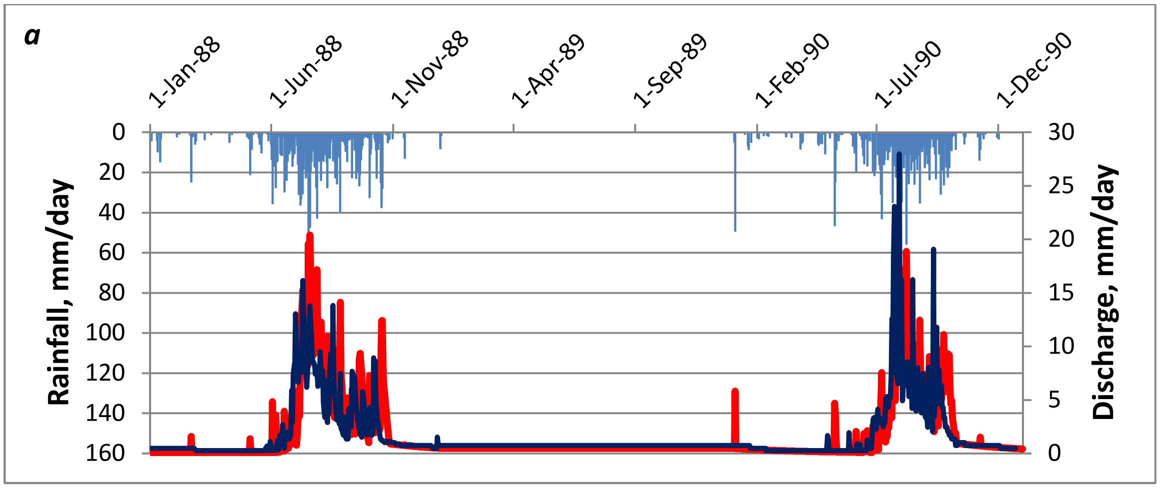

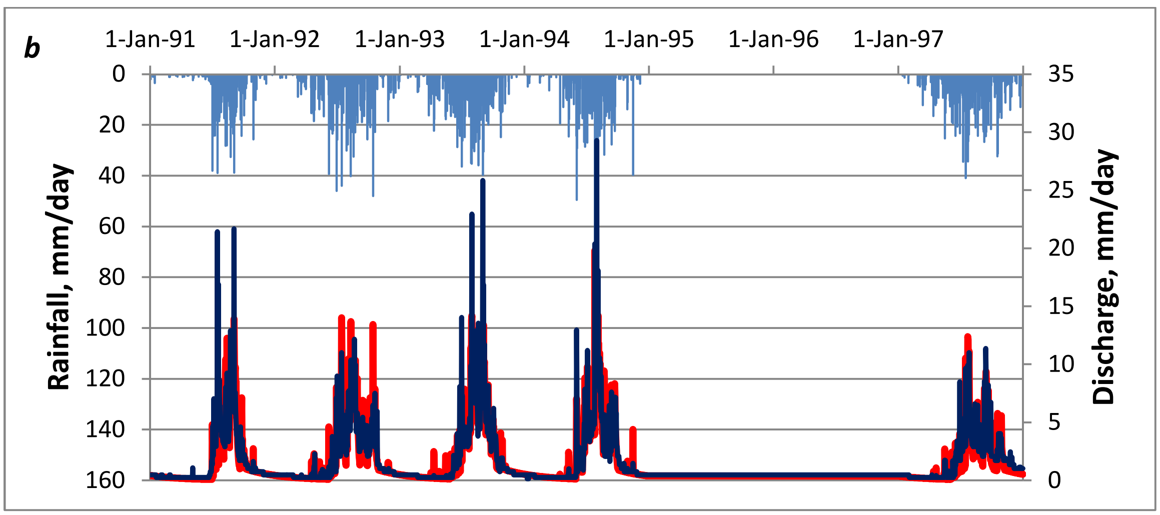

Figure D1-1: Predicted (red line) and observed (blue line) discharge data for Anjeni a) calibration and b) validation for daily discharge. Rainfall amounts expressed in mm/day is the solid blue area chart hanging from the top of each figure

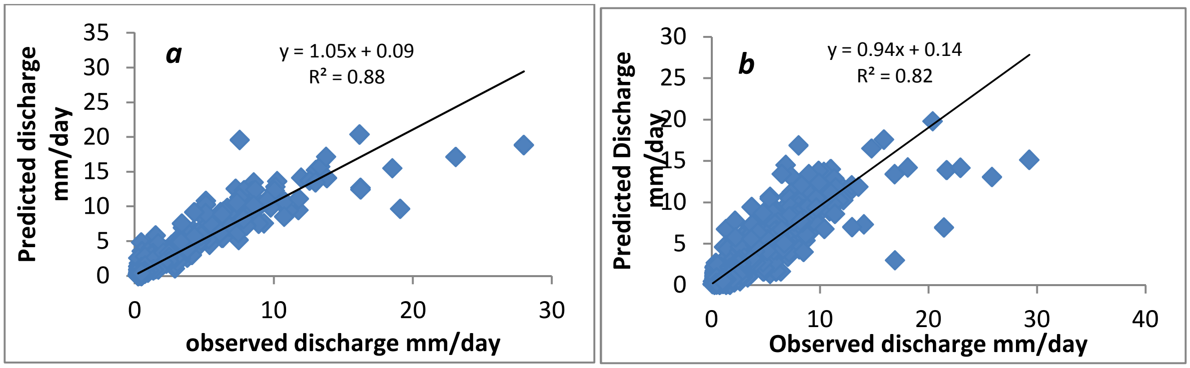

Figure D1-2: Stream flow scatter plot for Anjeni a) calibration b) validation for daily discharge.

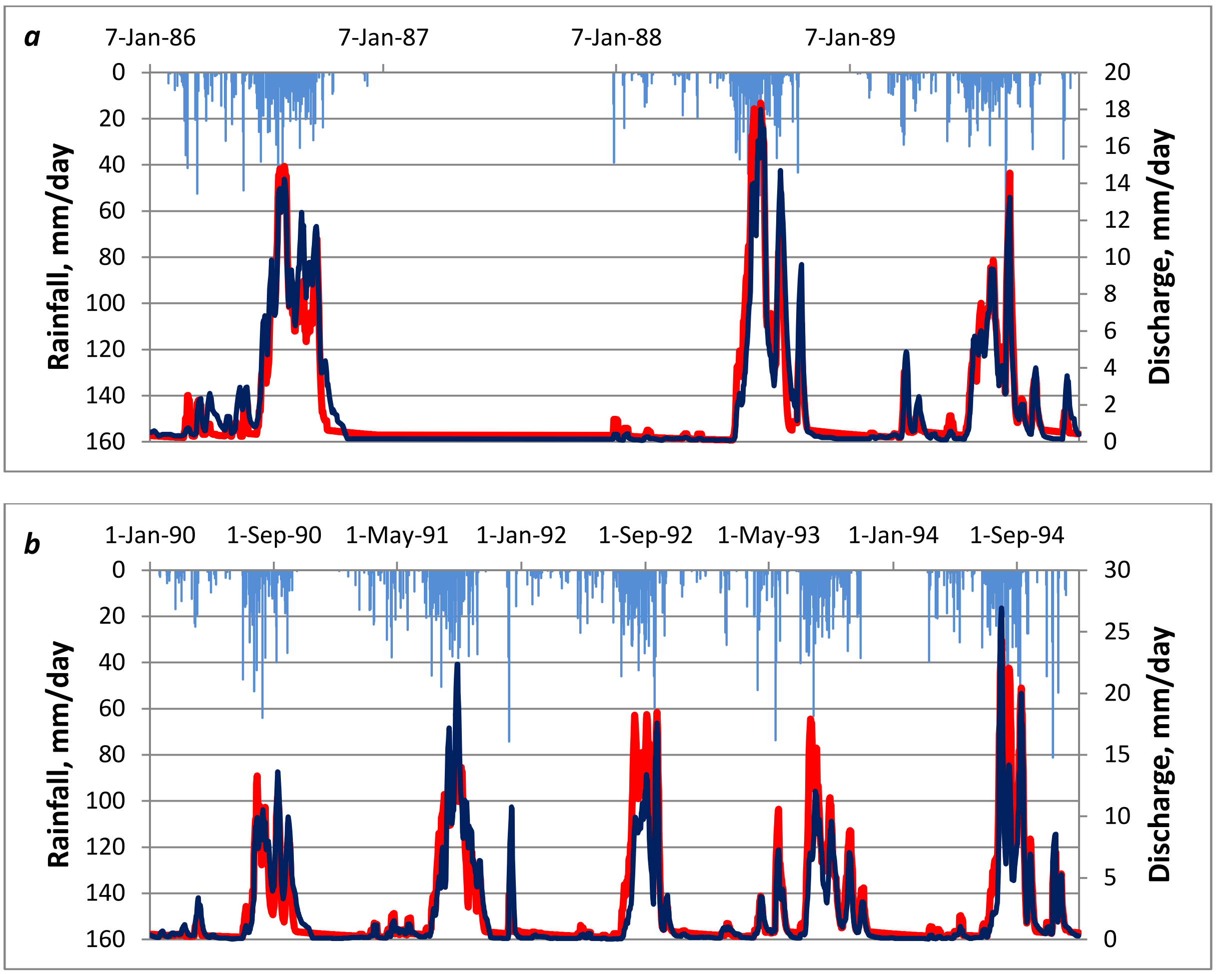

Figure D1-3: Predicted (red line) and observed (blue line) discharge data for Andit Tid a) calibration b) validation for daily discharge. Rainfall amounts expressed in mm/day is the solid blue area chart hanging from the top of each figure

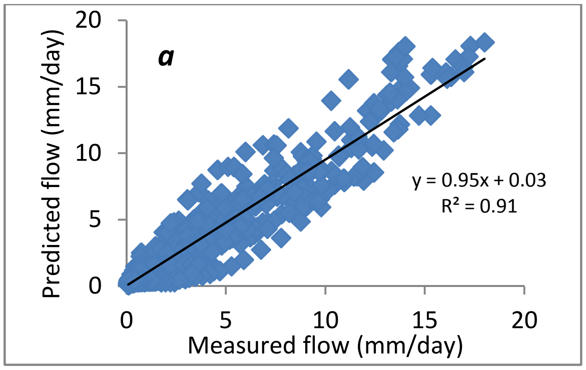

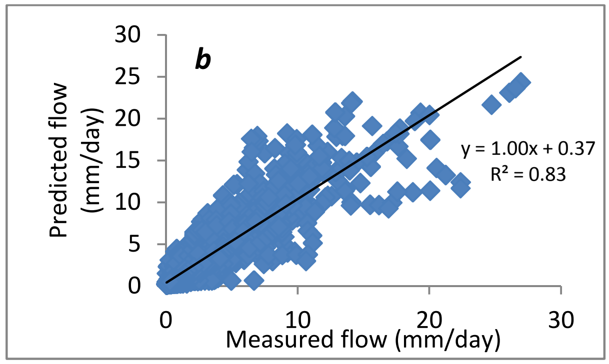

Figure D1-4. Stream flow scatter plot for Andit Tid a) calibration b) validation for weekly discharge.

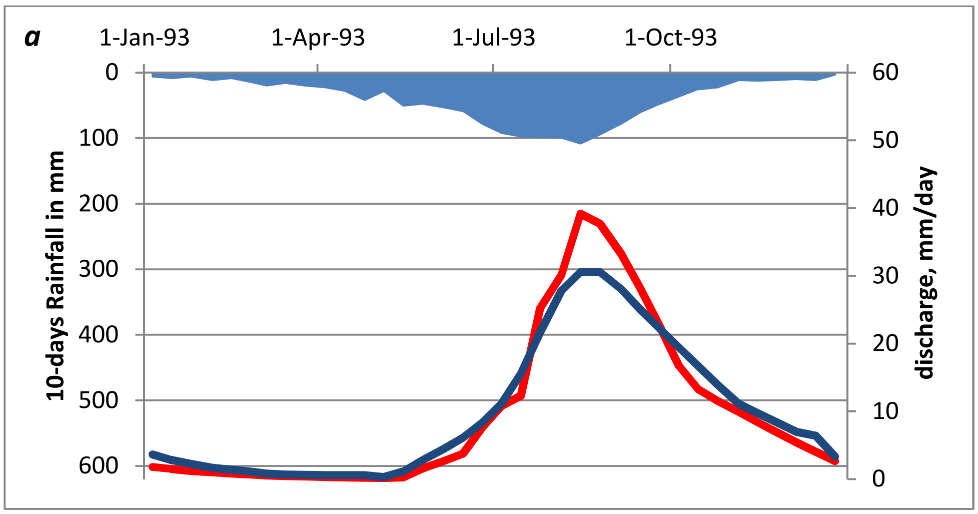

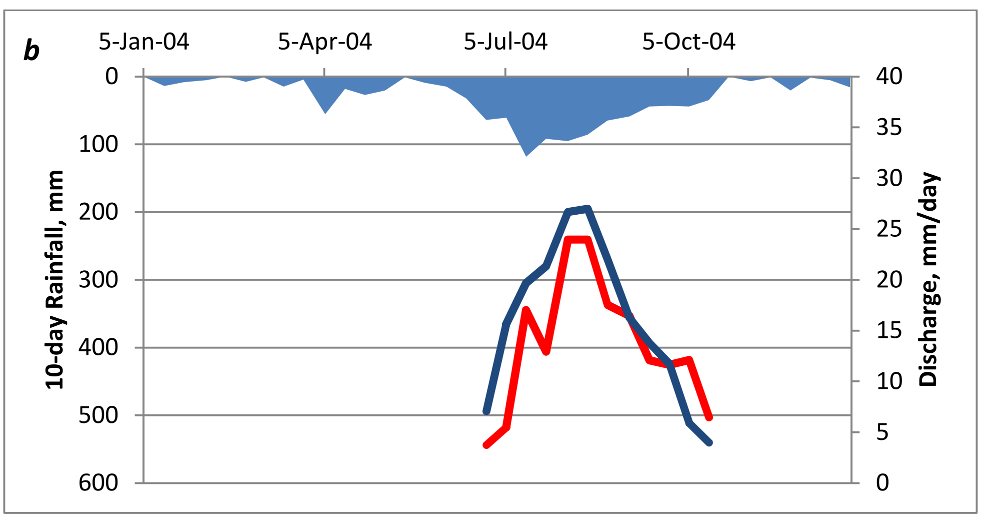

Figure D1-5: Predicted (red line) and observed (blue line) discharge data for Blue Nile Basin a) calibration b) validation for 10-daily discharge. Rainfall amounts expressed in mm/day is the solid blue area chart hanging from the top of each figure

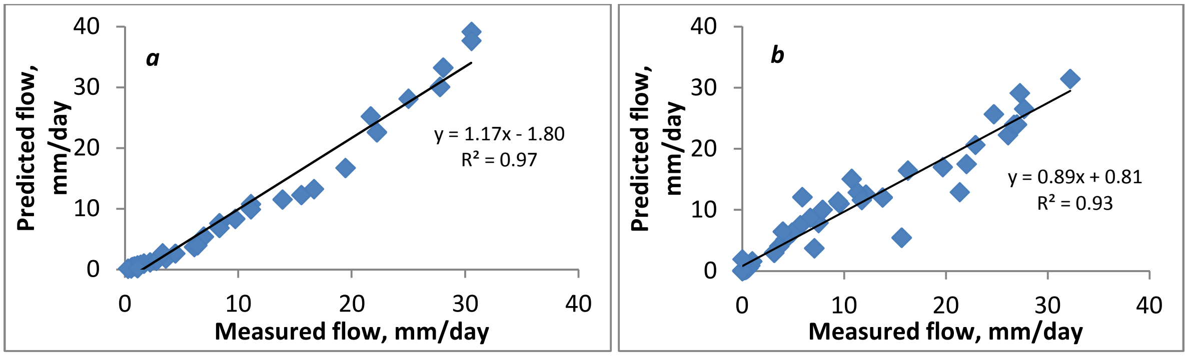

Figure D1-6: Stream flow scatter plot for Blue Nile Basin a) calibration b) validation for 10-days average discharge.

Appendix-D2: Sediment concentration time series plot and scatter plot

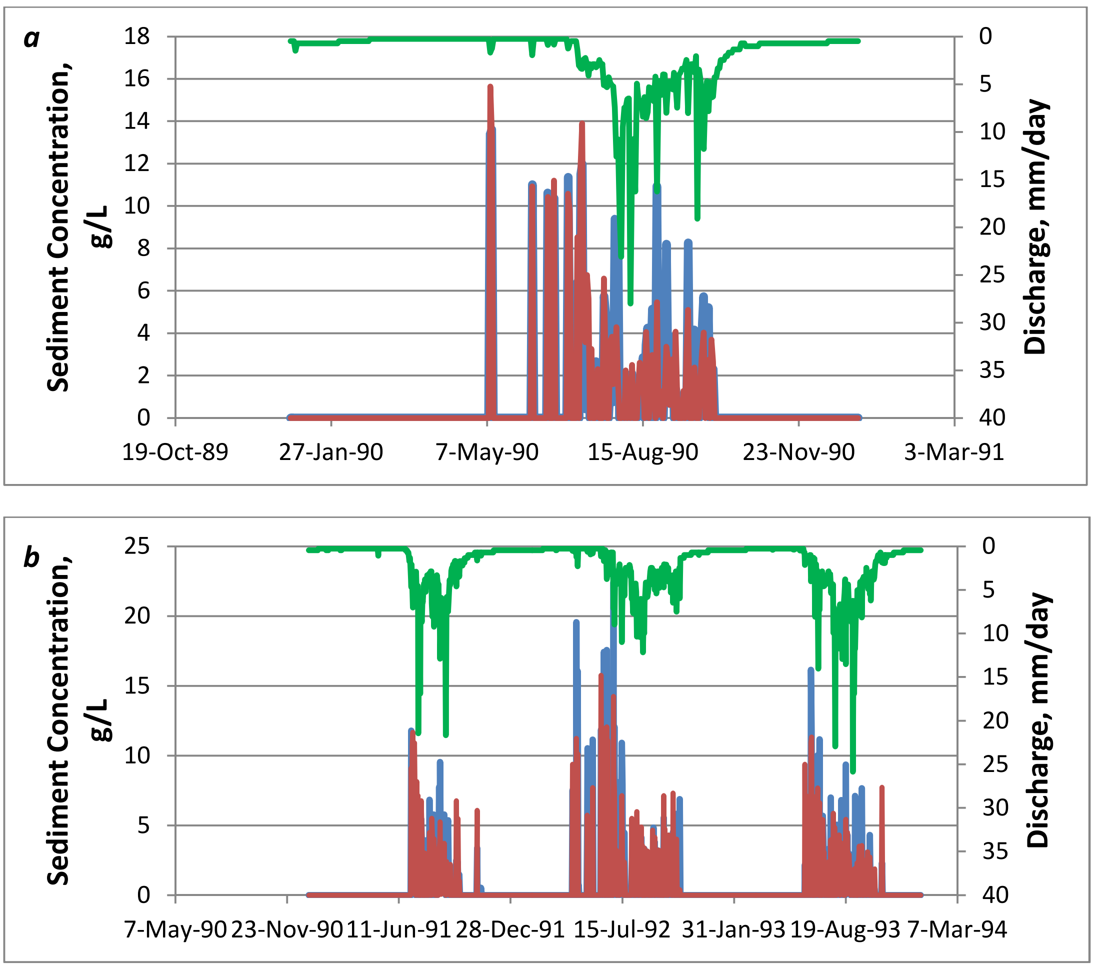

Figure D2-1: Predicted (red line) and observed (blue line) sediment concentration for Anjeni a) calibration b) validation. Discharge expressed in mm/day is the solid green area chart hanging from top of figure.

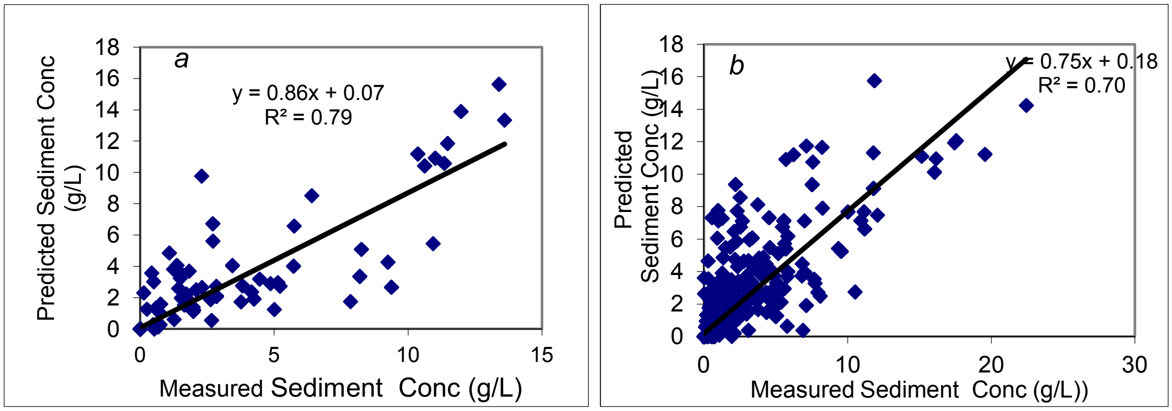

Figure D2-2: Sediment concentration scatter plot for Anjeni a) calibration b) validation for daily sediment concentration.

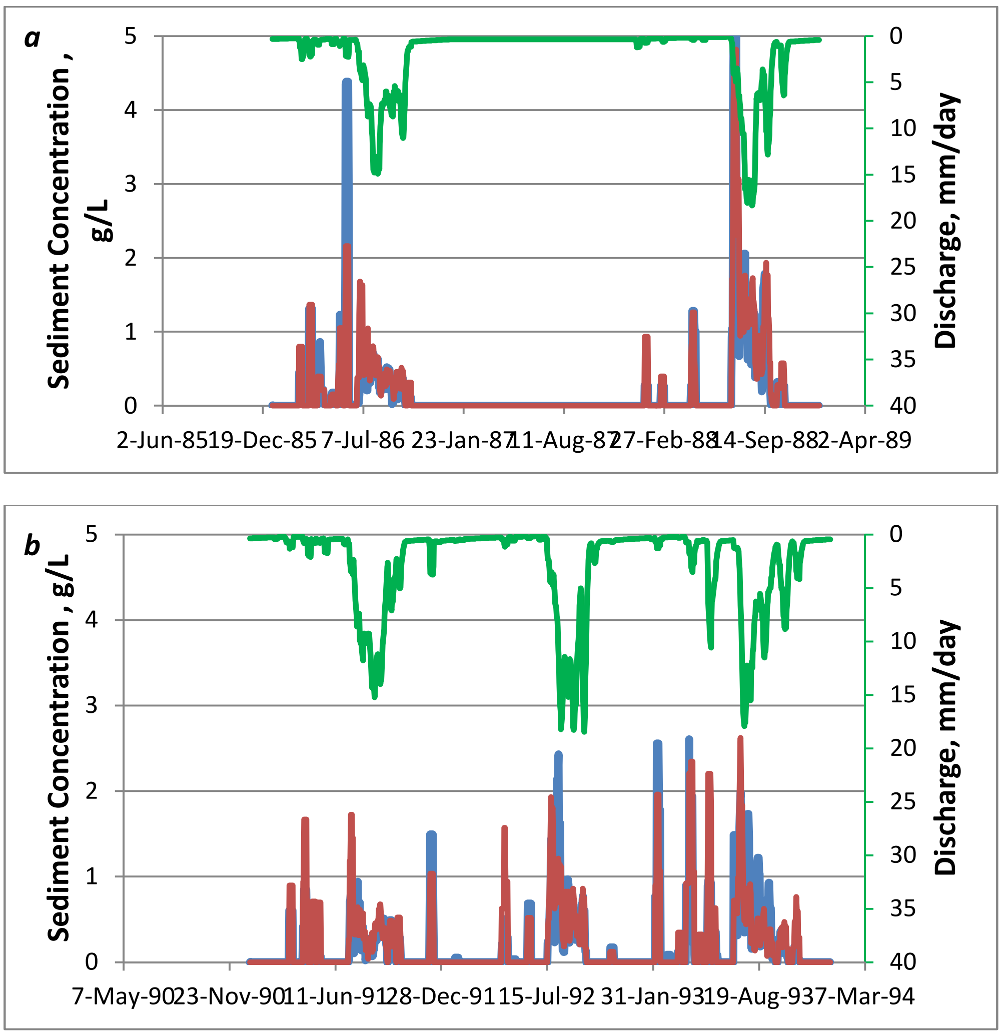

Figure D2-3: Predicted (red line) and observed (blue line) sediment concentration for Andit Tid a) calibration b) validation. Discharge expressed in mm/day is the solid green area chart hanging from top of figure.

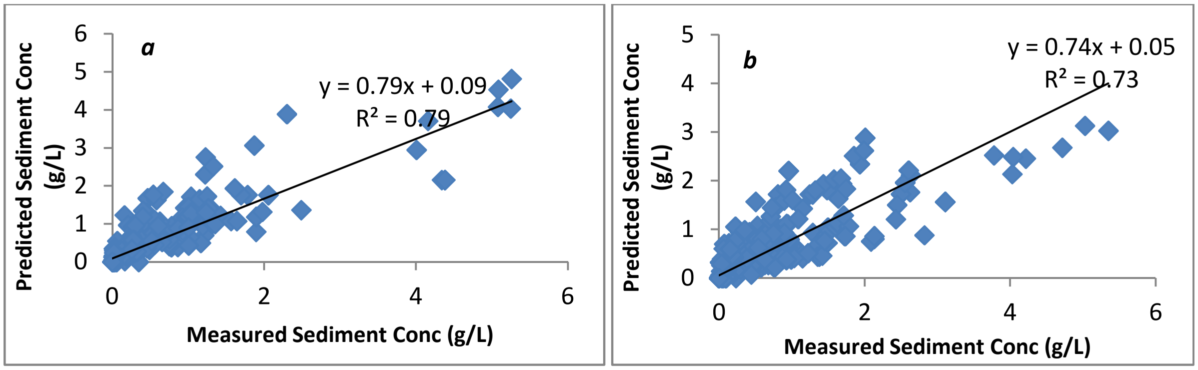

Figure D2-4: Sediment concentration scatter plot for Andit Tid a) calibration b) validation for weekly sediment concentration

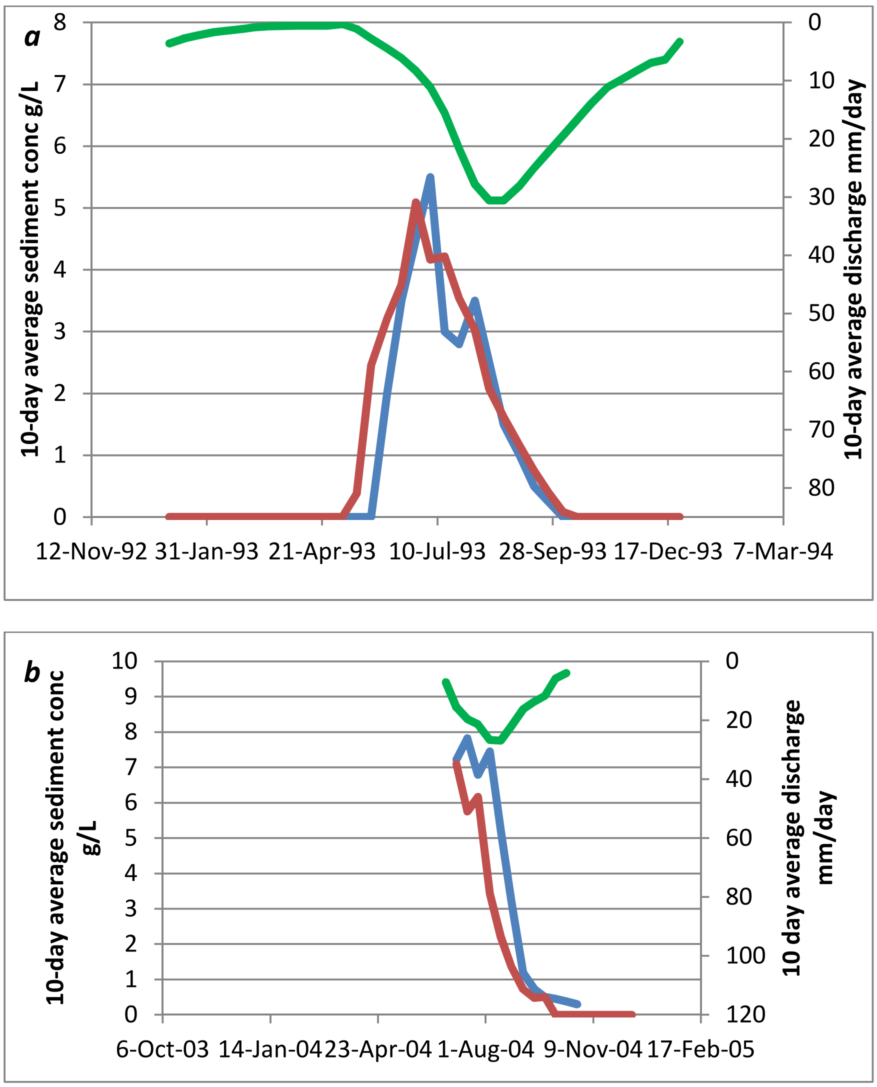

Figure D2-5: Predicted (red line) and observed (blue line) sediment concentration for Blue Nile Basin a) calibration b) validation. Discharge expressed in mm/day is the solid green area chart hanging from top of figure.

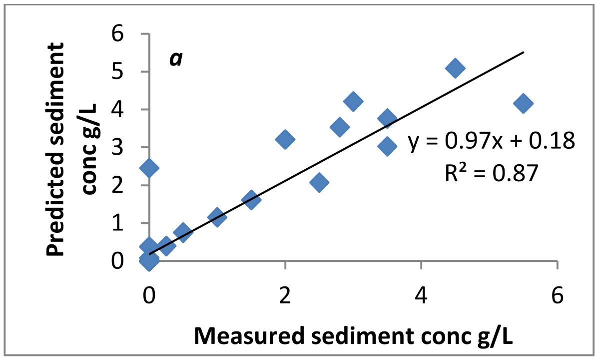

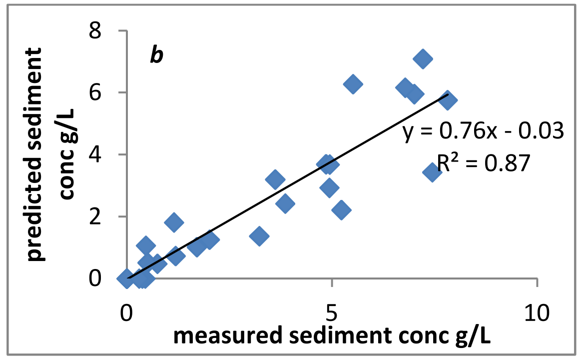

Figure D2-6: Sediment concentration scatter plot for Blue Nile Basin a) calibration b) validation for 10-days average sediment concentration

APPENDIX E: CHAPTER SIX

Appendix E1: Storm runoff simulation of Debre Mawi watershed at the outlet and its sub-watershed

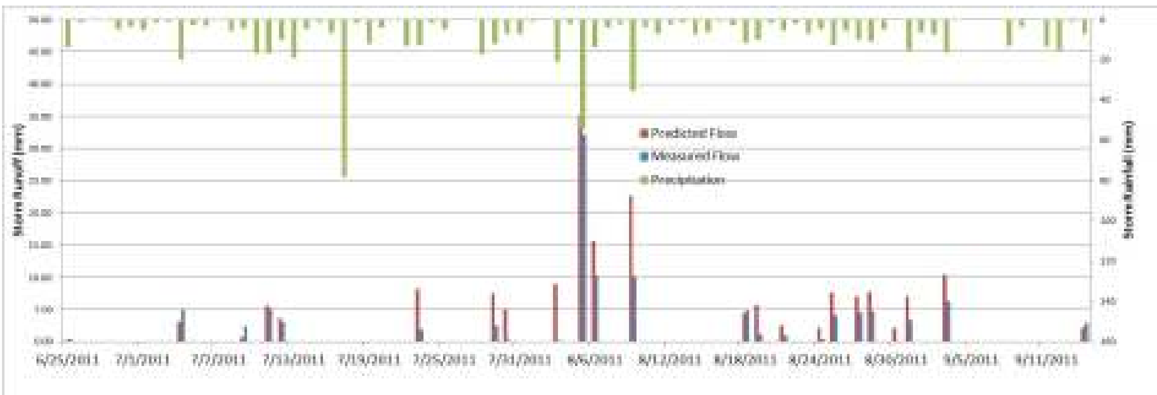

Figure E1-1: Measured and simulated storm runoff at weir-5 for the whole watershed for rainy period of 2011

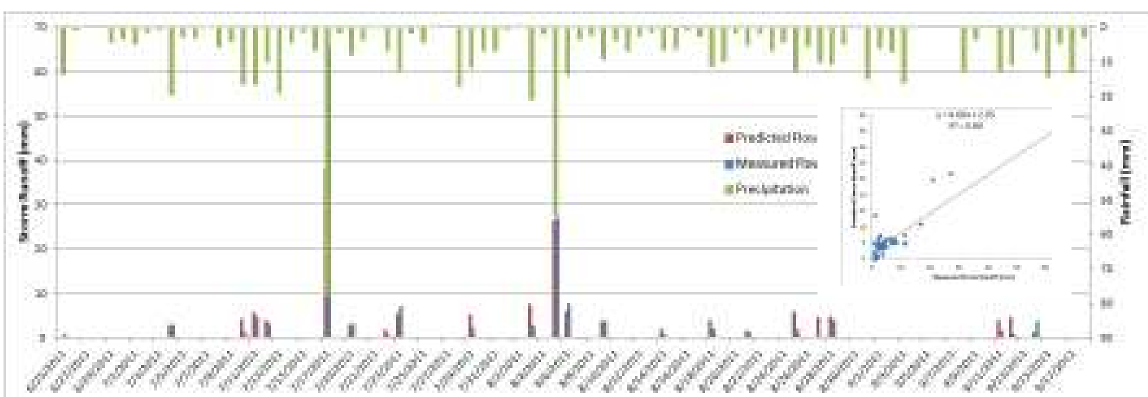

Figure E1-2: Measured and simulated storm runoff at weir-4 for sub-watershed 4 for rainy period of 2011 and scatter plot for 2010 and 2011 rainy period.

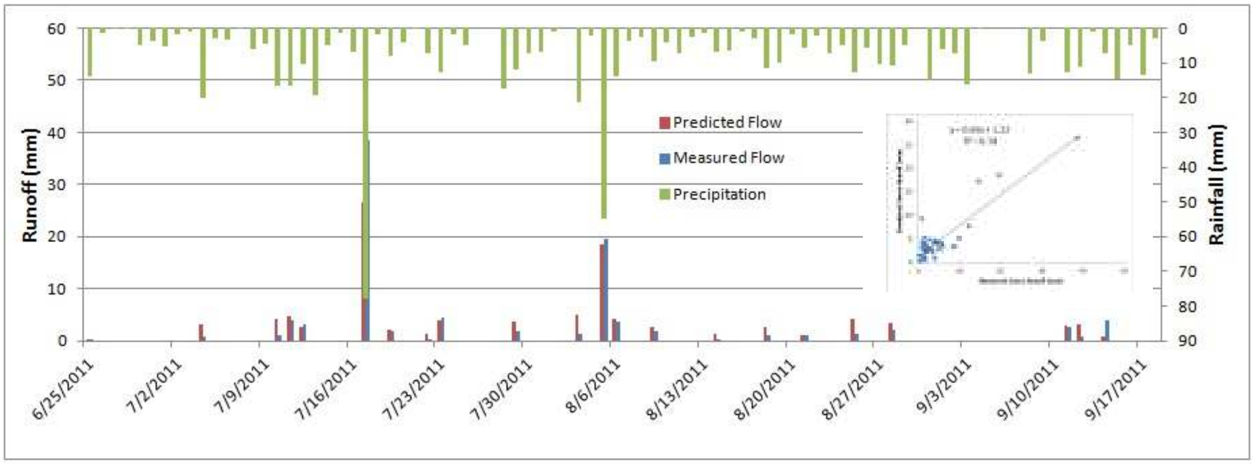

Figure E1-3: Measured and simulated sediment concentration at weir-3 for sub-watershed 3 for rainy period 2011 and scatter plot for 2010 and 2011 rainy period

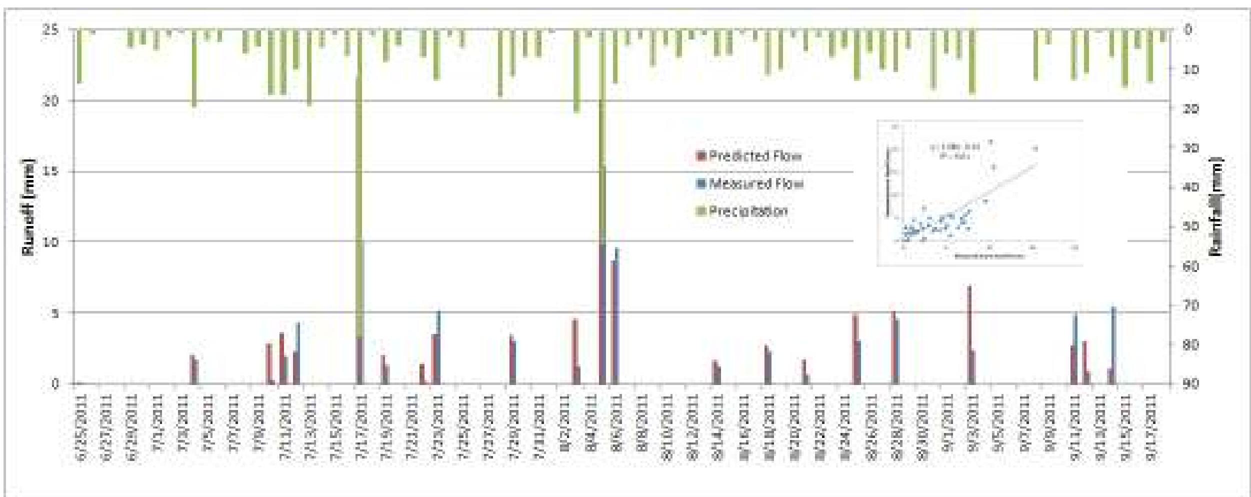

Figure E1-4: Measured and simulated storm runoff at weir-1 for sub-watershed 1 for rainy period of 2010 and scatter plot for 2010 and 2011 rainy period

Appendix E2: Sediment concentration simulation of Debre Mawi watershed at the outlet and its sub-watershed

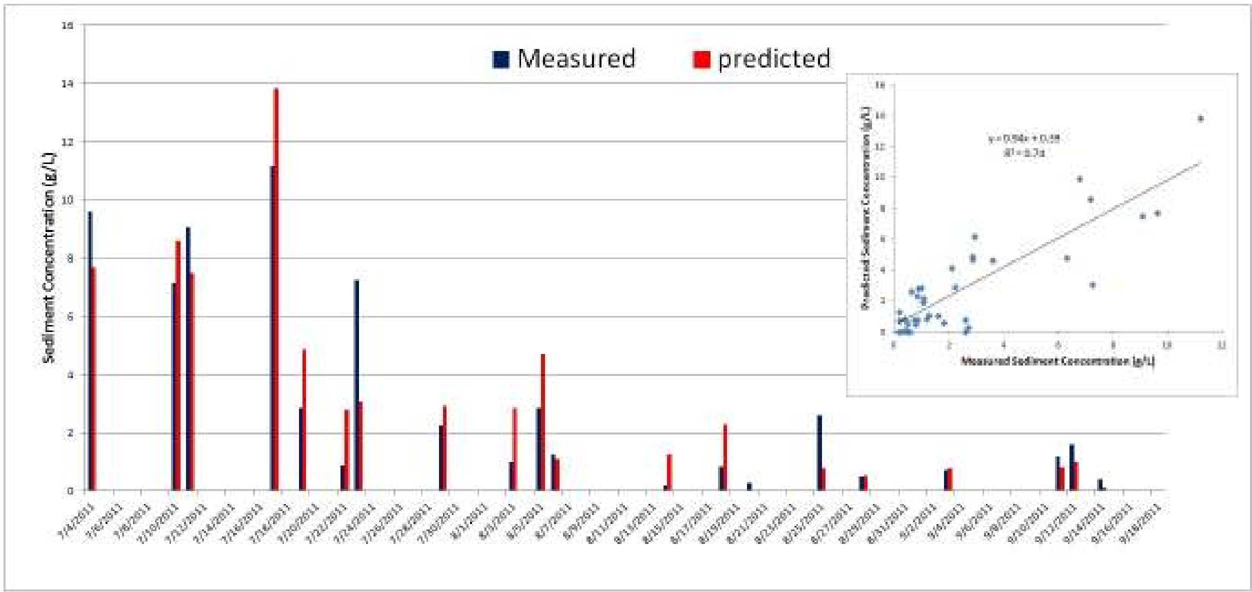

Figure 2-1: Measured and simulated sediment concentration at weir-1 for sub-watershed 1 for rainy period of 2010 and scatter plot for 2010 and 2011 rainy period

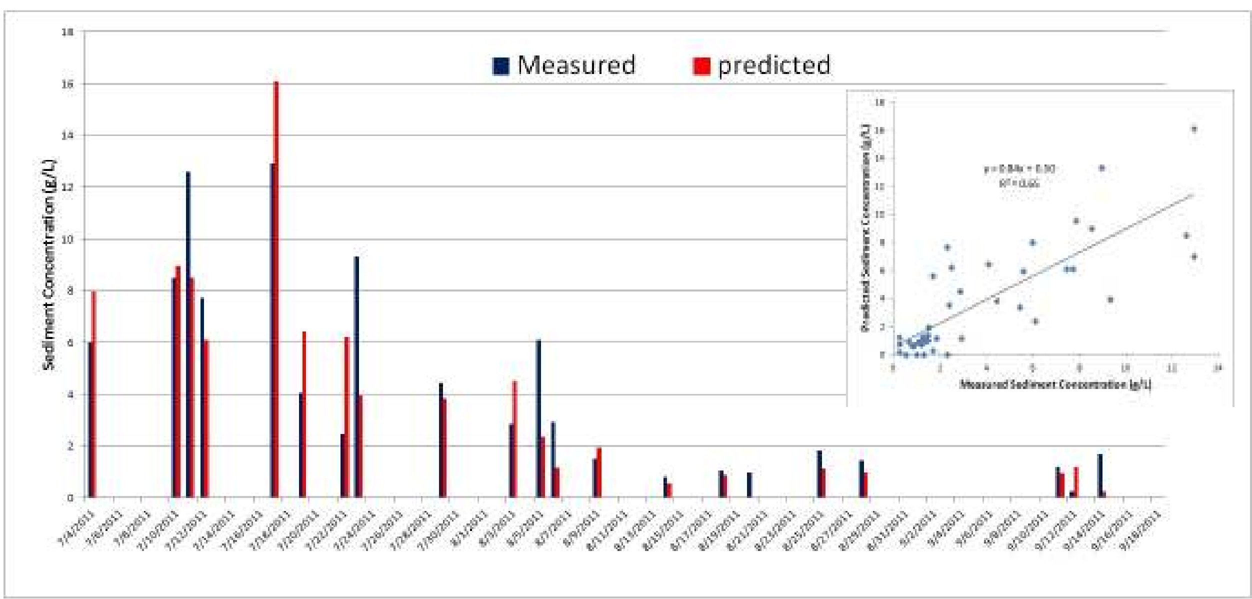

Figure E2-2: Measured and simulated sediment concentration at weir-3 for sub-watershed 3 for rainy period 2011 and scatter plot for 2010 and 2011 rainy period

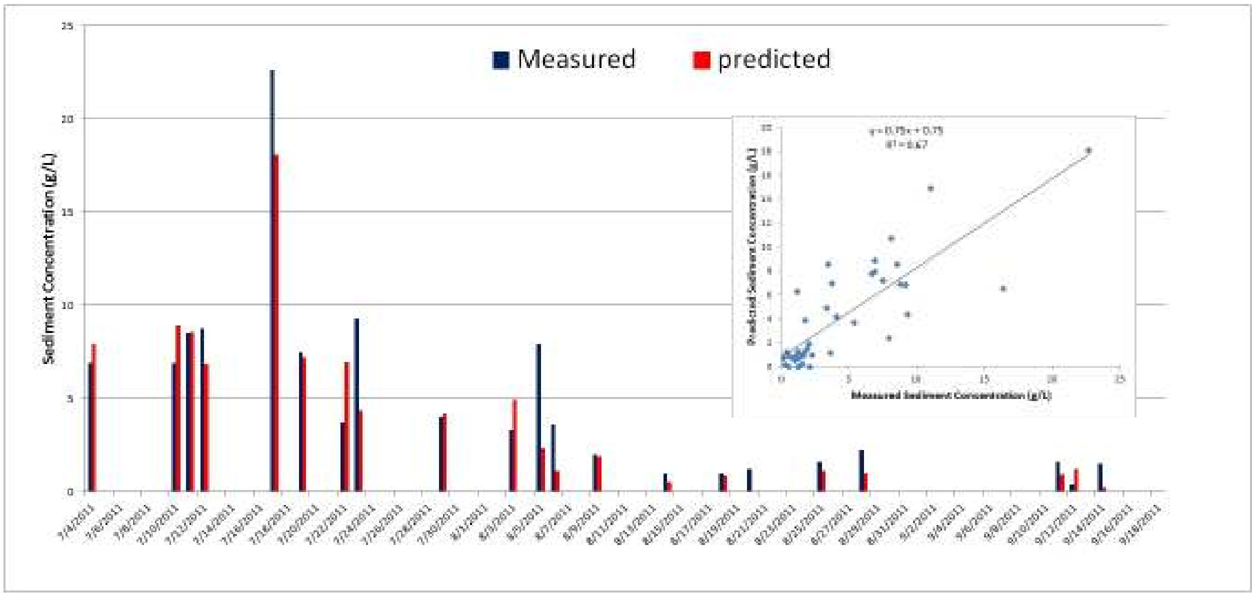

Figure E2-3: Measured and simulated sediment concentration at weir-4 for sub-watershed 4 for rainy period of 2011 and scatter plot for 2010 and 2011 rainy period.

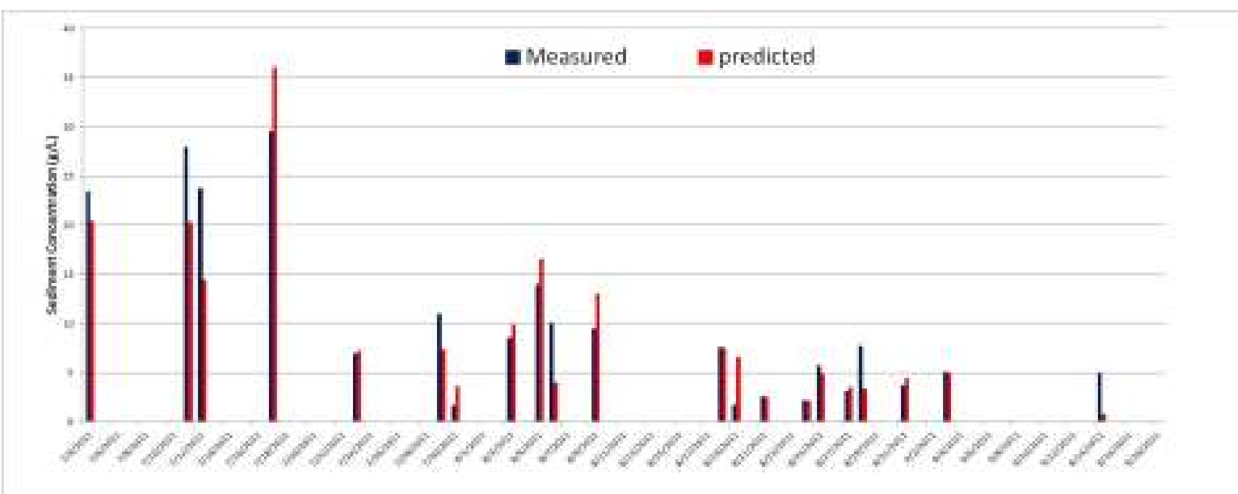

Figure E2-4: Measured and simulated sediment concentration at weir-5 for the whole watershed for rainy period of 2011